Isolation and Characterisation of Two Antiplasmodial Diterpenes from *Harpagophytum procumbens* (Devil's Claw) and Chemical Modification of a Related Analogue

Cailean Clarkson

Harpagophytum procumbens

Thesis presented for the degree of

Doctor of Philosophy in Pharmacology

University of Cape Town

Supervisors: Assoc. Prof. P.J. Smith, Dr W.E. Campbell, Dr K. Chibale

August, 2002

DECLARATION

Isolation and Characterisation of Two Antiplasmodial Diterpenes from *Harpagophytum procumbens* (Devil's Claw) and Chemical Modification of a Related Analogue

I, Cailean Clarkson hereby declare that the work on which this thesis is based is my original work (except where acknowledgements indicate otherwise) and that neither the substance nor any part of this work has been, is being, or is to be submitted for another degree at this University or at any other University.

I grant the University of Cape Town free license to reproduce the thesis in whole or in part, for the purpose of research.

This thesis is presented for examination for the degree of Doctor of Philosophy.

Signed by candidate

Signed:

Date: 12·08·2002

ACKNOWLEDGEMENTS

I am indebted to my three wonderful supervisors, Associate Professor Pete Smith, Dr Bill Campbell and Dr Kelly Chibale, whose insight, enthusiasm and guidance made this thesis possible. It was truly a pleasure and an honour working in your labs.

I am extremely grateful to Dr Gilbert Matsabisa for sharing his findings on *H. procumbens* and allowing me to pursue this work. Much appreciation goes to Gerard Hansford and Professor Earle Graven, from the Grassroots Natural Products Group, for generously supplying *H. procumbens*, without which this study may have taken an eternity.

Thank you to the University of Cape Town, Benfara Scholarship and the Ernst and Ethel Eriksen Trust for financial support and providing me with an opportunity to study further.

I would like to thank the Pharmacology postgraduate students, Donelly van Schalkwyk, Dale Taylor, Chiku Mtegha, Siya Ntutela, Jason Walden, Bongi Gumede, Susan Yeh, Justin Wilkins, Malefa Tselanyane, Paul Waako and Gary Gabriels as well as the ex-students Dr Gilbert Matsabisa, Dr Natalie Brine and Jennifer Norman for sharing their expertise on everything and anything, and for providing a stimulating working environment. Thank you to the Medicinal Chemistry students, Chitalu Musonda, Manie Gamieldien, Kevin Wellington and Alex Chipleleme for providing answers to copious questions and for making my experience in the Chemistry Department so enjoyable.

I would like to express my gratitude to Dr J. Bastida at the University of Barcelona for running the NMR samples, and to Dr M. Bredenkamp at the University of Stellenbosch for allowing us to use their polarimeter. I am grateful to Professor P. Folb for his commitment towards the success of every student that passes through the department, and for sharing his unequalled statistical knowledge.

To all of the people who successfully run the Pharmacology Department, Sumaya Salie, Noor Salie, Noel Jordan, Jessica Petersen, Sherlayne Koonin and Marion Newman, thank you for all of your input.

A big thank you to family and friends for their years of love and support, and for asking about the well being of my mosquitos. It is greatly appreciated. A heartfelt thanks to Grant Langdon for the emotional support and for sponsoring my write up with biscottis.

ABSTRACT

Malaria is recognised as one of the leading public health problems in Sub-Saharan Africa. The treatment and control of the disease depends largely on a limited number of chemotherapeutic agents, most of which have been used for the past 30 years. The emergence and spread of drug resistance parasites has highlighted the need for new chemically diverse, effective drugs. One of the major sources of antimalarial agents and novel template compounds is higher plants. Reliance on medicinal plants for the treatment of malaria is widespread in South Africa and represents a diverse resource of potential antimalarial drugs. This thesis describes the investigation of one of South Africa's medicinal plants, *Harpagophytum procumbens* (Devil's Claw) as a source of antiplasmodial hit compounds, and the subsequent synthesis of potential leads based on the active compounds.

The initial screening of the root extracts of *H. procumbens* showed that the petroleum ether extract possessed *in vitro* antiplasmodial activity (IC_{50}=13μgml^{-1}). Bioassay-guided fractionation, using a combination of flash and high pressure liquid chromatography, yielded an active diterpene that was identified as $C_{20}H_{28}O_3$. The isolated compound displayed *in vitro* activity (IC_{50}<0.6μgml^{-1}) against a chloroquine resistant (K1) and sensitive (D10) strain of *P. falciparum*, and low *in vitro* cytotoxicity against a mammalian cell line (Rat-1). Since the yield of the active principle was extremely low (<0.003% by weight), an improved purification procedure was developed using solid phase extraction techniques. This enabled the isolation of two antiplasmodial diterpenes in a high enough yield for full structure elucidation and thorough evaluation of *in vitro* antiplasmodial activity and cytotoxicity. The active components, (+)-8,11,13-totaratriene-12,13-diol ($C_{20}H_{30}O_2$) and (+)-8,11,13-abietatrien-12-ol ($C_{20}H_{30}O$), were identified using high resolution electron impact mass spectrometry and detailed nuclear magnetic resonance spectroscopy. The compounds were found to exhibit potent *in vitro* antiplasmodial activity (IC_{50}<1μgml^{-1}) against several strains of *P. falciparum* (D10, 3D7, RSA11, K1 and W2) and low *in vitro* cytotoxicity (IC_{50}>50μgml^{-1}) against two mammalian cell lines (CHO and HepG2). Although the compounds have previously been isolated from other plants and synthesised, this is the first report of their isolation from *H. procumbens.* Furthermore, the compounds

modification purposes. Five novel β-amino alcohols, which varied in the structural features of the amine moiety, were synthesised using classical synthetic organic chemistry approaches. The new compounds were characterised and tested for *in vitro* antiplasmodial activity and cytotoxicity. All of the synthesised compounds showed an improved activity and revealed favourable chemical modifications to optimise the activity of the hit compounds. In terms of lead development, two of the synthesised compounds showed considerable potential and warrant further investigation as promising leads.

TABLE OF CONTENTS

CHAPTER 1

Malaria, Traditional Medicines, Drug Discovery & Development

CHAPTER 2

Harpagophytum procumbens

CHAPTER 3

Antiplasmodial Activity of *H. procumbens* (batch I and II)

CHAPTER 5

Synthesis and Activity of Totarol Derivatives

CHAPTER 6

Research Summary, Prospects and Conclusions

CHAPTER 7

Materials and Methods

LIST OF FIGURES, PLATES AND SCHEMES

CHAPTER 5

CHAPTER 7

APPENDIX 1

APPENDIX 2

APPENDIX 2

APPENDIX 2

LIST OF TABLES

CHAPTER 7

LIST OF ABBREVIATIONS

ACN	acetonitrile
APAD	3-acetylpyridine adenine dinucleotide
ca	approximately
CHO	Chinese hamster ovarian (cells)
COSY	proton-proton homonuclear shift correlated spectroscopy
CQ	chloroquine
DHFR	dihydrofolate reductase
DHPS	dihydropteroate synthetase
DMEM	Dulbecco's Modified Eagles' Medium
DMSO	dimethylsulphoxide
DN	daunomycin
et al.	and all others
EtOAc	ethyl acetate
FC	flash chromatography
FCS	fetal calf serum
g	gram(s)
Hams-F_{12}	Ham's Nutrient Mixture F-12
HepG2	Heptoma G (cells)
HMBC	heteronuclear multiple bond connectivity
HPLC	high pressure liquid chromatography
HREIMS	high resolution electron impact mass spectrometry
hrs	hours
HSQC	heteronuclear single quantum coherence
Hz	hertz
IC_{50}	50% inhibitory concentration
IR	infra red
J	coupling constant
kg	kilogram(s)
MeOH	methanol
mg	milligram(s)
MIC	minimum inhibitory concentration
min	minute(s)

ml	millilitre
MTT	3-(4,5-dimethylthiazol-2-yl)-2,5-diphenyltetrazoliumbromide
ND	not determinable
NMR	nuclear magnetic resonance
NOESY	nuclear Overhauser enhancement and exchange spectroscopy
PBS	phosphate buffered saline
PE	petroleum ether
pLDH	parasite lactate dehydrogenase
ppm	parts per million
QN	quinine
R_I	resistance index
rpm	revolutions per minute
SD	standard deviation
S_I	selectivity index
SPE	solid phase extraction
TLC	thin layer chromatography
TMS	tetramethylsilane
UV	ultraviolet (radiation)
WHO	World Health Organisation
λ	wavelength (nm)
μg	microgram(s)
μM	micromolar

Chapter 1

Malaria, Traditional Medicines, Drug Discovery & Development

1.1 Brief History of Malaria

Malaria has been present since time immemorial and remains one of the worlds most prevalent health problems. In the 4th century BC, the Greeks noted an association between people exposed to swamp lands and the subsequent development of fevers. The Romans later called this disease mal'aira (bad air), due to the foul smelling air near the swamps. It was only in the 1890s that parasite gametocytes were first observed in blood and it was postulated that they were transmitted by mosquitos. Pioneering work by Sir Ronald Ross established the main features of the parasitic life cycle, for which he received the Nobel Prize in 1902. During the 20th century, a number of advances were made towards understanding the parasite, developing antimalarial drugs and to controlling the mosquito vector (Prescott *et al.*, 1993).

1.2 Prevalence of Malaria

Although the geographical distribution of malaria has been reduced over the past 50 years, 40% of the world's population is still affected by the disease (Figure 1.2.).

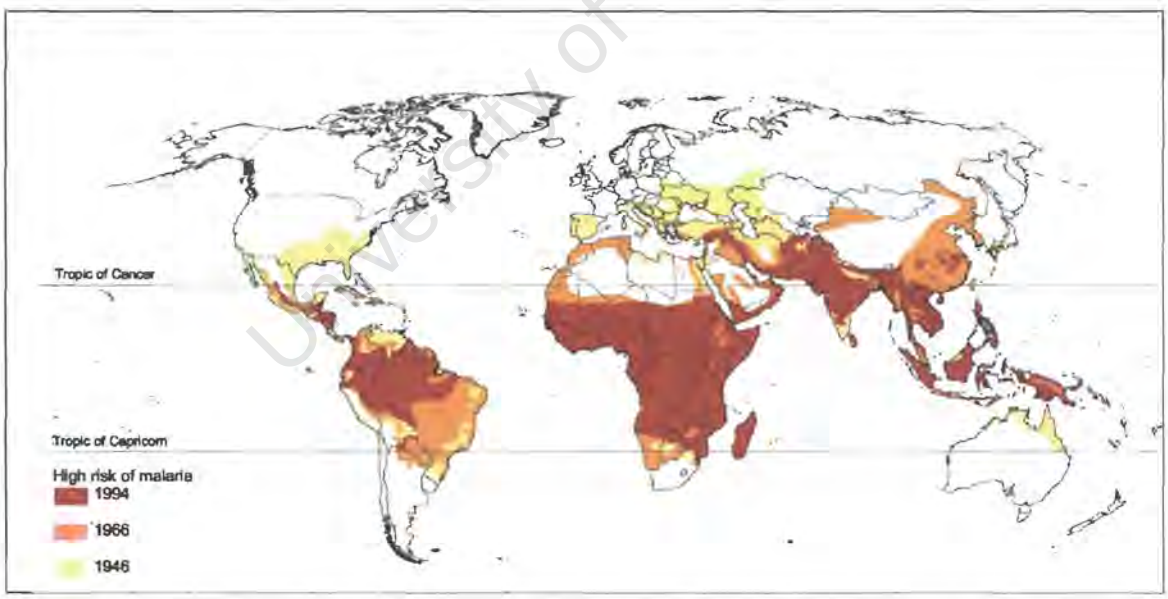

Figure 1.2. Global distribution of malaria from 1946- 1994 (Reproduced with permission from A. Mellinger, The Centre for International Development, Cambridge, Massachusetts)

It is estimated that malaria is responsible for 300-500 million clinical cases and over 1 million deaths per year (WHO, 1998). The majority of the malaria cases occur in sub-

Saharan Africa, where the disease continues to be one of the most widespread health problems.

The high incidence of malaria in Africa can be attributed to a number of reasons. Climatic suitability for malaria transmission occurs over a large area of Africa, and global climatic warming combined with changes in land use are extending the areas of transmission. Malaria is geographically specific, but mankind also influences the epidemiology of the disease. The mass movement of refugees, migrant workers and non-immune travellers facilitate the spread of the disease, particularly across borders. Moreover, methods of intervention aimed at preventing the disease and treating the patients have been hampered by a lack of political commitment, failure to use existing tools and poor health care facilities. The emergence of multi-drug resistant parasites and resistance of mosquitos to insecticides has further complicated efforts to eradicate malaria.

1.2.1 Malaria in South Africa

In the first half of the 20th century measures were taken in South Africa to control malaria due to its devastating impact on the economy. Before large-scale intervention, the disease reached epidemic levels as far south as Durban and the highlands of Pretoria (Sharp and le Sueur 1996). Currently, the malaria distribution is confined to Kwazulu-Natal, Mpumalanga and the Northern Province (Figure 1.2.1.).

The high-risk transmission areas are concentrated along the international borders, particularly the Mozambican border. This stresses the impact of imported malaria and the need for malaria control to be regional and not country specific. In South Africa the disease is distinctively seasonal and there is a large inter-annual variation in the number of cases. The annual number of notified malaria cases in the year 2000 was approximately 62 000 and in 2001 it was 25 000 (Wille, Department of Health, 2001). The relatively large inter-annual variation is attributed to favourable climatic conditions, population migration and the emergence of drug resistant parasites (Sharp and le Sueur, 1996). Despite intensive efforts by the Department of Health, the control of malaria continues to be a challenge for South Africa as it does worldwide.

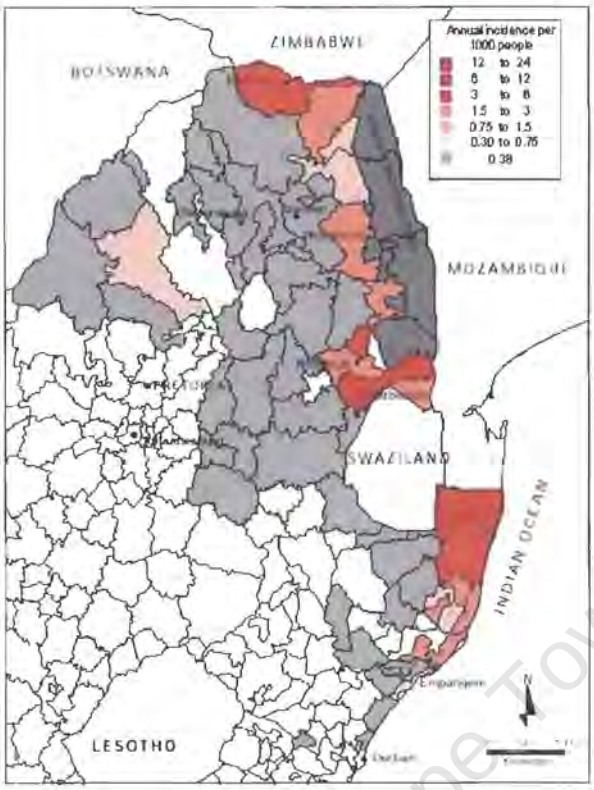

Figure 1.2.1. Distribution of malaria in South Africa, 1995 (Reproduced with permission from B. Sharp, National Research Programme , MRC, Durban, South Africa)

1.3 Economic Burden of Malaria

The economic and social burden of the disease has resulted in lower rates of economic growth in malaria endemic countries (Sachs and Malaney, 2002). Medical costs of prevention, treatment and care puts an additional strain on health systems, which usually have limited resources. A bout of malaria would result in a loss of at least 5 workdays for an individual, a loss of income for a family and reduced productivity for an employer. In the rural areas where farming is often the sole means of income, working days off result in a reduced harvest production. In school children, malaria leads to poor school attendance and impairment of learning. Women are at a higher risk of getting malaria during pregnancy than any other time. For pregnant women, malaria often causes anaemia, maternal death and is associated with a low birth weight among newborns. The prevalence of malaria in an area can lead to a decline in international trade and tourism and foreign investment, which are essential for economic growth.

There is a strong correlation between malaria, poverty and development, which is often underestimated (Sachs and Malaney, 2002). The cost to human and social wellbeing is large and is exacerbated in the poorer communities.

1.4 Life cycle of the Malaria Parasite

Malaria is caused by the protozoan parasite *Plasmodium falciparum* and is transmitted by the female *Anopheles* mosquito. The life cycle of the malaria parasite is complex and consists of four stages. Two asexual stages occur in the human host and one asexual and sexual stage take place in the mosquito vector (Figure 1.4.).

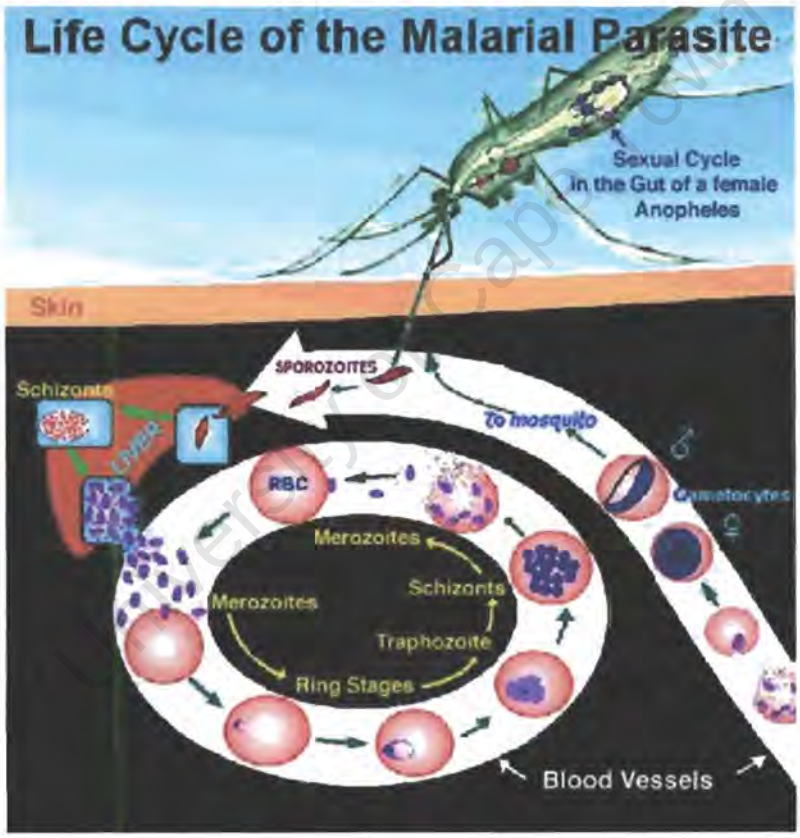

Figure 1.4. Life cycle of the malaria parasite (Reproduced with permission from S. Sharma, The Institute of Fundamental Research, Bombay, India)

When an infected mosquito bites an individual, a small amount of saliva containing an anticoagulant and sporozoites enters the bloodstream. Once in the bloodstream the sporozoites invade liver cells where they undergo asexual fission to produce merozoites. On release from the liver cells, the merozoites can either invade other liver cells or infect erythrocytes.

In the intra-erythrocytic stage the parasites feed upon the host cell's haemoglobin and occupy up to 80% of its volume (Francis *et al.*, 1997). Symptoms of malaria only begin once the parasite starts to divide asexually in the red blood cells. Inside the erythrocytes, each merozoite matures into a trophozoite, which divides asexually to give a schizont with a number of nuclei. The schizont then divides to produce numerous merozoites that lyse the erythrocytes and are released back into the bloodstream. The release of merozoites, toxins and other cellular debris into the circulatory system causes the characteristic fevers and chills associated with malaria. This intra-erythrocytic stage of the parasite is cyclic and is repeated every 48 or 72 hours depending on the species of the parasite. Merozoites also have the ability to develop into gametocytes that can be ingested by a mosquito during a blood feed. Once inside the mosquito gut, the gametocytes fuse to produce a zygote. The zygote penetrates the mosquito gut wall and forms an oocyst on the outer layer. Here the oocyst asexually multiplies and differentiates to form sporozoites that migrate to the mosquito's salivary glands. This completes the multi-stage life cycle of the parasite (Prescott *et al.*, 1993).

There are four species of *Plasmodium*; *P. falciparum, P. malariae, P. vivax and P. ovale*. Of the four human *Plasmodium* species, *P. falciparum* is the most common form and poses the greatest risk of complications and death.

1.5 Prevention and Cure

A wide range of preventative measures and effective treatment are available for malaria. For most countries this includes a combination of vector control programs integrated with early diagnosis and treatment of the disease. Many factors influence the choice of malaria intervention in a country or region. One of the main considerations is cost-effectiveness. Especially in Africa, for malaria control to be appropriate it not only has to be effective, but also cost effective.

Malaria prevention involves the measures taken to protect against infection and against the progression of the disease. Intervention methods aimed at controlling the vector include house spraying with insecticides, larvicides and environmental management to limit the number of breeding sites. Personal protection would encompass the use of insecticide-treated nets (bednets and curtains), repellents and protective clothing.

Measures involving chemoprophylaxis prevent the development of the disease but not the initial infection.

One of the most important strategies to reduce the burden of the disease is the provision of effective treatment. This involves early diagnosis followed by the correct use of efficacious, safe and affordable antimalarial drugs. Ideally, a protective vaccine would be a powerful tool in the control of malaria. Although there have been great advances in sequencing the genome of *P. falciparum*, the development of a vaccine has been complicated by *Plasmodium* being genetically diverse and having a multi-stage life cycle. It is hoped that a vaccine will be available for widespread use in the next 7-15 years. Until a vaccine for malaria has been developed, the treatment and control of the disease relies heavily on chemotherapeutic agents.

1.6 Classes of Drugs Used in the Treatment of Malaria

There are a limited number of antimalarial drugs that are in widespread use. The majority of them target the intra-erythrocytic stages of parasite growth, thereby preventing the development of the disease and further transmission. There are three main groups of antimalarial drugs in use. The first and most commonly used are the quinoline based antimalarials, which include quinine and its derivatives chloroquine, amodiaquine and mefloquine. The antifolate drugs are a second major group and are represented by the dihydrofolate reductase inhibitors, pyrimethamine and proguanil as well as the sulfonamides and sulfones. The last group comprises artemisinin and its derivatives artesunate and artemether. Resistance to most of the drugs in current use has highlighted the need not only for novel antimalarials, but to understand the mechanisms acquired by parasites to evade the action of the drugs. With an understanding of drug resistance, one could design new antimalarials that circumvent these mechanisms or even reverse resistance.

1.6.1 Quinoline-containing antimalarials

One of the first treatments for malaria in the Western world was quinine (QN) (Figure 1.6.1.), an active ingredient from the bark of the *Cinchona* tree. Presently, QN is still used for treatment, but only as an intravenous injection for severe malaria. Chloroquine (CQ), which was the most widely used of the 4-aminoquinoline compounds was synthesised in

the 1930s as a less toxic analogue of QN and has been used extensively ever since. It is a low-cost drug, safe and suitable for oral administration. Unfortunately, resistance to CQ was first reported in the 1960s and has now spread to every malaria endemic country. CQ's reduced efficacy led to the development of the synthetic analogues mefloquine and amodiaquine for the treatment of CQ-resistant parasites. Despite the widespread use of this group of antimalarial drugs, the precise mode of action remains to be understood.

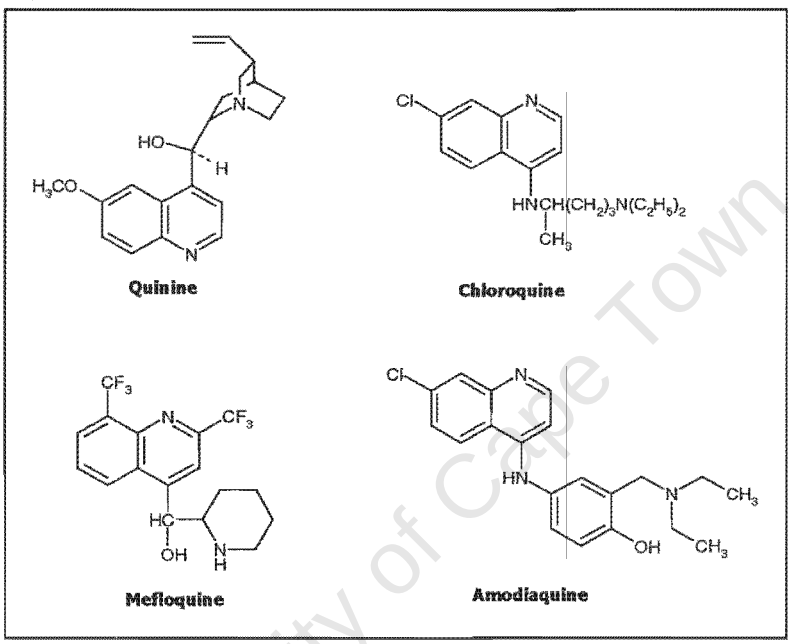

Figure 1.6.1. Structures of the quinoline antimalarial drugs quinine, chloroquine, mefloquine and amodiaquine

1.6.1.1 Mechanism of chloroquine action

A number of possible mechanisms have been proposed for the action of CQ and its related compounds. Initially, it was hypothesised that CQ bound to plasmodial DNA and inhibited DNA and RNA synthesis (Parker and Irvin, 1952). This theory has since been refuted along with the proposals that CQ causes the inhibition of a vacuolar proteinase (Vander Jagt *et al.*, 1986), or of protein synthesis (Surolia *et al.*, 1991).

The most common hypothesis is that CQ acts primarily by interfering with haem polymerization in the intra-erythrocytic stage of the parasite lifecycle. CQ is a weak base (pka_1=8.1, pka_2=10.2) and in its unprotonated form it can diffuse across the membranes

of parasitised erythrocytes and accumulate in the acidic digestive vacuole of the parasite (Yayon *et al.*, 1984). During the intra-erythrocytic stage, the parasite feeds by ingesting haemoglobin from the host cytoplasm and degrading it in the digestive vacuole. The catabolism of haemoglobin releases amino acids and a toxic by-product ferriprotoporphyrin, also known as haem. The parasite detoxifies the haem molecules in the food vacuole by polymerising them into an inert form called haemozoin (Goldberg *et al.*, 1990). It is proposed that the principal action of CQ is to inhibit the haem polymerisation resulting in the toxic build up of haem or drug-haem complexes (Orjih *et al.*, 1994). This theory is supported by the observation that CQ is capable of inhibiting the spontaneous formation of β-haematin, a synthetic polymer of haem identical to haemozoin, in a chemical system (Egan *et al.*, 1994). Furthermore, for CQ like drugs a strong correlation has been demonstrated between haem binding, inhibition of haem polymerisation and the *in vitro* antimalarial activity (Dorn *et al.*, 1998). Evidence that CQ may inhibit the degradation of haem by glutathione suggests an additional mechanism of action (Ginsburg *et al.*, 1998). In this hypothesis CQ prevents the polymerisation of haem and therefore increases the efflux of haem out of the food vacuole. Under normal conditions the haem would be degraded by glutathione, but in the presence of CQ this process is competitively inhibited, enabling haem to accumulate in the parasite membrane. The presence of haem in the membrane disrupts its barrier properties, thereby disturbing homeostasis in the parasite, leading to parasite death.

Although there is substantial evidence that CQ inhibits haem polymerisation and causes toxic levels of haem to build up, the precise mechanism by which this occurs is still uncertain. It has been shown that a haem-CQ complex can bind to haemozoin, preventing further polymersiation by 'capping' the growing polymer and obstructing further growth (Sullivan *et al.*, 1998). An alternative mechanism of action proposes that CQ reduces the availability of monomeric haem for polymerisation (Dorn *et al.*, 1998). In order for haem to be incorporated into the haemozoin polymer, it needs to exist in the monomeric form. In the absence of CQ, equilibrium exists between the monomeric and dimeric forms of haem and in an acidic environment like in the parasitic vacuole, the monomer is the more stable structure (Brown *et al.*, 1970). Under experimental conditions, it was observed that CQ binds preferentially to the dimer and it is postulated that this stabilises the dimer, relative to the monomer, shifting the dimerisation equilibrium and reducing the amount of available monomer. Moreover, it was suggested that the stabilised CQ-dimer could bind to

the growing haemozoin polymer and inhibit polymerisation, which is consistent with the 'capping' theory (Dorn *et al.*, 1998).

1.6.1.2 Mechanism of cholorquine resistance

It is generally accepted that CQ resistant parasites accumulate less CQ than sensitive parasites, thereby preventing lethal concentrations of the drug being reached within the parasitic food vacuole (Fitch, 1970). The molecular explanation for this process remains a subject of much debate. Hypotheses for the decrease in CQ accumulation can be broadly classified into three areas, a higher rate of CQ efflux, a lower rate of CQ uptake, or varying combinations of both of these processes.

1.6.1.2.1 Increased efflux of chloroquine

CQ resistance in *Plasmodium* has been compared to multidrug resistance (MDR) in cancer cells. One of the distinguishing features of MDR cells is that they express high levels of a plasma membrane protein, P-glycoprotein (PgP) (Riordan *et al.*, 1985). Pgp is a member of the superfamily of ATP-binding cassette transport proteins and operates as an energy dependant drug exporter. A variety of chemically diverse compounds are transported out of the cell by Pgp, thereby decreasing the internal concentrations of the drug (Fojo *et al.*, 1985). MDR phenotypes can be reversed by chemosensitisers that inhibit Pgp drug transport and increase the sensitivity of the cells to the drugs (Ford, 1996). Several parallels can be drawn between CQ resistance and multidrug resistance in cancer cells, namely decreased accumulation of drug, drug efflux mechanisms, cross resistance and resistance modulation by chemosensitisers.

It has been reported that CQ resistant parasites efflux CQ at a much faster rate than sensitive parasites, resulting in a decrease in drug accumulation (Krogstad *et al.*, 1987). These findings were later observed to be ATP dependant, which suggests an active Pgp-like drug efflux (Krogstad *et al.*, 1992). Genetic investigations have shown that the MDR phenotype is due to the over-expression of the human *mdr1* gene and similar genes, *pfmdr1* and *pfmdr2* have been identified in *P. falciparum.* The *pfmdr* gene product, a P-glycoprotein homologue Pgh1, has been localised on the digestive vacuole membrane, (Cowman *et al.*, 1991), but there is still conflicting evidence about the link between CQ resistance and the over expression of Pgh1 (Wellems *et al.*, 1990 and Foote *et al.*, 1989).

More recent observations of the transfection of mutant *pfmdr* genes from CQ resistant strains to sensitive strains, supports the involvement of Pgh1 in the decreased CQ accumulation in resistant parasites (Reed *et al.*, 2000). Furthermore, it has been shown that changes in Pgh1 could modulate resistance to quinine, mefloquine and halofantrine (Reed *et al.*, 2000).

One of the characteristics of MDR cells is their ability to transport a wide range of unrelated compounds out of the cell (Nielsen and Skovsgaard, 1992). Although some cross resistance to the quinoline antimalarials has been reported, the cross resistance patterns are not as broad as those observed for MDR cells (Bray *et al.*, 1998).

When MDR cells are exposed to verapamil and a number of other unrelated compounds, their sensitivity to the drugs is increased and resistance is reversed (Ford, 1996). The observation that CQ resistance can also be reversed by verapamil (Martin *et al.*, 1987) and by a number of other chemosensitisers, provides additional evidence for the analogy to MDR cells.

1.6.1.2.2 Decreased chloroquine uptake

A reduced uptake of CQ has also been proposed to explain the lower levels of CQ in resistant strains. Since CQ is a weak base, it accumulates in the acidic digestive vacuole in the parasite. The degree of accumulation is thought to be pH dependant and an increase in vacuolar pH would cause a decrease in CQ accumulation. A vacuolar ATPase proton pump maintains the pH and is thought to have weakened activity in CQ resistant parasites (Bray *et al.*, 1992). Recent evidence suggests that a vacuole transmembrane protein PfCRT (chloroquine resistance transporter) is linked to CQ resistance (Fidock *et al.*, 2000). Transfection of a mutant *pfcrt* gene from a resistant parasite to a sensitive parasite conferred the resistant phenotype. It was proposed that mutations in the transmembrane protein could decrease the influx of CQ across the parasite membrane (Fidock *et al.*, 2002). Furthermore, the transfected strains were found to have a lower vacuole pH, which contradicts the theory that CQ resistant parasites have an elevated vacuole pH. In a complementary study, it was shown that the pH of the digestive vacuole is actually lower in resistant parasites than sensitive parasites (Dzekunov *et al.*, 2000). It was proposed that the lower pH favours the formation of an insoluble form of haem that CQ is unable to bind to. This is consistent with earlier hypotheses, which suggested that the

ability of CQ to associate with free haem is the determining factor in CQ resistance (Fitch *et al.*, 1970 Bray *et al.*, 1998). Although a number of hypotheses have been put forward for the possible mechanism of CQ resistance, it is thought that resistance is not conferred by a single mechanism, but is a combination of several possible processes.

1.6.2 Antifolate antimalarials

The antifolate group of drugs was generated through synthetic medicinal chemistry and an understanding of the parasites' biochemical pathways. This class of antimalarials is still commonly used, even though their activity is being restricted by the rapid emergence of drug resistance (Plowe *et al.*, 1998). Traditionally the antifolates are divided into two classes, the dihydrofolate reductase (DHFR) inhibitors pyrimethamine and proguanil, and the dihydropteroate synthetase (DHPS) inhibitors, which include the sulfonamide drugs, sulfadoxine and dapsone (Figure 1.6.2.).

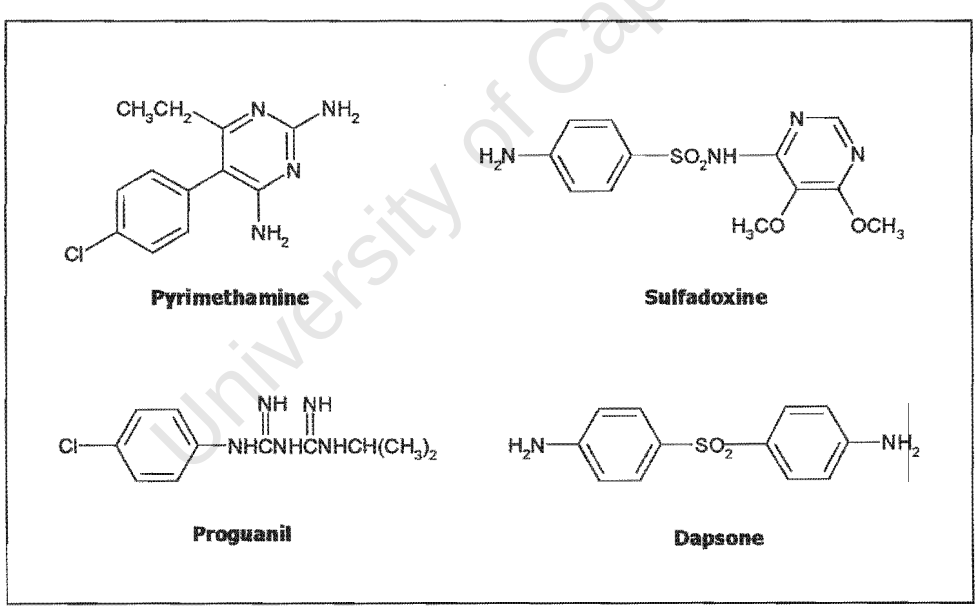

Figure 1.6.2. Structures of the antifolates pyrimethamine, sulfadoxine, proguanil and dapsone

1.6.2.1 Mechanism of antifolate action

Both classes of the antifolates act by inhibiting the synthesis of folic acid. Folic acid is an essential cofactor for the synthesis of pyridines and purines, which are the bases required for the construction of DNA, RNA and other cellular constituents (Schellenberg and

Coatney, 1961 and Gutteridge and Trigy, 1971). Humans cannot synthesise folic acid and obtain it from their diet, whereas parasites synthesise their own and are susceptible to folate metabolism inhibitors. The antifolates are active at all the growing stages of the parasite life cycle.

Folate synthesis is essential for parasite survival and is carried out in a number of steps catalysed by various enzymes. The sulfonamide-like drugs inhibit the action of one of the enzymes DHPS by competing with the natural substrate *p*-aminobenzoic acid for the active site of the enzyme (Zhang and Meshnick, 1991). Similarly, pyrimethamine and proguanil competitively inhibit the enzyme DHFR by mimicking the structure of the natural substrate (Diggens *et al.*, 1970). Pyrimethamine and sulfadoxine are often used in combination as they target the same metabolic pathway, producing a synergistic effect.

1.6.2.2 Mechanism of antifolate resistance

Resistance to the antifolates drugs is now very common in malaria parasites. Studies have shown that resistance to DHPS and DHFR inhibitors is conferred by mutations in the target enzymes (Wang *et al.*,1997). The acquired mutations reduce the ability of the inhibitor to bind to the enzyme, thereby enabling the parasite to tolerate higher concentrations of the drugs. Humans obtain preformed folate from their diet and parasites are exposed to this in the bloodstream. An additional mechanism of antifolate resistance is for the parasite to take up preformed folate from its surroundings and bypass the blockage of folate synthesis (Wang *et al.*, 1997). Antifolate resistance is usually due to a combination of mutations in the target enzymes and the use of an alternative pathway to salvage folate.

1.6.3 Artemisinin antimalarials

The antimalarial qinghaosu (artemisinin) was first isolated from the Chinese medicinal plant *qing hao* (*Artemisia annua*) in 1972. The natural extract artemisinin has since been used to generate a number of semi-synthetic derivatives, dihydroartemisinin, artesunate, artemether and arteether (Figure 1.6.3.).

Motivation for the derivatisation of artemisinin was to increase its poor solubility and to enhance its antimalarial activity. This group of compounds is the most rapidly acting of all

the available antimalarial drugs and is effective against multi-drug resistant strains of *P. falciparum* (Hein and White, 1993). Currently, artemisinin and its derivatives are being used increasingly to treat uncomplicated and severe forms of malaria.

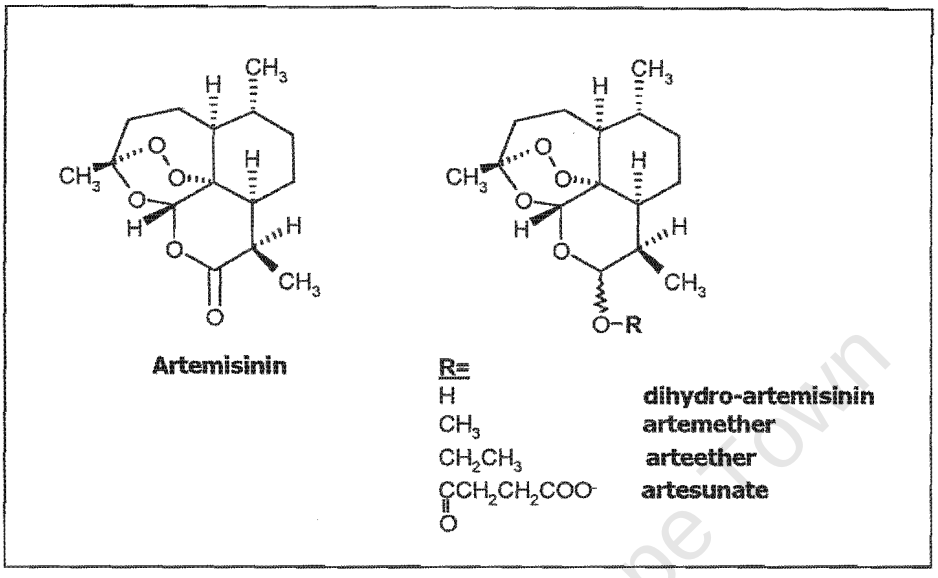

Figure 1.6.3. Structures of artemisinin and its derivatives

1.6.3.1 Mechanism of artemisinin action

The precise mode of action of artemisinin and its derivatives is not completely understood, but appears to involve two steps. In the first step, the endoperoxide bridge is cleaved to generate artemisinin-derived free radicals. The free radicals are strong alkylating agents and in the second step they form covalent bonds with various parasite proteins (Meshnick, 1994).

The initial activation of artemisinin appears to be catalysed by ferrous haem and free iron (Fe II), and is assumed to be responsible for the selective toxicity to malaria parasites, since the parasites live in a haem rich environment (Meshnick *et al.*, 1993, Meshnick, 1994 and Zhang *et al.*, 1992). However, the exact mechanism of activation has not been elucidated and remains a contentious issue (Olliaro *et al.*, 2001). This iron-induced cleavage of artemisinin results in the formation of carbon and oxygen centered radicals and an epoxide (Cumming *et al.*, 1996), all of which are capable of alkylating proteins. Although labeled artemisinin has been shown to covalently bind to a number of proteins,

the significance of this binding or how it brings about parasite death remains unknown (Yang *et al.*, 1993). It has been proposed that the generated radicals invoke oxidative stress, which could cause general damage to the parasite (Krungkrai and Yuthvong, 1987).

1.6.3.2 Mechanisms of artemisinin resistance

Although the use of artemisinin and its derivatives is increasing, there have been very few reports of resistance. Artemisinin resistance has been achieved *in vitro* in *P. falciparum* after mutagenic treatment with N-methyl-N-nitronitrosoguanidine, demonstrating the possibility of resistance (Indelburg, 1985). More recently, low levels of resistance have been induced under drug pressure, however this was not maintained once the drug was removed (Peters and Robinson, 1999).

1.6.4 Need for new antimalarial drugs

With the combined availability of antimalarial drugs and vector control programs, it was thought that malaria would soon be eradicated. Unfortunately, these hopes were dampened with the development of drug resistance and the subsequent resurgence of malaria. The phenomenon of drug resistance is an achievement that the malaria parasite has repeated for nearly every drug used against it. Since the control of malaria still relies heavily on chemotherapeutic agents, it is imperative to generate new antimalarial compounds to meet the challenge of resistance when it arises. One approach to antimalarial drug discovery is the investigation of medicinal plants and natural products.

1.7 Traditional Medicines: A Global Perspective

Traditional medicine refers to remedies that have been handed down from generation to generation to restore health or well-being. These are generally indigenous to countries or communities and often constitute an unwritten body of beliefs or customs. Over the past few decades, a renewed interest in traditional medicines, particularly in the Western world, has made some traditional therapies more accessible and increased public awareness of alternative systems of medicine. This has resulted in an increasing number

of traditional medicines being used outside of the communities they originated from, as individuals seek alternative or complementary remedies to conventional medicine. Many diverse therapies fall into this group, including herbal medicine from different cultures, Oriental therapies, Ayuverdic medicine, acupuncture, homeopathy and aromatherapy. Although traditional medicines are varied and have different perceptions of what constitutes health and disease, they all aim to restore mental and physical well-being to their patients.

While modern medicine is well established in most parts of the world, the WHO estimates that 80% of the world's population still relies solely on traditional medicine for their physical and psychological health needs. In view of the widespread usage of traditional systems of medicine, the WHO has developed a policy to reassess traditional medicines as a potential health care resource. This involves the evaluation, registration, regulation and inclusion of proven traditional medicines into national health care systems (WHO, 1998).

1.7.1 Traditional medicine in South Africa

Long before allopathic remedies were available in South Africa, traditional medicine provided an informal health care system for the population, and continues to be an important resource for the delivery of health care. There are an estimated 200 000 indigenous traditional healers practising in South Africa, which is eight times as many healers as doctors of modern medicine (Kale, 1995). Traditional healers have thrived in the face of competition from modern medicine and approximately 60% of the South African population consult them, usually in addition to seeking conventional treatment (van Wyk *et al.*, 1997 and Kale, 1995). The large patronage of traditional healers in South Africa is thought to be due to the strong cultural belief system and modern medical facilities often being unavailable or too expensive (Edwards, 1986). Within the framework of the African culture, an illness is often perceived as a supernatural phenomenon involving ancestral spirits, social relations or the environment (Cocks and Møller, 2002). A traditional healer can relate to the patient's culture, beliefs and concept of illness and treats them accordingly. Furthermore, traditional healers are highly respected in the communities and are often opinion leaders (Kale, 1995).

Due to the rich cultural diversity of the South African population, a traditional healer is the general term used to describe a practioner of indigenous medicine. Within the Zulu, Xhosa

and Sotho communities, a traditional healer can be classified into three main groups. Firstly, an *inyanga* (Zulu), *ixwele* (Xhosa) or *nqaka* (Sotho) refer to herbalists who are predominately male and have an extensive knowledge about medicinal herbs and plant-derived medicines. The second group includes the *isangoma* (Zulu), *amagquira* (Xhosa) and *dingaka* (Sotho), who are diviners and incorporate ancestral spirits and supernatural forces into healing rituals. The last group, the *umthandazi* (Zulu), are faith healers of a Christian denomination and heal through religious intervention and prayer (Edwards, 1986). In addition to these three types of healers, there are also traditional healers within the Khoi-San people of the Kalahari and amongst the descendants of the Dutch settlers who brought their folk remedies to South Africa. Although traditional medicines practised in South Africa have different origins, there is a large degree of overlap as remedies have been adopted from other cultures and incorporated into the array of indigenous medicines (Cocks and Møller, 2002). Some of these traditional medicines are documented, while a large portion of this knowledge remains unwritten and has been carried orally from one generation to the next through traditional healers.

Traditional medicines represent a wealth of information and the South African government recognises traditional healers as an important resource for primary health care. In accordance with the WHO's traditional medicine policy, the government aims to integrate traditional medicine into the national health care system by collaborating with traditional healers and evaluating the rational use of indigenous medicines (Edinburg, 1998). Although this is an ongoing process, the main objectives include registration of qualified traditional healers, co-operation between modern and traditional practioners, promotion of research for the evaluation of traditional medicines, registration of proven traditional medicines and the introduction of quality assurance systems (Edinburg, 1998 and Baleta, 1998). Hopefully, this approach will extend primary healthcare coverage to the many varied people and communities as well as preserve indigenous systems of medicine. Within a country, herbal medicines vary enormously from one community to the other, in both the choice of plants and the preparation.

1.7.2 Use of plants in traditional medicines

Higher plants were once the primary source of medicines in the world, and continue to form the basis of traditional medicine systems. The WHO estimates that the majority of

the world's inhabitants rely almost entirely on plant-derived medicines, with some 20 000 species of higher plants being used medicinally (Phillipson, 1994).

A number of countries have extensive texts describing their herbal lore, often dating back thousands of years. The first records of the use of medicinal plants were written on clay in Mesopotamia and date from about 2600 BC. Among the plants listed were *Papaver somniferum* (poppy juice), *Commiphora* species (myrrh), *Glycyrrhiza glabra* (liquorice), *Cupressus sempevrens* (cypress) and *Cedrus* species (cedar), all of which are still used today as treatment for a range of ailments (Cragg and Newman, 2001). There is also evidence that herbs were used extensively by ancient Egyptian, Chinese, Indian and Greek civilisations. Early herbal expertises were often developed through acute observations coupled to trial and error (Chevallier, 1996). This observed plant lore was handed down from generation to generation and varies between countries in keeping with their social and cultural heritage.

1.7.2.1 Medicinal plants used in South Africa

Medicinal plants are used widely in South Africa and are an important part of indigenous knowledge. In terms of species richness, the country is considered to have one of the most diverse temperate flora in the world. With more than 30 000 species of higher plants, South Africa has an unequalled botanical diversity (van Wyk *et al.*, 1997). It is estimated that 3000 of these species are utilised for medicinal purposes and that one tenth of them are used commonly and traded as medicines (van Wyk *et al.*, 1997). The volumes of plants sold in the informal and commercial sectors of the economy are considerable. In 1998, it was estimated that some 20 000 tonnes of over 700 medicinal plant species are traded in South Africa annually, with a market value of about $60 million (Mander, 1998). Unsustainable harvesting activities of popular medicinal plants have led to conservation measures being implemented and certain plants being cultivated to reduce the pressure on wild populations (van Wyk *et al.*, 1997). In addition to the local demand for medicinal plants, a few South African plants have become popular worldwide. These include *Harpagophytum procumbens* (Devil's claw), *Aloe ferox* (Cape aloes), *Agathosma betulina* (buchu), *Hypoxis hemerocallidea* (Africa potato) and *Aspalathus linearis* (rooibos tea), (George *et al.*, 2001).

Although South Africa contains about 10% of the earth's plant diversity, relatively little work has been done on medicinal plants from this region (Eloff, 1998). South Africa's rich heritage of indigenous medicines coupled to its biodiversity is an extremely valuable resource. The importance of plants lies not only in their chemotherapeutic effect, but also in their role as a source of model compounds for drug development. In addition to plant constituents being used directly as therapeutic agents, they can be utilised as starting materials or templates for drug synthesis.

1.7.3 Plant-derived drugs

Crude plant extracts, or combinations of several medicinal plants, are frequently used in traditional medicines and contain numerous components that are thought to contribute to the overall curative effect. This differs fundamentally from allopathic medicine, which uses a single active ingredient to target a specific illness. In 1819, the isolation of the analgesic morphine from the opium poppy (*Papaver somniferum*) laid the foundation for the purification of pharmacologically active compounds from medicinal plants. Since then, a number of plant compounds have been used in, or have provided the models for modern medicine. Analysis of prescription drugs in the US and Canada showed that 25% of the drugs contained components either isolated or derived from plants (Farnsworth, 1984). Furthermore, 119 plant metabolites were used globally as drugs, and 74% of these were discovered as a result of phytochemical studies of plants used in traditional medicine (Farnsworth and Soejarto, 1991). Plants investigated for pharmacologically active compounds are usually selected on the basis of ethnomedical information, since there is a correlation between biological activity and the use of the plant in traditional medicine (Hostettman *et al.*, 1996). As opposed to random collection of plant material, this targeted collection is guided by the belief that plants that have acquired the status of a traditional herbal remedy have already undergone some form of screening and have a higher probability of yielding an active substance.

Well-known examples of plant-derived drugs include the analgesic morphine, isolated from the opium poppy *Papaver somniferum*; the antimalarial quinine, extracted from the bark of the *Cinchona* species; the anticancer agent vincristine, which is obtained from the Madagascar periwinkle *Catharanthus roseus*; atropine, the anticholinergic from *Atropa belladonna*; the antihypertensive reserpine, isolated from *Rauwolfia serpentina*; and salicylic acid, which was originally isolated from the bark of the *Salix* species and served

as a template for aspirin (De Smet, 1997). More recently the important anticancer drug taxol, originally isolated from the T*axus* species and the antimalarial artemisinin, extracted from *Artemisia annua,* have been developed from higher plants. In addition to purified plant-derived drugs, there has been a resurgence of interest in crude herbal remedies for self-medication in the Western world (George *et al.*, 2001). Popular herbal preparations include *Ginkgo biloba*, *Hypericum perforatum* (St John's wort), *Crataegus monogyna* (Hawthorn), *Aesculus hippocastanum* (Horse chestnut), *Piper methysticum* (Kava-kava), *Panax ginseng* (Ginseng), *Oenothera biennis* (Evening primrose) and *Echinacea* species, (De Smet, 1997). The isolation of an active component, or the use of the crude plant extract, with therapeutic properties is particularly relevant to diseases lacking effective chemotherapeutic agents.

1.7.3.1 Plant-derived antimalarial drugs

The majority of drugs active against malaria parasites originate from plants or are based upon plant-derived compounds. One of the first forms of treatment in the Western world for malaria was quinine, which was extracted from the bark of the *Cinchona* tree. Peruvian Indians in South America used to chew the bark of the *Cinchona* tree to treat fever like symptoms associated with malaria. Knowledge of this 'fever tree' spread to Spain and *Cinchona* bark was imported to Europe in the 17th century for antimalarial use. In 1820, the alkaloid quinine was isolated and identified by French chemists as the active ingredient of *Cinchona* bark. Quinine-like drugs came into widespread use in the 1930s and are still used extensively, even though resistance to this group of antimalarial drugs is common (Cowman, 1995). Another well-known plant-derived antimalarial is artemisinin. A search for novel antimalarials from Chinese traditional medicine resulted in the isolation of artemisinin (*qinghaosu*) from the leaves of *Artemisia annua* (*qing hao*). This plant was recommended for fevers in a medical handbook written in 341 AD, and has appeared in several Chinese materia medica texts as a treatment for febrile illness (Hien and White, 1993). Artemisinin was first isolated in 1972 and is now the starting material for several semi-synthetic derivatives with enhanced antimalarial activity (van Agtmael *et al.*, 1999). The artemisinin drugs are the most rapidly acting antimalarials and are being used increasingly in South-East Asia and Africa. Besides quinine and artemisinin, several other antimalarial compounds have been isolated from medicinal plants. Table 1.7.3.1. lists examples of plants used in traditional medicines to treat malaria and their active constituents.

Table 1.7.3.1. Examples of traditional herbal medicines with antimalarial activity

Plant	Traditional use	Active constituents	Remarks	References
Alstonia angustifolia	The bark is used throughout Malaysia as a treatment for malaria and dysentery	Echitamine and dimeric indole alkaloids- macrocarpamine, macralstonine and villastonine	Significant *in vitro* antimalarial activity against *P. falciparum* and comparatively low *in vitro* cytotoxicity	Phillipson, 1993
Artabotrys uncinatus	Used in Southern China as treatment for malaria	Yingzhaosu	A synthetic derivative of yingzhaosu, arteflene is undergoing Western development for the treatment of malaria	De Smit, 1997
Azadirachta indica	The neem tree has a strong reputation throughout Asia and India as folklore antimalarial	Terpenoids, mainly limonoids- nimbolide, nimbinin, gedunin and dihydrogedunin	Strong *in vitro* antimalarial activity against *P. falciparum* and relatively low *in vitro* cytotoxicity	Phillipson, 1995 De Smet, 1997 Dhar, 1998
Brucea javanica	Plants used in China, Thailand and other South-East Asian countries for treatment of malaria and amoebiasis	Series of quassinoids - bruceine and bruceantin	Active against *P. falciparum in vitro*, but show *in vitro* and *in vivo* cytotoxicity. Quassinoids are biosynthetically related to liminoids	Phillipson, 1993 De Smet, 1997 O'Neil, 1986
Cryptolepis sanguinolenta	The roots and leaves are used in Ghana and Guinea Bissau for treatment of malaria	Alkaloid - cryptolepine	Highly active against *P. falciparum in vitro*, but inactive in mouse *P.berghei* model	Phillipson, 1993 Paulo, 2000 Kirby, 1995a
Dichroa febrifuga	The roots have been used in China for centuries against malaria fevers and amoebiasis	Alkaloids - febrifugine and isofebrifugine	Higher *in vitro* potency than chloroquine and artemisinin. Clinical use suggests liver toxicity	Phillipson, 1991 Takaya, 1999 De Smit, 1997
Enantia chlorantha	The bark is used as a traditional antimalarial medicine in Nigeria	Protoberberine alkaloids palmatine, berberine, jatrorrhizine and columbamine	*In vitro* antimalarial activity against *P. falciparum* is comparable to quinine, but did not display *in vivo* activity in mouse model	Phillipson, 1993 De Smit, 1997
Triclisia patens *Triclisia dictyophylla* *Triclisia triandra*	Used in Sierra Leone to treat malaria Herbal antimalarial treatment in Ghana Used in Thailand as an antimalarial pant	Bisbenzylisoquinoline alkaloids - phaethine, pycnamine, tiliacorinine and tiliacorine	Phaethine showed good *in vitro* antimalarial activity, but lacked *in vivo* activity. None of the isolated alkaloids were cytotoxic *in vitro*	Phillipson, 1993 De Smet, 1997
Triphyophyluum peltatum	Commonly used in West African traditional medicine to treat fevers, malaria and other diseases	Naphthylisoquinoline alkaloids- dioncophylline and dioncopeltine	Highly active against *P. falciparum, in vitro*	Phillipson, 1995 François, 1994

A number of extracts from South African plants have been evaluated for *in vitro* antiplasmodial activity, but little is known about their active constituents (Prozesky *et al.*, 2001 and Matsabisa, 2001).

Research of medicinal plants with antimalarial activity has resulted in the isolation of several potential hits and in some instances has provided evidence supporting their use in traditional medicines. When investigating medicinal plants as a source of antimalarial drugs, two problems are commonly encountered; a) the crude extracts or compounds show *in vitro* antimalarial activity but are extremely toxic and b) those which are active *in vitro* fail to display *in vivo* activity. One of the difficulties when isolating antimalarial drugs is identifying compounds that have sufficient selectivity to kill the parasite without harming the host. Protozoa share many biochemical pathways with the human host and often antimalarial compounds destroy both parasites and mammalian cells at similar concentrations, limiting their use as a potential drug (Kirby, 1996). The lack of *in vivo* antimalarial activity is subject to the pharmacodynamic and pharmacokinetic properties of the extract or compound. This would include absorption, distribution to the site of action and whether the compound is metabolised too quickly or to a less active form (Kirby, 1996). Furthermore, *P. berghei* in the mouse model is not ideal and an alternative animal model might be required to demonstrate *in vivo* activity. Although many possibilities exist, in terms of potential antimalarial drugs, only a limited number achieve drug candidate status and even fewer are ultimately registered as drugs. In order to achieve a higher hit rate, it is necessary to generate a larger choice of plant-derived antimalarials and obtain scientific information about their mechanism of action.

1.8 Drug Discovery and Development

In the drug discovery process, an initial hit compound is identified in the primary screens by giving a positive result in a bioassay. A hit can be defined as a prototype compound that has a desired pharmacological activity, and often requires chemical modification to improve its medical properties. The hit is optimised by analogue synthesis and developed into promising lead compounds, which are further modified to generate pre-clinical candidates. The candidate compounds then enter the developmental process and ultimately clinical trials. The criteria used to establish whether a compound is a hit, lead or pre-clinical candidate are listed in Table 1.8.

Table 1.8. Criteria for determining if a compound is a hit, lead or pre-clinical candidate

	Hit	Lead	Pre-clinical candidate
In vitro activity	✓	✓	✓
In vivo activity		✓	✓
Structure-activity relationship trends		✓	✓
Known mechanism of action		✓	✓
Pharmacokinetic profile		✓	✓
Acceptable estimated daily dose			✓
Selectivity: related systems		✓	✓
Selectivity: wide range systems			✓
Acceptable Cyp450 profile			✓
Physical properties: Mwt, logP		✓	✓
Solubility			✓
Chemically tractable		✓	✓
Synthetic routes		✓	✓
Clean in early toxicity (e.g. 7 day rat)			✓

1.8.1 Drug discovery

Drug discovery involves finding novel biologically active hits that give positive results in the initial screening process. Bioassays relevant to the therapeutic targets are essential in the screening stage and provide important information to monitor the activity of the hits. In general the bioassays are *in vitro* tests against isolated sub-cellular systems, lower organisms or culture cells, which are usually quicker and less expensive than *in vivo* methods. Once a suitable bioassay has been identified, different types of chemical compounds can be screened for activity. Broadly speaking, four different approaches are used to discover new hit compounds. These are: empirical screening methods, rational drug design, drug metabolism studies and clinical observations. The empirical approach relies on screening large numbers of diverse drug-like compounds. The source of compounds could be synthetic chemical libraries, historical compound collections, combinatorial libraries or natural product libraries including plant, marine and microbial compounds (Harvey, 1999). With the empirical process, there is no attempt to design an active compound and the large number and variety of structures that the libraries offer increase the probability of getting a hit (Terret *et al.*, 1995). The other major source of hits is the rational approach. This method is based on identifying a biological target and

designing a compound to interact with that particular target (Silverman, 1992). Rational drug design often makes use of computer-aided techniques and requires a molecular understanding of biological processes. The third source of hit compounds is drug metabolism studies, whereby drug metabolites are isolated and screened for activity to determine if the metabolite or the drug is responsible for the activity. Clinical observations of drug side effects have also led to drug discovery. During clinical trials a drug may display an additional activity, which could be an effective treatment for a different condition (Silverman, 1992). Each of these approaches to hit discovery has its benefits and disadvantages and the selection depends on the aim of the research and the available resources. In the course of this study higher plants will be focused on for hit discovery.

Historically, many clinically successful drugs have been derived from higher plants, but there has been a decline in natural product research with the increasing use of molecular and combinatorial approaches to drug discovery (Harvey, 1999). Nevertheless, higher plants continue to provide active substances and remain a valuable source of novel template compounds. One of the main attractions of working with plants is the structural diversity provided by natural compounds. The chemical diversity and stereospecificity of complex natural products is greater than provided by most synthetic chemistry approaches. In addition to the wide range of structural types, many plant-derived compounds are relatively small and have drug-like properties. Furthermore, plant constituents often occur as a group of structurally related metabolites, making it possible to isolate analogues of the active compound and obtain structure-activity information (Harvey, 1999). Since only a fraction of the estimated 250 000 species of higher plants have been investigated for pharmacological activity, it is most likely that plants will continue to offer novel hits for lead and drug development.

1.8.2 Drug development: lead modification

In this phase, a hit that has attracted attention in the primary screening is modified so that its desired pharmacological activity is enhanced and its undesirable properties are minimised. Prior to modification, the parts of the compound responsible for the biological activity are usually identified and are collectively known as the pharmacophore (Silverman, 1992). Once the essential structural elements of the compound have been established, functional group modification can be used to optimise the activity. This

involves the synthesis of analogues to determine the relationship between molecular structure and activity. For lead modification, both combinatorial and normal chemical techniques can be employed. The traditional approach involves the synthesis of a single target molecule with a defined structure. Selected structures are generated one after another and are submitted for pharmacological assays. This procedure is repeated for individual compounds until optimal lead activity is achieved. Combinatorial chemistry uses a combinatorial process to prepare classes of compounds from sets of building blocks, and covers a range of techniques and reactions that are conventionally performed on solid supports. The key feature of combinatorial chemistry is that a large number of diverse compounds are synthesised simultaneously in a time and resource-effective manner (Terret *et al.*, 1995). A library of compounds is tested for activity and the most active representatives are selected. The combinatorial selection process differs from the traditional optimisation cycles in that the active compounds are chosen from a family of synthesised molecules rather than through sequential modification steps (Wess *et al.*, 2001). In modern drug discovery, combinatorial chemistry impacts at the hit generation and lead optimisation stages.

In addition to potency and selectivity other factors are also taken into account during lead optimisation, namely absorption, distribution, metabolism, excretion and toxicity (ADMET), (Wess *et al.,* 2001). The pharmacological properties of a compound are a function of its physiochemical profile and can be estimated using the 'rule of 5' (Lipinski *et al.*, 1997). These rules define drug-like properties and are used as guidelines to predict the solubility and permeability of compounds in the discovery and developmental setting. The 'rule of 5' states that poor absorption and permeation are more likely when: the molecular weight is over 500, there are more than 5 H-bond donors, the LogP (where P is a measurement of lipophilicity) is over 5 and there are more than 10 H-bond acceptors (Lipinski *et al.*, 1997). The set of rules do not apply to compounds that are substrates for biological transporters. Although there are exceptions, the rules are commonly used to estimate the absorption of an active substance and to guide lead optimisation (Wess *et al.,* 2001). In the drug development process, a lead compound is modified until its profile of properties fulfils the defined criteria for a pre-clinical candidate (see Table 1.8.). At this stage the drug candidate will enter pre-clinical and clinical safety and efficacy studies and if these are successful a marketable drug will be produced, manufactured and registered.

1.9 Scope of Study

It is the intention of this study to combine ethnopharmacological and traditional medicinal chemistry approaches to generate potential lead compounds for antimalarial drugs.

This study aims to:

1. Investigate the *in vitro* antiplasmodial activity of a South African medicinal plant, *Harpagophytum procumbens*
2. Identify, isolate and characterise hit compounds with *in vitro* antiplasmodial activity
3. Develop the hits into promising leads using traditional medicinal chemistry approaches and the active plant-derived compound as a central scaffold

Chapter 2

Harpagophytum procumbens

2.1 *Harpagophytum procumbens* (Burch.) DC. ex Meissn. subsp. *procumbens*

Harpagophytum belongs to the botanical family *Pedaliaceae* and two species occur in Southern Africa, *H. procumbens* and *H. zeyheri*. Both are used for medicinal purposes and are thought to have similar chemical compositions (van Wyk *et al.*, 1997). *H. procumbens* is commonly known as Devil's Claw, *sengaparile* (Tswana) and *duiwelsklou* (Afrikaans). This name is derived from the translation of the German name *teufelskralle* (Devil's Claw) given by the Namibian farmers to the plant (Iwu, 1993). The *Harpago* in the genus name translates to hook, based on the appearance of its barbed fruit.

2.2 Distribution and Botanical Description

H. procumbens is found in the northwestern parts of Southern Africa and thrives in dry sandy or clay soils. Natural habitats include the Kalahari dessert and savanna in Namibia and adjacent parts of South Africa, Angola, Botswana and Zimbabwe.

H. procumbens is a weedy perennial plant with an extensive tuberous root system. To survive dry periods the plant forms water-storing secondary root tubers that branch off horizontally from a central tap root (Wegener, 2000). The tubers are longitudinally striated and can vary considerably in size and shape. At the beginning of the rainy season, the succulent tap roots produce flat lying creeping stems that can grow up to 1.5m in length (Iwu, 1993). Their leaves are usually irregularly divided into several lobes and are a greyish-green (van Wyk *et al.*, 1997). Although the young shoot and leaf may be browsed on in time of necessity, it is not recommended since the stem is tough and may form an entangled mass in the stomach (Watt and Breyer-Brandwijk, 1962) Towards the end of spring the plant produces tubular flowers that are usually dark violet with a yellow center. A characteristic feature of *H. procumbens* is the claw-like fruit with rows of curved arms bearing sharp hooked thorns. The length of the arms of the fruit and the arrangement of the seeds differ between *H. procumbens* and *H. zeyheri* and can be used to distinguish between the two. The fruit may cling tenaciously to the fur or foot of an animal and is often dispersed in this way. Furthermore, the fruit can fatally wound an animal if it gets jammed in their hoof or in their mouth (Watt and Breyer-Brandwijk, 1962). Photographs of the different features of *H. procumbens* are displayed in Plate 2.

Plate 2. Photograph gallery of *Harpagophytum procumbens*

a) Harpagophytum procumbens

b) Characteristic fruit of *H. procumbens*

c) Secondary tubers of *H. procumbens*

d) *H. procumbens* under cultivation at Grassroots

e) Sliced and dried roots of *H. procumbens*

f) Examples of *H. procumbens* products

Photographs a,b,d,e and f reproduced with permission from van Wyk B.E, Medicinal Plants of South Africa and People's Plants. A Guide to Useful Plants of Southern Africa. Briza Publications, Pretoria. Photograph c was taken by the author

2.3 Harvesting and Cultivation

The thick fleshy secondary root tubers are the parts of the plant used medicinally. To harvest these, the soil is shoveled away usually by hand, from the primary tap root and the secondary roots that lead to the tubers. The secondary root tubers are then unearthed, collected, washed, sliced and dried (Plate 2c,e.). To ensure continuous harvesting, minimal damage is done to the primary tap root, which is covered with soil once harvesting is complete (Wegener, 2000). Traditionally *H. procumbens* was obtained solely from wild-harvested material, with approximately 500 tons being traded annually. Since, the international interest in the therapeutic potential of this plant is growing, there is a danger of over-exploitation of the wild resources (van Wyk and Gericke, 2000). Presently in South Africa, *H. procumbens* is obtained by wild collection as well as by harvesting cultivated plant material. Over the past few years, a number of private ventures based in South Africa and Namibia have successfully propagated *H. procumbens* on a commercial scale. In 1996, the Grassroots Natural Products Group started growing *H. procumbens* in the Western Cape to provide a sustainable supply of raw material and reduce the pressure on wild plants (Plate 2d.). *H. procumbens* does not grow naturally in the Western Cape and primary roots of the plants were sourced from the Northern Cape, propagated and successfully cultivated under intensive farming conditions. Specific chemical constituents of the secondary root tubers are monitored using high pressure liquid chromatography (HPLC) to evaluate the quality of the raw material. The plant is traded worldwide, but the majority of the raw material produced is exported to European countries where there is an increasing demand for Devil's Claw. The cultivation of *H. procumbens* has great commercial potential and the Agricultural Research Council of South Africa is exploring the possibility of transferring propagation technologies to small local farmers in the interest of rural development (van Wyk and Gericke, 2000).

2.4 Phytochemistry

The secondary root tubers of *H. procumbens* contain a complex mixture of chemical constituents. The roots are rich in sugars (50%), consisting mainly of the tetrasaccharide stachyose and smaller amounts of raffinose, sucrose and monosaccharides (Bradley, 1992). They also contain iridoid glycosides (0.5 – 3%), such as harpagoside, harpagide and procumide (Figure 2.5.), (Litchi and von Wartburg, 1964 and Tunman and Stierstorfer, 1964)). Harpagoside was the first glycoside to be isolated from *H.*

procumbens in 1962 and is regarded by some as the main pharmacologically active constituent. The other glycosides harpagide and procumide were isolated several months later and are possibly degradation products of the main glycoside harpagoside (van Wyk *et al.*, 1997). Recent *in vitro* studies have shown that the main iridoid glycosides from *H. procumbens* are transformed into the pyridine monoterpene alkaloid acucubine B (Figure 2.4) by human intestinal bacteria (Baghdikian *et al.*, 1999).

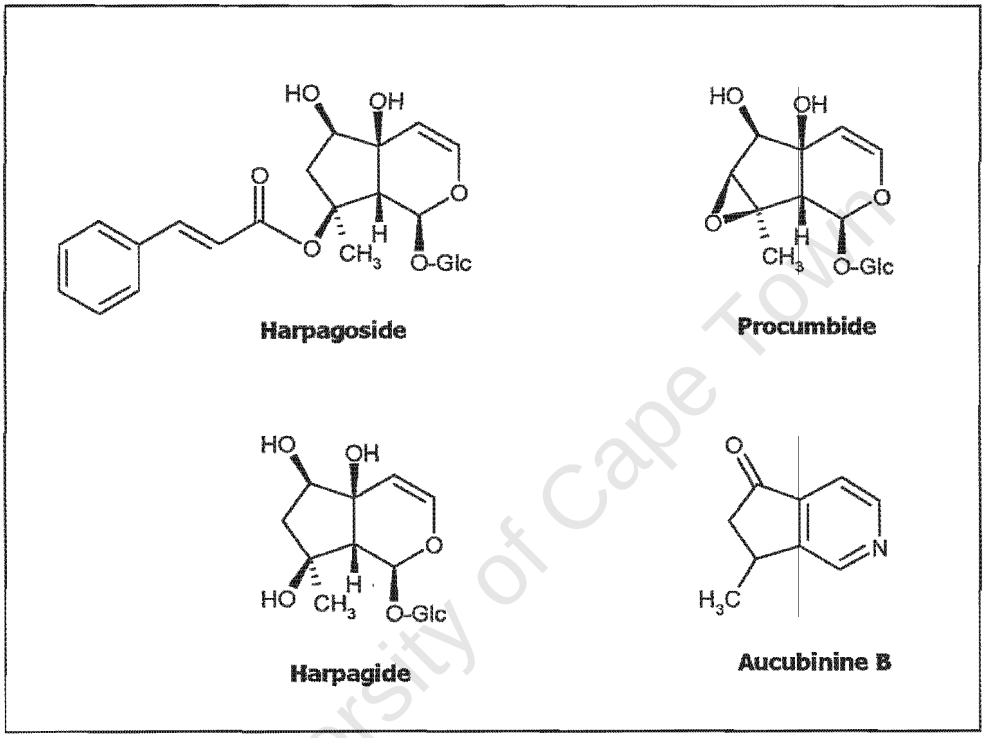

Figure 2.5. Structures of the main iridoid glycosides, harpagoside, harpagide and procumide from *H. procumbens* and the alkaloid acucubine B

Minor chemical constituents include; flavonoids, luteolin and kaempferol; phenolic acids, cinnamic acid, caffeic acid and chlorogenic acid; harpagoquinone; phytosterols, stigmasterol and ß-sitosterol; triterpenes, oleanolic, ursolic and 3ß-acetyloleanolic acid derivatives and esters (Bradley, 1992 and Iwu, 1993).

2.5 Traditional and Current Uses

Medicinal preparations of the secondary root tubers have been used in traditional medicine in Southern Africa for centuries. The plant is traditionally used for the relief of

fevers and other blood diseases and to treat digestive disorders, arthritic and rheumatic conditions (Watt and Breyer-Brandwijk, 1962 and van Wyk *et al.*, 1997). The roots are also used as a general analgesic and are applied in an ointment form to sores, ulcers and boils. Dried roots are administered during pregnancy and continued after labour for pain relief (Watt and Breyer-Brandwijk, 1962).

H. procumbens was introduced into Europe as a herbal tea in the 20th century. This occurred *via* a German soldier who studied the traditional medicine systems of the Namibian people (Wegener, 2000). The Western use of *H. procumbens* is generally in line with the traditional application, although attention has been focused on its anti-inflammatory and anti-rheumatic use. Decoctions, tinctures and tablet forms of the dried roots (Plate 2f.) are readily available in pharmacies and health food shops and are used to stimulate appetite, relieve indigestion and to treat a range of joint and muscular problems. These would include rheumatic and arthritic conditions, back pain, gout and fibrositis (Chevallier, 1996). The British Herbal Pharmacopoeia recognizes *H. procumbens* as possessing analgesic, sedative and diuretic properties. Furthermore, extracts and drugs of the secondary tubers are approved in monographs published by the German Commission E as well as by the European Scientific Cooperative on Phytotherapy (ESCOP), for the treatment of osteoarthritis and tendonitis (Wegener, 2000).

2.6 Pharmacological and Clinical Studies

2.6.1 Anti-inflammatory, analgesic and anti-rheumatic activity

Over the past 4-5 decades, many scientific studies have been conducted on animals and humans to assess the effectiveness of *H. procumbens* as an anti-inflammatory, anti-rheumatic and analgesic agent. The results of these studies have been conflicting.

The first pharmacological effects of *H. procumbens* were studied more than 40 years ago, using the formaldehyde-induced arthritis test in rats. Subcutaneous injections and oral ingestions of an infusion of *H. procumbens* significantly reduced the swelling of arthritic joints (Zorn, 1985). Subsequent studies have supported these observations in various animal experimental models (Eichler and Koch, 1970 and Erdoes *et al.*, 1978). More recent research evaluated the aqueous extract of *H. procumbens* and its main iridoid glycoside, harpagoside for anti-inflammatory and analgesic effects in mice and rats

(Lanhers *et al.*, 1992). Although the extract exerted significant dose-dependant activity, harpagoside did not appear to have anti-inflammatory properties and had little analgesic effect. These results suggest that the activity exhibited by *H. procumbens* is due to the interaction of various active principles present in the crude aqueous extract and not harpagoside alone. However, conflicting studies have indicated that *H. procumbens* lacks any anti-inflammatory and analgesic activity (Whitehouse *et al.*, 1983 and Grahame and Robinson, 1981).

Numerous clinical studies have assessed the efficacy of *H. procumbens* in patients with rheumatoid arthritis, osteoarthritis and lower back pain (Wegener, 2000). One of the largest studies involved 630 patients, suffering from various arthritic conditions, that were treated for 6 months with dried aqueous extract of *H. procumbens* (Bélaiche, 1982). An improvement of pain and other complaints was demonstrated. While several clinical studies have supported these findings, others have demonstrated that *H. procumbens* has little, if any anti-inflammatory, anti-rheumatic and analgesic activity (Wegener, 2000). As a result of these conflicting findings, a number of researchers have cited different methodological approaches and the lack of standardization of *H. procumbens* preparations to explain these discrepancies. In addition, studies have shown that *H. procumbens* is less active if administered orally, compared to intraperitoneally and intraduodenally, suggesting inactivation in the stomach (Soulimani *et al.*, 1994). Therefore, the route of administration of *H. procumbens* could also influence the outcome of the study. The mechanism of action of the observed anti-inflammatory, anti-rheumatic and analgesic activity of *H. procumbens* has not been elucidated.

2.6.2 Anti-oxidant activity

Recent studies have indicated that *H. procumbens* exerts significant *in vivo* anti-oxidant activity at the doses required to induce anti-inflammatory and analgesic effects (Bhattacharya, 1998). Since oxidative free radicals are known to be involved in inflammation, the anti-oxidant activity of *H. procumbens* could be responsible for the reported anti-inflammatory activity.

2.6.3 Digestive activity

Infusions of *H. procumbens* are commonly used as a dyspeptic aid, however there is no scientific evidence to support its efficacy. It is thought that the strong bitter-tasting preparations of the roots of *H. procumbens* stimulate gastric acid secretion and digestion (Chevallier, 1996). The roots have been reported to have 6000 or more bitterness equivalence to that of gentian root (Iwu, 1993).

Several other pharmacological effects of *H. procumbens* have been observed. The extracts have been shown to cause a reduction of arterial blood pressure in rats, to have a protective effect against arrhythmias induced by calcium chloride and epinephrine-chloroform in rats and rabbits (Circosta *et al.*, 1984) and to interfere with the mechanisms that regulate the influx of calcium into cells (Occhiuto *et al.*, 1985).

2.6.4 Pharmacokinetics

There is no absorption, distribution, metabolism and excretion data for whole *H. procumbens* extracts. A few studies have detected harpagoside in plasma, following oral administration of *H. procumbens* extracts to humans and pigs (Wegener, 2000). However, it is not known whether harpagoside is the metabolically active constituent of the extract.

2.6.5 Toxicology and contraindications

The toxicity of *H. procumbens* extracts observed in animal experiments is very low (Whitehouse *et al.*, 1983 and Erdoes *et al.*, 1978). Preparations of the dried roots appear to be well tolerated in the clinical studies conducted, with only a few mild gastrointestinal complaints (Wegener, 2000). Despite the long history of usage of *H. procumbens* there have been no reports of adverse side effects or of negative interactions with conventional drugs usually prescribed for rheumatic and arthrosic conditions (Wegener, 2000).

H. procumbens is reported to have oxytoxic properties and should not be taken during pregnancy (Iwu, 1993). Due to its stimulating effect on the digestive system, it should be avoided in patients suffering from stomach or duodenal ulcers (Chevallier, 1996).

2.7 Antimalarial Activity of *H. procumbens*

Infusions of *H. procumbens* are traditionally used for the relief of fevers and to treat blood diseases (Watt and Breyer-Branwijk, 1962). A fever is defined as a persistent or recurrent elevation of body temperature and is often associated with malaria, particularly in Africa. Some traditional healers classify all fevers together, whilst others distinguish between the various types and treat them accordingly (Iwu, 1993). Since preparations of *H. procumbens* are used to treat fevers, which probably encompass those associated with malaria, it is likely that the plant has been used traditionally for the treatment of malaria.

A scientist from Botswana initially provided the South African Traditional Medicines Research Unit (SATMRU) in the Department of Pharmacology at UCT, with a sample of *H. procumbens* roots to test for anti-inflammatory activity. The plant was later included in a suite of plants, which were screened for *in vitro* antiplasmodial activity by Dr Matsabisa (unpublished data, UCT). The results indicated that the dichloromethane extract of the *H. procumben's* roots had *in vitro* antiplasmodial activity against a chloroquine sensitive strain of *P. falciparum*. Although a few pharmacological effects of *H. procumbens* have been published pertaining to anti-inflammatory and anti-rheumatic activity, no antimalarial properties have been reported to date, to the best of my knowledge. Considering the long history of usage in Africa, the absence of side effects and these recent findings, *H. procumbens* warranted further investigation as an antimalarial agent.

Chapter 3

Antiplasmodial Activity of *H. procumbens* (batch I and II)

3. *In vitro* Antiplasmodial Activity of *H. procumbens* (batch I and II)

3.1 Introduction

Initial screens aimed at identifying active plants for further research, showed that the dichloromethane extract of the roots of *H. procumbens* had significant *in vitro* antiplasmodial activity. This sample of *H. procumbens* roots (20g) originated from Botswana and little is known about its growing conditions or time of harvest. To study the antiplasmodial activity of *H. procumbens*, additional plant material was required and sourced from a Health Shop in Cape Town (The Sunflower Health Shop, Long Market Street). The dried, cut root sections were obtained from wild harvested material that was collected towards the end of the rainy season (early autumn) in the Namibian region. This chapter assesses the *in vitro* antiplasmodial activity of *H. procumbens* dried root extracts. It investigates the active components in the roots and characterises their *in vitro* antiplasmodial activity and cytotoxicity. In the course of this chapter, two separate batches (I and II) of *H. procumbens* roots are examined.

3.2 Results

3.2.1 *In vitro* antiplasmodial activity of the *H. procumbens* extracts

Both hot and cold water (H_2O), methanol (MeOH) and petroleum ether (PE) extractions were performed on the dried root sections of *H. procumbens* (batch I), (Table 3.2.1).

Table 3.2.1. Yield of the extracts obtained from dried *H. procumbens* roots (batch I)

Extract	% Yield
H_2O	25.04
MeOH	14.08
PE	0.26

The concentrated *H. procumbens* extracts were tested *in vitro* against a CQ-sensitive strain of *P. falciparum* (D10), (Figure 3.2.1). The parasites were maintained in continuous culture using a modified version of the Trager and Jensen (1976) method and parasite lactate dehydrogenase activity was used as a measure of parasite viability (Makler *et al.*,

1993). The D10 strain was found to be CQ-sensitive with a 50% inhibitory concentration (IC_{50}) value of 7.81± 0.69ngml^{-1} (n=3). For both the H_2O and MeOH extracts, the IC_{50} values were not determinable (ND), since the parasite viability exceeded 50% even at the highest concentrations (100μgml^{-1}) of the extracts. For the crude *H. procumbens* extracts tested, antiplasmodial activity was only observed for the PE extract, which had an IC_{50} value of 13.57±1.63μgml^{-1} (n=5). This result corresponds to the IC_{50} value of 13μgml^{-1}, obtained for the dichloromethane extract of the *H. procumbens* sample from Botswana, (experiment performed by Dr Matsabisa).

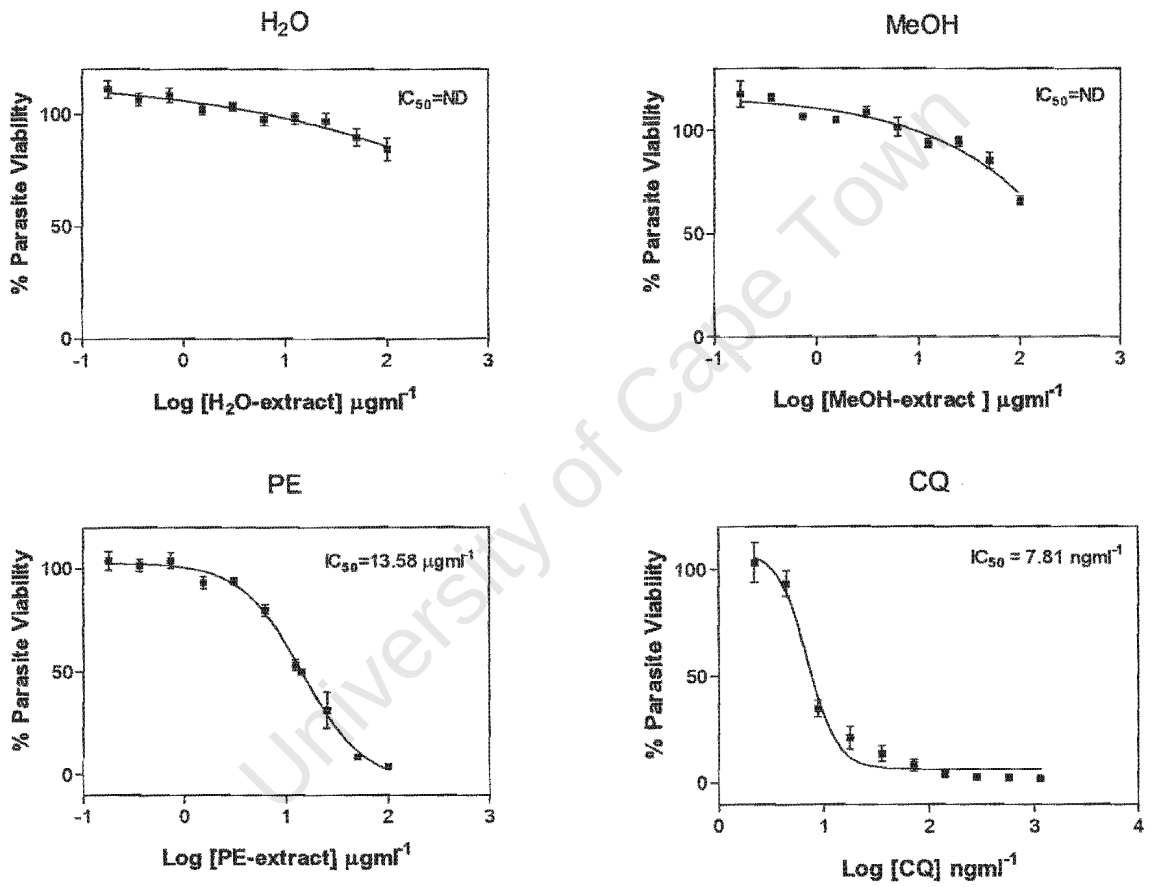

Figure 3.2.1. Dose response curves of chloroquine and the water, methanol and petroleum ether extracts of *H. procumbens* on *P. falciparum* strain D10. Each point represents the mean of 3 independent experiments performed in duplicate

In the cold MeOH extract, a significant amount of a white crystalline substance precipitated out of solution, and was filtered off and tested for antiplasmodial activity against D10. The crystals did not possess any antiplasmodial activity (data not shown) and had no apparent effect on parasite viability. Since the roots of *H. procumbens* are rich

in sugars, the phenol-sulfuric acid reaction (Rao and Pattabiraman, 1989) for the detection of sugars was performed on the crystals and gave a strong positive result.

3.2.2 Bioassay-guided fractionation of the *H. procumbens* PE extract

Bioassay-guided fractionation techniques were used to isolate the active principles from the PE extract. The selection, testing and isolating procedure was based on antiplasmodial activity, rather than chemical considerations.

3.2.2.1 *In vitro* antiplasmodial activity of the flash chromatography fractions of the PE extract of *H. procumbens*

The crude PE extract of *H. procumbens* was fractionated using flash chromatography (silica gel eluted with a step gradient of increasing polarity, PE – EtOAc - MeOH) to yield a total of 11 pooled fractions (A-K). Details of the eluting solvent system, TLC profiles and yields for each fraction are given in Chapter 7 (Section 7.3.1). All of the fractions were subjected to antiplasmodial tests against *P. falciparum* D10 (Figure 3.2.2.1a).

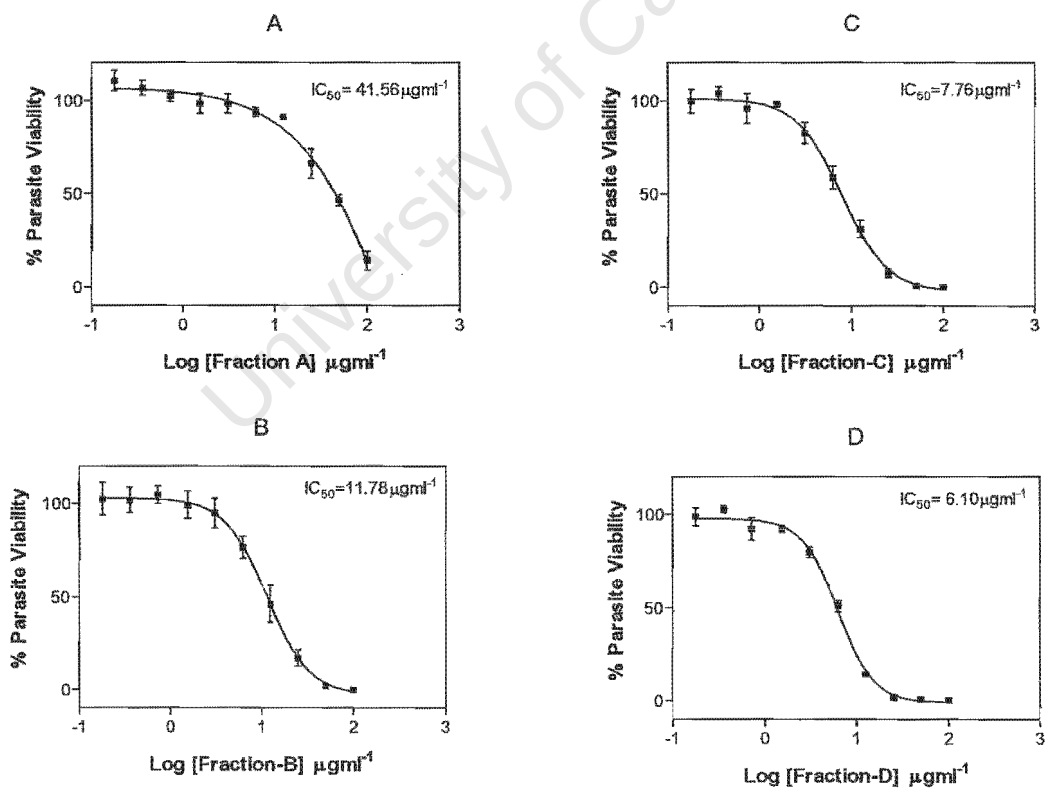

Figure 3.2.2.1a. Dose response curves of the fractions (A-D) generated by flash chromatography on the PE extract of *H. procumbens*. Each point represents the mean of 2 independent experiments each in duplicate

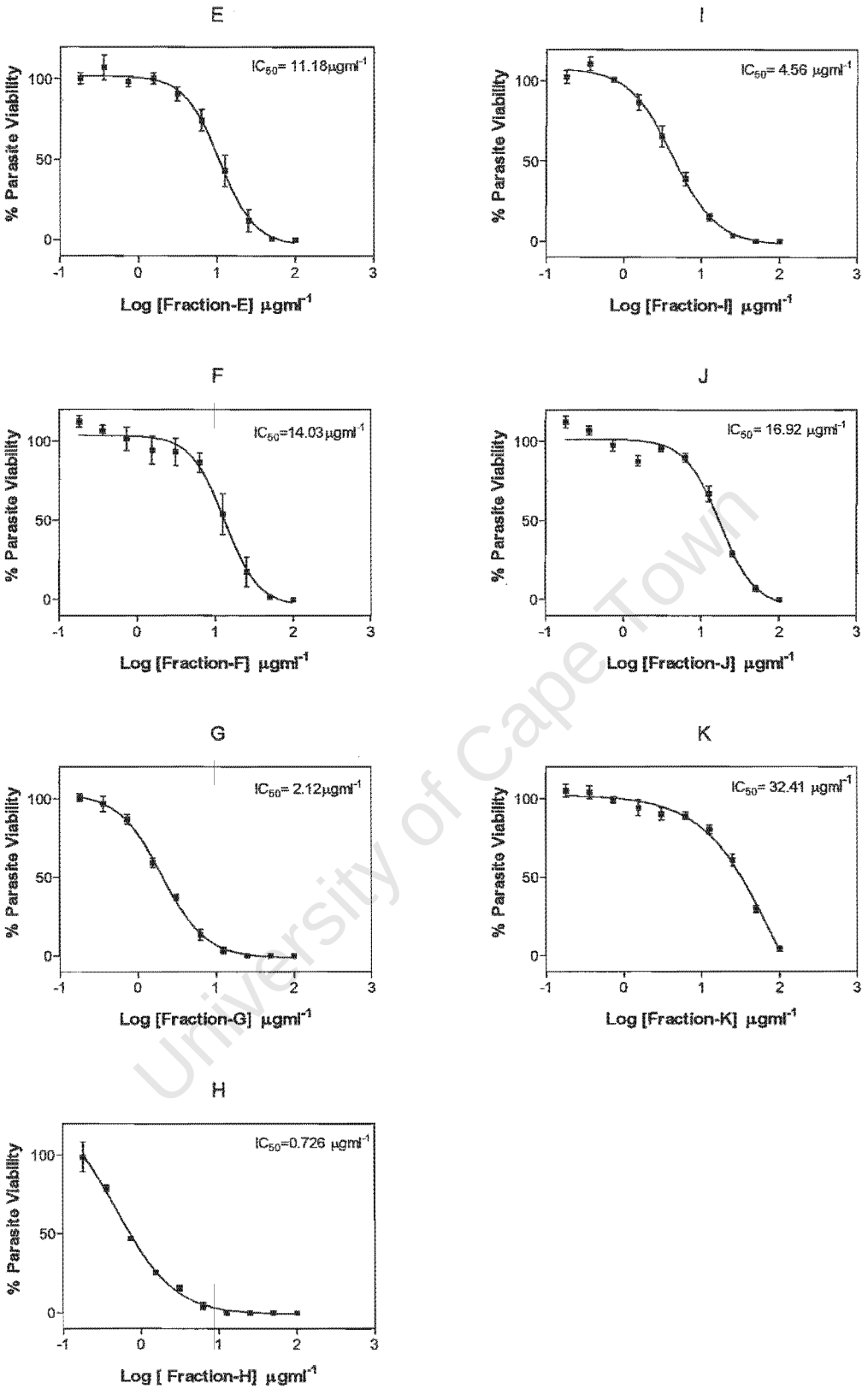

Figure 3.2.2.1a. (Continued) Dose response curves of the fractions (E-K) generated by flash chromatography on the PE extract of *H. procumbens*. Each point represents the mean of 2 independent experiments each performed in duplicate

The mean (n=2) IC_{50} values for the fractions (A-K) are summarised in Figure 3.2.2.1b. Among the 11 fractions tested, the strongest antiplasmodial activity was observed for fractions G and H, which were purified further by HPLC. The yields of fractions G and H were approximately 1.5% by weight of the crude PE extract of *H. procumbens*.

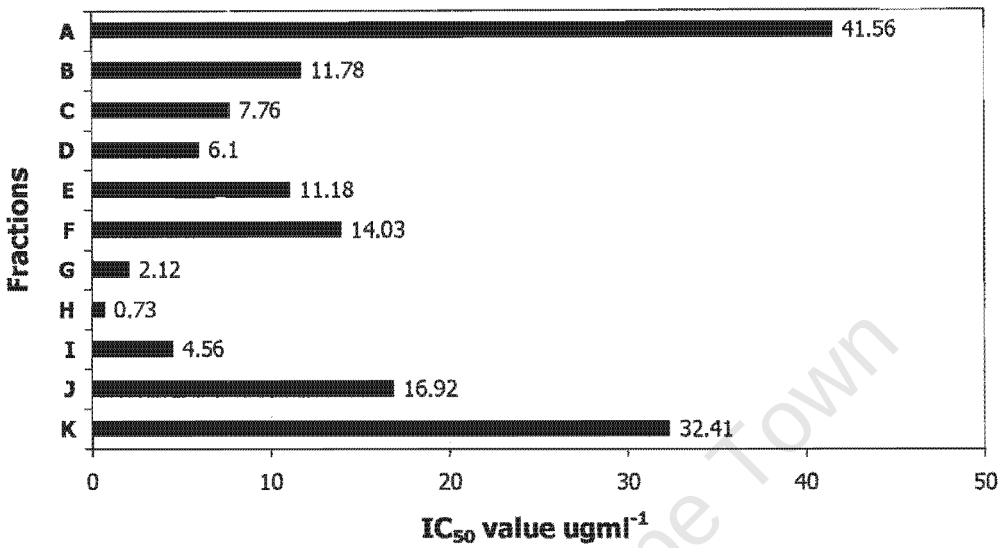

Figure 3.2.2.1b. Summary of the IC_{50} values of the fractions (A-K) generated by flash chromatography. These values represent the mean IC_{50} value of 2 independent experiments each performed in duplicate

3.2.2.2 Purification of the most active FC fractions by high-pressure liquid chromatography (HPLC)

Fractions G and H (combined mass of 60mg), had very similar HPLC profiles and were both used for the isolation of the active principle. Using a semi-preparative HPLC column (Details in Chapter 7, 7.5), fraction H was subdivided into fractions (H1-H5) (Figure 3.2.2.2.), which were collected, concentrated and tested for antiplasmodial activity using *P. falciparum* D10.

Although a quantitative analysis was impracticable due to the low yields of the collected fractions, a qualitative comparison of activity was achieved. Fraction H5 showed the greatest antiplasmodial activity, followed by fraction H4. In order to isolate individual components, H5 was subdivided further by collecting fractions at narrower time intervals within this section (fractions a,b,c Figure 3.2.2.2.). A qualitative comparison of the activity of these H5 fractions was carried out, and the most active peak **H5a**, R_t=36.72 mins was identified.

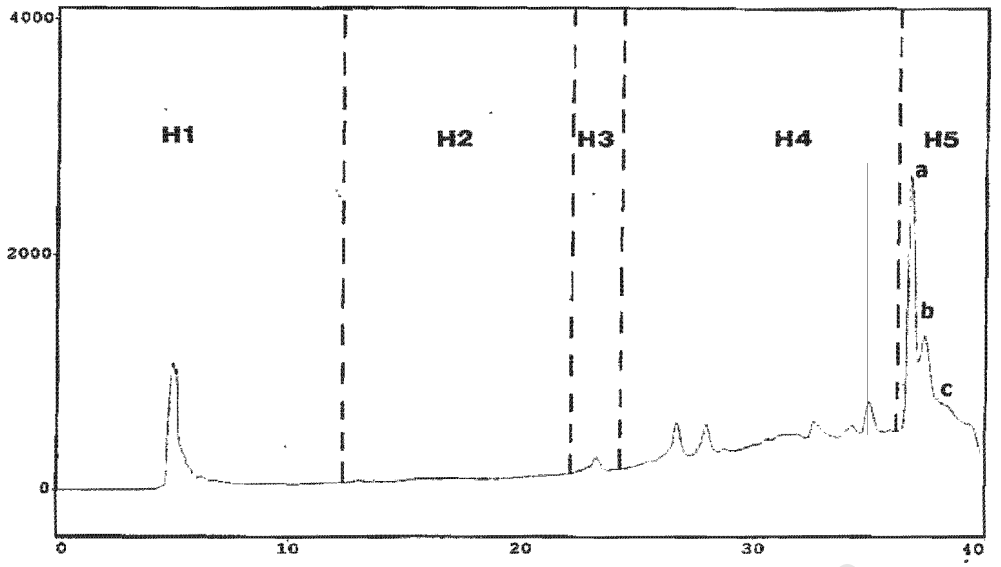

Figure 3.2.2.2. HPLC chromatogram of fraction H. The demarcated regions represent the collected fractions (H1-H5)

After several repeat injections of fractions H and G, a measurable amount of the component **H5a** was collected, concentrated and tested for *in vitro* antiplasmodial activity and cytotoxicity. A small aliquot of the concentrated **H5a** fraction was run on the HPLC to determine its purity, and was found to be in excess of 85% pure and consisted of one major peak with minor impurities (Appendix 2, A2.1). Furthermore, the UV absorbance (Appendix 2, A2.1) across the main peak was uniform, suggesting a single compound was present. The flash chromatography fractions C and D, which showed moderate activity, were also run on HPLC to monitor their purity. Both of these fractions were extremely waxy and contained numerous compounds.

3.2.3. *In vitro* antiplasmodial activity and cytotoxicity of H5a

The IC_{50} value of the active component **H5a** was determined in a CQ-sensitive (D10) and CQ-resistant (K1) strain of *P. falciparum* (Figure 3.2.3.1.). *P. falciparum* K1 was confirmed to be CQ-resistant with a CQ IC_{50} value of 111.69±50.04ngml^{-1} (n=3). Experiments with **H5a** resulted in a dose-dependant inhibition of parasite growth with an IC_{50} value of 0.53±0.120μgml^{-1} (n=3) in D10 and 0.33±0.08μgml^{-1} (n=3) in K1. Using the Mann Whitney two-tailed test, it was established that there was a significant difference (P=0.008) in the activity of **H5a** against D10 and K1, with K1 being slightly more sensitive to H5a.

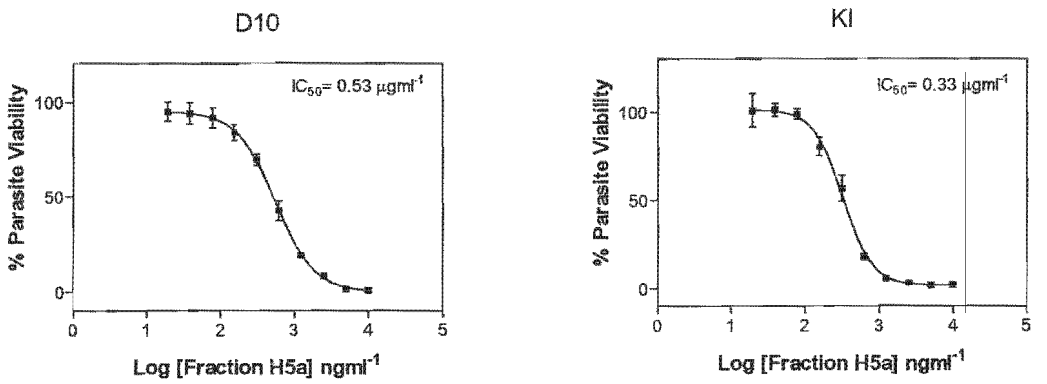

Figure 3.2.3.1. Dose response curves for **H5a** on D10 and K1 strains of *P. falciparum*. Each point represents the mean of 3 independent experiments each performed in duplicate

To determine the selectivity index (ratio of cytotoxicity to antiplasmodial activity), fraction H and **H5a** were evaluated for *in vitro* cytotoxicity against a Rat fibroblast cell line (Rat-1-cells), (Figure 3.2.3.2.). The Rat-1-cells were maintained in culture and cell viability was measured using a modified version of the MTT assay (Mosmann, 1983). For the cytotoxicity assays daunomycin was used as a positive control.

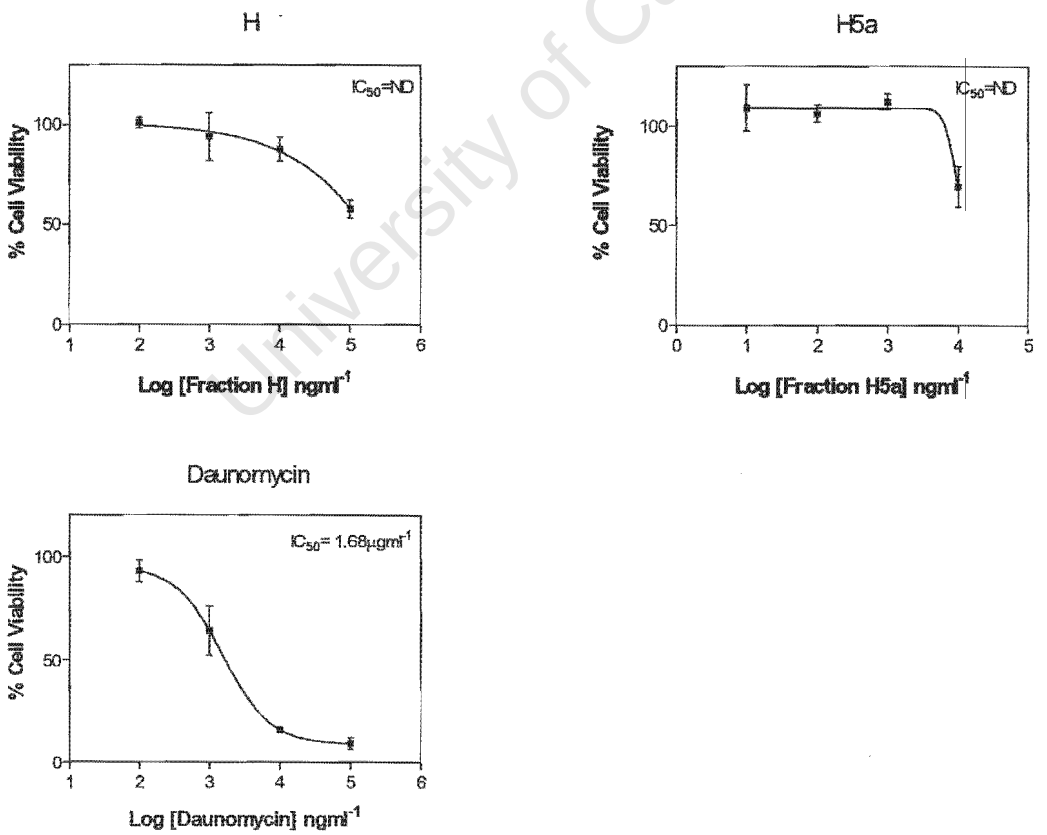

Figure 3.2.3.2. Dose response curves for daunomycin, fraction H and **H5a** on Rat-1-cells. Each point represents the mean of 2 independent experiments each performed in quadruplicate

The Rat-1-cells were sensitive to daunomycin, with an IC_{50} value of 1.68μgml^{-1} (n=2). For both fraction H and H5a, the IC_{50} values on Rat-1-cells could not be determined as the cell viability exceeded 50%, even at the highest concentrations of the compounds. As a result of this, the selectivity index could not be calculated.

3.2.4 UV spectrum, mass spectrometry (MS), nuclear magnetic spectroscopy (NMR) of H5a

The UV spectrum of **H5a** (Appendix 2, A2.1) displayed absorption maxima at 200, 224 and 270nm. Although **H5a** was not a single compound, it was sufficiently pure for mass spectrometry analysis (Appendix 2, A2.1). The HREIMS of the active compound showed a molecular ion peak at *m/z* 316.2038, which corresponded to a molecular formula of $C_{20}H_{28}O_3$. Unfortunately, the NMR sample could not be run as an insufficient amount of **H5a** remained.

In an attempt to obtain a larger quantity of the active principle **H5a** for full structure elucidation, an additional 3kgs of dried root sections (batch II) were obtained from the same supplier (The Sunflower Health Shop).

3.2.5 *In vitro* antiplasmodial activity of *H .procumbens* (batch II)

Since the PE extract of the previous batch of *H. procumbens* showed antiplasmodial activity, only the PE extraction was performed on the second batch. The PE extract of the *H. procumbens* roots (batch II) had an IC_{50} value of 25μgml^{-1} against *P. falciparum* D10.

3.2.6 Bioassay-guided fractionation of the *H. procumbens* (batch II) PE extract

3.2.6.1 Antiplasmodial activity of the flash chromatography fractions from the PE extract of *H. procumbens* (batch II)

The PE extract of *H. procumbens* (batch II) was fractionated using flash chromatography. Details of the eluting solvent systems and the TLC profiles of the fractions are given in Chapter 7 (Section 7.3.2). A total of 24 fractions $(A\text{-}X)_{II}$ were produced and tested for *in vitro* antiplasmodial activity against *P. falciparum* D10. The dose response curves for the

fractions A-X are in Appendix 1 (Figure 3.2.6.1), and the corresponding IC_{50} values are summarised in Figure 3.2.6.1.

Fractions V_{II} and W_{II} showed the greatest antiplasmodial activity, but only yielded a few milligrams. Fractions E_{II}, F_{II}, G_{II} and I_{II} had similar IC_{50} values in the range of 9-12μgml^{-1}, and were focused on for further purification.

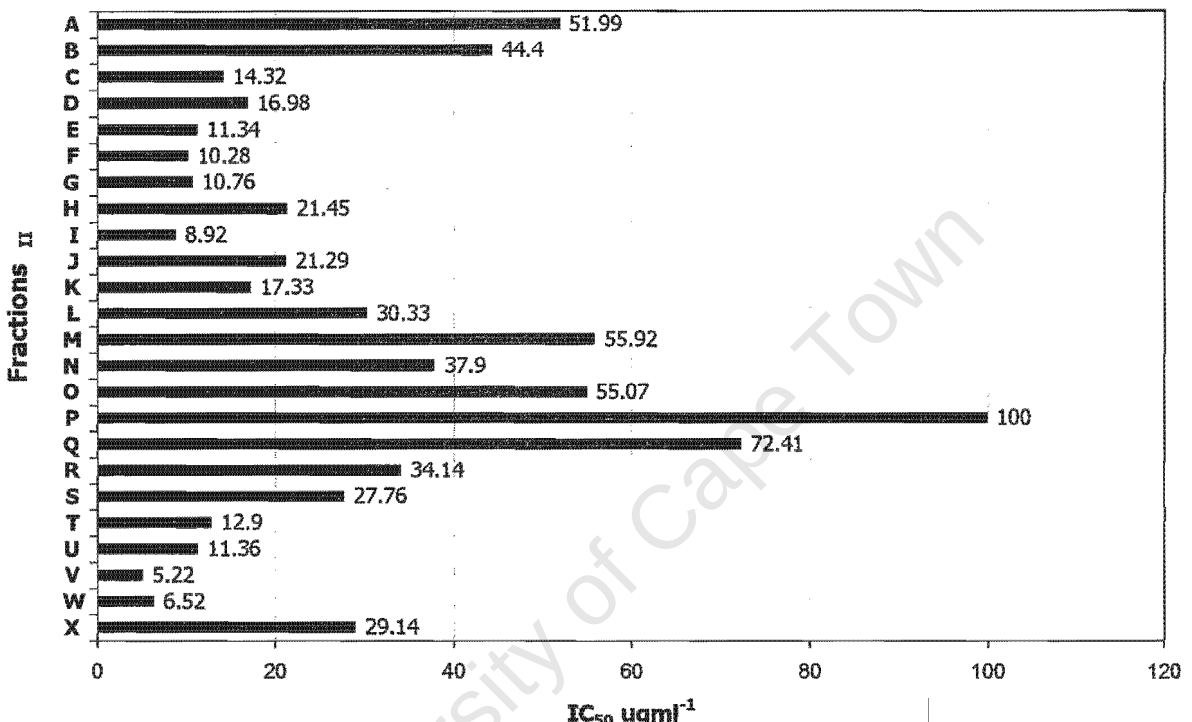

Figure 3.2.6.1. Summary of the IC_{50} values for the fractions $(A\text{-}X)_{II}$ generated by flash chromatography on *H. procumbens* (batch II). The values represent the mean IC_{50} value of two independent experiments each performed in duplicate

3.2.6.2 Purification of the active flash chromatography fractions by HPLC

The HPLC profiles of fractions V_{II} and W_{II} were very similar and consisted of several peaks. Since there were only a few milligrams of each fraction, further purification for full structure elucidation was not feasible. The HPLC chromatograms of the fractions E_{II}, F_{II}, G_{II} and I_{II} contained numerous peaks, with several common peaks within each fraction. These common peaks were identified, collected as smaller fractions, concentrated and tested for antiplasmodial activity against *P. falciparum* D10. The most active fraction collected had an IC_{50} value of 4.43μgml^{-1} and only yielded a few milligrams. This active fraction consisted of 3 prominent peaks, which when separated and tested had IC_{50}

values in the range of 10-18μgml^{-1}. The yields of these purified compounds were very low and the quantities obtained were, yet again not sufficient for NMR analysis.

3.3 Discussion

3.3.1 *In vitro* antiplasmodial activity of *H. procumbens* extracts

Of the crude *H. procumbens* extracts, only the PE extract showed *in vitro* antiplasmodial activity. In traditional medicines the aqueous extracts of *H. procumbens* are used to treat fevers, which would contain very little if any of the non-polar compounds extracted by PE. Research on plants has shown that water extracts used in traditional medicine do not necessarily contain the active principles isolated through *in vitro* bioassay guided fractionation of organic solvent extracts (Phillipson *et al.*, 1993). In some instances, precursors or structural analogues of the active principles are present in the aqueous extract and have to be modified in some way before activity is exhibited. A notable example of this is the lipophilic quassinoid terpenoids, which have shown potent *in vitro* and *in vivo* antiplasmodial activity. The isolated quassinoids are mainly chloroform soluble, yet the plant they are derived from is used as an aqueous extract that has shown little *in vitro* activity. Chromatographic investigation of the aqueous extract indicated that a small amount of potent lipophilic quassinoids were present, with a much larger quantity of polar quassinoids. Acid hydrolysis of the dry aqueous extract yielded a number of lipophilic quassinoids with significant *in vitro* antiplasmodial activity (Phillipson *et al.*, 1993). These results indicate that precursors of the active principles may be present in the aqueous extract but have to be converted, possibly *in vivo*, before activity is exhibited.

An additional explanation for the low levels of the active component in traditional water preparations, is that plants contain complex mixtures of chemicals and synergism could exist between the various compounds (Kirby, 1996). This has been demonstrated for artemisinin, which is highly lipophillic and is extracted from *A. annua* with organic solvents. An aqueous infusion of the plant is commonly used in traditional medicines and contains relatively low levels of artemisinin. Research on the chemical composition of *A. annua* extracts has resulted in the isolation of a number of compounds, including several flavonoids (structurally unrelated to artemisinin) that can enhance the *in vitro* antiplasmodial activity of artemisinin (Elford *et al.*, 1987). Hence, low levels of artemisinin

in an aqueous extract could exhibit antimalarial activity if a synergistic relationship exists with other compounds. In addition, studies on *A. annua* tea, prepared by traditional methods, have shown that the levels of artemisinin are surprisingly higher than would be expected (Mueller *et al.*, 2000). It has been suggested that other plant constituents could help extract and keep the lipophilic compound in an aqueous solution. All of these factors could account for the antimalarial activity of aqueous extracts used in traditional medicines, which on investigation *in vitro* have relatively low levels of the isolated active principle.

Furthermore, the extracts in this study were assayed for direct *in vitro* antiplasmodial activity. There may be compounds present in the aqueous extract that act as antipyretics or immune stimulants, which could help to relieve the symptoms of the disease and contribute to the overall activity of the plant (Phillipson *et al.*, 1993). Experimental investigations for such effects, as well as the analysis of the chemical composition of the water extract were not carried out in this study. From the observed results, all that can be concluded is that the component that showed positive antiplasmodial activity was concentrated in the PE extract and that the water and MeOH extracts did not show activity in the *in vitro* assay system used. Although these results support the use of *H. procumbens* for the treatment of malaria, the activity was not observed in the aqueous extract.

3.3.2 Purification and identification of the active principle from *H. procumbens*

In vitro bioassay-guided fractionation of the PE extract led to the isolation of an active principle **H5a**. Although the most active flash chromatography fractions G and H were focused on for further purification, fractions C and D were also relatively active and could potentially have been used for the isolation of antiplasmodial agents. The HPLC chromatograms of C and D indicated that the fractions contained a complex mixture of waxy compounds, which would have been difficult to separate. Bearing this in mind, as well as the higher IC_{50} values obtained, fractions C and D were not purified any further. Considering the different polarities of the fractions, the compounds responsible for the observed activity in fractions C and D were probably different to the active principle isolated from fraction G and H. Many plant compounds exist as groups of structurally related metabolites, which often possess common features necessary for activity. Fractions C and D may contain biosynthetically related analogues of the isolated

compound with different degrees of potency. The other possibility is that they contain structurally diverse compounds with a different mechanism of action.

An active principle in excess of 85% purity (HPLC analysis) was isolated from fractions G and H with an approximate yield of 0.003% by weight of the dried root sections. The UV spectrum of the active component indicated some degree of conjugation, but without the NMR data the structure could not be elucidated. From the mass spectrum the molecular weight of the active principle was found to be 316.2038, which corresponded to the molecular formula $C_{20}H_{28}O_3$. Considering the molecular formula of the compound, it is most likely a diterpene. Diterpenes (diterpenoids) are a diverse class of secondary metabolites found in many genera of higher plants, fungi, insects and microorganisms (Buckingham *et al.*, 1994)).

Although the milligram quantities of **H5a** isolated were sufficient for bioactivity screening purposes and HREIMS analysis, additional material was needed for structural elucidation. Typically, active natural products are present in very low (usually <0.01 percent by weight) quantities in natural sources (Cragg and Newman, 2001). This was the case for the antiplasmodial component in *H. procumbens*, which could only be identified as far as the molecular weight and corresponding molecular formula.

3.3.3 *In vitro* antiplasmodial activity and cytotoxicity of the active principle

The active principle **H5a**, isolated from the PE extract of *H. procumbens* roots, was approximately 26 times more potent than the crude PE extract. **H5a** showed potent antiplasmodial activity against both CQ-sensitive and resistant strains of *P. falciparum*, demonstrating no cross-resistance with CQ. Moreover, statistical analysis indicated that **H5a** was significantly more active against the CQ-resistant strain (K1) strain than in the CQ-sensitive strain (D10). Since both the mechanism of CQ-resistance and mode of action of **H5a** are not known, no explanations can be provided at this stage for K1's increased sensitivity to **H5a**.

There is over a 10-fold difference in the sensitivity of the two strains to CQ, but for the isolated compound the activities were the same order of magnitude. This suggests that the mechanism of action of the isolated compound is possibly different to that of CQ. Alternatively, if the mode of action is similar, then the isolated compound circumvents the

mechanisms of resistance. Although the active principle is not as effective as CQ, it could play a role in the treatment of CQ-resistant parasites. Furthermore, the active component could be used to study structure-activity relationships, which would identify structural modifications that might lead to a more active candidate for antimalarial drug development.

Although *H. procumbens* extracts are used extensively and pharmacological studies have shown very little toxicity, it is usually the crude aqueous extract that is used, which would have a different toxicity profile to a purified compound. If an isolated compound affects parasite viability, it is logical to screen for *in vitro* cytotoxicity to determine the selectivity index. Due to the limited quantities of fraction H and **H5a**, the highest concentrations that the Rat-1-cells were exposed to were 100 and 10μgml^{-1} respectively. Since the cell viability exceeded 50% at these concentrations, the IC_{50} values and selectivity index could not be calculated. These results indicate that the concentrations of fraction H and **H5a** required to kill the parasites had no measurable effect on Rat-1-cell viability. Although the results are encouraging, dose response experiments should be done at much higher concentrations to identify the toxic range of the isolated compound. This would be necessary to assess whether the active principle is sufficiently selective to kill the malaria parasites without damaging host cells. Even if the active component is toxic to mammalian cells, attempts can be made to synthesise structural analogues with favourable cytotoxic to antiplasmodial ratios. In conclusion, the isolated compound appeared to have selective antiplasmodial activity against a drug resistant and sensitive strain of *P. falciparum*.

3.3.4 Comparison of antiplasmodial activity of two different batches of *H. procumbens'* roots

In an attempt to produce a larger quantity of the active principle, additional plant material (batch II) was obtained, extracted and fractionated. The crude PE extract of this second batch was only half as potent as the first batch, suggesting that it contained either less of the active principle or less active analogues of the isolated compound. The most active flash chromatography fraction from this PE extract had an IC_{50} value of 4μgml^{-1} and when this fraction was separated and tested for activity, the individual components all had IC_{50} values exceeding 10μgml^{-1}. The combination of compounds in this fraction show greater antimalarial activity than the individual compounds, suggesting synergism between the

different compounds. Instability of the purified compounds could also be an explanation for the reduced activity on separation. Yet again, the quantities isolated of the active components were not sufficient for structure elucidation.

By comparing the polarities of the compounds, the active principles isolated from batch II appear to be different from the active compound from batch I. Numerous studies have shown that the chemical composition of a plant can vary considerably depending on the stage of growth, onset of flowering and fruit development. Metabolic changes in plants are also influenced by the soil content, climate and environmental factors, which include stress conditions such as limited water, high UVB levels and chilling conditions. Furthermore, the same phenotype of a plant can have different chemotypes that produce different levels of metabolites under identical growing conditions. Although both of the batches of dried roots were obtained from the same source, the plant material originated from wild-harvested *H. procumbens*. This would probably include a variety of *H. procumbens* plants sourced from different locations. The *H. procumbens'* roots are usually collected towards the end of the rainy season, but besides this there is very little standardisation in terms of harvesting of wild material. These studies have shown that the chemical content, particularly the active antimalarial principle, of *H. procumbens'* roots can vary considerably from one batch to another.

3.4 Conclusion

The crude PE root extract of *H. procumbens* showed *in vitro* antiplasmodial activity against a CQ-sensitive strain of *P. falciparum* and was focused on for further purification. An active principle was isolated and its molecular formula $C_{20}H_{28}O_3$ was determined by analysing its HREIMS molecular ion. The yield of the compound was very low and the quantities isolated were sufficient for bioactivity screening, but not for structure determination. The active component showed significant *in vitro* antiplasmodial activity against both a CQ-sensitive and CQ-resistant strain of *P. falciparum*. The *in vitro* cytotoxicity assays indicated that the compound was not toxic to Rat-1-cells at the concentrations required to kill the *P. falciparum* parasites. Studies on another batch of *H. procumbens* roots suggest that the levels and structures of the antiplasmodial components can vary from one batch to another.

Considering the potent *in vitro* antiplasmodial activity against drug sensitive and resistant parasites and the lack of toxicity, the roots of *H. procumbens* represent a potential source of antimalarial drugs. To investigate this further, a third batch of *H. procumbens* plants was collected and evaluated for activity.

Chapter 4

Activity of *H. procumbens* (batch III) and the Active Compounds

4. *In vitro* Antiplasmodial Activity of *H. procumbens* (batch III) and Isolation of the Active Compounds

4.1 Introduction

The previous chapter examined the *in vitro* antiplasmodial activity of wild harvested *H. procumbens* roots (batch I and II). The results were promising, but varied considerably from one batch to another. In an attempt to isolate larger quantities of the active principles for full structure elucidation and extensive antiplasmodial and cytotoxicity evaluation, a third batch of *H. procumbens* was investigated. The plant material was obtained from the Grassroots Natural Products Group, which grow *H. procumbens* under controlled conditions on a farm in the Western Cape. Since the plant does not grow naturally in this area, cuttings of *H. procumbens* were sourced from the Northern Cape, propagated and then transferred to well-drained sandy soils. Two whole *H. procumbens* plants were acquired from Grassroots Natural Products for this study. Voucher specimens and details of the growing conditions were deposited in the Bolus Herbarium, Department of Botany, University of Cape Town.

This chapter examines the *in vitro* antiplasmodial activity of different sections of the *H. procumbens* plants from the Grassroots Natural Products Group. It describes the purification of the active extract and the isolation of pure compounds with a high enough yield for structure elucidation and thorough evaluation of activity.

4.2 Results

4.2.1 *In vitro* antiplasmodial activity of the PE extracts of different parts of *H. procumbens* (batch III)

Two *H. procumbens* plants A94 and A47, which originated from different cuttings, were randomly chosen from the cultivated *H. procumbens* plants on the Grassroots farm. In addition to root sections, aerial parts (leaves and stems) and fruits of the plants were acquired, extracted with PE and tested for *in vitro* antiplasmodial activity against *P. falciparum* D10 (Figure 4.2.1.).

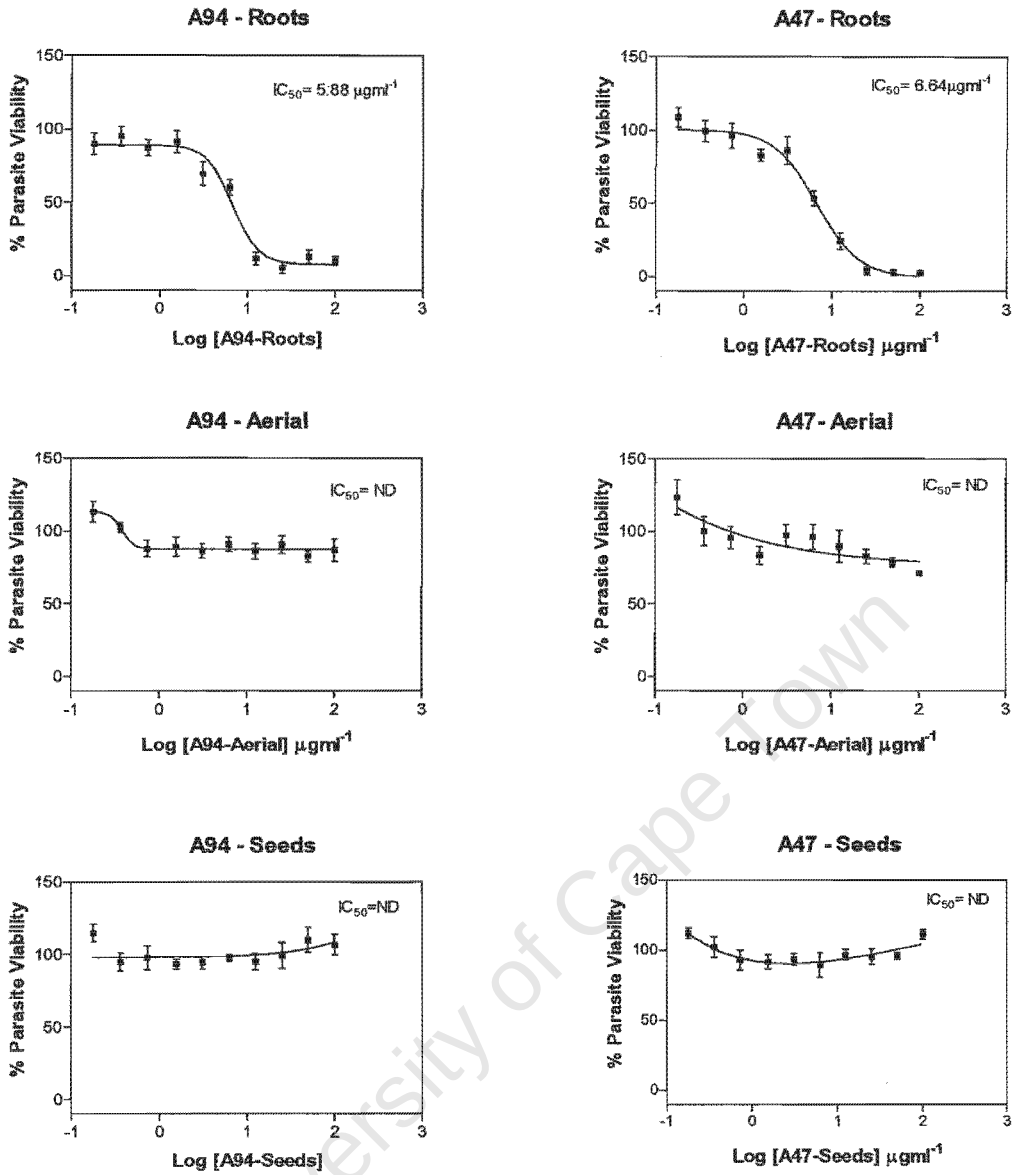

Figure 4.2.1. Dose response curves of the PE extracts of the roots, aerial parts and seeds of *H. procumbens* plants A94 and A47, using *P. falciparum* D10. Each point represents the mean of 3 independent experiments each performed in duplicate

The same order of activity was observed for the two different *H. procumbens* plants A94 and A47. The PE extracts of the aerial parts and the seeds of both of the plants showed no activity against *P. falciparum* D10 at the highest concentrations tested (100µgml^{-1}). A dose-dependant inhibition of parasite growth was observed for the PE root extracts, with IC_{50} values of 5.88±1.33 µgml^{-1} for A94 and 6.64±2.44µgml^{-1} for A47. Since the antiplasmodial component was concentrated in the roots of *H. procumbens* (batch III), an additional 10kgs of powdered root material was obtained from Grassroots. The PE extract of this composite root material was tested for antiplasmodial activity and was found to be as active as the A94 and A47 PE root extracts.

4.2.2 Bioassay-guided fractionation of the root PE extract

The PE extract of the roots was fractionated using a solid phase extraction (SPE) C_{18} cartridge and an acetonitrile (ACN)-water solvent system, eluting with a step gradient of decreasing polarity (Details in Chapter 7, 7.4). All of the fractions generated by SPE were subjected to *in vitro* antiplasmodial tests against D10. In the preliminary fractionation procedure (using 5% increments of ACN), the active principles were eluted between 60% and 65% ACN. When the eluant was fine-tuned to 1% increments of ACN within this range, the most active fractions were collected at 60% and 61% ACN. The dose response curves for these fractions are in Appendix 1 (Figure 4.2.2.1a) and the corresponding IC_{50} values are summarised in Figure 4.2.2.1b.

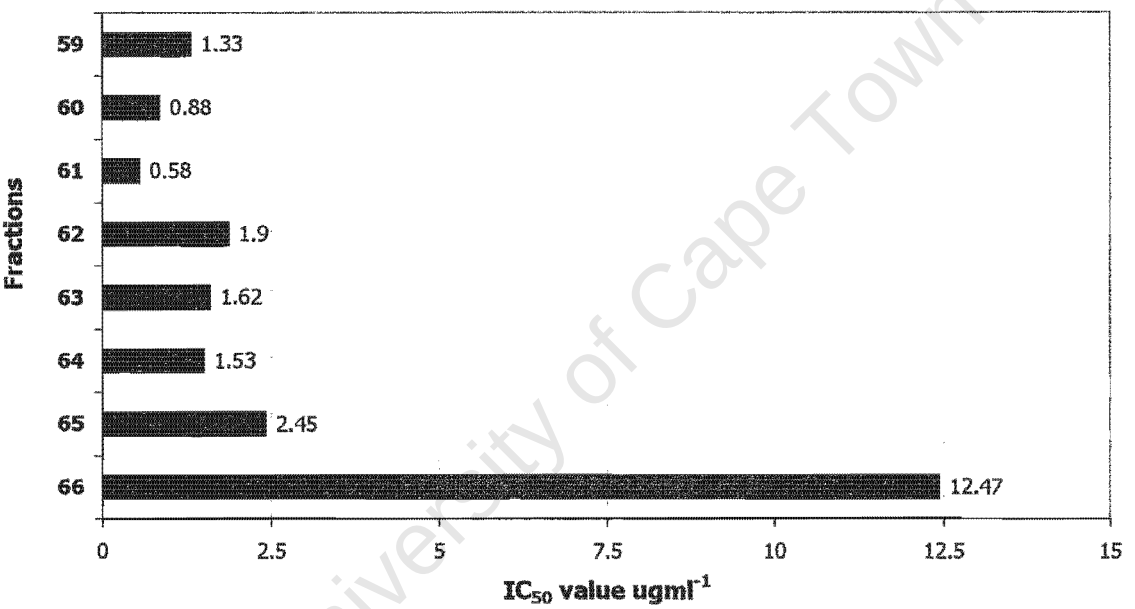

Figure 4.2.2.1b. Summary of the IC_{50} values of the fractions 59-66% ACN generated by SPE. The fractions are identified by the % of ACN they were eluted with. The values represent the mean IC_{50} value of two independent experiments each performed in duplicate

Whilst eluting with 1% increments of ACN in the 55-63% range, the elution volumes were modified to optimise separation. This resulted in the isolation and identification of two fractions, eluted with 56% ACN and 60% ACN, that exhibited significant antiplasmodial activity. The HPLC analysis (Figure 4.2.2.2.) of these fractions showed a single prominent peak for each fraction (56% ACN, R_T=29.6min and 60% ACN, ~~R_T=30.8min),~~ with minor impurities on either side. Integration of the area under the peaks indicated that the 56% ACN fraction was 82% pure and that the 60% ACN fraction was 84% pure. The UV

spectrum of the main peak in the 56% ACN fraction (Appendix 2, A2.2) and in the 60% ACN fraction (Appendix 2, A2.3) were identical, showing absorption maxima at approximately 210nm and 280nm. Furthermore, the UV spectra across the main peaks were uniform, suggesting a single compound within the peak. Since the fractions eluted with 56% ACN and 60% ACN were found to be greater than 80% pure, they were not subjected to further fractionation and will be referred to as compounds **56** and **60** respectively.

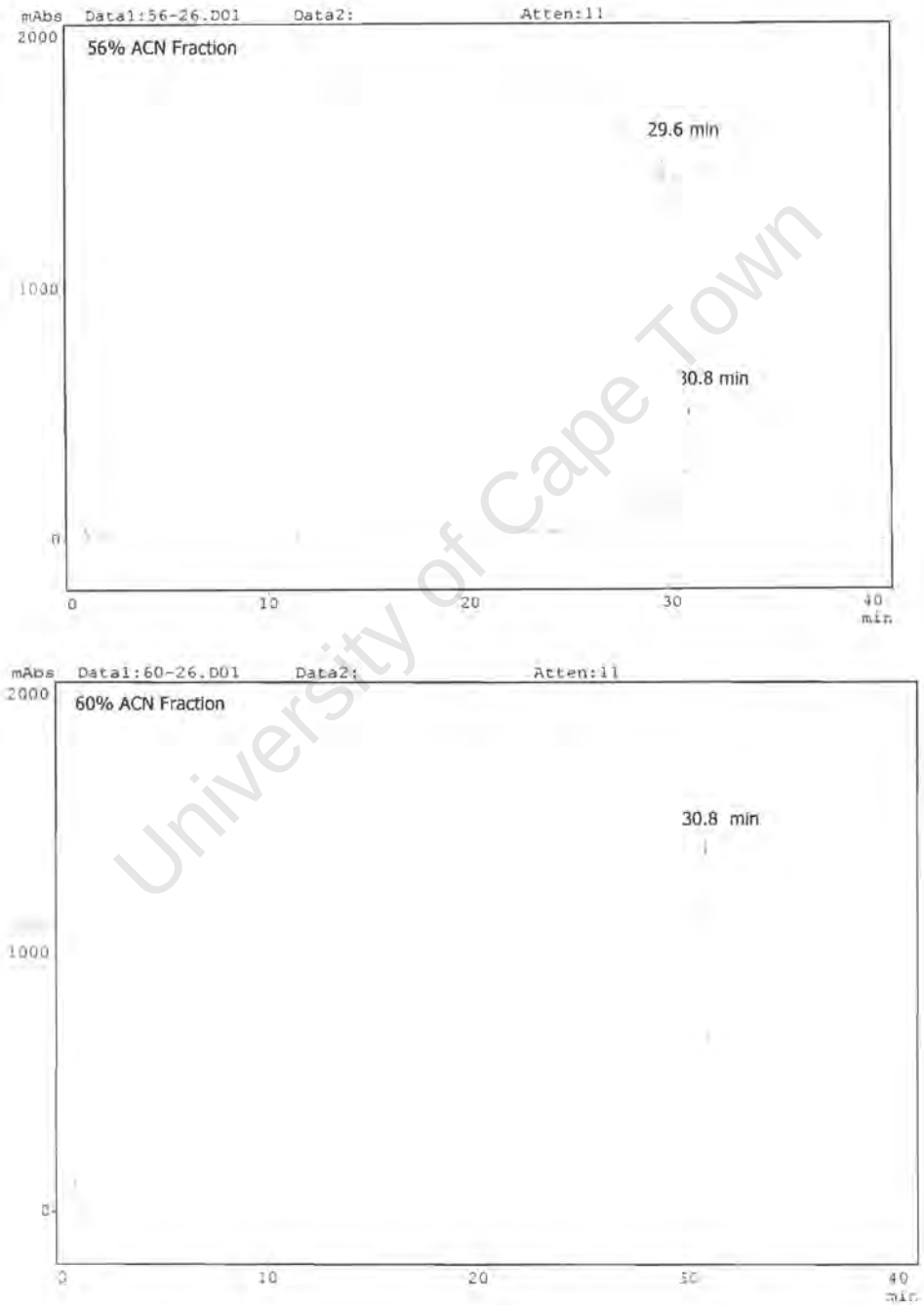

Figure 4.2.2.2. HPLC chromatograms of the active SPE fractions eluted with 56% and 60% ACN

The other SPE fractions produced between 56% and 60% ACN showed moderate activity, and HPLC analysis indicated that these fractions contained tailing amounts of compounds **56** and **60** (Chapter 7, 7.4.1). Since **56** and **60** displayed the greatest antiplasmodial activity, they were focused on for further investigations. The yield of **56** was approximately 0.033% and of **60** it was 0.015% by weight of the powdered *H. procumbens* roots. Of the 10 kgs of the powdered *H. procumbens* roots acquired, several kilograms were exhaustively extracted with PE and purified by SPE to yield measurable amounts of compounds **56** and **60** for structure elucidation.

4.2.3 Identification and characterisation of compounds 56 and 60 from *H. procumbens*

The identity of **56** and **60** (Figure 4.2.3.) was determined by mass spectrometry (HREIMS), infrared spectroscopy, specific rotation, melting point determination, ^{1}H, ^{13}C, HSQC, HMBC, COSY and NOESY NMR experiments. The ^{1}H, ^{13}C, HMBC, COSY and NOESY NMR results for **56** and **60** are summarised in Tables 4.2.3.2 and 4.2.3.3. For convenience purposes, the structure elucidation discussion of the isolated compounds will follow their respective NMR data tables. Copies of the HREIMS, NMR and IR spectra are in Appendix 2 (A2.2 and A2.3). The molecular weight and formula, melting point, specific rotation and IR data for the isolated compounds are given in Table 4.2.3.4.

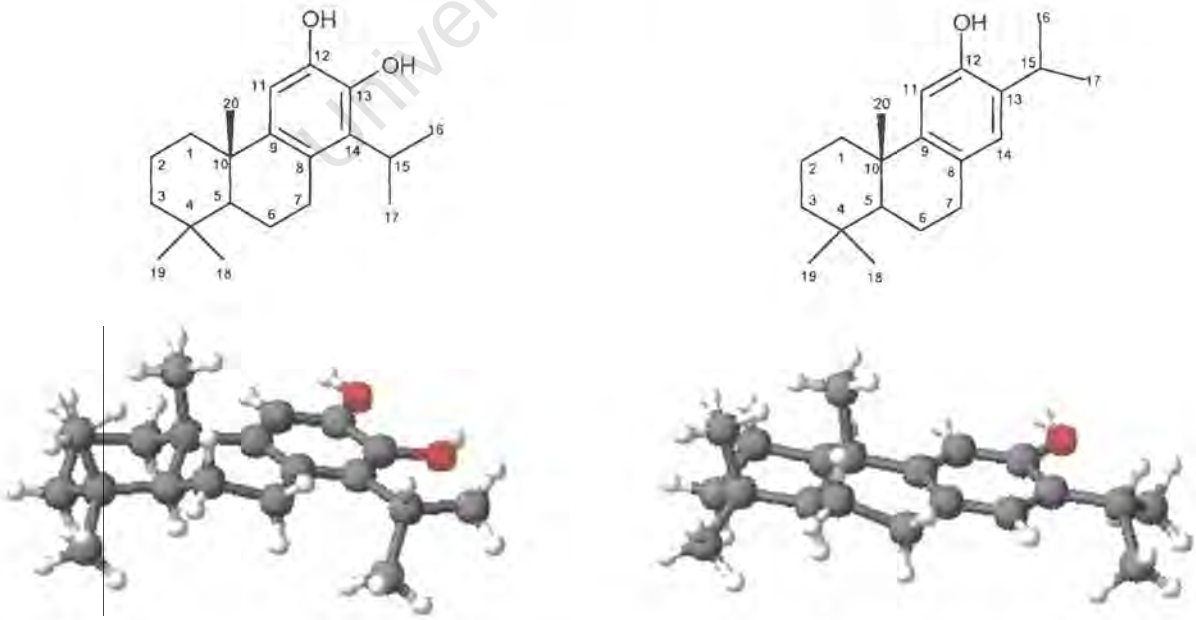

Figure 4.2.3. Structures, numbering and stereochemistry of compounds **56** and **60**

Table 4.2.3.2. ^{1}H, ^{13}C, HMBC, COSY and NOESY spectral data of compound **56**. (* Overlapping spectra. • Values are interchangeable within the same column)

Position		δ ^{1}H	J (Hz)	δ ^{13}C	HMBC	COSY	NOESY
1	α	(1.15 – 1.12)	*m*	41.1	C-3, C-5	H-1β, H-2β	H-1β, H-2β, H-11
	β	2.09	*br d* (12.5)		C-3, C-5	H-1α, H-2α	H-1α, H-2α, H-11, H-20
2	α	1.47	*dt* (*, 3.4)	20.6	-	H-1β, H-2β, H-3β	H-1β, H-2β, H3β
	β	1.66	*dt* (13.7, 3.4)		-	H-1α, H-2α, H-3α	H-1α, H-2α, H-3α, H-19, H-20
3	α	(1.14 – 1.12)	*m*	42.9	*	H-2β, H-3β	H-2β, H-3β, H-18
	β	1.36	*br d* (13.2)		-	H-2α, H-3α	H-2α, H3α, H-18, H-19
4		-	-	34.2	-	-	-
5		(1.13 – 1.12)	*m*	51.5	*	H-6β	H-6β, H-7α, H-18
6	α	1.80	*dd* (13.2, 7.8)	20.8	C-4, C-5, C-7, C-8, C-10	H-6β, H-7α	H-6β, H-7α, H-18
	β	1.54	*m*		C-4, C-5, C-7, C-10	H-5, H-6α, H-7α, H-7β	H-5, H-6α, H-7α, H-7β, H-19, H-20
7	α	2.51	*m*	29.5	C-5, C-6, C-8, C-9	H-6α, H-6β, H-7β	H-5, H-6α, H-7β, H-15
	β	2.73	*dd* (16.8, 5.9)		C-5, C-6, C-8, C-9	H-6β, H-7α	H-6β, H-7α, H-15, H-16, H-17
8		-	-	121.5	-	-	-
9		-	-	142.5	-	-	-
10		-	-	38.8	-	-	-
11		6.49	*s*	109.7	C-8, C-9, C-10, C-12, C-13	-	H-1α, H-1αβ
12		-	-	144.0	-	-	-
13		-	-	144.0	-	-	-
14		-	-	132.3	-	-	-
15		3.10	*septet* (7.0)	28.9	-	H-16, H-17	H-7α, H-7β, H-16, H-17
16		1.21•	*d* (7.0)	20.6•	C-14, C-15, C17	H-15	H-7β, H-15
17		1.22•	*d* (7.0)	20.6•	C-14, C-15, C16	H-15	H-7β, H15
18		0.85	*s*	33.8	C-3, C-5, C-19	-	H-3α, H-3α, H-5 H-6α
19		0.82	*s*	22.4	C-3, C-5, C-18	-	H-2β, H-3β, H-6β, H-20
20		1.06	*s*	25.6	C-1, C-5, C-9, C-10	-	H1β, H2β, H-6β, H-19

4.2.3.2 Structure of compound 56

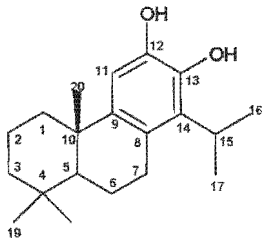

The molecular formula of **56**, $C_{20}H_{30}O_2$ was determined by analysing its HREIMS molecular ion at m/z 302.22565 (calculated value 302.22458). The initial evaluation of the ^{1}H-NMR spectrum of **56** showed a single aromatic proton, along with an isopropyl and three methyl groups. The construction of the main skeleton was initiated at the aromatic ring, with the identification of H-11 as the deshielded proton resonating at δ 6.49. Using the HMBC contours, H-11 was correlated to C-12 and C-13 at δ 144.0 (overlapping signals). The chemical shift values for these quaternary carbons suggested that a hydroxyl group was attached to both C-12 and C-13. HMBC data also linked the H-11 proton with the quaternary carbons C-9 (δ 142.5) and C-8 (δ 121.5). The dd at δ 2.73 was assigned to the benzylic H-7β, which showed geminal coupling (J=16.8Hz) to H-7α and vicinal coupling (J=6.0Hz) to H-6β. Based on a molecular model, the dihedral angle between H-7β and H-6α was 90°, therefore no vicinal coupling with H-6α was observed. From the HSQC and COSY experiments, H-7α was identified as a multiplet at δ 2.51. In the COSY spectrum, H-7α was linked to H-7β as well as the vicinal H-6 protons, which should furnish a ddd for the H-7α signal. The dd resonating at δ 1.80 was identified as H-6α and showed geminal coupling (J=13.2Hz) to H-6β and vicinal coupling (J=7.8Hz) to H-7α. Additional coupling with H-5 and H-7β was not observed due to the 90° dihedral angle between the respective protons. The COSY and HSQC spectra enabled the identification of the H-6β signal at δ 1.54. The multiplicity of H-6β appeared to be a ddd, whereas the COSY correlations between H-6β and H-5, H-6α, H-7β and H-7α would suggest a dddd splitting pattern. Due to the complexity of the overlapping signals, the coupling constants for H-6β could not be calculated. The COSY spectrum indicated that H-6β was coupled to a signal at δ(1.13-1.12) that was identified as H-5. Complementary evidence for this assignment was provided by the HMBC experiments, which showed two and three bond correlations with H-6 and H-7 to C-5 (δ 51.5). Since H-5 was interlinked through NOESY correlations to H-7α and H-18, an α-orientation could be assigned to this proton. Due to spectral overlap in the region δ(1.15 – 1.12), the exact chemical shift value, multiplicity and coupling constant could not be determined for H-5.

The isopropyl group was identified by a methine septet at δ 3.10 (J=7.0Hz, H-15) that was coupled to methyl signals at δ 1.21 and δ 1.33 (H-16, H-17, d, J=7.0Hz). Since the isopropyl group can rotate freely, the chemical shifts for H-16 and H-17 are interchangeable. The position of the isopropyl group was determined by the three bond correlations from H-16 and H-17 to C-14 (δ 132.2). Moreover, NOESY correlations between the H-7 protons and the H-15, H-16 and H-17 protons confirmed the location of the isopropyl group.

The broad doublet resonating at δ 2.09 was assigned to H-1β. Although the COSY spectrum indicated that H-1β was coupled to H-1α (J=12.5Hz) and H-2α, the vicinal coupling was not resolved. This would account for the appearance of a broad doublet for H-1β when a dd would be expected. In the HSQC spectrum H-1β and a multiplet at δ(1.15-1.12), which was identified as H-1α, were both linked to C-1. The chemical shift value and multiplicity of H-1α could not be determined due to overlap with the H-3α and H-5 signals. The COSY spectrum linked H-3α to a broad doublet (J=13.2Hz) that was assigned to H-3β. While H-3β and H-1β appeared as broad doublets, the COSY data revealed that these protons were coupled to geminal protons as well as to H-2α, which should afford a dd. It is proposed that the vicinal coupling to the H-2α is too small to be completely resolved, therefore only the large geminal coupling is observed. From a molecular model, the orientation of the interacting H-3β and H-2α protons as well as the H-1β and H-2α protons is almost identical, which would account for the similar splitting patterns. The H-2β proton resonates at δ 1.66 and occurs as a double triplet (J=13.7 and 3.4Hz). The large coupling constant would be due to geminal coupling with H-2α and the smaller coulping constant would be from the interaction with H-1α and H-3α. The fact that first order splitting patterns (n+1) are exhibited for the vicinal coulping suggests that the H-1α and H-3α protons are interacting identically with H-2β. A similar phenomenon was observed for H-2α (δ 1.47). This proton also resonated as a double triplet and was coupled to the vicinal protons H-1β and H-3β. The interaction of H-2β with H-1α and H-3α, and H-2α with H-1β and H-3β defines the dihedral angles between the above-mentioned protons and the subsequent conformation of the cyclic ring.

Three methyl singlets at δ 0.82, 0.85 and 1.06 were observed with corresponding carbon signals at δ 22.0, 33.8 and 25.6 respectively. Through relevant HMBC and NOESY correlations the methyl groups were identified as H-19 (δ 0.82), H-18 (δ 0.85) and H-20 (δ 1.06). The NOESY correlations from H-1β, H-2β and H-6β to H-20 indicate that H-20 is

in a β-orientation. This was confirmed by further NOESY correlations displayed between H-20 and H-19. Other prominent NOESY correlations were from H-19 to H-2β, H-3β and H-6β, and from H-18 to H-3α and H-6α, which would define the conformation preference of the H-19 and H-18 methyl groups to be a β and α-orientation respectively. The ^{1}H spectrum of **56** was similar to previously reported data (Burnell *et al.*, 1988), although a number of their resonances were recorded as multiplets and no 2D NMR experiments were described.

The ^{13}C-NMR spectrum showed 18 signals and a HSQC experiment allowed the correlation of the protonated carbons with the corresponding hydrogens. The C-16 and C-17 signals resonated at the same chemical shift values, which would be expected for a freely rotatable isopropyl group. The data gathered from the ^{13}C and HMBC spectrum indicated that the deshielded C-12 and C-13 signals were also overlapping. Although the ^{13}C-NMR spectrum would be expected to display 20 signals, the overlap of two sets of signals would explain why only 18 resonances were observed. HMBC data correlated H-6 to C-4, C-8 and C-10, H-20 to C-9 and C-10, H-16 to C-14, H-17 to C-14, H-11 to C-8, C-10, C-12 and C-13 enabling identification of the 7 quaternary carbons. The ^{13}C-NMR spectral chemical shifts were similar (δ±2ppm) to published data (Evans *et al.*, 2000).

The IR spectrum showed absorption bands for a hydroxyl group at 3390cm^{-1} and an aromatic ring system at 1627cm^{-1}, providing support for the determined structure. Compound **56** was crystalline and had a sharp melting point between 51-52°C. The specific rotation of **56** indicated that it was optically active and was dextrorotatory (+). Since compound **56** was dark yellow in colour, it had to be diluted considerably before reproducible specific rotation values were obtained. At higher concentrations the coloured compound absorbed the polarised light as opposed to rotating and transmitting it, which interfered with the readings. Due to the dilute concentrations used, the measured specific rotation of **56** probably has a large associated error. Nevertheless, the value indicates that **56** rotates the plane of polarised light in a clockwise direction (+). Based on the HREIMS data, IR spectrum, optical rotation and detailed NMR experiments, compound **56** was unambiguously identified as (+)-8,11,13-totaratriene-12,13-diol.

Table 4.2.3.3. ^{1}H, ^{13}C, HMBC, COSY and NOESY spectral data of compound **60**. (* Overlapping spectra.* Values are interchangeable within the same column)

Position		δ ^{1}H	(J in Hz)	δ ^{13}C	HMBC	COSY	NOESY
1	α	1.39	*m*	39.1	-	H-1β, H-2β	H-1β, H-2β
	β	2.17	*br d* (12.6)		-	H-1α, H-2α	H-1α, H-11, H-20
2	α	(1.58 - 1.65)	*m*	19.5	-	H-1β, H-2β, H-3β	H-2β
	β	(1.71 - 1.77)	*m*		-	H-1α, H-2α, H-3α	H-2α, H-20
3	α	(1.20 – 1.23)	*m*	41.9	-	H-2β, H-3β	H-3β, H-18
	β	1.46	*br d* (13.2)		-	H-2α, H-3α	H-3α, H-18, H-19
4		-	-	33.5	-	-	-
5		1.30	*m*	50.6	C-4, C-7, C-10, C-18, C-19, C-20	H-6β	*
6	α	1.85	*dd* (13.2, 7.3)	19.5	C-7	H-6β, H-7α	H-6β, H-18
	β	(1.71 – 1.65)	*m*		C-7	H-5, H-6α, H-7β, H-7α	H-6α, H-20
7	α	2.77	*m*	29.9	C-6, C-8, C-9	H-6β, H-6α, H-7β	H-7β
	β	2.86	*dd* (16.8, 7.0)		C-6, C-8, C-9	H-6β, H-7α	H-7α
8		-	-	127.5	-	-	-
9		-	-	148.9	-	-	-
10		-	-	37.7	-	-	-
11		6.63	*s*	111.2	C-8, C-10, C-12, C-13	-	H-1β
12		-	-	150.9	-	-	-
13		-	-	131.6	-	-	-
14		6.83	-	126.8	C-7, C-9, C-12, C-15	-	H-16, H-17
15		3.11	*septet* (6.8)	27.0	C-13, C-14, C-16, C-17	H-16, H-17	-
16		1.22*	*d* (6.8)	22.8*	C-13, C-15, C-17	H-15	-
17		1.24*	*d* (6.8)	22.9*	C-13, C-15, C-16	H-15	-
18		0.94	*s*	33.5	C-3, C-4, C-5, C-19	-	H-3α, H-3β, H-5, H-6α
19		0.91	*s*	21.8	C-3, C-4, C-5, C-18	-	H-3β, H-20
20		1.17	*s*	25.0	C-1, C-5, C-9, C10	-	H-1β H-2β, H-6β, H-19

4.2.3.3 Structure of compound 60

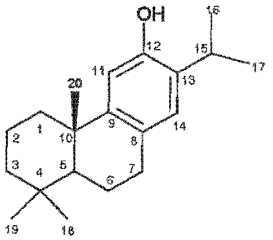

The HREIMS of **60** showed a molecular ion peak at m/z 286.23061, analysing for $C_{20}H_{30}O$ (calculated 286.22967). The ^{1}H-NMR spectrum of compound **60** closely resembled that of **56**, showing three methyl groups, an isopropyl group on an aromatic ring and an aromatic proton. A comparison of the ^{1}H and ^{13}C-NMR spectrum of **56** and **60** showed that a number of the chemical shifts and multiplicities were similar, suggesting common structural features.

A thorough investigation of the ^{1}H and ^{13}C NMR, COSY, HSQC, HMBC and NOESY experiments performed on **60** showed that the main skeleton was identical to that of **56**. The proton resonances from the fused cyclic rings were the same for **56** and **60**, including the spectral overlap for the H-2 and H-6β signals, as well as for the H-5, H-1α and H-3α signals. One of the noticeable differences in the ^{1}H-NMR spectrum of **60** was the presence of an additional aromatic proton resonating at δ 6.83. Using the HMBC contours, this proton was correlated to C-7, C-9, C-12 and C-15 and was identified as H-14. In the NOESY experiment, H-14 was clearly correlated with the isopropyl methyls, indicating the location of the isopropyl group at C-13. The other aromatic proton H-11 (δ 6.63) was correlated to C-8, C-10, C-12 and C-13, but was not linked to the isopropyl group through both HMBC and NOESY experiments, confirming the position of the isopropyl group at C-13. Using the HMBC contours, both H-11 and H-14 were correlated to C-12, whose relatively high chemical shift value suggested the presence of a hydroxyl group. Through HMBC correlations with H-11 to C-8, C-10, C-12 and C-13, H-14 to C-7, C-9, C-12 and C-15, H-15 to C-13, C-14, C-16 and C-17, H-16 and H-17 both to C-13 and C-15, the sequence of the above-mentioned protons on the aromatic ring was verified.

A comparison of the ^{13}C NMR data of **60** and **56** showed that the majority of the carbon chemical shifts were very similar. The noticeable difference between the spectra was the shift of the C-13 signal from δ 144 to δ 132. This would be due to the replacement of the hydroxyl group at C-13 with an isopropyl group.

All of the protonated carbon resonances could be assigned from the HSQC spectrum, while HMBC correlations from H-11 to C-8, C-10, C-12 and C-13; H-14 to C-9 and C-12; H-18 to C-4; H-20 to C-1, C-5, C-9 and C-10, and H-15, H-16 and H-17 to C-13 enabled the identification of the six quaternary carbons. Although 20 carbon resonances were expected only 19 were observed, which could be explained by the overlapping C-4 and C-18 signals. The ^{13}C spectral chemical shifts of **60** were identical ($\delta \pm 1.0$ppm) to published data (Harrison *et al.*, 1987). 2D-NMR (HMBC and HSQC) correlations were recently described for the first time for compound **60** (Aboul-Ela and El-Lakany, 2000), although four of their carbon assignments based on this data did not agree with the 2-D experiments in this study or with previously published ^{13}C chemical shift values (Evans *et al.*, 1999). One of the differences is their chemical shift values for the aromatic protons H-11 and H-14, which they identified at δ 6.88 and δ 6.67 respectively. These values are interchanged with the assignments in this study of H-11 at δ 6.63 and H-14 at δ 6.83. The informative 3-bond correlations from H-14 to C-7 and H-11 to C-10 observed in our HMBC experiments clearly identifies the H-14 proton as the more deshielded aromatic proton. The other variation in chemical shift values is for H-18 and H-19, which have also been interchanged compared to the assignments in this study. Using the NOESY data the correlation from H-18 to H-6α and H-5, and from H-19 to H-3β and H-20 indicate that the H-18 proton signal is slightly downfield from that of H-19.

As for compound **56**, the IR spectrum of **60** supported the presence of a hydroxyl group with an absorption band at 3406cm^{-1}. The UV absorption at 278nm confirmed the aromatic nature of the compound. The melting point of compound **60** could not be determined since it did not crystallize. This was most probably due to minor impurities, which were indicated in the HPLC profile. The melting point range of **60** has been reported to be 56-57°C (Evans *et al*, 2000). The specific rotation of **60** revealed that the compound was dextrorotatory (+), which has previously been reported for compound **60** isolated from a natural source (Yang *et al.*, 2001). Since **60** was dark yellow in colour, the same problems encountered for **56** were experienced for **60** when measuring the specific rotation.

The main differences observed in the ^{1}H and ^{13}C-NMR spectra of compounds **56** and **60** originated from the structural diversity located on the aromatic ring. From the specific rotation, HREIMS spectrum and thorough evaluation of detailed NMR experiments compound **60** was identified as (+)-8,11,13-Abietatrien-12-ol, also known as ferruginol.

As suggested by the HPLC retention times and the identical UV absorbances, compounds **56** and **60** were very similar in structure and are probably related metabolites derived from a common synthetic pathway. A comparison of the molecular formulae of **56** ($C_{20}H_{30}O_2$), **60** ($C_{20}H_{30}O$) and the active component isolated from the first batch of *H. procumbens*, **H5a** ($C_{20}H_{28}O_3$), suggests that the latter is a related analogue of **56** and **60**. As plant compounds often exist as part of a family of related molecules, it is likely that other less active analogues were present in the crude extract. Since compounds **56** and **60** showed the greatest antiplasmodial activity, they were focused on for the isolation of sufficient material for structural characterisation.

Table 4.2.3.4. Compound characterization data for **56** and **60**

Cmpd	Molecular weight	Molecular formula	Melting pt /°C	Specific rotation	IR absorbance ν_{max} cm^{-1}
56	302.22565	$C_{20}H_{30}O_2$	51 - 52	$[\alpha]_D^{26.5}$ +95.0° (c; 0.842)	3390 (OH), 2927, 1627, 1458,1272, 1110, 873, 736
60	286.23061	$C_{20}H_{30}O$	ND	$[\alpha]_D^{26.7}$ +20.7° (c; 10.15)	3406 (OH), 2925, 1710, 1460, 1264, 1113, 891, 740

ND- not determinable. [α] – measured in $CDCl_3$, c ($mgml^{-1}$)

4.2.4 *In vitro* antiplasmodial activity and cytotoxiciy of the active compounds 56 and 60

Compounds **56** and **60** were tested for *in vitro* antiplasmodial activity against 5 different *P. falciparum* strains with varying degrees of CQ sensitivity. The CQ dose-response relationships were also evaluated for the 5 strains to assess their sensitivity to CQ. The dose response curves are in Appendix 1 (Figure 4.2.4.1) and the corresponding IC_{50} values are listed in Table 4.2.4.1.

Table 4.2.4.1. Summary of the mean IC_{50} values (± SD) for CQ and compounds **56** and **60** in 5 strains of *P. falciparum*

Strain	IC_{50} ± SD			P value
	56 μgml^{-1}	**60** μgml^{-1}	**CQ** $ngml^{-1}$	
D10	0.76 ± 0.09	0.95 ± 0.08	11.83 ± 1.46	0.180
3D7	1.37 ± 0.39	1.89 ± 0.37	11.71 ± 1.53	0.128
K1	0.83 ± 0.07	0.63 ± 0.05	181.76 ± 10.69	0.310
W2	1.16 ± 0.01	0.80 ± 0.13	134.11 ± 15.80	0.004
RSA11	0.78 ± 0.15	0.84 ± 0.29	110.52 ± 14.01	0.484

Values represent the mean IC_{50} (± SD) of three independent experiments each performed in duplicate
P value obtained using the Mann-Whitney two-tailed test to compare the activity of **56** and **60** within each strain

Compounds **56** and **60** showed significant antiplasmodial activity against CQ-resistant and sensitive strains of *P. falciparum*. As indicated by the P value, **56** and **60** were equipotent in strains D10, 3D7, K1 and RSA11. A statistically significant difference in activity was observed between compound **56** and **60** in the W2 strain

The *in vitro* cytotoxicity of the compounds was determined using Chinese hamster ovarian (CHO) cells and Human heptoma (HepG2) cells. The cells were maintained in continuous culture and a modified version of the MTT assay was used to measure cell viability. The cytotoxicity dose response curves for the positive control daunomycin (Dn) and **56** and **60** are in Appendix 1 (Figure 4.2.4.2), and their IC_{50} values are summarised in Table 4.2.4.2.

Table 4.2.4.2. IC_{50} values for compounds **56**, **60** and daunomycin against CHO and HepG2 cells

Cell line	IC_{50} ± SD		
	56 μgml^{-1}	**60** μgml^{-1}	**Dn** μgml^{-1}
CHO	51.45 ± 7.79	51.69 ± 2.67	1.53 ± 0.15
HepG2	59.01 ± 5.76	43.71 ± 6.07	1.46 ± 0.20

Values represent the mean IC_{50} (± SD) of three independent experiments each performed in quadruplicate

Both **56** and **60** showed low cytotoxicity in CHO and HepG2 cells compared to the positive control daunomycin. Since the observed IC_{50} values against the CHO and HepG2 cell lines were approximately the same, the selectivity indexes for **56** and **60** were calculated using the CHO IC_{50} concentrations. The selectivity index (S_I) is a ratio of

cytotoxicity to antiplasmodial activity and gives a general indication of the specific activity (Table 4.2.4.3).

Table 4.2.4.3. S_I values for the compounds **56** and **60** in the 5 strains of *P. falciparum*

Strain	56 (S_I)	60 (S_I)
D10	67.70	54.16
3D7	37.55	27.22
K1	61.99	81.67
W2	44.35	64.31
RSA11	65.96	61.25

The average S_I value for compounds **56** and **60** exceeded 55, demonstrating that the compounds were 55 fold more potent to the parasites than the mammalian cells.

4.3 Discussion

4.3.1 *In vitro* antiplasmodial activity of different parts of *H. procumbens*

Among the PE root, aerial and fruit extracts of *H. procumbens*, the strongest antiplasmodial activity was found in the root extract. Both of the plants' root extracts were equipotent, suggesting that A94 and A47 belong to the same chemotypes. The root extracts of these cultivated plants were twice as potent as the wild harvested material, indicating either a higher concentration of the active components or the presence of more active analogues. Often the profile of compounds in plant material originating from their wild habitat differs from that of cultivated plants. This is usually attributed to the different growing conditions and reduced exposure to stress such as limited water and nutrients, excessive wind, predation and competition from other vegetation. Since the levels of other compounds were not investigated, all that can be concluded is that the antiplasmodial component in *H. procumbens* was concentrated in the roots and that the cultivated plants displayed greater antiplasmodial activity than the wild harvested material.

4.3.2 Isolation of the active compounds 56 and 60

Bioassay-guided fractionation using solid phase extraction led to the isolation of the compounds **56** and **60**. Although the active SPE fractions 56% ACN and 60% ACN were not pure compounds, HPLC analysis and NMR experiments showed that the fractions were sufficiently (>80%) pure for structure elucidation and *in vitro* testing. Both **56** and **60** had very similar retention times and identical UV spectra, suggesting common structural features. This is not surprising since many plant compounds exist as biosynthetically related metabolites.

The SPE separation techniques were more effective, in terms of the number of steps involved in isolating pure compounds, compared to flash chromatography followed by HPLC, which was initially used. The improvement in separation methods and increased yields of the active components in the cultivated *H. procumbens*, facilitated the isolation of **56** and **60**. Although the yields were improved, they were still relatively low at 0.015 – 0.033% by weight of the powdered root material. In the extraction procedure the powdered roots were exhaustively extracted with PE to effect maximum removal of the active components. Since the extraction and separation procedures were optimised and the yields remained low, the antiplasmodial component was probably a minor constituent of the root material. Unless the yields can be greatly improved by manipulating the growing conditions, selecting for a favourable chemotype or interfering with the biosynthetic pathway of the active components, the *H. procumbens* roots are not a viable source of the isolated antiplasmodial compounds. Despite the low yields, the quantities isolated of the compounds **56** and **60** were sufficient for structure elucidation.

4.3.3 *In vitro* antiplasmodial activity and cytotoxicity of 56 and 60

The compounds **56** and **60** were tested for *in vitro* antiplasmodial activity against five strains of *P. falciparum*. Of the strains used, D10 and 3D7 had IC_{50} values consistent with CQ-sensitive parasites and K1, W2 and RSA11 had IC_{50} values consistent with CQ-resistance. The difference in CQ sensitivity of the strains was greater than 15 fold. However, the isolated compounds were equally active against the sensitive and resistant strains, and showed no cross-resistance with CQ. This would suggest either an alternative mechanism of action for compounds **56** and **60**, or an ability to circumvent resistance. Both of which would warrant further investigation as potential antimalarials. Furthermore, **56** and **60** have very different structural features to any of the current antimalarial drugs.

By comparing the structures of **56** and **60**, the position of the isopropyl and hydroxyl group does not appear to influence the antiplasmodial activity, but at this stage there is insufficient data to make definite conclusions about the structure-activity relationships. Although the compounds are not as active as CQ, structure-activity studies could identify desirable modifications to optimise their activity.

The 5 strains used in the study showed slightly different sensitivities to the isolated compounds, which were not correlated with their CQ sensitivity. As indicated by the P values obtained from the Mann-Whitney test, compounds **56** and **60** were equipotent against strains D10, 3D7, K1 and RSA11. A statistically significant difference in activity was observed in the W2 strain, with compound **60** being more potent than **56**. The majority of the IC_{50} values obtained were less than $1\mu gml^{-1}$, with the exception of the 3D7 strain that seemed to be less sensitive to **56** and **60** compared to the rest of the strains. Since very little is known about the genotype of the individual strains, no inferences could be made regarding their varying susceptibility to the isolated compounds.

The cytotoxicity assays against CHO and HepG2 cells revealed that **56** and **60** were selectively active against the *P. falciparum* strains. These observations were confirmed by the selectivity index values, which indicated that the compounds were approximately 55 times more potent against *P. falciparum* strains than the mammalian cell lines. One of the problems in discovering antiplasmodial drugs is that the parasites share many biochemical pathways with the human host, making it difficult to identify compounds with selective activity (Kirby, 1996). At relatively low concentrations, compounds **56** and **60** were sufficiently selective to kill the parasites without damaging mammalian cells. While these results are promising in terms of antiparasitic action and lack of toxicity, compounds **56** and **60** would have to be subjected to extensive *in vivo* toxicity tests before host toxicity could be assessed. In conclusion, both compounds **56** and **60** showed significant antiplasmodial activity against various *P. falciparum* strains, and minimal cytotoxicity to the two mammalian cell lines.

4.3.4 Occurrence of compounds 56 and 60 and their reported biological activities

Compound **56** has previously been isolated from the plant *Podocarpus nagi* as well as being identified as a pyrolysis product of maytenone and has served as an intermediate in

the sythesis of totarane-like structures. In the early 1960s a bisditerpene maytenone (Figure 4.3.4.1) was isolated from the root bark of the tree *Maytenus dispermus* (Johnson *et al.*, 1961). Whilst characterising the compound, it was found that it decomposed on melting to give propene and a mixture of a C_{20} and a C_{17} catechol. Through chemical analysis, the former was identified as 8-isopropylpodocarpane-6,7-diol (**56**). Later work confirmed the identity of the C_{20} catechol by synthesising **56** and proving it to be identical with the pyrolysis product of maytenone (Elmore and King, 1961).

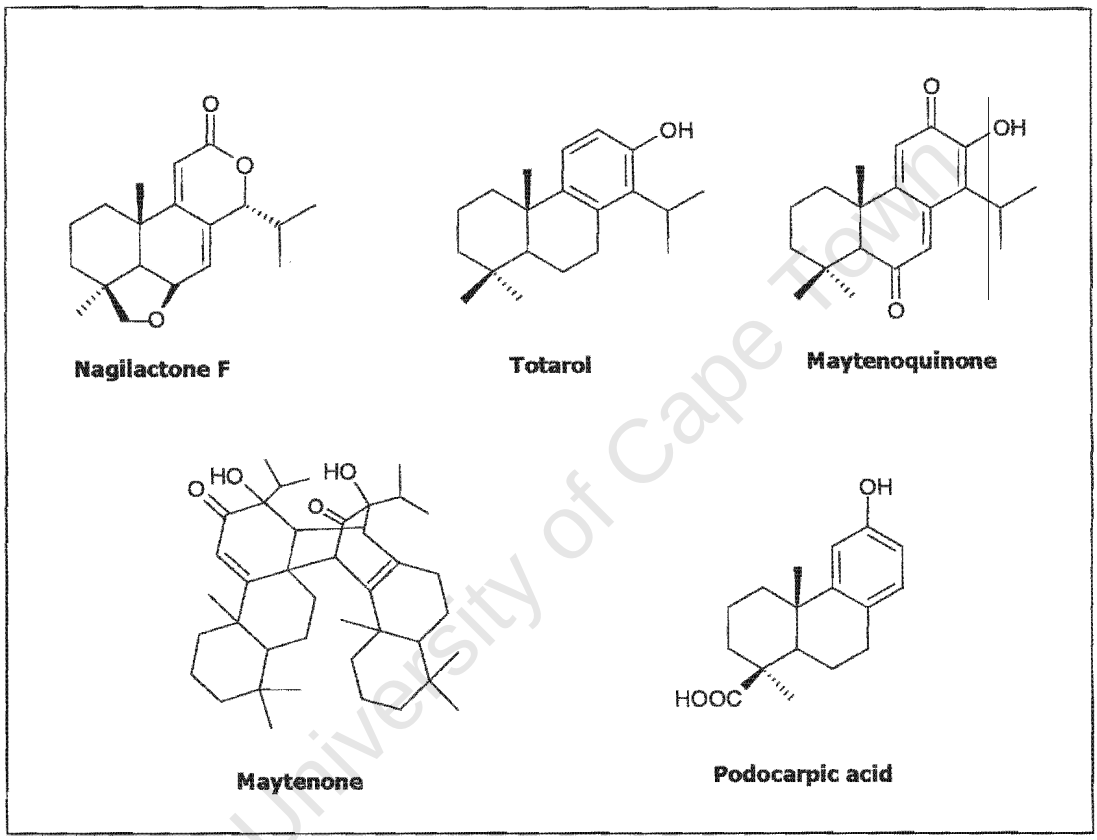

Figure 4.3.4.1. Structures of a nagilactone, totarol, maytenone, maytenoquinone and podocarpic acid

A few years later, **56** was isolated from *Podocarpus nagi* along with a series of nagilactones (Hayashi *et al.*, 1967). This research focused on the isolation and structure elucidation of the nagilactones, which were found to possess a totarane-like skeleton (Figure 4.3.4.1). Since compound **56** was reported to co-occur with the nagilactones in *P. nagi,* it was proposed that it was a biogenetic precursor of the nagilactones. The nagilactones have been isolated from various species of *Podocarpus*, and form an important class of compounds due to their antitumour activity (Hayashi *et al.*, 1975). On

account of this activity, efforts were directed towards their synthesis. One of the studies modelled the synthetic route on the previously proposed biogenetic pathway that involved compound **56** (Cambie *et al.*, 1982). This resulted in **56** being synthesised from totarol (Figure 4.3.4.1), and chemically characterised as an intermediate. Compound **56** has also been reported as an intermediate in the synthesis of maytenoquinone (Figure 4.3.4.1), (Burnell *et al.*, 1988). Maytenoquinone is another diterpene isolated from the root bark of the tree *Maytenus dispermus* (Martin, 1973). In this study **56** was generated from podocarpic acid (Figure 4.3.4.1) and was characterised by ^{1}H and ^{13}C NMR. Although compound **56** has previously been isolated, characterised and prepared as an intermediate in the above mentioned reactions and variations thereof, its biological activity was not examined in any of these studies.

Only recently was the biological activity of compound **56** investigated as part of a larger study on the synthesis and antibacterial activity of totarol derivatives (Evans *et al.*, 2000). The phenolic diterpene totarol has been shown to exhibit significant antibacterial activity (reviewed in Chapter 5), and as a result of the interest in the development of new antibiotics, research was aimed at identifying the structural features on which the biological activity depends (Evans *et al.*, 1999 and Evans *et al.*, 2000). This involved the synthesis of various analogues of totarol, including compound **56**, and evaluating their activity in drug resistant bacteria. The results of this study are summarised in Table 4.3.4.1. The antibacterial properties of totarol and **56** indicated that the derivatization of the aromatic ring of totarol at C-12 (to generate **56**) had an undesirable effect on its *in vitro* activity.

Table 4.3.4.1. Minimum inhibitory concentrations, MIC μgml^{-1} (values in brackets are μM) of totarol, **56** and **60** against drug resistant bacteria

	MIC μgml^{-1} (μM)			
Compound	***Enterococcus faecalis*** ^{GR}	***Streptococcus pneumoniae*** ^{PR}	***Staphylococcus aureus*** ^{MR}	***Klebsiella pneumoniae*** ^{MDR}
Totarol	2 (7)	2 (7)	2 (7)	>32
56	32 (106)	8 (26)	8 (26)	>32
60	8 (28)	2 (7)	8 (28)	>32

^{GR} Gentamycin resistant, ^{PR} Penicillin resistant, ^{MR} Methicillin resistant, ^{MDR} Multi-drug resistant. *K. pneumoniae* is Gram-negative and the other bacteria used are Gram-positive. References (Evans *et al*, 1999) and (Evans *et al*, 2000)

This research also included compound **60** (ferruginol) as an analogue of totarol (Evans *et al*, 1999). Compared to totarol, **60**'s antibacterial activity was equipotent for one of the bacterial strains, and was reduced by a factor of 4 for the other two Gram-positive bacteria. In these studies none of the generated analogues retained totarol's potency against all 3 Gram-positive bacteria. The ferruginol (**60**) for this investigation was synthesised from ferruginyl benzoate, hence the reported antibacterial activity was that of racemic (±)-ferruginol. A recent report described the enantioselective synthesis of (+) and (–)-ferruginol and their respective *in vitro* antibacterial activity (Yang *et al*, 2001). The activity against drug resistant Gram-positive bacteria is listed in Table 4.3.4.2. The results suggested that the unnatural (–)-ferruginol was more potent than both the natural (+) and racemic (±)-ferruginol. For comparative purposes, the ferruginol (**60**) isolated from *H. procumbens* in this study was dextrorotatory (+).

Table 4.3.4.2. Minimum inhibitory concentrations (MIC) values of synthesised (+), (–) and (±)-ferruginol against MRSA644 and VREVanc

	MIC $\mu g ml^{-1}$	
Compounds	**MRSA644**	**VREVanc**
(±)-ferruginol	125	62.5
(+)-ferruginol	>125	>125
(–)-ferruginol	62.5	31.3

MRSA644- methicillin resistant *Staphylococcus aureus*, strain 644. VREVanc-vancomycin resistant Enterococcus Reference (Yang *et al.*, 2001)

The actual MIC value obtained for the (±)-ferruginol in Table 4.3.4.1 differs considerably from that in Table 4.3.4.2 and could be attributed to the different *in vitro* experimental approaches used in the different studies.

Besides the above mentioned synthesis of ferruginol, the naturally occurring (+)-ferruginol has been isolated from a number of plants, namely *Torreya nucifera* (Harrison and Asakawa, 1987), *Thuja plicata* (Sharp *et al.*, 2001), *Taiwania cryptomerioides* (He *et al.*, 1997) as well as from several species of *Salvia* including, *S. syriaca* (Ulubelen *et al.*, 2000), *S. apiana* (González *et al.*, 1992), *S. viridis* (Ulubelen *et al.*, 2000), *S. candidissima* (Ulubelen *et al.*, 1992), *S. sclarea* (Ulubelen *et al.*, 1993), *S. miltiorrhiza* (Nakanishi *et al.*, 1983), *S. lanigera* (Aboul-Ela and El-Lakany, 2000) and *S. hypargeia* (Ulubelen *et al.*, 1988). In the majority of the studies on the *Salvia* species, the roots were investigated

and yielded ferruginol in addition to several other abietane-type diterpenes. Species of the genus *Salvia* have been credited with medicinal properties in many parts of the world and have been reported to possess antibacterial (Martinez-Vazquez *et al*, 1998), antiviral (Tada *et al.*, 1994), antifungal (Kalemba, 1999), antihypertensive (Ulubelen *et al.*, 2000), antioxidant (Malencic *et al.*, 2000) and antitumour activity (Ulubelen *et al*, 1992). Despite their pronounced biological activities, an extensive literature search showed that the antiplasmodial activity of the *Salvia* species has not been reported.

In addition to the antibacterial activity, several other biological studies have been performed on the ferruginol isolated from these natural sources. Using an experimental rat model, ferruginol was found to exhibit antihypertensive activity by reducing blood pressure as much as the positive controls regitine and propranolol (Ulubelen *et al.*, 2000). Ferruginol has also shown interesting bioactivities in the brine shrimp lethality test (BST) for antitumour compounds, the yellow fever mosquito (YFM) microtitre plate assay for pesticides, and in cytotoxicity tests against 3 human solid tumour cell lines (He *et al*, 1997). The results of these tests are summarised in Table 4.3.4.3. Ferruginol displayed moderate activity in the BST test and was selectively toxic against human colon adenocarcinoma (HT-29). Only slight cytotoxicity was observed for the other cell lines. In the YFM assay, ferruginol did not show significant (LC_{50} <1 μgml^{-1}) activity as a lead for insecticide development. Although the activity of ferruginol (**60**) has been evaluated in a range of biological assays, there have been no reports on its antiplasmodial activity to date.

Table 4.3.4.3. Activity and cytotoxicity of ferruginol in the BSL, YFM assays and against human tumour cells

	LC_{50} μgml^{-1}		ED_{50} μgml^{-1}		
Compound	**BST[a]**	**YFM[b]**	**MCF-7[c]**	**A-54[d]**	**HT-29[e]**
Ferruginol	9.4	2.0	13.05	11.09	7.78×10^{-1}
Adriamycin[f]	-	-	1.89×10^{-1}	4.99×10^{-3}	3.57×10^{-1}

[a] Brine shrimp lethality test, [b] Yellow fever mosquito larvae test, [c] Human breast cancer carcinoma, [d] Human lung carcinoma, [e] Human colon adenocarcinoma, , [f] the standard positive control. Reference: (He *et al.*, 1997)

In conclusion, both **56** and **60** have previously been isolated from plants and several studies have described their synthesis. However, this is the first report of the isolation of **56** and **60** from *H. procumbens*. Furthermore, a few biological activities of the

compounds have been published, but no antiplasmodial properties have been documented, to the best of my knowledge.

4.3.5 Reported abietane diterpenes with antiplasmodial activity

Many of the abietane diterpenes extracted from natural sources have displayed intrinsic antimicrobial activity. A thorough literature search revealed that a single abietane-type ester, 3-O-benzoylhosloppone (Figure 4.3.5), as well as four tanshinones, including cryptotanshinone (Figure 4.3.5), with abietane-type skeletons have been shown to possess *in vitro* antiplasmodial activity.

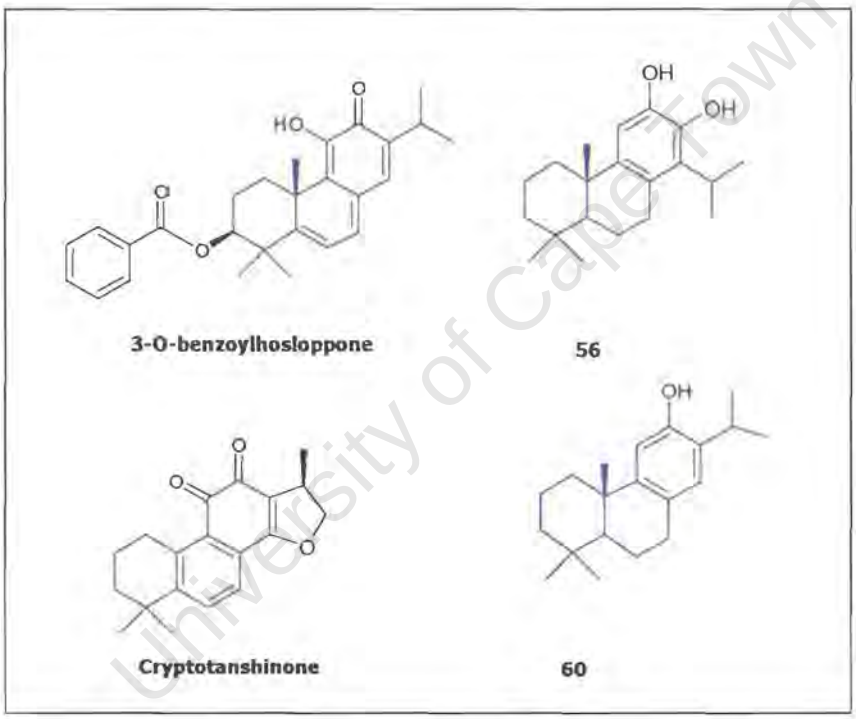

Figure 4.3.5. Compound 3-O-benzoylhosloppone, cryptotanshinone, 56 and 60

The compound 3-O-benzoylhosloppone was isolated from a hexane extract of the root bark of the plant *Holsundia opposita* (Achenbach *et al.*, 1992). *H. opposita* is widely distributed in East and West Africa and is traditionally used to treat malaria (Achenbach *et al.*, 1992). The crude extract of the root bark was found to exhibit significant *in vitro* activity against *P. falciparum*, with an IC_{50} value of 5.6μgml^{-1}. Purification of the extract led to the isolation of 3-O-benzoylhosloppone, which showed *in vitro* activity against both a CQ-resistant strain K1 (IC_{50}=0.40μgml^{-1}) and a CQ-sensitive strain NF54 (IC_{50}

=0.22μgml^{-1}). Although three other abietane-type esters were isolated from the extract, the yields were extremely low and the quantities were not sufficient for antiplasmodial testing (Achenbach *et al.*, 1993).

The other abietane-type compounds that have been shown to possess antiplasmodial activity are tanshinones. Tanshinones are norditerpenes with an abietane-type skeleton containing a quinone moiety. In recent work four tanshinones were isolated from the plant *Pervoskia abrotanoides* (Sairafianpour *et al.*, 2001) and were tested for *in vitro* antiplasmodial activity. All of the compounds showed moderate activity against a CQ-sensitive strain of *P. falciparum* (3D7), with IC_{50} values in the range of 12 - 27μM. The IC_{50} value of cryptotanshinone (illustrated in Figure 4.3.5) was 12.5μM compared to compounds **56** and **60** that had IC_{50} values of 4 - 6μM against the 3D7 strain. In addition to antiplasmodial activity, the isolated tanshinones were found to exhibit leishmanicidal activity. These findings support the use of *P. abrotanoides* in Iranian folk medicine to treat leishmaniasis (Sairafianpour *et al.*, 2001). Even though leishmaniasis and malaria are both protozoal diseases, they are caused by different protozoa and have little in common.

The *in vitro* antiplasmodial activity displayed by 3-O-benzoylhosloppone was comparable to that of compounds **56** and **60**, whereas the tanshinones were slightly less active. Common structural features of the compounds, illustrated in Figure 4.3.6, suggest that the position of the isopropyl and hydroxyl group as well as the addition of a benzoyl group does not influence the activity. The reduced potency of the tanshinones could be due to the loss of an isopropyl and hydroxyl group or a result of the addition of a quinone moiety. Although these studies give some indication of structure-activity relationships, a more detailed investigation would be required to identify the essential structural elements responsible for the antiplasmodial activity. In order to modify **56** and **60** for structure-activity studies, sufficient quantities of the relatively pure compounds would be required.

4.3.6 Commercial availability of compounds 56 and 60

Due to the very low yields of compounds **56** and **60** from *H. procumbens*, an alternative source of the compounds was investigated for further work. Several reports have described the synthesis of both **56** and **60**, however the synthetic routes were extremely complicated and involved numerous steps. Besides trying to extract more of the compounds from plant material, the other alternative was a commercial supply of **56** and

60. On-line searches of chemical catalogues showed that neither compound **56** nor **60** were readily available. The closest match was the analogue totarol, which could be purchased at a price of US$300 per gram. Since the structure of totarol was very similar to **56** and **60**, a few hundred milligrams were purchased with the objective of; i) testing it for antiplasmodial activity and ii) using it for chemical modification to generate leads of compounds **56** and **60**.

4.4 Conclusion

In this chapter, the roots of cultivated *H. procumbens* were shown to possess *in vitro* antiplasmodial activity. A purification process for the crude plant extract was developed, and led to the isolation of two active compounds (+)-8,11,13-totaratriene-12,13-diol (**56**) and (+)-8,11,13-Abietatrien-12-ol (**60**), which were identified using HREIMS and detailed NMR experiments. Although both of the compounds have previously been isolated from plants and synthesised, this if the first report of their isolation from *H. procumbens*. Furthermore, the antiplasmodial properties of these compounds have not been investigated before. The isolated compounds were found to have selective *in vitro* antiplasmodial activity against drug resistant and sensitive strains of *P. falciparum*. While previous work on the *in vitro* antiplasmodial activity of more complex abietane-type diterpenes suggest some structure-activity relationships, a more detailed investigation would be required to determine the features of the compound responsible for the activity.

In addition to their potent antiplasmodial activity and low cytotoxicity, the isolated compounds are structurally different to any of the current antimalarials. The activity of these hits could be optimised using traditional medicinal chemistry to generate lead compounds for antimalarial drug development. To address structure-function studies and synthesise potential leads of the isolated compounds, an analogue (totarol) of the compounds was obtained for chemical modification.

Chapter 5

Synthesis and Activity of Totarol Derivatives

5. The Synthesis and *In Vitro* Antiplasmodial Activity of Totarol Derivatives

5.1 Introduction

Due to the low yields of the active compounds isolated from *H. procumbens*, the analogue totarol was obtained from commercial sources for chemical modification purposes. The isolation, characterisation, synthesis and biological activity of totarol has been studied extensively and will be reviewed in this chapter. In addition to reviewing the previous work on totarol, this chapter describes the synthetic approach used to generate some totarol derivatives. The characterisation and evaluation of *in vitro* antiplasmodial activity and cytotoxicity of these novel derivatives is also reported.

5.1.1 Totarol – structure determination and occurence

Totarol, a naturally occurring phenolic diterpene, was first isolated from the heartwood of the *Podocarpus totara* tree (Easterfield and Mcdowell, 1911). The preliminary studies on totarol resulted in the correct analysis of $C_{20}H_{30}O$, and highlighted the fact that no other compound had ever been cited in the chemical literature with this formula (Easterfield and McDowell, 1915). On the basis of a series of chemical degradations and spectroscopic work, the structure of totarol (Figure 5.1.1.1.) was determined (Short *et al.*, 1951). Confirmation of this structure was provided by the total synthesis of the racemate (±)-totarol, whose IR spectrum was identical to that of the naturally occurring (+)-totarol (Barltrop and Rogers, 1958).

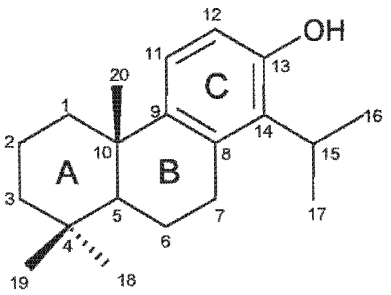

Figure 5.1.1.1. Chemical structure of (+)-totarol (8,11,13-Totaratrien-13-ol)

The ^{1}H-NMR spectroscopic data for totarol was first measured in 1964 (Brieskorn *et al.*, 1964), followed by the ^{13}C-NMR data, which was studied in 1969 (Wenkert *et al.*, 1969). Prior to 1991, there was no complete set of ^{1}H-NMR data for totarol as most of the ^{1}H signals of the A and B rings overlapped. However, Ying and co-workers managed to obtain resolved signals at 500MHz and used 2D NMR experiments to provide evidence for all the proton assignments (Ying *et al.*, 1991). In addition to the NMR data, the mass spectra and fragmentation pathways of totarol have been described (Enzell, 1966). The mass spectral fragmentation patterns serve as a 'molecular fingerprint' as each compound fragments in a unique way. Figure 5.1.1.2. shows the breakdown pattern of totarol, which was established through investigation of a series of deuterated totarol derivatives (Enzell, 1966).

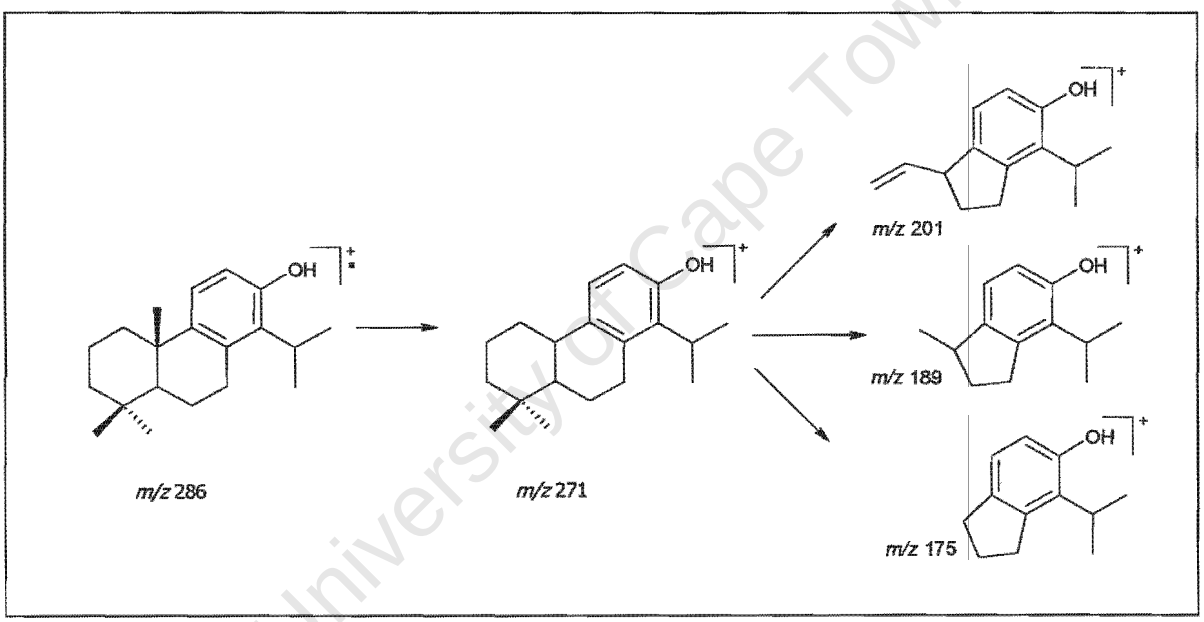

Figure 5.1.1.2. Fragmentation pathway of totarol

Totarol has been isolated from a large variety of plants, including several species of *Podocarpus*, *Dacrydium*, *Cupressus* and *Juniperus* (Detailed review: Bendall and Cambie, 1995). The most abundant source of totarol appears to be the heartwood of the tree *Podocarpus totara*, which is indigenous to New Zealand. The hexane extract of *P. totara* has been reported to yield 5.07% totarol, by weight of the dry timber (Cambie and Mander, 1962). Along with totarol, a number of oxygenated derivatives, biphenyl dimers and analogues, including ferruginol, were extracted from a large number of the plants (Bendall and Cambie, 1995). Since these derivatives have been found to co-occur naturally with totarol, it is believed that they share a common biosynthetic pathway.

5.1.2 Biogenesis and total syntheses of totarol

Diterpene biogenesis generally occurs by ring closure of geranyl geranyl pyrophosphate to produce a labdane skeleton. This structure can then undergo methyl group migration followed by oxidation and aromatization to yield a typical diterpene such as ferruginol, with the isopropyl group at the C-13 position (Figure 5.1.2.1), (Geissmann and Crout, 1969).

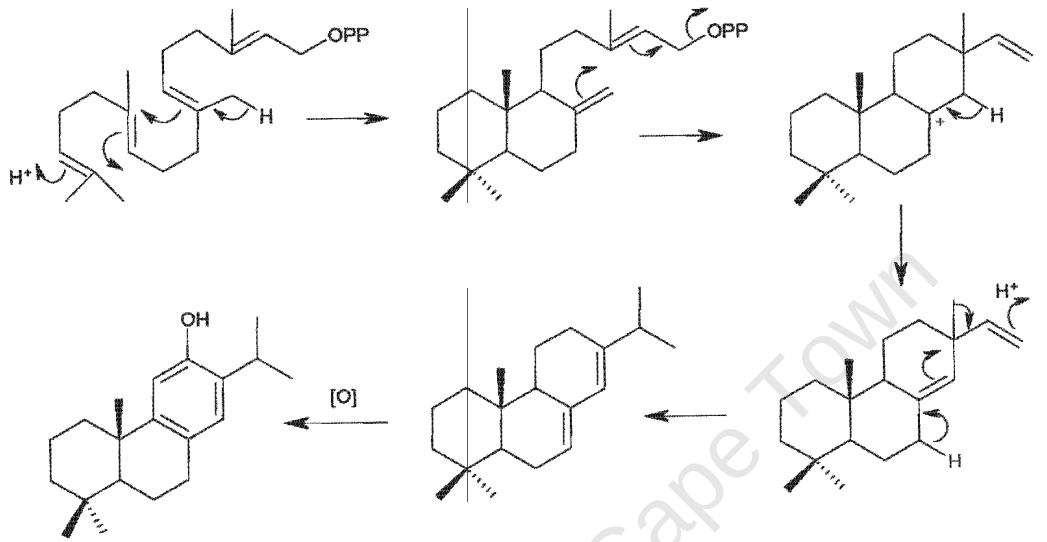

Figure 5.1.2.1. Proposed biogenetic pathway of ferruginol

In totarol the isopropyl group is located at the C-14 position, which could be achieved by a rearrangement of ferruginol. An additional pathway was then proposed for the biogenesis of totarol from ferruginol (Figure 5.1.2.2.), (Wenkert and Jackson, 1958).

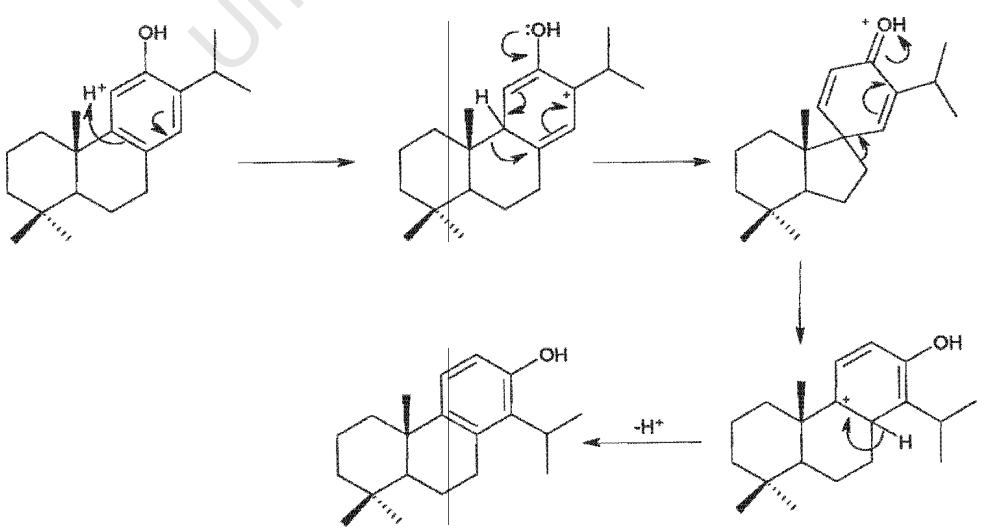

Figure 5.1.2.2. Proposed biogenetic pathway of totarol

The isopropyl group of totarol exerts steric hindrance upon the phenolic group at C-13, giving the molecule unique chemistry. This was first observed by Short and colleagues who realised that totarol is unable to take part in intermolecular hydrogen bonding like ordinary phenols (Short *et al.*, 1951). Furthermore, the steric crowding of the phenolic group also decreases the apparent polarity of totarol (Bendall and Cambie, 1995) as well as the relative reactivity of the phenolic group (Matsumoto *et al*, 1977 and 1978).

In addition to the biogenetic pathway, four total syntheses of totarol have been reported (Detailed review: Bendall and Cambie, 1995). The initial interest in totarol was due to its novel structure, non-conventional reactivity and chemical properties. At a later stage, the biological activity of totarol derivatives, particularly the nagilactones, made totarol an attractive target for synthesis. Of the four different synthetic routes reported, only one of them was enantioselective and described the synthesis of the natural (+)-totarol (Matsumoto and Suetsugu, 1979).

5.1.3 Biological properties of totarol

5.1.3.1 *In vitro* antibacterial activity

The antimicrobial activity of totarol has been investigated along with 5 other diterpenoids isolated from *Podocarpus nagi*. Totarol, the most abundant of the compounds, was found to exhibit significant *in vitro* antibacterial activity against various Gram-positive bacteria (Table 5.1.3.1), but was not active against Gram-negative bacteria or fungi (Kubo *et al.*, 1992).

Table 5.1.3.1. *In vitro* antibacterial activity of totarol and penicillin

	MIC $\mu g ml^{-1}$	
Bacterium	**Totarol**	**Penicillin G**
Bacillus subtilis	1.56	50
Brevibacterium ammoniagenes	0.78	0.39
Staphylococcus aureus ATCC 12598^{S}	1.56	0.049
Staphylococcus aureus ATCC 29247^{R}	0.78	>800
Streptococcus mutans	0.78	0.049
Propionibacterium acnes	0.39	0.012

^{S} Penicillin-sensitive strain. ^{R} Penicillin-resistant strain. Reference: (Kubo *et al.*, 1992)

In light of the potent antibacterial activity of totarol, efforts were directed towards identifying the structural features on which the activity depends. A series of studies on the activity of totarol and its derivatives showed that out of 72 synthesised derivatives, none were more potent than totarol itself (Evans *et al.*, Part 1 – 1999, Part 2 – 2000 and Part 3 - 2000). The results of this research were evaluated in terms of structure-activity relationships and revealed that; (i) a phenolic moiety was essential for antibacterial activity, (ii) derivatization at C-12 had an undesirable effect on antibacterial activity, (iii) lipophilic substitutions at C-12 diminish activity and (iv) the most active compounds examined all possessed a primary or secondary alkyl substitution in the *ortho* – position to the hydroxyl group.

In addition to intrinsic antibacterial activity, totarol has also been reported to reduce the MIC of methicillin against methicillin-resistant *Staphylococcus aureus* (MRSA). The MIC of methicillin was reduced 8-fold when combined with 1μgml^{-1} of totarol (MIC of totarol in MRSA = 2μgml^{-1}), (Nicolson *et al.*, 1999). The ability of totarol to enhance the activity of methicillin against MRSA expands the arsenal of antibiotics against drug resistant bacteria. This could prove to be useful in countering the increasing problem of bacterial resistance to antibiotics.

5.1.3.1.1. Mode of antibacterial action of totarol

Considering totarol's antibacterial activity, attempts have been made to understand its molecular mechanism of action. From mode of action studies on antibiotic diterpenes structurally related to totarol, it was proposed that the activity was due to the inhibition of DNA (Kobayashi *et al.*, 1989) and peptidoglycan synthesis (Kobayashi *et al.*, 1988). However, other researchers have reported that totarol does not inhibit the synthesis of DNA or peptidoglycan in *S. aureus*, but reduces the respiration rate by 70% (Nicolson *et al.*, 1999). These findings are supported by research on the antioxidative properties of totarol, which revealed that the compound inhibits oxygen consumption and respiratory-driven proton translocation in Gram-negative bacteria cells (Haraguchi *et al.*, 1996). Furthermore, recent experiments by Evans and colleagues have shown that totarol modestly uncouples oxidative phosphorylation in isolated mitochondria. This led to the proposal that totarol disrupts bacterial energy metabolism by increasing the proton permeability of the membrane, either by acting as an uncoupler or by disrupting the membrane (Evans *et al.*, Part 3 – 2000).

To determine the nature of the interaction and location of totarol in a biomembrane model system, the intrinsic fluorescent properties of totarol were studied in aqueous and phospholipid phases (Mateo *et al.*, 2000). The results showed that totarol has a preference for phospholipid systems and is located in the inner region of the membrane, away from the phospholipid/water interface. These observations suggest that the action of totarol is mediated through its interaction with membranes by disturbing the membrane structure. Although the primary bacterial target for totarol appears to be the respiratory chain, further research is required to define the specific site of action.

5.1.3.2 *In vitro* cytotoxicity

To further assess the potential of totarol as an antibiotic, the cytotoxicity was evaluated against against 3 human cell lines at concentrations of 21, 14 and 7μgml^{-1} (Evans *et al.*, Part 1 – 1999). The results are summarised in Table 5.1.3.2.

Table 5.1.3.2. *In vitro* cytotoxicity of totarol

Compound	[μgml^{-1}]	[μM]	Cell Growth (%)		
			CH 2983	HeLa	MG 63
Totarol	21	73	36	13	15
Totarol	14	49	103	96	97
Totarol	7	25	115	106	105

CH 293 – Human fibroblasts, normal diploid strain. HeLa – carcinoma cell line. MG 63 – osteosarcoma cell line. Reference: (Evans *et al.*, 1999)

From this study it was concluded that totarol was not significantly cytotoxic and that the MIC against multidrug resistant bacteria was 7-fold lower than the minimum concentration at which cytotoxicity was evident.

5.1.3.3 Hypocholesterolemic activity

Totarol has also been shown to exhibit *in vivo* hypocholesterolemic activity in a rat model (Enomoto *et al.*, 1977). It was suggested that this occurred mainly by inhibition of cholesterol absorption from the intestines and possibly by stimulation of cholesterol excretion or catabolism.

A thorough literature search on the biological activity of totarol revealed that its antiplasmodial properties have not been studied.

5.1.4. Summary

Totarol has been isolated from several species of plants and is well characterised in terms of NMR data, high-resolution mass spectrum and the fragmentation pathway. In addition to the proposed biogenesis of totarol, the total synthesis has been described. The positioning of the substituents on totarol give the molecule unique properties, reactivity and biological activity. Several studies have shown that totarol exhibits potent *in vitro* antibacterial activity, although the molecular mechanism of action remains unclear.

Combined with the facts that the compound has previously been characterised, shows little toxicity, is commercially available and is structurally similar to compounds **56** and **60**, totarol is an ideal candidate for chemical modification to generate potential leads of compounds **56** and **60**.

5.2 Hit development

In the previous chapter, two hit compounds with *in vitro* antiplasmodial activity were isolated and identified. The compounds were very similar in structure and represent biologically privileged scaffolds for antimalarial drug discovery and development. The ultimate objective would be to improve these hits such that their profile of characteristics fulfils criteria for pre-clinical candidates (Table 1.8 – Introduction). The parameters that are focused on in this process are the potency, selectivity, absorption, distribution, metabolism and toxicity (Wess *et al.*, 2001). The aim of this study is to develop the hits into promising lead compounds with an initial focus on the *in vitro* antiplasmodial activity, potency, selectivity and cytotoxicity.

5.2.1 Hit modification

Usually only a small part of a hit compound interacts with the biological target. These structural elements (substructures) that are responsible for activity are collectively known as the pharmacophore (Silverman, 1992). One approach to identifying the pharmacophore is to dissect the molecule to determine which sections are essential for activity. Although this was not accomplished in this study, the possible general features of the pharmacophore were identified by comparing the common structural features of

compounds **56** and **60** with the previously reported abietane diterpenes with antiplasmodial activity (Figure 4.3.6 – Chapter 4).

Once the pharmacophore has been established, the next stage of lead development involves functional group modification. Since there is a relationship between the molecular structure of a compound and its activity, functional group modification usually provides structure-activity information. A multitude of chemical modifications can be made when considering functional group modification. As opposed to a random process to optimise potency, a rational approach was used in this study. In deciding the nature of the synthetic modifications to be made, chemical features known to be present in existing antimalarial agents were considered.

5.2.2 Modification of totarol

As mentioned in section 5.1, due to the low yields of compounds **56** and **60**, totarol was used as the scaffold for chemical modification. The initial objective was to prepare compounds **56** and **60** for subsequent modification from totarol. The isolated compounds and totarol have a limited number of reactive sites at which further chemical modifications could be carried out. Since the isopropyl group exerts steric hindrance upon the adjacent phenolic group (Matsumoto *et al.*, 1977 and 1978), it was presumed that if the hydroxyl group was at position C-12, as for compounds **56** and **60**, further steric hindrance would be encountered from ring-A and B substituents when trying to further functionalise these compounds at this position. For this reason, totarol was used directly to generate leads of compounds **56** and **60**. An additional consideration was that the conversion of totarol to **60** involves several steps, which may decrease the yield of the ultimate product. Coupled with the fact that only a small amount of totarol was available for exploratory studies, a more efficient means of lead generation was decided on.

There are many potential classes of totarol derivatives that could be targeted, one of them being the β-amino alcohols. The rationale for choosing this class of derivatives is based on the fact that the β-amino alcohol moiety is present in a number of potent antimalarial drugs such as quinine and other quinolylcarbinol amines (Fishman and Cruickshank, 1968). The combination of a potentially active substructure with a biologically relevant structure (totarol) could create a hybrid of two active motifs in addition to generating chemical diversity.

One common method for accessing β-amino alcohols involves opening of an epoxide with amines (Scheme 5.2.2). The wide range of amines commercially and readily available, including anilines, primary, secondary and heterocyclic amines, is particularly attractive for potential generation of diverse libraries of totarol derived β-amino alcohols.

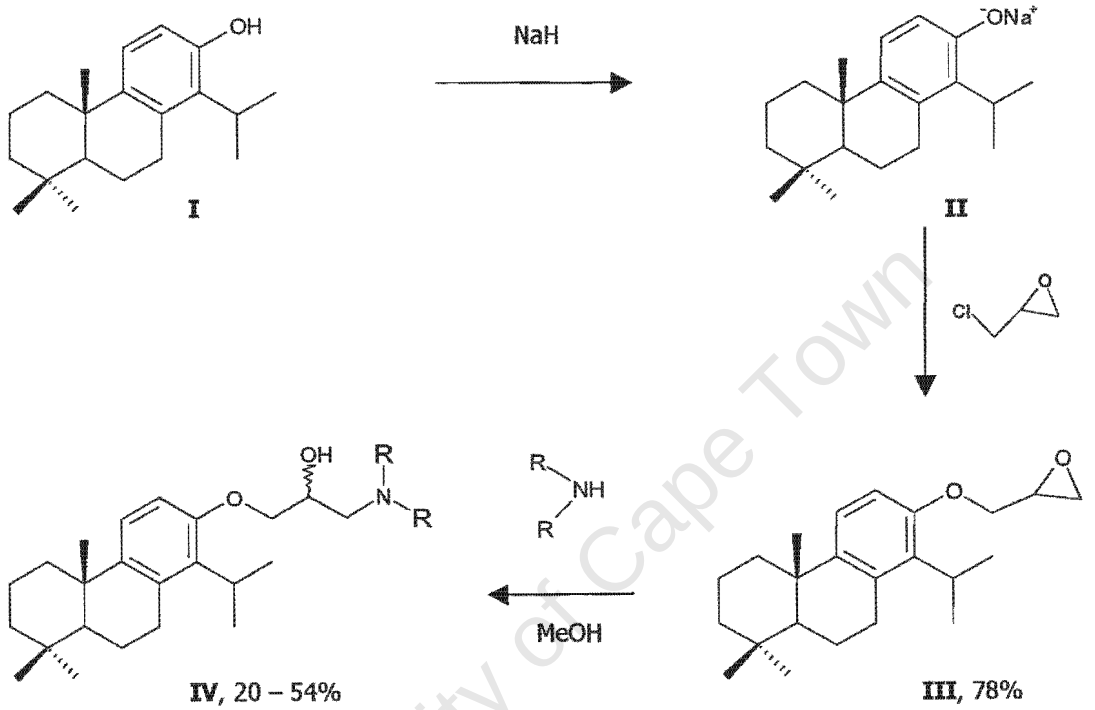

Scheme 5.2.2. Synthesis of totarol derived β-amino alcohols

Where RRNH are:

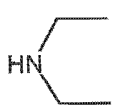

(2)

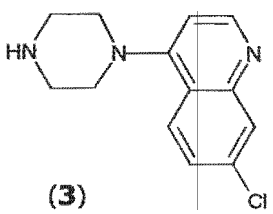

(3)

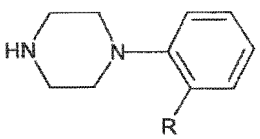

(4) R= H

(5) R=Cl

(6) R=OEt

In this study, the approach to the synthesis of β-amino alcohols involved sodium hydride-mediated generation of a phenoxide anion (**II**), followed by a nucleophillic substitution reaction with epichlorohydrin that gave an intermediate epoxide (**III,** 78%). The epoxide was subsequently reacted with the amines to produce β-amino alcohols of the general structure **IV** (Scheme 1), (Details in Chapter 7, 7.9). All of the synthesised compounds were purified using preparative TLC methods. Although the number of compounds synthesised is not sufficient to make definite conclusions regarding structure-activity relationships, the effect of introducing the β-amino alcohol moiety could be determined. Furthermore, the structural variations of the amines could provide additional structure-activity information for the development of potential leads. These new compounds were characterised by HREIMS as well as 1D and 2D NMR experiments.

5.3 Results

5.3.1 Characterisation of the totarol derivatives

The novel products (Figure 5.3.1.) were characterised by infrared spectroscopy, mass spectrometry (HREIMS) and ^{1}H, ^{13}C, HSQC, HMBC and COSY NMR experiments. The melting point and specific rotation were also recorded. The molecular weight and formula, melting point, specific rotation and IR data for the compounds are listed in Table 5.3.1. The NMR results for totarol, the intermediate epoxide (**1**) and the synthesised compounds **2** – **6** are summarised in Tables 5.3.1.1 - 7. For convenience purposes, the structure elucidation discussion of each compound will follow its respective NMR data table. A summary of the ^{13}C-NMR data for the compounds is also given in Table 5.3.1.8.

The NMR spectrum for the epoxide intermediate and compound **3**, suggested there may be a mixture of stereoisomers (details in discussion), therefore some of the signals appear to be duplicated and have been denoted as either "i or ii" in the NMR tables. NOESY experiments were not performed on any of the compounds. As a result of this, the spatial orientation of geminal hydrogens could not be determined and have been described as either Ha or Hb. The absolute configuration at the newly generated chiral centre (C-22) remains to be established. Hence the compounds are drawn with undefined stereochemistry at this centre. The NMR, HREIMS and IR spectra of totarol and the synthesised compounds are in Appendix 2 (A2.4 - A2.10)

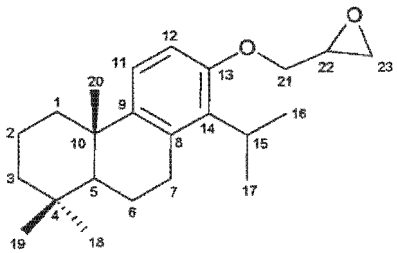

1

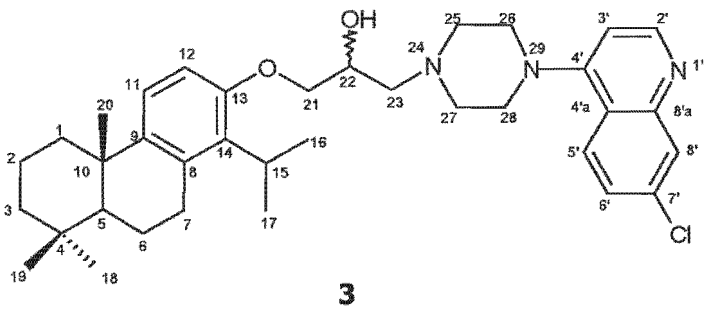

3

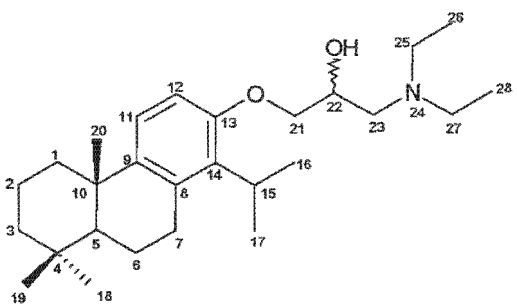

2

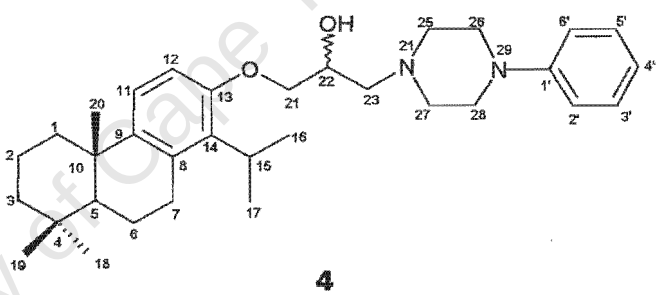

4

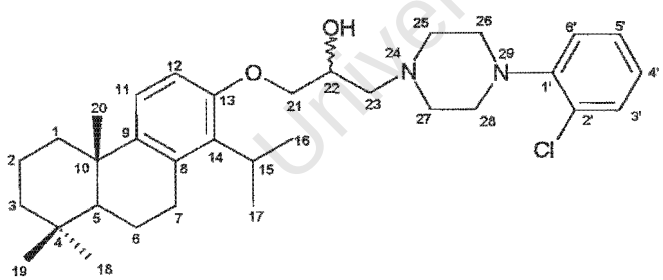

5

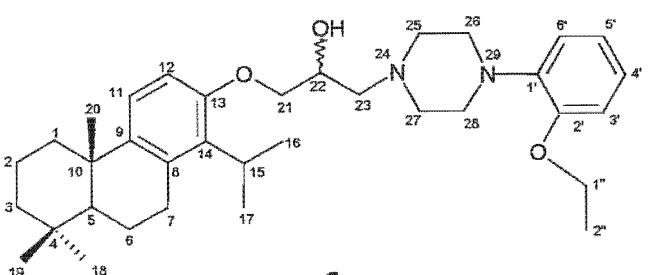

6

Figure 5.3.1. Structures and numbering of the 5 new compounds (**2**-**6**) synthesised from totarol, as well as the epoxide intermediate (**1**)

Table 5.3.1. Compound characterization data for totarol, the epoxide intermediate (**1**) and the compounds **2 - 6**

Compound	Molecular weight	Molecular formula	Melting point /°C	Specific rotation	IR ν_{max} cm^{-1}
Totarol	286.23 (calc.)	$C_{20}H_{30}O$	126 - 127	$[\alpha]_D^{23.0}$ +36.5° ($CHCl_3$, c;10.15)	3435 (OH), 2943, 2867, 1636, 1456, 1271
1	342.25585	$C_{23}H_{34}O_2$	94 - 95	NM	NM
2	415.34612	$C_{27}H_{45}NO_2$	71 - 72	$[\alpha]_D^{26.0}$ +24.4° ($CHCl_3$, c;4.50)	3412 (OH), 2925, 1455, 1260, 1114, 754
3	589.34432	$C_{36}H_{48}N_3O_2Cl$	86 - 87	$[\alpha]_D^{25.3}$ +20.7° ($CHCl_3$, c;10.15)	3400 (OH), 2924, 1575, 1456, 1260, 930, 872, 823, 736
4	504.37256	$C_{33}H_{48}N_2O_2$	50 - 52	$[\alpha]_D^{25.0}$ +24.3° ($CHCl_3$, c;10.29)	3435 (OH), 2925, 1599, 1455, 1263, 928, 802, 738
5	538.33254	$C_{33}H_{47}N_2O_2Cl$	55 - 56	$[\alpha]_D^{25.7}$ +21.8° ($CHCl_3$, c;6.42)	3434 (OH), 2941, 1588, 1479, 1263, 935, 802, 739
6	548.39818	$C_{35}H_{52}N_2O_3$	50 - 51	$[\alpha]_D^{24.2}$ +21.1° ($CHCl_3$, c;10.92)	3434 (OH), 2941,1588, 1479, 1263, 935, 802, 739

NM- not measured, due to insufficient amount of sample. [α] - c ($mgml^{-1}$)

Table 5.3.1.1. ^{1}H, ^{13}C, COSY and NOESY spectral data of totarol. Chemical shifts are in ppm

Position		δ ^{1}H	(J in Hz)	δ ^{13}C	COSY	NOESY
1	α	(1.31 - 1.19)	*m*	39.8	H-1β, H-2β	H-1β, H-2β
	β	2.22	*br d* (12.7)		H-1α, H-2α	H-1α, H-11
2	α	1.48	*dt* (13.5, 3.2)	19.7	H-1β, H-2β, H-3β	H-2β, H-3β
	β	1.76	*dt* (13.5. 3.4)		H-1α, H-2α, H-3α	H-2α, H-19, H-20
3	α	(1.31 - 1.19)	*m*	41.8	H-2β, H-3β	H-2β, H-3β, H-18
	β	1.46	*br d* (13.1)		H-2α, H-3α	H-3α, H-18, H-19
4		-	-	33.5	-	-
5		(1.31 - 1.19)	*m*	49.8	H-6β	H-6β, H-18
6	α	1.91	*dd* (13.2, 7.9)	19.6	H-6β, H-7α	H-6β, H-18
	β	(1.56 - 1.71)	*m*		H-5, H-6α, H-7β	H-6α, H-19
7	α	2.75	*m*	28.9	H-6α, H-7β	H-7β
	β	2.94	*dd* (17.0, 6.2)		H-6β, H-7α	H-7α
8		-	-	134.2	-	-
9		-	-	143.4	-	-
10		-	-	37.9	-	-
11		6.99	*d* (8.6)	123.2	H-12	H-1β, H-12
12		6.53	*d* (8.6)	114.5	H-11	H-11
13		-	-	152.2	-	-
14		-	-	131.2	-	-

*Overlapping signals . ♦Values are interchangeable within the same column

Table 5.3.1.1 (Continued) ^{1}H, ^{13}C, COSY and NOESY spectral data of totarol. Chemical shifts in ppm.

Position	δ ^{1}H	J (Hz)	δ ^{13}C	COSY	NOESY
15	3.29	*sept* (7.1)	27.4	H-16, H-17	H-7β, H-16, H-17
16	1.34♦	*d* (7.1)	20.6♦	H-15	H-15
17	1.35♦	*d* (7.1)	20.6♦	H-15	H-15
18	0.95	*s*	33.5	-	H-3α, H-3β, H-5 H-6α,
19	0.91	*s*	21.8	-	H-2β, H-3β, H-6β, H-20
20	1.18	*s*	25.4	-	H-2β, H-6β, H-19
OH	4.43	*s*	-	-	-

*Overlapping signals . ♦Values are interchangeable within the same column

5.3.1.1 Structure of totarol

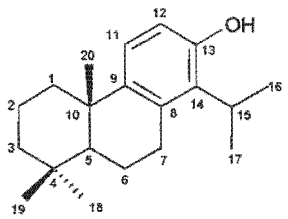

Although complete ^{1}H and ^{13}C NMR assignments of totarol have previously been reported, ^{1}H, ^{13}C, HSQC, COSY and NOESY NMR experiments were still performed to confirm the authenticity of the commercial sample. Furthermore, the identification of the ^{1}H and ^{13}C signals was necessary for interpretation of the spectral data of the totarol derivatives.

The ^{1}H NMR spectrum of totarol closely resembled that of ferruginol (**60**), which would be expected considering the similar structural features. A noticeable difference in the spectra was the multiplicity of the aromatic hydrogens. Furthermore, the carbon resonances in the aromatic region were slightly different, suggesting that the structural diversity was located on the aromatic ring.

The construction of the main skeleton was initiated at the aromatic proton H-11 (δ 6.99), which resonated as a doublet (J=8.6Hz). In the COSY spectrum, H-11 coupled with a doublet at δ 6.53 that was identified as H-12. Complementary evidence for this assignment was provided by the NOESY spectrum, which showed a correlation between H-11 and H-1β. H-12 resonates upfield relative to H-11 due to the mesomeric effect of the hydroxyl group at C-13. The hydroxyl group was identified at δ 4.43 by using a D_2O wash. The septet at δ 3.29 (H-15) coupled (COSY) to two methyl doublets (H-16 and H-17) at δ 1.34 and δ 1.35 indicated the presence of the isopropyl group. The methyl groups CH_3-16 and CH_3-17 are diastereotopic and therefore the chemical shift values are interchangeable. Through the COSY experiment the methyl protons (H-16 and H-17) were linked to H-15, which in turn was correlated to H-7β in the NOESY spectrum. Thus, the position of H-7β was established at δ 2.94. The H-7β proton resonated as a dd (J=17.0 and 6.2Hz) and was coupled to H-7α and H-6β in the COSY spectrum. Based on a molecular model, the dihedral angle between H-7β and H-6α was 90°, therefore no vicinal coupling was observed between these protons. In addition to the COSY coupling with H-7β, the identity of H-7α was established by the HSQC experiment that linked both H-7β and H-7α to the same carbon (C-7, δ 28.9). H-7α appeared as a multiplet at δ 2.75 and since it was coupled to H-7β and H-6α in the COSY spectrum, a dd would be expected for

the multiplicity. Although additional coupling between H-7α and H-6β was not observed in the COSY spectrum, coupling between these protons may contribute to the multiplicity of the H-7α signal. H-6α was identified as a dd (J=13.2 and 7.9Hz) at δ 1.91. The large geminal coupling constant would be due to its interaction with H-6β and the vicinal coupling is from H-7α. Through relevant COSY and NOESY contours, the multiplet that appeared at δ(1.56 – 1.71) was assigned to H-6β. Complementary evidence for this assignment was provided by the HSQC spectrum, which showed that H-6β and H-6α were both attached to a single carbon at δ 19.6 (C-6). The COSY spectrum indicates that H-6β is coupled to H-6α and H-7β, which should afford a dd as the multiplicity. The exact chemical shift value of the H-5 signal could not be resolved as proton signals from H-5, H-1α and H-3α overlapped in the region δ(1.31 – 1.19). NOESY correlations between H-5 and H-18 suggest an α-orientation for H-5. The α-orientation of the H-18 was confirmed by additional NOESY correlations with H-6α. The methyl signals at δ 0.95 and δ 0.91 were assigned to H-18 and H-19 respectively. A β-orientation was assigned to H-19 due to its NOESY correlation with H-6β and H-20. The H-20 signal was identified as a singlet resonating at δ 1.18. The NOESY spectrum displayed correlations between H-20 and H-2β, H-6β and H-19 verifying the orientation of these protons. The broad doublet at δ 2.22 (J=12.7) was assigned to H-1β. In the COSY spectrum, this proton was coupled with H-1α and H-2α, which should give rise to a dd. It is proposed that the splitting due to the vicinal H-2α proton is not resolved, thus only the geminal coupling is observed. As complementary evidence for the orientation of H-1β, a NOESY experiment correlated H-1β with H-11. The HSQC spectrum correlated C-1 (δ 39.8) with H-1β and a multiplet at δ (1.31 – 1.19) that was identified as H-1α. As for compound **60**, a double triplet was observed for H-2β (δ 1.76, J=13.5 and 3.4Hz). From the COSY data of totarol, H-2β was coupled to H-2α, H-1α and H-3α. The fact that H-2β was split into a triplet suggests that H-1α and H-3α appear almost identical to H-2β. A similar phenomenon was also observed for H-2α, which occurred as a double triplet (δ 1.48, J=13.5 and 3.2Hz). The COSY spectrum showed that H-2α was coupled to H-2β, H-1β and H-3β. The broad doublet (δ 1.46) that overlapped with the H-2α signals was assigned to H-3β. Although the COSY spectrum showed coupling between H-3β and H-3α as well as H-3β and H-2α, only the vicinal coupling was evident. The β-orientation of this proton was supported by the NOESY correlation from H-3β to H-18 and to H-19.

In the ^{13}C NMR spectrum, all of the protonated carbon resonances could be assigned from the HSQC spectrum. Although we were not able to obtain an HMBC spectrum for totarol,

the HMBC data from compound **60** coupled to the published NMR data on totarol (Ying *et al.*, 1991) enabled the identification of the five quaternary carbons. The ^{1}H and ^{13}C NMR spectra of totarol were similar to previously reported data (Ying *et al.*, 1991). The most significant differences were the chemical shifts for C-13, which was shifted upfield by approximately 3ppm (from δ 154.9 to 152.2), and the OH signal that was shifted upfield by 6ppm (from δ 10.7 to 4.4). These differences can be attributed to the use of pyridine in the reference experiments and $CDCl_3$ in this study and not to incorrect assignments.

From the NMR data, the structure of totarol was found to be consistent with the expected structure. In addition to the NMR spectra, the melting point 126 - 126°C (Lit. 126 - 128°C – Ying *et al.*, 1991) provided further evidence for the purity of the sample. This was confirmed by HPLC analysis (HPLC spectrum in Appendix 2, A2.4), which indicated that the totarol was 91% pure. The optical rotation reading showed that the compound was dextrorotatory (+). In conclusion, the purchased sample was confirmed to be (+)-totarol.

Table 5.3.1.2. ^{1}H, ^{13}C, HMBC and COSY spectral data of the epoxide intermediate (**1**). Chemical shifts are in ppm

Position		δ ^{1}H	J (Hz)	δ ^{13}C	HMBC	COSY
1	α	(1.29 – 1.19)	*m*	39.6	-	H-1β, H-2β
	β	2.24	*d* (12.5)		-	H-1α, H-2α
2	α	1.47	*dt* (13.5, 3.2)	19.5	-	H-1β, H-2β
	β	1.73	*dt* (13.5. 3.4)		-	H-1α, H-2α, H-3α
3	α	(1.29 – 1.19)	*m*	41.6	*	H-2β
	β	1.47	*d* (13.1)		-	H-3α
4		-	-	33.3	-	-
5		(1.29 – 1.19)	*m*	49.5	C-6, C-7, C-10, C-18, C-19, C-20	H-6β
6	α	1.92	*dd* (13.2, 7.9)	19.4	C-5, C-7, C-8, C-10	H-6β, H-7α
	β	(1.72 – 1.59)	*m*		C-5, C-7, C-10	H-5, H-6α, H-7α, H-7β
7	α	(2.82 – 2.70)	*m*	28.7	C-6, C-8, C-9	H-7β, H-6β, H-6α
	β	2.95	*dd* (16.7, 5.9)		C-5, C-6, C-8, C-9	H-6β, H-7α
8		-	-	133.9	-	-
9		-	-	143.7	-	-
10		-	-	37.7	-	-
11		7.08	*d* (8.7)	122.8	C-8, C-10, C-13	H-12
12		6.68	*d* (8.7)	110.2	C-9, C-14	H-11
13		-	-	155.1	-	-
14		-	-	133.6	-	-

*Overlapping signals . ♦Values are interchangeable within the same column

Table 5.3.1.2. (Continued) ^{1}H, ^{13}C, HMBC and COSY spectral data of the epoxide intermediate (**1**). Chemical shifts are in ppm

Position	δ ^{1}H	J (Hz)	δ ^{13}C	HMBC	COSY
15	3.29	*Sept* (7.0)	27.5	C-16, C-17	H-16, H-17
16i	1.31♦	*d* (7.0)	20.4♦	C-14, C-15, C-17	H-15
16ii	1.33♦	*d* (7.0)		C-14, C-15, C-17	H-15
17i	1.32♦	*d* (7.0)	20.5♦	C-14, C-15, C-16	H-15
17ii	1.33♦	*d* (7.0)		C-14, C-15, C-16	H-15
18	0.95	*s*	33.2	C-3, C-5, C-19	-
19	0.92	*s*	21.6	C-3, C-5, C-18	H-21b, H-22
20	1.18	*s*	25.2	C-1, C-5, C-9, C-10	-
21ai	4.17	*dd* (3.5, 2.1)	68.7	C-13, C-22, C-23	H-21b, H-22
21aii	3.98	*dd* (5.6, 1.7)		C-13, C-22, C-23	H-21b, H-22
21bi	4.13	*dd* (3.5, 2.1)		C-13, C-22, C-23	H-21a, H-22
21bii	3.95	*dd* (5.6, 1.7)		C-13, C-22, C-23	H-21a, H-22
22	3.36	*m*	50.4	-	H-21a, H-21b, H-23a
23a	2.89	*dd* (5.0, 4.4)	44.8	-	H-22, H-23b
23b	2.75	*dd* (5.0, 2.7)		-	H-23a

*Overlapping signals . ♦Values are interchangeable within the same column

5.3.1.2 Structure of the intermediate epoxide (1)

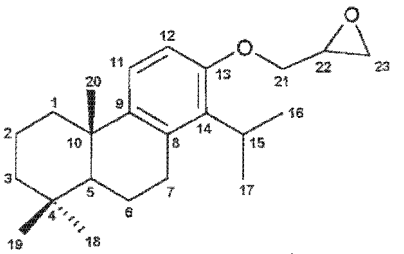

The molecular formula of the intermediate $C_{20}H_{34}O_2$ was determined by analysing its HREIMS molecular ion at m/z 342.25585 (calculated 342.25588). The ^{1}H-NMR spectrum of the epoxide closely resembled that of totarol, where noticeable similarities were the aromatic region, an isopropyl group, five methyl signals and the proton resonances of the fused cyclic rings. To avoid repetition, only the main differences in the spectrum will be discussed.

The most striking difference in the ^{1}H-NMR spectrum was the H-21a and H-21b signals. Each H-21 signal should be split by a geminal proton, which in turn would be split by the vicinal H-22, furnishing a dd. In the spectrum, the signals for the H-21 protons appeared to be duplicated with H-21a resonating as a set of dd at δ_i 4.17 (J=3.5 and 2.2Hz) and δ_{ii} 3.98 (J=5.6 and 1.7Hz). Similarly H-21b appeared as two dd at δ_i 4.13 (J=3.5 and 2.1Hz) and δ_{ii} 3.95 (J=5.6 and 1.7 Hz). The HSQC spectrum correlated C-21 (δ 68.7) with δ_i 4.17, δ_{ii} 3.98 (H-21a$_i$ and H-21a$_{ii}$) as well as δ_i4.13 and δ_{ii}3.95 (H-21b$_i$ and H-21b$_{ii}$), supporting the assignment of these two sets of dd to the H-21 protons. As complementary evidence, the HMBC experiment linked the H-21 signals with C-13, C-22 and C-23. The COSY spectrum revealed that H-21a was coupled to H-21b as well as H-22, and that H-21b was coupled to H-21a and H-22, which should only give a dd for each H-21 proton. A possible explanation for the apparent duplication of the H-21 signals is that the epoxide intermediate consists of diastereoisomers or regioisomers (Figure 5.3.1.2). The intensity of the duplicated signals was approximately the same, suggesting an equal ratio of the presumed isomers. In epichlorohydrin there are three electrophilic carbons (indicated as 1, 2 and 3 in Figure 5.3.1.2) at which nucleophilic substitution could potentially occur, depending on the reaction conditions. In the first option [Figure 5.3.1.2 (1)], the phenoxide anion attacks at C-1 to generate diastereoisomeric epoxides (i) and/or (ii) in a substitution nucleophilic bimolecular (S_N2) fashion. Another option would be for the phenoxide anion to attack at C-3. Attack at C-3 would produce an alkoxide intermediate followed by an intramolecular S_N2 displacement of Cl to effect cyclisation to the same

epoxides [(i) and/or (ii)]. If the phenoxide anion were to attack at C-2, an alternate alkoxide intermediate would be generated, followed by intramolecular displacement of Cl to give an oxetane (iii) derivative. This process would result in regioisomers. Since the epichlorohydrin is a racemate, option (1) would generate equal quantities of diastereoisomers (i) and (ii). Both options (1) and (2) would result in a mixture of diastereoisomers of the epoxide.

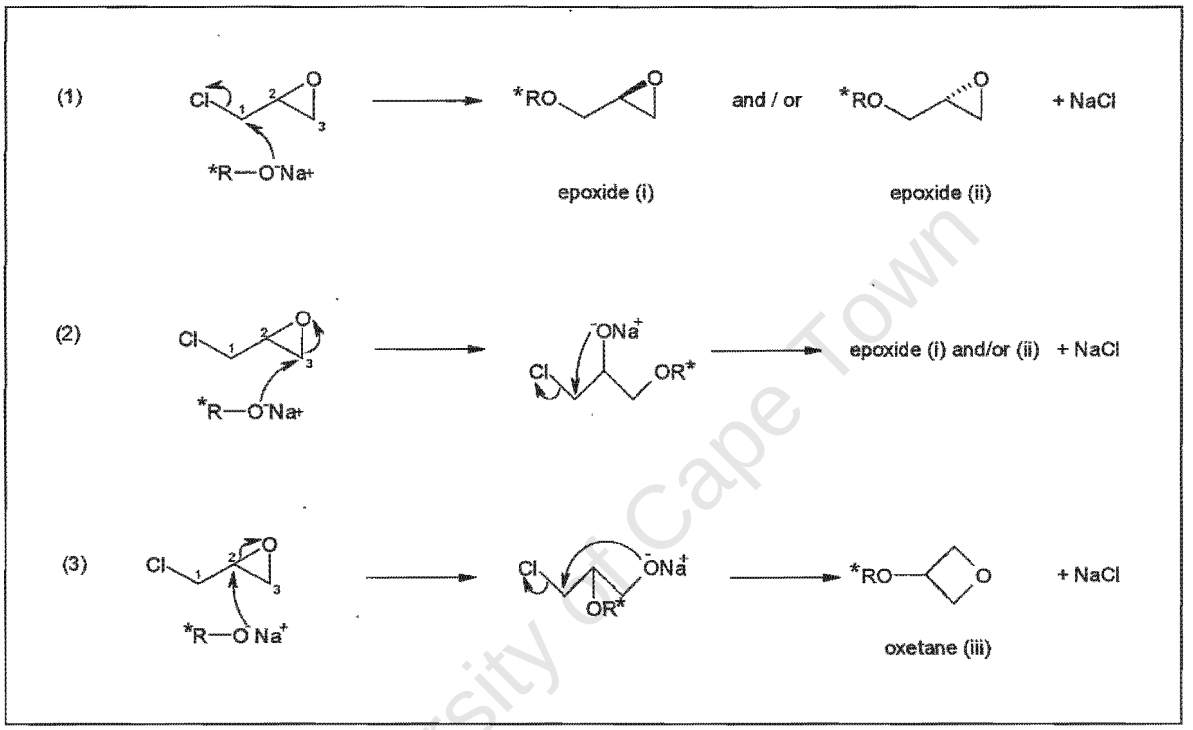

Figure 5.3.1.2. Generation of the epoxide diastereoisomers (i) and (ii) and the regioisomer (iii) (*R denotes a chiral moiety like that in totarol)

The regiochemistry of epoxyalkyl halide reactions has been reported to be markedly dependant upon the solvent used (Cruickshank and Fishman, 1969). It was found that in aprotic solvents the carbon-halide bond is susceptible to nucleophilic attack [option (1)]. In alcoholic solvents hydrogen bonding at the oxirane group weakens the carbon-oxygen bond, such that nucleophilic attack at this site is favoured [option (2)]. In the presence of an acid (Bronsted or Lewis acid) the oxygen of the epoxide is protonated or complexed to the Lewis acid. This results in preferential attack at the secondary C-2 where the developing positive charge is better stabilised [option (3)]. Since dimethylformamide (DMF) was used as a solvent in this study, the epoxides (i) and (ii) would have preferentially been formed.

Another possible explanation for the duplication of certain ^{1}H NMR signals is that the epoxide might have undergone an acid catalysed ring opening in the NMR tube due to the slight acidic nature of the NMR solvent $CDCl_3$ and the presence of a molecule of water. The resulting diol would have slightly different chemical shift values relative to the epoxide.

The only other signals at which this phenomenon was observed was H-16 and H-17. The set of doublets resonating at δ_i 1.31 (J=7.0Hz) and δ_{ii} 1.33 (J=7.0Hz) was assigned to H-16_i and H-16_{ii}, and the pair of doublets at δ_i 1.32 (J=7.0Hz) and δ_{ii} 1.34 (J=7.0Hz) was identified as H-17_i and H-17_{ii}. Since the CH_3-16 and CH_3-17 methyls are diastereotopic, the chemical shift values for H-16 and H-17 are interchangeable. In the COSY spectrum, the H-16 and H-17 proton signals were coupled to H-15. Further evidence for the assignment of these signals was provided by the HSQC experiment, which showed that these two sets of doublets were linked to a single carbon at δ 20.5 (C-16 and C-17 overlapped). Based on the analysis of a molecular model, the isopropyl methyls could interact through space with the H-21 protons and could possibly be influenced by their stereoisomeric conformation. The duplication of the H-16, H-17 as well as the H-21 signals suggested the presence of isomers, whilst the remaining resonances of the possible isomers were perfectly superimposable.

Using the COSY experiment, the H-21 protons were coupled to a multiplet at δ 3.36 that was identified as H-22. The COSY data revealed that H-22 was coupled to H-23a and the H-21 protons, which should afford a ddd as the multiplet. The coupling of H-22 with H-23 enabled the identification of the H-23 signals. The dd resonating at δ 2.89 (J=6.7 and 4.1Hz) was assigned to H-23a, and H-23b was observed as a dd at δ 2.75 (J=6.7 and 2.7Hz). The HMBC contours correlated the H-21 protons to C-22 and C-23, confirming the assignment of the above-mentioned protons and carbons.

The HSQC and HMBC experiments enabled the assignment of all the carbon signals. As for totarol, the C-16 and C-17 resonances overlapped. A comparison of the ^{13}C NMR data of totarol and the epoxide showed three additional resonances at δ 68.7, δ 50.4 and δ 44.8, which were assigned to C-21, C-22 and C-23 respectively. None of the ^{13}C signals were duplicated. Theoretically, the carbon chemical shifts values would not be influenced by the spatial orientation of the hydrogens and should remain constant for

diastereoisomers. If an oxetane intermediate was formed, through acid-catalysed ring opening, then the ^{13}C signals should differ slightly.

The NMR experiments coupled with the HREIMS analysis, confirmed that the intermediate epoxide had been synthesised. Although the ^{1}H NMR data suggested that either diastereoisomers, regioisomers or an open ring intermediate of the epoxide were formed, this remains to be shown.

Table 5.3.1.3. ^{1}H, ^{13}C, HMBC and COSY spectral data of compound **2**. Chemical shifts are in ppm

Position		δ ^{1}H	J (Hz)	δ ^{13}C	HMBC	COSY
1	α	(1.29 – 1.21)	*m*	39.6	-	H-1β, H-2β
	β	2.25	*br d* (12.8)		-	H-1α, H-2α
2	α	(1.49 – 1.44)	*m*	19.5	-	H-1β, H-2β
	β	1.78	*dt* (13.6. 3.2)		-	H-1α, H-2α, H-3α
3	α	(1.29 – 1.21)	*m*	41.6	*	H-2β, H-3β
	β	1.46	*br d* (12.9)		-	*
4		-	-	33.3	-	-
5		(1.29 – 1.21)	*m*	49.5	C-6, C-7, C-10, C-18, C-19, C-20	H-6β
6	α	1.91	*dd* (13.5, 8.0)	19.4	C-8, C-10	H-6β, H-7α
	β	(1.72 – 1.56)	*m*		C-5, C-7, C-10	H-5, H-6α, H-7α, H-7β
7	α	(2.78 – 2.69)	*m*	28.7	*	H-6α, H-6β, H-7β
	β	2.95	*dd* (16.8, 6.6)		C-5, C-6, C-8, C-9	H-6β, H-7α
8		-	-	133.7	-	-
9		-	-	143.3	-	-
10		-	-	37.7	-	-
11		7.07	*d* (8.8)	122.8	C-8, C-10, C-13	H-12
12		6.71	*d* (8.8)	109.8	C-9, C-13, C-14	H-11
13		-	-	155.2	-	-
14		-	-	133.1	-	-

*Overlapping signals . ♦Values are interchangeable within the same column

Table 5.3.1.3. (Continued) ^{1}H, ^{13}C, HMBC and COSY spectral data of compound **2**. Chemical shifts are in ppm

Position	δ ^{1}H	J (Hz)	δ ^{13}C	HMBC	COSY
15	3.39	*br m*	27.5	-	H-16, H-17
16	1.31♦	*d* (7.0)	20.6	C-14, C-15, C-17	H-15
17	1.32♦	*d* (7.0)	20.6	C-14, C-15, C-16	H-15
18	0.94	*s*	33.2	C-3, C-5, C-19	-
19	0.92	*s*	21.6	C-3, C-5, C-18	-
20	1.18	*s*	25.2	C-1, C-5, C-9, C-10	-
21a	4.01	*dd* (9.2, 4.6)	70.1	C-22, C-23	H-21b, H-22
21b	3.90	*dd* (9.2, 5.8)		C-22, C-23	H-21a, H-22
22	4.05	*m*	65.9	-	H-21a, H-21b, H-23
23a	(2.71 – 2.64)	*m*	56.8	C-22, C-25, C-27	H-22, H-23b
23b	(2.71 – 2.64)	*m*		C-22, C-25, C-27	H-22, H-23a
25	(2.74 – 2.69)	*m*	47.4	C-23, C-27, C-26	H-26, H-27
26	1.08	*t* (7.1)	11.6	C-25	H-25
27	(2.67 – 2.60)	*m*	47.4	C-23, C-25, C-28	H-25, H-28
28	1.08	*t* (7.1)	11.6	C-27	H-27

*Overlapping signals . ♦Values are interchangeable within the same column

5.3.1.3 Structure of compound 2

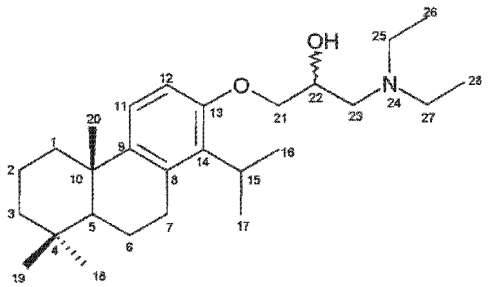

The HREIMS of **2** showed a molecular ion peak at m/z 415.34612 (calculated 415.34503) analysing for $C_{27}H_{45}NO_2$. Since the NMR data of **2** is similar to that of the epoxide, with respect to the totarol moiety, only the main differences will be highlighted. Analysis of the NMR spectrum indicated that none of the proton signals were duplicated.

H-21a was identified as a dd at δ 4.01 (J=9.2 and 4.6 Hz) and the dd at δ 3.90 (J=9.2 and 5.8Hz) was assigned to H-21b. In the COSY spectrum, the H-21 protons were coupled to their geminal proton as well as H-22. The H-22 protons resonated as a multiplet at δ 4.05. Since H-22 was coupled to both the H-21 protons and H-23a, a ddd splitting pattern would be expected. Although the H-22 signal overlapped slightly with the H-21a signal, their relative positions could be determined from the HSQC spectrum. The COSY data showed coupling between H-22 and the H-23 protons. The H-23 signal appeared as a multiplet and spectral overlap of this signal with the H-7α, H-25 and H-27 resonances prevented the chemical shift values from being determined. The HMBC data correlated the H-21 protons to C-22 (δ 65.9) and C-23 (δ 56.8). When coupled with the HSQC spectrum, this information confirmed the assignment of the H-21, H-22 and H-23 protons.

Additional proton signals were observed at δ 1.08, which were assigned to H-26 and H-28. These resonances showed a triplet splitting pattern and integrated for 6 Hs, supporting the assignment to the two identical H-26 and H-28 methyl signals. Using the COSY spectrum, H-26 and H-28 were coupled to H-25 and H-27, respectively. Although the H-25 and H-27 resonances only overlapped slightly, the spectrum in this region was complicated by further spectral overlap with the H-23 and H-7α signals. HMBC correlations from H-25 to C-23, C-26 and C-27 and from H-27 to C-23, C-25 and C-28 supported the identity of these proton signals.

were observed. The C-22 signal was shifted downfield (from δ 50.4 to 65.9) relative to the epoxide, due to the presence of the hydroxyl group. C-23 was also shifted (from δ 44.8 to 56.8), under the influence of the nitrogen atom. The IR spectrum of **2** supported the presence of a hydroxyl group, showing an absorbance at 3412cm^{-1}. From the HREIMS, NMR data and IR spectrum, the determined structure of **2** corresponded to the expected structure.

Table 5.3.1.4. ^{1}H, ^{13}C, HMBC and COSY spectral data of compound **3**. Chemical shifts are in ppm

Position		δ ^{1}H	J (Hz)	δ ^{13}C	HMBC	COSY
1	α	(1.29 – 1.21)	*m*	39.7	-	H-1β, H-2β
	β	2.25	*d* (12.5)		C-10	H-1α, H-2α
2	α	(1.50 – 1.41)	*m*	19.6	-	H-1β, H-2β
	β	1.74	*dt* (13.6. 3.3)		-	H-1α, H-2α, H-3α
3	α	(1.29 – 1.21)	*m*	41.6	*	H-2β
	β	1.43	*br d* (13.6)		-	H-3α
4		-	-	33.4	-	-
5		(1.29 – 1.21)	*m*	49.6	C-4, C-6, C-10, C-18, C-19, C-20	H-6β
6	α	1.92	*dd* (13.1, 8.0)	19.5	-	H-6β, H-7α
	β	(1.73 – 1.57)	*m*		-	H-5, H-6α, H-7α, H-7β
7	α	(2.82 – 2.71)	*m*	28.8	C-5, C-8	H-6α, H-6β, H-7β
	β	(3.01 – 2.92)	*m*		C-5, C-8	H-6β, H-7α
8		-	-	134.0	-	-
9		-	-	143.6	-	-
10		-	-	37.7	-	-
11		7.10	*d* (8.9)	122.9	C-8, C-10, C-12, C-13	H-12
12		6.73	*d* (8.9)	109.9	C-9, C-13, C-14	H-11
13		-	-	155.0	-	-
14		-	-	133.2	-	-
15		(3.33 – 3.23)	*m*	27.5	-	H-16, H-17
16i		1.34✦	*d* (6.9)	20.8	C-14, C-15, C-17	H-15
16ii		1.32✦	*d* (6.9)		C-14, C-15, C-17	H-15

*Overlapping signals . ✦Values are interchangeable within the same column

Table 5.3.1.4. (Continued) ^{1}H, ^{13}C, HMBC and COSY spectral data of compound **3**. Chemical shifts in ppm

Position	δ ^{1}H	J (Hz)	δ ^{13}C	HMBC	COSY
17i	1.35*	*d* (6.9)	20.8	C-14, C-15, C-16	H-15
17ii	1.33*	*d* (6.9)		C-14, C-15, C-16	H-15
18	0.95	*s*	33.3	C-3, C-5, C-19	-
19	0.92	*s*	21.6	C-3, C-5, C-18	-
20	1.19	*s*	25.2	C-1, C-5, C-9, C-10	-
21a	4.04	*dd* (9.5, 5.1)	70.1	C-22, C-23	H-21b, H-22
21b	3.97	*dd* (9.5, 5.3)		C-22, C-23	H-21a, H-22
22	4.21	*m*	66.1	-	H-21, H-23a, H-23b
23a	(2.82 – 2.71)	*m*	61.3	-	H-22, H-23b
23b	(2.82 – 2.71)	*m*		-	H-22, H-23a
25	(3.01 – 2.92)	*m*	53.4	C-27	H-26
26	3.28	*m*	52.3	C-28	H-25
27	(2.82 – 2.71)	*m*	53.4	C-25	H-28
28	3.28	*m*	52.3	C-26	H-27
2′	8.72	*d* (5.0)	151.9	C-3′, C-4′, C-8′a	H-3′
3′	6.85	*d* (5.0)	109.0	C-2′, C-4′a	H-2′
4′	-	-	150.2	-	-
4′a	-	-	121.9	-	-
5′	7.95	*d* (8.9)	125.1	C-4′, C-7′, C-8′a	H-6′
6′	7.42	*dd* (8.9, 2.1)	126.2	C-4′a	H-5′, H-8′
7′	-	-	134.9	-	-
8′	8.05	*d* (2.1)	134.0	C-6′, C-7′	H-6′
8′a	-	-	156.8	-	-

*Overlapping signals . ♦Values are interchangeable within the same column

5.3.1.4 Structure of compound 3

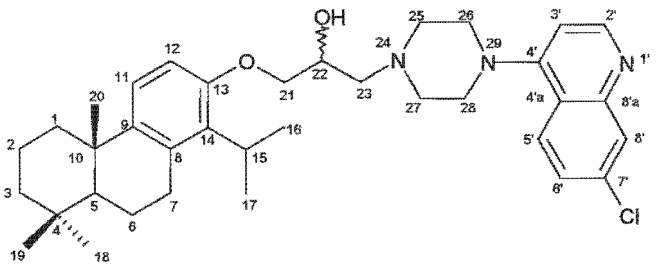

The HREIMS of **3** indicated a molecular ion at m/z 589.34432 (calculated 589.34351) that corresponded to a molecular formula of $C_{36}H_{48}N_3O_2Cl$. As with compound **2**, only the noticeable differences between the NMR spectrum of the epoxide and **3** will be discussed.

The most striking signals in the ^{1}H-NMR were the five additional aromatic resonances. The most deshielded proton at δ 8.72 was assigned to H-2′, which resonated as a d (J=5.0Hz). In the COSY spectrum, H-2′ was coupled to a d (J=5.0Hz) at δ 6.85 that was assigned to H-3′. HMBC correlations from H-2′ to C-3′, C-4′ and C-8′a, and from H-3′ to C-2′ and C-4′a verified the positions of H-2′ and H-3′ on the ring. The d at δ 8.05 was identified as H-8′ and displayed meta coupling (J=2.1Hz) with H-6′. Through the COSY spectrum, H-6′ was found to be coupled to H-8′ as well as H-5′, furnishing a dd at δ 7.42 (J=8.9 and 2.1 Hz). The informative 3-bond correlations in the HMBC spectrum from H-5′ to C-7′, C-4′ and C-8′a supported the determined positions of the aromatic protons.

Another noticeable difference in the spectrum of **3** was the presence of the multiplet at δ 3.28, which was assigned to H-26 and H-28. These resonances overlapped with the H-15 signal, resulting in a broad multiplet. The COSY experiment coupled H-26 and H-28 with H-25 and H-27, respectively. Due to signal overlap between H-25 and H-7β, and H-27 with H-7α and the H-23 protons, the exact chemical shift values could not be determined. However, the relative positions of H-25 (δ 2.92 - 3.01) and H-27 (δ 2.2 – 2.71) could be established from the HSQC spectrum. The H-23 protons also resonated in the range δ(2.82 – 2.71), and were coupled to H-22 (δ 4.21). H-22 appeared to be two overlapping multiplets, when a dddd splitting pattern would be expected. The most logical explanation for this is the presence of diastereoisomers. H-21a was identified as a dd at δ 4.04 (J=9.5 and 5.1 Hz) and the adjacent dd at δ 3.97 (J=9.5 and 5.3Hz) was assigned to H-21b. The coupling constants indicated that the H-21 protons were coupled to a geminal proton as well as a vicinal proton (H-22), which was confirmed in the COSY spectrum.

Analysis of the resonances from the totarol skeleton indicated that the H-16 and H-17 signals were duplicated, suggesting there may be a mixture of diastereoisomers. The d (J=6.9Hz) at δ 1.34 was assigned to H-16_i and the d (J=6.9Hz) at δ 1.32 to H-16_{ii}. Similarly the d (J=6.9Hz) at δ 1.35 was identified as H-17_i and the d (J=6.9Hz) resonating at δ 1.33 was assigned to H-17_{ii}. In the HSQC spectrum, the two sets of doublets were linked to a single carbon at δ 20.8 (C-16 and C-17 overlapped). The intensity of the (i) and (ii) signals was approximately the same, suggesting an equal ratio of the presumed diastereoisomers. Another possible explanation for the duplication of the H-16 and H-17 signals is that a mixture of compound **3** and its intramolecularly hydrogen bonded conformation might have existed in the NMR solvent solution. The hydrogen bonded conformation referred to is the one involving the β-nitrogen and the OH group.

For the ^{13}C-NMR spectrum, the HSQC and HMBC experiments allowed the assignment of all the carbon signals. Through relevant HMBC correlations, the four new quaternary carbons on the aromatic ring were identified. The presence of 13 additional carbon resonances, compared to the epoxide spectrum, indicated that the intended reaction had occurred. None of the ^{13}C signals was duplicated. As mentioned earlier, theoretically, the spatial orientation of the hydrogens as well as the formation of an intramolecular H-bond should not influence the carbon chemical shift values. Thus, diastereoisomers and an intramolecularly H-bond conformation of **3** should all have identical ^{13}C chemical shift values.

From the HREIMS, IR and NMR data, compound **3** was found to be consistent with the expected structure. Although the duplicated ^{1}H signals suggested the presence of either diastereoisomers or an intramolecularly H-bonded conformation of **3**, this remains to be shown.

Table 5.3.1.5. ^{1}H, ^{13}C and COSY spectral data of compound **4**. Chemical shifts are in ppm

Position		δ ^{1}H	J (Hz)	δ ^{13}C	COSY
1	α	(1.28 – 1.19)	*m*	39.8	H-1β
	β	2.24	*d* (12.6)		H-1α, H-2α
2	α	1.58	*dt* (13.8, 3.3)	19.6	H-1β, H-2β
	β	1.76	*dt* (13.8, 3.5)		H-1α, H-2α, H-3α
3	α	(1.28 – 1.19)	*m*	41.7	H-2β
	β	1.46	*d* (13.2)		H-3β
4		-	-	33.4	-
5		(1.28 – 1.19)	*m*	49.7	H-6β
6	α	1.91	*dd* (9.9, 7.9)	19.5	H-6β, H-7α
	β	(1.67 – 1.63)	*m*		H-5, H-6α, H-7α, H-7β
7	α	(2.79 – 2.71)	*m*	28.9	H-6α, H-6β, H-7β
	α	2.94	*dd* (12.8, 6.7)		H-6β, H-7α
8		-	-	134.0	-
9		-	-	143.6	-
10		-	-	37.8	-
11		7.01	*d* (8.8)	122.9	H-12
12		6.71	*d* (8.8)	110.0	H-11
13		-	-	155.0	-
14		-	-	133.3	-
15		3.29	*m*	27.6	H-16, H-17
16		1.31[♦]	*d* (7.0)	20.8	H-15

[*] Overlapping signals . [♦] Values are interchangeable within the same column

Table 5.3.1.5. (Continued) ^{1}H, ^{13}C and COSY spectral data of compound **4**. Chemical shifts are in ppm

Position	δ ^{1}H	J (Hz)	δ ^{13}C	COSY
17	1.32*	*d* (7.0)	20.8	H-15
18	0.94	*s*	33.3	-
19	0.91	*s*	21.7	-
20	1.17	*s*	25.3	-
21a	4.01	*dd* (7.0, 5.1)	70.3	H-21b, H-22
21b	3.94	*dd* (7.0, 5.2)		H-21a, H-22
22	4.16	*m*	66.1	H-23a, H-23b
23a	(2.66 – 2.64)	*m*	61.4	H-22, H-21
23b	(2.66 – 2.64)	*m*		H-22
25	(2.86 – 2.80)	*m*	53.6	H-26
26	3.21	*t* (3.3)	49.4	H-25
27	(2.66 – 2.64)	*m*	53.6	H-28
28	3.23	*t* (3.3)	49.4	H-27
1′	-	-	151.3	-
2′	6.92	*d* (8.6)	116.3	H-3′
3′	(7.28 – 7.24)	*m*	129.2	H-2′
4′	6.85	*2d* (7.3, 0.7)	119.9	-
5′	(7.28 – 7.24)	*m*	129.2	H-6′
6′	6.92	*d* (8.6)	116.3	H-5′

*Overlapping signals. ♦Values are interchangeable within the same column

5.3.1.5 Structure of compound 4

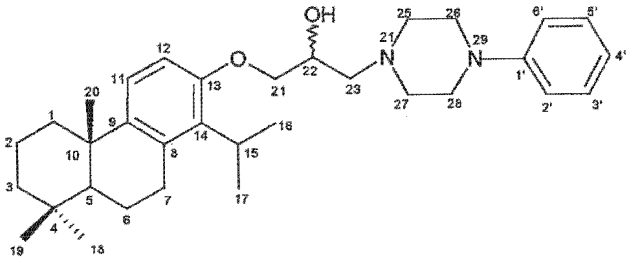

The HREIMS of compound **4** showed a molecular ion peak at m/z 504.37256 (calculated 504.37158), analysing for $C_{33}H_{48}N_2O_2$. The ^1H and ^{13}C NMR data of **4** was similar to that of the epoxide and only the differences between the two will be discussed.

A noticeable difference in the ^1H spectrum was the appearance of five additional aromatic resonances. The most shielded signal was assigned to H-4′ (δ 6.85) and appeared as two overlapping doublets (J=7.3 and 0.7Hz). The COSY spectrum showed that H-4′ was ortho coupled to H-3′ as well as H-5′, which would furnish two doublets. Unresolved meta coupling (J=0.73Hz) suggested that H-4′ was also coupled to H-6′ and H-2′. The dd at δ 6.92 was assigned to H-6′ and H-2′. The doublet integrated for 2Hs, supporting its assignment to both H-6′ and H-2′. Using the COSY spectrum, H-6′ and H-2′ were ortho coupled (J=8.6Hz) to H-5′ and H-3′. The H-5′ and H-3′ resonances occurred as multiplets in the range δ(7.28 – 7.24). Spectral overlap with the H-5′, H-3′ and the $CDCl_3$ signal prevented the exact chemical shift values from being determined.

The spectrum in the region δ(2.86 - 2.60) closely resembled that of **3**, with the H-25 signal overlapping that of H-7α, as well as the H-27 resonance overlapping the H-23 signals. COSY data coupled the H-23 protons to H-22, which resonated as a multiplet at δ 4.16. As observed for **3**, the H-22 signal appeared to be a quintet, although the distances between the peaks suggested a series of overlapping doublets. The dd at δ 4.01 and at δ 3.94 was assigned to H-21a and H-21b respectively. In the COSY experiment, the H-21 protons were coupled to their geminal proton (J=7.0Hz) as well as the vicinal H-22 proton (J *ca* 5.1Hz). The two overlapping triplets resonating at δ 3.21 and δ 3.23 were identified as H-26 and H-28. The COSY experiment showed coupling (J=3.3Hz) between these triplets and the H-25 and H-27 signals. The fact that first order splitting patterns were observed for H-26 and H-28 suggests that the H-25 protons are equivalent as are the H-27 protons. None of the ^1H resonances were duplicated in **4**.

Although HSQC and HMBC experiments were not performed on **4**, all of the ^{13}C signals could be assigned by comparing the ^{13}C NMR data with that of the epoxide, compound **5** and **6**. Compared to the epoxide, noticeable differences in the spectrum were the additional aromatic carbon resonances at δ 129.2 (C-3′ and C-5′) and δ 116.3 (C-6′ and C-2′) as well as the two methylene signals resonating at δ 49.4 (C-28 and C-26) and δ 53.6 (C-27 and C-25). Furthermore, the C-22 signal was more deshielded (from δ 50.4 to 66.1) as was the C-23 resonance (from δ 44.8 to 61.4), which could be explained in terms of their proximity to the nitrogen and hydroxyl group. The IR spectrum of **4** supported the presence of a hydroxyl group showing a peak at 3425cm^{-1}. A combination of the HREIMS data, NMR and IR spectrum of **4** verified that the structure corresponded to the expected structure.

Table 5.3.1.6. ^{1}H, ^{13}C, HMBC and COSY spectral data of compound **5**. Chemical shifts are in ppm

Position		δ ^{1}H	J (Hz)	δ ^{13}C	HMBC	COSY
1	α	(1.30 – 1.21)	*m*	39.7	-	H-1β, H-2β
	β	2.25	*d* (12.4)		-	H-1α
2	α	1.47	*dt* (13.8, *)	19.5	-	H-2β
	β	1.78	*dt* (13.8. 3.3)		-	H-1α, H-2α, H-3α
3	α	(1.30 – 1.21)	*m*	41.6	*	H-2β, H-3β
	β	1.47	*d* (13.3)		-	H-3α
4		-	-	33.3	-	-
5		(1.30 – 1.21)	*m*	49.6	C-6, C-7, C-10,C-18, C-19, C-20	*
6	α	1.92	*dd* (13.2, 8.0)	19.4	C-5, C-7, C-8, C-10	H-6β, H-7α
	β	(1.72 – 1.57)	*m*		C-5, C-7, C-10	H-5, H-6α, H-7β
7	α	(2.76 – 2.65)	*m*	28.8	C-6, C-8, C-9	H-6α, H-7β
	β	2.96	*dd* (*, 6.4)		C-5, C-6, C-8, C-9	H-6β, H-7α
8		-	-	133.9	-	-
9		-	-	143.4	-	-
10		-	-	37.7	-	-
11		7.09	*d* (8.9)	122.8	C-8, C-10, C-13	H-12
12		6.73	*d* (8.9)	109.8	C-9, C-14, C-13	H-11
13		-	-	155.2	-	-
14		-	-	133.2	-	-
15		3.30	*m*	27.5	C-16, C-17	H-16, H-17
16		1.32♦	*d* (6.8)	20.7	C-14, C-15, C-17	H-15

* Overlapping signals . ♦Values are interchangeable within the same column

Table 5.3.1.6. (Continued) ^{1}H, ^{13}C, HMBC and COSY spectral data of compound (**5**). Chemical shifts are in ppm

Position	δ ^{1}H	J (Hz)	δ ^{13}C	HMBC	COSY
17	1.34♦	*d* (6.8)	20.7	C-14, C-15, C-16	H-15
18	0.95	*s*	33.2	C-3, C-5, C-19	-
19	0.92	*s*	21.6	C-3, C-5, C-18	-
20	1.19	*s*	25.2	C-1, C-5, C-9, C-10	-
21a	4.03	*dd* (9.5, 5.0)	70.2	C-22, C-23	H-21b, H-22
21b	3.95	*dd* (9.5, 5.3)		C-22, C-23	H-21a, H-22
22	4.18	*m*	65.9	C-21, C-23	H-21, H-23a, H-23b
23a	(2.76 – 2.65)	*m*	61.2	C-22	H-22
23b	(2.76 – 2.65)	*m*		C-22	H-22
25	(2.92 – 2.79)	*m*	53.6	C-26, C-27	H-26
26	3.11	*m*	51.3	C-25, C-28	H-25
27	(2.76 – 2.65)	*m*	53.6	C-25, C-28	H-28
28	3.11	*m*	51.3	C-26, C-27	H-27
1′	-	-	149.2	-	-
2′	-	-	128.8	-	-
3′	7.36	*dd* (8.0, 1.5)	130.7	C-1′, C-2′, C-5′	H-4′
4′	6.98	*2dd* (7.7, 1.5)	123.8	C-2′, C-6′	H-3′, H-5′
5′	7.21	*m*	127.6	C-1′, C-3′	H-4′, H-6′
6′	7.05	*dd* (8.1, 1.5)	120.4	C-2′, C-4′	H-5′

* Overlapping signals . ♦Values are interchangeable within the same column

5.3.1.6 Structure of compound 5

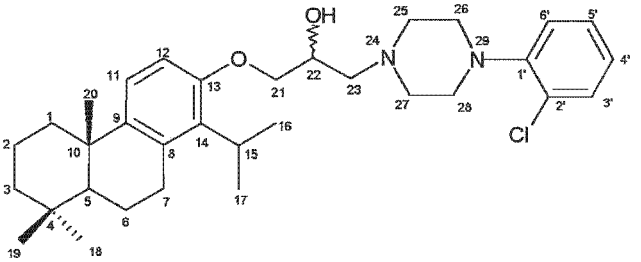

The molecular formula for compound **5**, $C_{33}H_{47}N_2O_2Cl$ was determined by analysing its HREIMS molecular ion at m/z 538.33254 (calculated 538.33261). Since the ^1H NMR spectrum of **5** closely resembled that of **4**, only the differences between the two will be highlighted.

In the ^1H NMR spectrum of **5**, the chlorine atom at C-2′ had a deshielding effect on the H-3′ proton and shifted it downfield to δ 7.36. This proton resonated as a dd and showed ortho coupling (J=8.0Hz) with H-4′ as well as long range meta coupling (J=1.5Hz) with H-5′. In the COSY spectrum H-3′ was clearly coupled to H-4′. This enabled the identification of the H-4′ signal as two overlapping doublets at δ 6.98. The COSY experiment revealed that H-4′ was coupled to H-3′ and H-5′, which should afford two doublets. The unresolved splitting of the overlapping doublets indicated that H-4′ was also meta coupled (J=1.5Hz) to H-6′. The H-6′ signal (δ 7.05) overlapped slightly with that from the H-11 proton, and resonated as a dd (J=8.1 and 1.5Hz). The ortho coupling of H-6′ would result from the interaction with H-5′, while the meta coupling is due to the H-4′ proton. The multiplet at δ 7.21 was assigned to H-5′ and its splitting pattern resembled that of H-4′. HMBC correlations from H-3′ to C-1′, C-2′ and C-5′, and from H-5′ to C-1′ and C-3′ verified the sequence of the above mentioned protons on the aromatic ring. The proximity of the nitrogen atom coupled with the inductive effect of the chlorine substituent caused the aromatic protons to resonate at slightly different chemical shift values, compared to **4**. Complete assignments of the carbon signals were achieved by HSQC and HMBC experiments. A comparison of the ^{13}C-NMR data of **5** and **4** showed that the majority of the chemical shifts were very similar. The only differences were the C-2′, C-4′ and C-6′ resonances which were all shifted downfield under the influence of the chlorine atom at C-2′. The presence of a hydroxyl group was confirmed by the IR spectrum showing an absorbance at 3435cm^{-1}. The combined HREIMS, IR and NMR data of **5** were found to be in complete accordance with the expected structure.

Table 5.3.1.7. ^{1}H, ^{13}C, HMBC and COSY spectral data of compound **6**. Chemical shifts are in ppm

Position		δ ^{1}H	J (Hz)	δ ^{13}C	HMBC	COSY
1	α	(1.29 – 1.21)	*m*	39.7	-	H-1β
	β	2.25	*d* (13.0)		-	H-1α, H-2α
2	α	(1.77 – 1.56)	*m*	19.5	-	H-1β
	β	(1.77 – 1.56)	*m*		-	*
3	α	(1.29 – 1.21)	*m*	41.6	*	*
	β	(1.77 – 1.56)	*m*		*	*
4		-	-	33.3	-	-
5		(1.29 – 1.21)	*m*	49.5	C-6, C-7, C-10, C-18, C-19, C-20	H-6β
6	α	1.91	*dd* (13.5, 8.0)	19.4	C-7, C-8, C-10	H-6β, H-7α
	β	(1.77 – 1.56)	*m*		C-5, C-7, C-10	H-5, H-6α, H-7α, H-7β
7	α	(2.85 – 2.73)	*m*	28.8	C-6, C-8	H-6α, H-6β, H-7β
	β	2.95	*dd* (16.9, 6.1)		C-5, C-6, C-8, C-9	H-6β, H-7α
8		-	-	133.2	-	-
9		-	-	143.4	-	-
10		-	-	37.7	-	-
11		7.09	*d* (8.8)	122.8	C-8, C-10, C-13	H-12
12		6.73	*d* (8.8)	109.8	C-9, C-13, C-14	H-11
13		-	-	155.2	-	-
14		-	-	133.2	-	-
15		3.30	*m*	27.5	-	H-16, H-17
16		1.32♦	*d* (7.0)	20.7	C-14, C-15, C-17	H-15

* Overlapping signals . ♦Values are interchangeable within the same column

Table 5.3.1.7. (Continued) ^{1}H, ^{13}C, HMBC and COSY spectral data of compound **6**. Chemical shifts are in ppm

Position	δ ^{1}H	J (Hz)	δ ^{13}C	HMBC	COSY
17	1.34♦	*d* (7.0)	20.7	C-14, C-15, C-16	H-15
18	0.95	*s*	33.2	C-3, C-5, C-19	-
19	0.92	*s*	21.6	C-3, C-5, C-18	-
20	1.18	*s*	25.2	C-1, C-5, C-9, C-10	-
21a	4.02	*dd* (9.5, 5.0)	70.2	C-22, C-23	H-21b, H-22
21b	3.94	*dd* (9.5, 5.2)		C-22, C-23	H-21a, H-22
22	4.17	*m*	65.9	-	H-21, H-23a, H-23b
23a	(2.70 – 2.64)	*m*	61.4	-	H-22
23b	(2.70 – 2.64)	*m*		-	H-22
25	(2.91 – 2.78)	*m*	53.7	C-26, C-27	H-26
26	3.14	*m*	50.6	-	H-25
27	(2.70 – 2.64)	*m*	53.7	C-25	H-26
28	3.14	*m*	50.6	-	H-27
1′	-	-	141.3	-	-
2′	-	-	151.6	-	-
3′	(7.00 – 6.92)	*m*	122.8	C-2′, C-4′	*
4′	(6.94 – 6.90)	*m*	118.2	C-3′	*
5′	(6.97 – 6.92)	*m*	121.0	C-1′, C-3′	*
6′	6.85	*d* (7.2)	112.6	C-1′, C-5′	*
1″	4.10	*q* (7.0)	63.6	C2″	H-2″
2″	1.45	*t* (7.0)	14.9	C-1″	H-1″

* Overlapping signals . ♦Values are interchangeable within the same column

5.3.1.7 Structure of compound 6

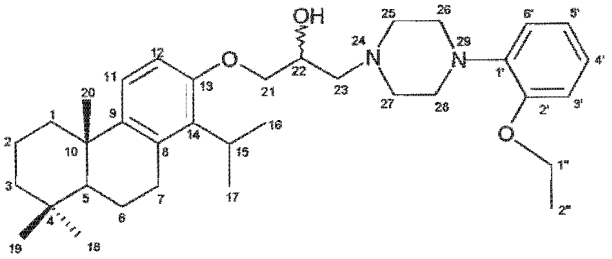

The HREIMS of compound **6** indicated a molecular ion peak at m/z 548.39818 (calculated 548.39779), corresponding to a molecular formula of $C_{35}H_{52}N_2O_3$. The ^{1}H NMR spectrum of **6** closely resembled those of **4** and **5**. A readily noticeable difference in the spectrum was the presence of an additional methyl group at δ 1.45 and a methylene group at δ 4.10. The methyl group was assigned to H-2″ and resonated as a triplet (J=7.0Hz). In the COSY experiment the H-2″ protons were coupled (J=7.0Hz) only with a quartet at δ 4.10, which was identified as H-1″. In addition to the COSY data, the coupling between H-1″ and H-2″ was confirmed by the magnitude of the coupling constants. Furthermore, the HMBC contours correlated H-1″ to C-2″, and H-2″ to C-1″ providing additional support for this assignment. The broad doublet at δ 6.85 was assigned to H-6′ and showed ortho coupling (J=7.2Hz) with H-5′ and unresolved long range meta coupling. The aromatic protons H-3′, H-4′ and H-5′ were not as resolved as those for **5** and overlapped in the region δ(7.0 – 6.9). Although the exact chemical shift values could not be determined, the relative positions of these protons were established through HSQC and HMBC experiments. The remaining proton signals resembled those of **5**. For the ^{13}C NMR spectrum, the HSQC and HMBC data enabled the identification of all the carbon signals. Compared to the ^{13}C spectrum of **5**, the C-2′, C-4′ and C-6′ signals were all shifted downfield due to the presence of the oxygen atom at C-2′. The other noticeable difference was the presence of two additional resonances at δ 63.6 and δ 14.9, which were identified using the HSQC spectrum, as C–1″ and C-2″ respectively. The combined HREIMS, IR and NMR data confirmed that **6** was consistent with the expected structure. The ^{13}C NMR data for totarol, the epoxide intermediate (**1**) and compounds **2 - 6** is summarised in Table 5.3.1.8. The collective data illustrates that the carbon resonances from the totarol skeleton remain constant, while the additional signals vary according to the structure of the reacting amine. The NMR data combined with the HREIMS spectra and IR measurements confirmed that all of the synthesised compounds corresponded to the expected structures.

Table 5.3.1.8 Summary of ^{13}C NMR data for totarol, the epoxide intermediate (**1**) and compounds (**2-6**). Chemical shifts (δ) are reported in ppm

Position	Totarol	1	2	3	4	5	6
1	39.6	39.6	39.6	39.7	39.8	39.7	39.6
2	19.5	19.5	19.5	19.6	19.6	19.5	19.5
3	41.6	41.6	41.6	41.6	41.7	41.6	41.6
4	33.3	33.3	33.3	33.4	33.4	33.3	33.3
5	49.6	49.5	49.5	49.6	49.7	49.6	49.5
6	19.4	19.4	19.4	19.5	19.5	19.4	19.4
7	28.7	28.7	28.7	28.8	28.9	28.8	28.8
8	134.0	133.9	133.7	134.0	134.0	133.9	133.2
9	143.2	143.7	143.3	143.6	143.6	143.4	143.4
10	37.7	37.7	37.7	37.7	37.8	37.7	37.7
11	123.0	122.8	122.8	122.9	122.9	122.8	122.8
12	114.3	110.2	109.8	109.9	110.0	109.8	109.8
13	151.9	155.1	155.2	151.9	155.0	155.2	155.2
14	131.0	133.6	133.1	133.2	133.3	133.2	133.2
15	27.1	27.5	27.5	27.5	27.6	27.5	27.5
16	19.4	20.5	20.6	20.8	20.8	20.7	20.7
17	19.5	20.5	20.6	20.8	20.8	20.7	20.7
18	33.2	33.2	33.2	33.3	33.3	33.2	33.2
19	21.6	21.6	21.6	21.6	21.7	21.6	21.6

Table 5.3.1.8. (Continued) Summary of ^{13}C NMR data for totarol, the epoxide intermediate (**1**) and compounds (**2-6**). Chemical shifts are in ppm

Position	Totarol	1	2	3	4	5	6
20	25.1	25.2	25.2	25.2	25.3	25.2	25.2
21	-	68.7	70.1	70.1	70.3	70.2	70.2
22	-	50.4	65.9	66.1	66.1	65.9	65.9
23	-	44.8	56.8	61.3	61.4	61.2	61.4
25	-	-	47.4	53.4	53.6	53.6	53.7
26	-	-	11.6	52.3	49.4	51.3	50.6
27	-	-	47.4	53.4	53.6	53.6	53.7
28	-	-	11.6	52.3	49.4	51.3	50.6
1′	-	-	-	-	151.3	149.2	141.3
2′	-	-	-	151.9	116.3	128.8	151.6
3′	-	-	-	109.0	129.2	130.7	122.8
4′	-	-	-	150.2	120.0	123.8	118.2
4′a	-	-	-	121.9	-	-	-
5′	-	-	-	125.1	129.2	127.6	121.0
6′	-	-	-	126.2	116.3	120.4	112.6
7′	-	-	-	135.0	-	-	-
8′	-	-	-	134.0	-	-	-
8′a	-	-	-	156.8	-	-	-
1″	-	-	-	-	-	-	63.6
2″	-	-	-	-	-	-	14.9

5.3.2 *In vitro* antiplasmodial activity of totarol

Prior to any modifications, totarol was tested for *in vitro* antiplasmodial activity against *P. falciparum* D10 (CQ-sensitive) and K1 (CQ-resistant), (Figure 5.3.2).

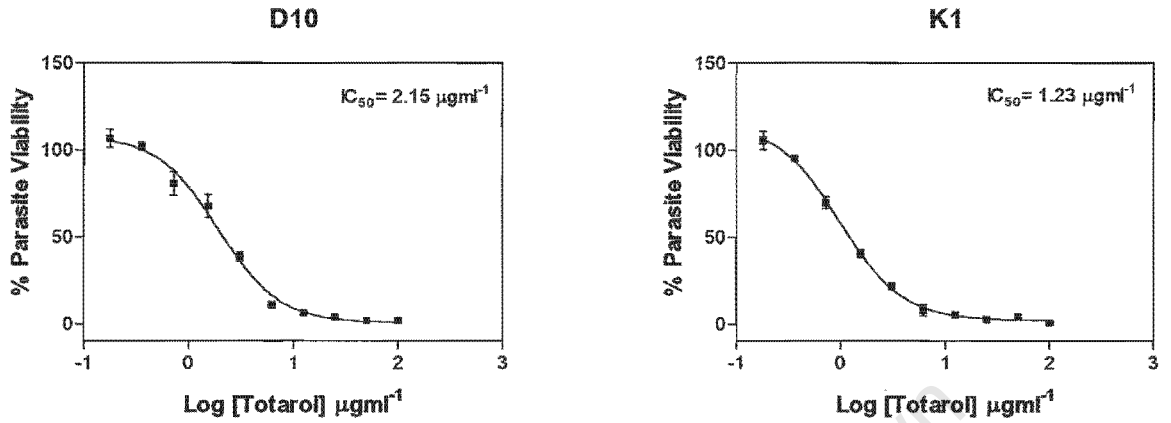

Figure 5.3.2. Dose response curves of totarol against *P. falciparum* D10 and K1. Each point represents the mean of 3 independent experiments each performed in duplicate

Totarol displayed antiplasmodial activity against a CQ-sensitive and CQ-resistant strain of *P. falciparum*. A comparison of the activity of totarol in the two strains using the Mann-Whitney two-tailed test, indicated that there was a statistically significant difference (P=0.0022), with K1 being approximately 1.7-fold more sensitive to totarol than D10.

5.3.3 *In vitro* antiplasmodial activity and cytotoxicity of the totarol derivatives

The synthesised β-amino alcohols (**2-6**), as well as the corresponding amines (**2-6**), were tested for *in vitro* antiplasmodial activity against a CQ-sensitive (D10) and CQ-resistant (K1) strain of *P. falciparum*. The compounds (**2-6**) were also tested for *in vitro* cytotoxicity using CHO cells, to determine the selectivity. The dose response curves are in Appendix 1 (Figure 5.3.3), and the corresponding IC_{50} values are summarised in Table 5.3.3. For comparative purposes the activity of totarol and compounds **56** and **60** can also be found in Table 5.3.3. In addition to the 50% inhibitory concentrations (IC_{50}), the resistance index (R_I= K1-IC_{50}/D10-IC_{50}), which gives an indication of the relative activity of the compounds in a drug resistant and sensitive strain of *P. falciparum*, was recorded. Furthermore, the ratio of cytotoxicity to antiplasmodial activity (S_I= CHO-IC_{50}/ K1-IC_{50}) is also listed in the Table.

Table 5.3.3. *In vitro* antiplasmodial activity and cytotoxicity of the amines (**2-6**), the new compounds (**2-6**), totarol and compounds **56** and **60**. The IC_{50} values in brackets are in μM

Compound	IC_{50} μgml^{-1} (μM)			S_I	R_I
	D10	**K1**	**CHO**		
Amine 2 	>100 (>1367)	85.73 ± 6.59 (1172 ± 90.10)	-	-	ND
Amine 3 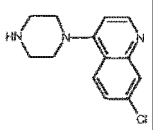	0.292 ± 0.002 (1.18 ± 0.008)	0.240 ± 0.014 (0.97 ± 0.057)	-	-	0.82
Amine 4 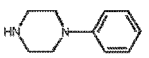	59.55 ±2.26 (367.05 ± 13.93)	3.32 ± 0.21 (20.46 ± 1.29)	-	-	0.06
Amine 5 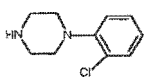	33.34 ± 3.85 (169.46 ± 19.57)	1.65 ± 0.05 (8.39 ± 0.25)	-	-	0.05
Amine 6 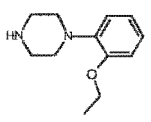	38.94 ± 5.45 (188.81 ± 26.43)	1.93 ± 0.15 (9.36 ± 0.73)	-	-	0.05
Intermediate 1 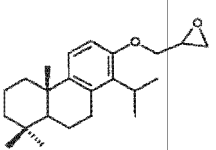	4.54 ± 0.71 (13.26 ± 2.07)	-	-	-	-
Product 2 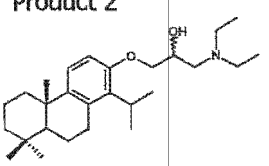	0.25 ± 0.08 (0.61 ± 0.19)	0.26 ± 0.06 (0.63 ± 0.15)	3.21 ± 0.46 (7.73 ± 1.11)	12.21	1.04
Product 3 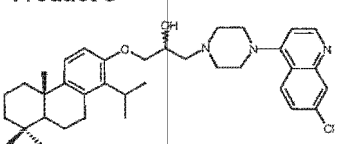	0.82 ± 0.14 (1.40 ± 0.23)	0.53 ± 0.08 (0.90 ± 0.14)	55.51 ± 4.65 (94.19 ± 7.89)	104.89	0.64

For D10 and K1, the values represent the mean IC_{50} (± SD) of three independent experiments each performed in duplicate. For CHO cells, the values represent the mean IC_{50} (±SD) of three independent experiments each performed in quadruplicate

Table 5.3.3. (Continued) *In vitro* antiplasmodial activity and cytotoxicity of the amines (**2-6**), totarol derivatives (**2-6**), totarol and compounds 56 and 60. The IC_{50} values in brackets are in μM

Compound	IC_{50} μgml^{-1} (μM)			S_I	R_I
	D10	**K1**	**CHO**		
Product 4 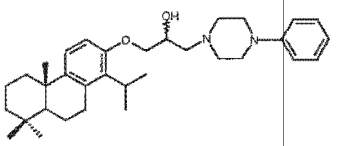	1.29 ± 0.15 (2.56 ± 0.30)	0.92 ± 0.06 (1.81 ± 0.11)	53.18 ± 1.47 (105.44 ± 2.91)	58.13	0.71
Product 5 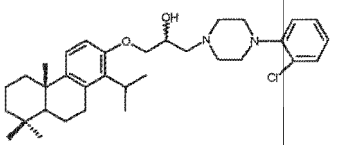	1.75 ± 0.11 (3.25 ± 0.20)	0.48 ± 0.19 (0.90 ± 0.35)	>100 (>186)	ND	0.28
Product 6 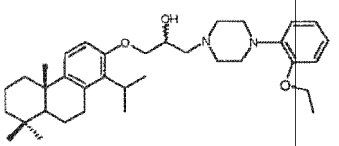	0.89 ± 0.18 (1.62 ± 0.33)	0.56 ± 0.042 (1.01 ± 0.08)	>100 (>182)	ND	0.62
Totarol 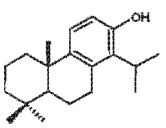	2.15 ± 0.59 (7.51 ± 2.06)	1.23 ± 0.15 (4.29 ± 0.52)	48.79 ± 0.96 (170.46 ± 3.35)	39.66	0.57
Compound 56 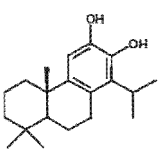	0.76 ± 0.09 (2.51 ± 0.30)	0.83 ± 0.07 (2.75 ± 0.23)	51.45 ± 7.79 (170.24 ± 25.78)	61.99	1.09
Compound 60 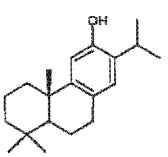	0.95 ± 0.08 (3.32 ± 0.28)	0.63 ± 0.05 (2.20 ± 0.17)	51.69 ± 2.67 (180.59 ± 9.33)	82.05	0.67

For D10 and K1, the values represent the mean IC_{50} (± SD) of three independent experiments each performed in duplicate. For CHO cells, the values represent the mean IC_{50} (±SD) of three independent experiments each performed in quadruplicate

The results from Table 5.3.3 are graphically illustrated in Figures 5.3.3.1 A, B and C and 5.3.3.2.

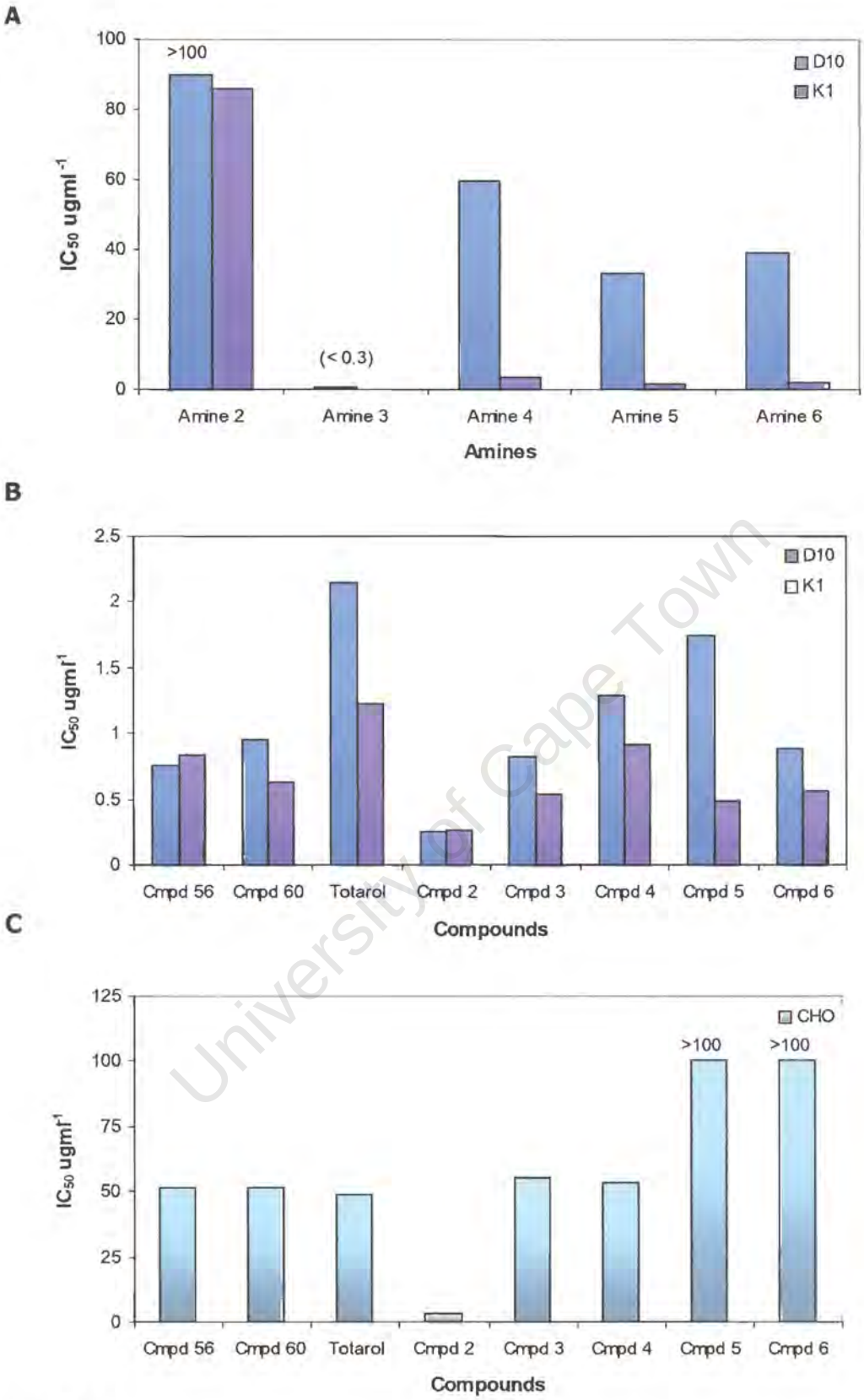

Figure 5.3.3.1.

A Summary of the IC_{50} values of the amines (**2-6**) against *P. falciparum* D10 and K1

B Summary of the IC_{50} values of compounds **56** and **60**, totarol, and the β-amino alcohols (**2-6**) against *P. falciparum* D10 and K1

C Summary of the IC_{50} values of compounds **56** and **60**, totarol and the β-amino alcohols (**2-6**) against CHO cells.

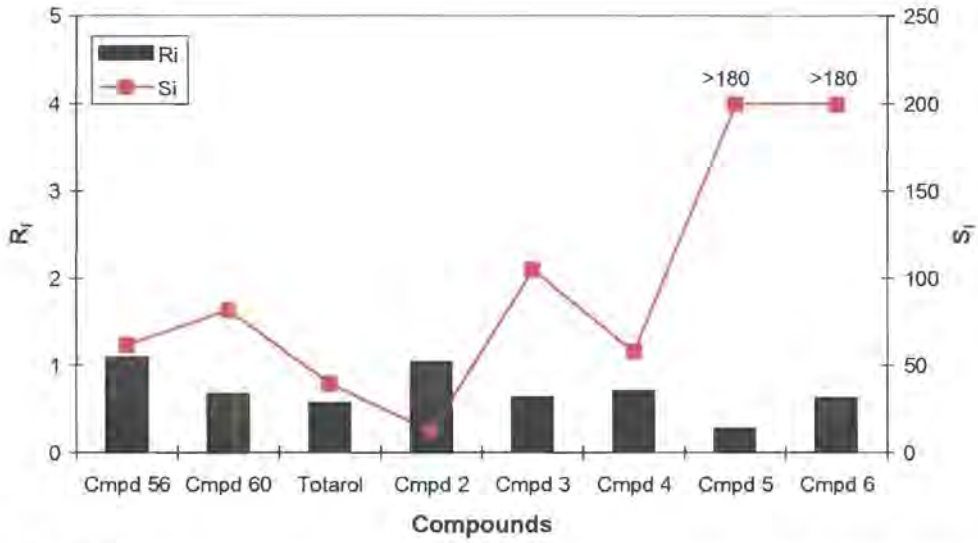

Figure 5.3.3.2 Summary of the selective (S_I) and resistance indexes (R_I) of the tested compounds

5.3.4 *In vitro* antiplasmodial activity of compound 56 and 6 when combined with chloroquine

When different antimalarial agents are taken simultaneously, they often interact in a specific way that can be classified as additive, synergistic or antagonistic. A technique adapted from Chawira and Warhurst (1987), using fixed ratios of predetermined concentrations needed to inhibit parasite growth by 50% (IC_{50}) was used to determine the interaction of compound **56** with CQ, and compound **6** with CQ (Details in Chapter 7, 7.6.1). Compound **6** was chosen as a representative of the synthesised β-amino alcohols. Similarly, compound **56** served as an example of the unmodified phenolic diterpenes. The results are illustrated in Figure 5.3.4.

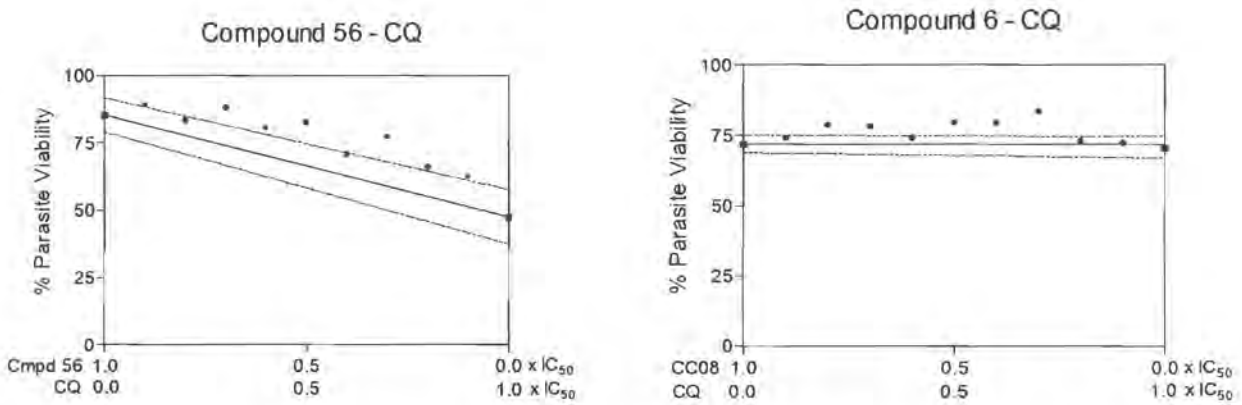

Figure 5.3.4. Additive effect shown by the compound **56** and CQ combination and by the ompound **6** and CQ combination on *P. falciparum* D10. The 95% confidence intervals for the observed IC_{50} values are joined by dashed lines to indicate the expected variability

If the effect of the combination is additive, then the parasite viability values for the fixed ratios lie on the straight line joining the values obtained for the drugs individually. Synergism is indicated by points below the line, and antagonism by points above the line. Although the variability within the set of data was high (i.e. the points did not lie on a straight line), the results indicate that a combination of CQ and compound **56** had an additive effect, as did the combination of compound **6** and CQ.

5.3.5 Separation of the possible diastereoisomers in compound 3

The duplication of a single pair of NMR resonances in compound **3** suggested that there may be a mixture of diastereoisomers. While enantiomers have identical physical properties, diastereoisomers have different physical properties and can usually be separated by techniques that utilise these. In an attempt to separate the possible diastereoisomers of **3**, successive development TLC was used in addition to HPLC (Details in Chapter 7, 7.5).

The TLC technique yielded a single spot after several developments. The HPLC profile of **3** (Figure 5.3.5.) indicated that the compound was 86% pure and contained a minor impurity.

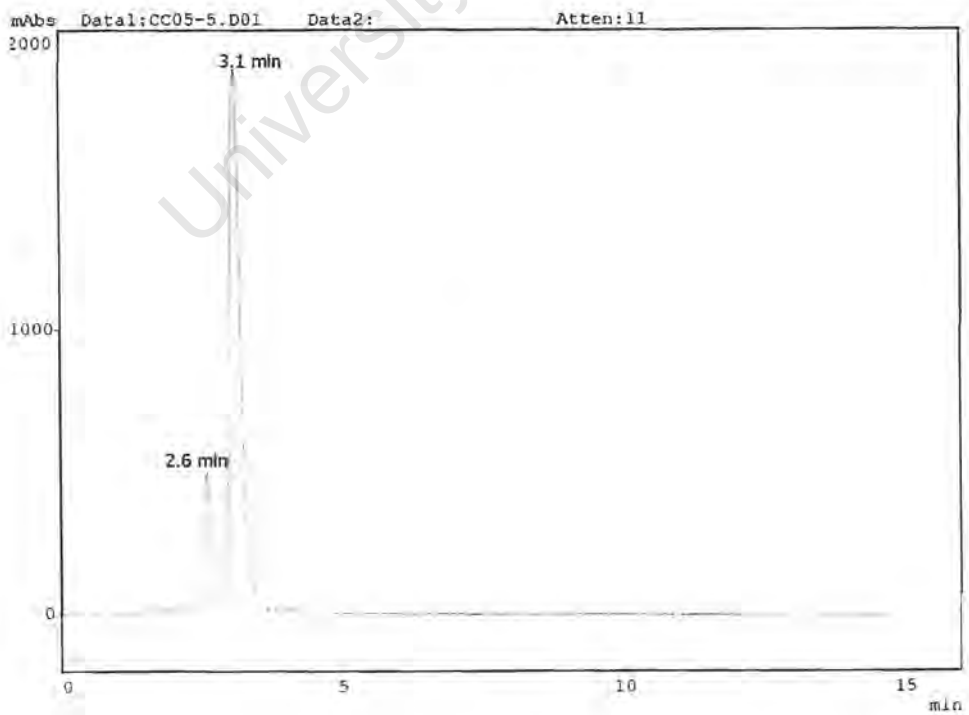

Figure 5.3.5. HPLC chromatogram of compound **3**

The UV spectrum (Appendix 2, A2.7) of the major peak (R_T=3.08min) differed from that of the minor constituent, suggesting that the two compounds had different structural features and were therefore not stereoisomers of each other. Neither the TLC nor HPLC techniques used supported the presence of diastereoisomers.

5.4 Discussion

5.4.1 Identity and purity of the synthesised compounds

The HREIMS and NMR data for the compounds **2** - **6** provided definite evidence that the compounds were consistent with their expected structures. Moreover, the IR spectra confirmed the presence of the hydroxyl group in all of the synthesised β-amino alcohols.

The compounds **2** - **6** were purified using preparative TLC until a single spot was obtained. In addition to the TLC profiles, the HREIMS and NMR spectrums indicated that the compounds were highly pure. This was further confirmed by the sharp melting points of **2** - **6**. The specific rotation measurements showed that all of the synthesised compounds were optically active and were dextrorotatory (+), although the optical purity of the compounds could not be determined at this stage.

Analysis of the NMR spectrum of **3** suggested that a mixture of **3** and either its intramolecularly H-bonded conformation or its diastereoisomers were generated. In an attempt to resolve the possible diastereoisomers of **3**, both TLC and HPLC separation techniques were used. The successive development TLC indicated that a single compound was present, while the HPLC profile showed that the compound was over 85% pure and contained a minor impurity. Since the UV absorption of the impurity differed from that of the main peak, it was concluded that these two compounds were probably not diastereoisomers. The lack of evidence for diastereoisomers would suggest that an intramolecularly H-bonded conformation of **3** was responsible for the duplicated ^{1}H NMR signals. The IR absorption of the O-H bond could be used as a test for and measure of the strength of the proposed intramolecularly H-bonding. However, an insufficient amount of 3 remained to measure the IR absorption in $CHCl_3$.

If diastereoisomers were present and their physical poperties were only marginally different, a chiral HPLC column may facilitate resolution as opposed to the normal phase TLC and HPLC, which were used in this study. A common method to separate diastereoisomers is recrystallization. Due to the small quantity of **3** that was synthesised in this study, further purification by recrystallization was not feasible. If the isomers could be separated by recrystallisation and there were sufficient quantities to grow an X-ray crystal, then X-ray crystallography could be used to determine the absolute stereochemistry at the new chiral. Although confirmation of a mixture of diastereoisomers was not necessary for the initial screening purposes, it would be interesting to determine the relative activity of the different isomers and to determine if the activity is stereo-dependent. Research on the antibacterial activity of enantiomers of ferruginol has shown that (-)-ferruginol is more potent than (+)-ferruginol (Yang *et al.*, 2001).

In conclusion, five new compounds were successfully synthesised and were shown to be consistent with the expected structures. Furthermore, the compounds showed a high level of purity.

5.4.2 *In vitro* antiplasmodial activity and cytotoxiciy of totarol

Totarol showed marked antiplasmodial activity against a CQ-sensitive and resistant strain of *P. falciparum*. Comparison of the IC_{50} values for D10 and K1 indicated that K1 was almost twice as sensitive to totarol than D10. Although the activity of totarol was comparable to that of the isolated compounds **56** and **60**, totarol was slightly less active (half as potent). The cytotoxicity assays revealed that the antiplasmodial activity was 40-fold greater than the cytotoxic effect. This demonstrates that totarol has sufficient selectivity to kill the parasites without damaging mammalian cells. The *in vitro* cytotoxicity of totarol has previously been reported (Evans *et al.*, 1999) and confirmed the finding that totarol was not toxic.This is the first time, to the best of my knowledge, that totarol has been shown to possess *in vitro* antiplasmodial activity.

5.4.3 *In vitro* activity of the synthesised compounds and their starting materials

For the five new compounds as well as their respective amines no attempt was made to determine the IC_{50} values in excess of 100μgml^{-1} as non-specific toxicity is often shown at these concentrations. Diethylamine (amine **2**) did not show significant antiplasmodial activity against D10 or K1. Although amine **2** has strong basic properties these did not appear to affect parasite viability.

The most active amine was **3**, which showed strong antiplasmodial activity against D10 (IC_{50}=0.29μgml^{-1}) and K1 (IC_{50}=0.24μgml^{-1}). Amine **3** and chloroquine both possess a 4-amino-7-chloroquinoline structure (Figure 5.4.3.), which has been shown to exhibit moderate *in vitro* antiplasmodial activity (Egan *et al.*, 2000).

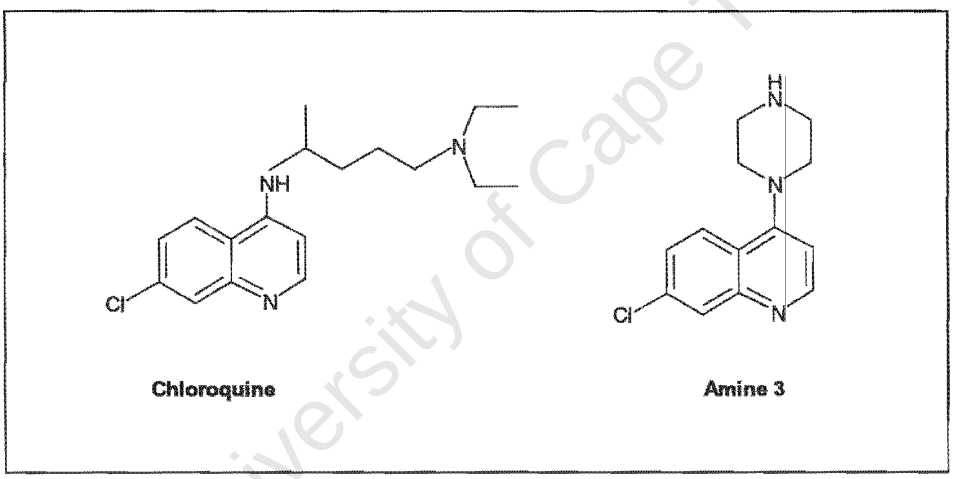

Figure 5.4.3. Structures of chloroquine and amine **3**

Research on the structure-function relationships in aminoquinolines has shown that the 4-aminoquinoline nucleus provides a haematin complexing template, while the 7-chloro group is responsible for the inhibition of β-haematin formation (Egan *et al.*, 2000). Although these groups are required for β-haematin inhibitory activity, the aminoalkyl side chain of CQ is necessary for potent antiplasmodial activity. Furthermore, changes in the length of the aminoalkyl side chain have been shown to have little effect on the activity in CQ-sensitive *P. falciparum* but a profound influence on the activity against CQ-resistant strains (De *et al.*, 1996). In light of the above, the observed activity of **3** is most likely due to the presence of the 4-amino-7-chloroquinoline structure. Amine **3** displays activity against both the CQ-sensitive and resistant strain (R_I=0.82). The fact that the activity is

not as strong as CQ, and that CQ cross resistance is not observed is probably due to the absence of the aminoalkyl side chain.

Among the amines tested, the most interesting results were those of amines **4**, **5** and **6**. These three amines showed little activity against the CQ-sensitive strain but were highly active against the resistant strain. The resistant indexes (R_I) indicated that the amines were approximately 20-times more potent in K1 than D10. Moreover, the attachment of a chlorine and OEt group to phenylpiperazine (amine **4**) caused a two-fold increase in antiplasmodial activity in both D10 and K1. Considering that the main difference between D10 and K1 is their CQ sensitivity, it can be speculated that the acquired mechanism of CQ resistance causes K1 to become more susceptible to amines **4**, **5** and **6**. At present, neither the mode of action of the amines nor the precise mechanism of CQ resistance is known. Thus, the exact reason for the increased sensitivity of K1 to the amines is unclear.

In order to establish which structural features were responsible for the antiplasmodial activity all of the starting materials, products and the epoxide intermediate were tested for activity. Compared to totarol, the epoxide showed reduced antiplasmodial activity. The fact that the epoxide was less soluble than totarol and the amines, could account for its reduced activity in the antiplasmodial tests.

Out of the newly synthesised compounds, **2** showed the greatest antiplasmodial activity. The resistant index (R_I=1.04) indicated that **2** was equally active against D10 and K1, with an IC_{50} value of 0.3μgml^{-1}. The antiplasmodial activity was found to be only 12-times greater than the cytotoxic effect. The low selectivity index suggests a slender safety margin, which would limit its potential as a useful antimalarial drug. In terms of developing compound **2** further, attempts could be made to produce chemical analogues with reduced cytotoxicity.

Compound **3** also showed significant antiplasmodial activity against D10 (IC_{50}= 0.82μgml^{-1}) and K1 (IC_{50}=0.53μgml^{-1}), although it was not as active as the starting amine (IC_{50} *ca* 0.27μgml^{-1}). As mentioned previously, the activity of amine **3** appears to be due to the 4-amino-7-chloroquinoline structural feature. When combined with totarol this activity is reduced, suggesting that the new compound prevents the 4-amino-7-chloroquinoline structure from either (i) being delivered to the requisite site of action within the parasite or (ii) prevents it from interacting with its target. Amine **3** is equally

active against D10 and K1, whereas compound **3** is 1.6-fold more potent to K1. Since totarol was 1.7-times more active in K1, the difference in activity of **3** in K1 and D10 is thought to stem from the totarol moiety of the compound. The selectivity index for **3** was 105, demonstrating a large safety margin. Despite the good antiplasmodial activity and lack of cytotoxicity, compound **3** was not as active as its amine. In light of this evidence, amine **3** would be a stronger candidate for antimalarial drug development compared to compound **3**.

The compounds **4**, **5** and **6** showed a remarkable improvement in activity compared to their respective amines. The amines all contained a phenylpiperazine nucleus and were 20-times more active against K1. Not only were compounds **4**, **5** and **6** considerably more active against both of the strains but the difference in sensitivity between D10 and K1 was approximately 2-fold. The antiplasmodial activity of **4**, **5** and **6** followed the relative activity of the amines, with **5** and **6** possessing the greatest activity followed by **4**. The different phenylpiperazine amines were chosen to probe the effect of a substituent on the aromatic ring. This showed that the attachment of a chlorine atom and an OEt group resulted in a significant increase in activity. Furthermore, **4** showed very little cytotoxicity while **5** and **6** were the least cytotoxic out of the synthesised compounds. The actual IC_{50} values for **5** and **6** could not be determined against the CHO cells since 100% cell viability was observed even at the highest concentrations ($100\mu gml^{-1}$) tested. The selective index for **5** and **6** exceeded 180, which demonstrated the large safety margin of these compounds. The synthesis of **4**, **5** and **6** involved generating a hybrid of totarol, a phenylpiperazine nucleus and an β-amino alcohol moiety. Since both the phenylpiperazine nucleus and totarol both showed initial activity, it is difficult to establish whether the improved activity of the hybrid compound is due to the combination of these two groups or if it is also influenced by the β-amino hydroxyl moiety. The precise structural features responsible for the activity could not be determined at this stage, but the overall combination does display favourable antiplasmodial activity and cytotoxicity.

Although the series of β-amino alcohols synthesised is relatively small, a number of interesting generalisations can be made on the strength of this data. The addition of a phenylpiperazine nucleus to totarol causes an increase in antiplasmodial activity, which is enhanced by the attachment of a chlorine or OEt substituent to the phenylpiperazine aromatic ring. Attachment of a 4-amino-7-chloroquinoline group to totarol reduces the

activity of the former, while the attachment of diethylamine to totarol greatly increases its activity.

In comparison to totarol, all of the new compounds showed improved antiplasmodial activity and no cross resistance with CQ. The most promising lead compounds in terms of selectivity and antiplasmodial activity are **5** and **6**. Both of these compounds exhibited significant antiplasmodial activity, high selective indexes and low resistance indexes. Although the antiplasmodial activity of **6** was comparable to that of the isolated compounds, **6** was less cytotoxic and would have a larger safety margin. In light of the above, compounds **5** and **6** showed the greatest potential for further lead development.

5.4.4 The effect of combining compounds 56 and 6 with chloroquine

The observations from these experiments suggest that the effect of **56** and CQ, and **6** and CQ is additive. Thus, the compounds and CQ had no influence on each other's activity. This information would be useful at a later stage if one of the compounds was developed into an antimalarial drug and there was a possibility that it could be co-administered with CQ. The use of combinations of antimalarials is being used increasingly to reduce the doses of individual drugs and as a possible means of circumventing or delaying the development of resistance (Kirby, 1996).

5.5 Conclusion

This study demonstrated for the first time that totarol possessed *in vitro* antiplasmodial activity against a drug resistant and sensitive strain of *P. falciparum*. Since the activity of totarol was comparable to that of **56** and **60**, it was used for chemical modification to generate potential lead compounds. A series of five β-amino alcohols were successfully synthesised, purified and fully characterised. The novel compounds were evaluated for *in vitro* antiplasmodial activity and cytotoxicity, and all showed an improved antiplasmodial activity. Although there is insufficient data at this stage to make definite structure-activity relationship conclusions, the addition of a phenylpiperazine structure to totarol showed the greatest improvement in antiplasmodial activity and selectivity. In terms of antimalarial drug development, compounds **5** and **6** showed the greatest potential and warrant further investigation as promising lead compounds.

Chapter 6

Research Summary, Prospects and Conclusions

6. Research Summary, Prospects and Conclusions

6.1 Research summary

In terms of mortality and morbidity, malaria is by far the world's most important parasitic disease and has a serious impact upon health and economic welfare in the tropical world. The increasing prevalence and distribution of malaria has been attributed to drug and insecticide resistance as well as social and environmental changes. Since the treatment and control of the disease relies heavily on chemotherapeutic agents, there is an urgent need to develop new antimalarial drugs to meet the challenge of resistance when it arises. Historically, the majority of antimalarial drugs have been derived from higher plants or from structures suggested by plant compounds. Although South Africa contains 10% of the earth's plant diversity, little is known about the antimalarial activity of South African plant species. The importance of indigenous plants lies not only in their chemotherapeutic effect, but also in their role as a potential source of novel structures for drug development. In light of South Africa's untapped biodiversity and the pressing need for new antimalarial agents, a South African medicinal plant was investigated for novel antimalarial drugs.

The plant *Harpagophytum procumbens* was selected after initial screens showed that the crude extract displayed *in vitro* antiplasmodial activity (IC_{50}=13μgml^{-1}). An extensive literature search revealed that this plant is widely used in traditional medicine to treat a variety of illnesses, including fevers and has not been examined for antiplasmodial activity. Bioassay-guided fractionation of the crude PE root extract resulted in the isolation of two active compounds that were identified as 8,11,13-Totaratriene-12-13-diol (**56**) and 8,11,13-Abietatrien-12-ol (**60**). Studies on three different batches of *H. procumbens* suggested that the structures and levels of the antiplasmodial components vary considerably between plants.

The active compounds exhibited significant *in vitro* antiplasmodial activity (IC_{50}<1μgml^{-1}) against several strains of *P. falciparum* and very little cytotoxicity (IC_{50}> 50μgml^{-1}) against mammalian cells (CHO and HepG2). Although the compounds have previously been isolated from other plants, they have not been isolated from *H. procumbens* and are not known to possess selective antiplasmodial activity. Furthermore, the compounds have different structural features compared to any of the current antimalarial drugs. Since the

active compounds were isolated in low yields (0.015 – 0.033% by weight) a commercial analogue (totarol) was obtained to generate potential leads of **56** and **60**. This study showed for the first time that totarol reduced parasite viability in a dose-dependant manner and that the activity was comparable to the isolated compounds. Thus, totarol was used as the scaffold to synthesise a series of β-amino alcohols that contained chemical features known to be present in existing antimalarial agents. Five novel compounds were successfully synthesised and evaluated for *in vitro* antiplasmodial activity and cytotoxicity. Compared to totarol, the synthesised compounds all showed improved activity against a drug sensitive and resistant strain of *P. falciparum* and displayed little cytotoxicity. Although a number of interesting generalisations could be made, at this stage there is insufficient data to make definite structure-activity conclusions. In terms of lead development, two of the synthesised compounds showed considerable potential and warrant further investigation as promising leads. This study identified two template molecules from *H. procumbens* for the design of new antimalarial drugs. Compelling evidence was also provided for the exploration of South African plants as a source of novel antimalarials.

6.2 Research prospects

Typically, active natural products are present in very low (<001 percent by weight) quantities in natural sources (Cragg and Newman, 2001). This was the case for the antiplasmodial compounds isolated from the *H. procumbens* roots. Furthermore, the yields of the active components remained low despite attempts to optimise the extraction and purification procedures. Since the Grassroots Natural Products Group grow *H. procumbens* on a commercial scale under controlled conditions, an opportunity exists to study the levels of the active compounds during a vegetation period and under different growing conditions. Insight may be obtained in the fluxes of and relationships between the active compounds and the different stages of growth and changes in environmental conditions. Additionally, if the levels of the active compounds are measured in plants of different origins, a high-producing chemotype could be selected for in the field and cultivated. This could potentially increase the production and yields of the desired compounds and make *H. procumbens* a viable source of the antiplasmodial components.

In addition to the isolated compounds **56** and **60**, it was suggested that a number of less active compounds were also present in the crude root extract. If these compounds are biosynthetically related to **56** and **60** and can be isolated in sufficient quantities for structure elucidation and *in vitro* testing, then structure-activity information could be obtained. Alternatively, a number of plant compounds exist as groups of structurally related metabolites within related species of plants. There are two species of *Harpagophytum*, *procumbens* and *zeyheri*, both of which are used for medicinal purposes. It may be useful to compare their *in vitro* antiplasmodial activity and establish whether the activity is due to biosynthetically related compounds. The activity of chemical analogues, either plant-derived or synthetic, of the isolated compounds would provide structure-activity information that could be used to determine the essential features of the molecule necessary for activity. This could also be achieved by chemically dissecting the molecule to probe the important regions for retention of activity. In some instances this has led to the identification of simpler analogues with similar or better activity.

As the yields of the isolated compounds were very low, a commercial analogue was used for chemical modification purposes. Although a series of β-amino alcohols was synthesised, a multitude of chemical modifications could potentially be made. Different substitution patterns of the totarol scaffold would create chemical diversity. This may facilitate identification of desirable modifications that might lead to more suitable candidates for drug development. An essential part of drug development is to screen the compounds for *in vivo* activity. This could be achieved by using a *Plasmodium berghei* mouse model and would provide valuable information on the *in vivo* antiplasmodial activity, intrinsic toxicity as well as pharmacokinetic and pharmacodynamic properties. The metabolism of the compounds could also be studied *in vivo* by incorporating a radioactive label (usually ^{14}C) and monitoring the metabolites. Drug metabolism studies could establish whether the compounds are metabolised to a more active, less active or inactive form. In an *in vitro* setting, radioactive labeling could also be used to determine the site and mode of action of the compounds.

While the isolated compounds showed potent antiplasmodial activity, totarol has previously been found to possess significant antibacterial activity. It may be useful to evaluate the isolated compounds against a range of microorganisms including other protozoa, bacteria and fungi. A number of *in vitro* assays for the different microorganisms exist and could easily be used to screen the compounds for additional activity.

In this study two antiplasmodial hit compounds were isolated from a medicinal plant and identified, and a series of promising lead compounds was synthesised. The ultimate objective would be to use structural variations to improve these compounds such that their *in vivo* profile of characteristics fulfils the defined criteria for a pre-clinical candidate. The development of these hits into potential drugs would require the combined *in vitro* and *in vivo* activity, selectivity, structure-activity relationship trends, mechanism of action and the pharmacokinetic profile. This thesis focused on drug discovery and the initial optimisation of the *in vitro* antiplasmodial activity of the compounds. This information could provide a basis for the development of a novel class of antimalarial drugs.

6.3 Conclusions

The investigation of *Harpagophytum procumbens* showed that the roots are a potential source of novel antiplasmodial compounds. Two diterpenes, 8,11,13-Totaratriene-12-13-diol (**56**) and 8,11,13-Abietatrien-12-ol (**60**) were isolated from the root extract and were found to possess potent *in vitro* antiplasmodial activity and little cytotoxicity. In light of their *in vitro* activity and different structural features, the compounds were used as models to generate lead compounds with enhanced antiplasmodial activity and reduced cytotoxicity. Five potential leads were synthesised from a commercial analogue of the isolated compounds. The *in vitro* activity of these new compounds revealed favourable modifications that could be used to optimise the activity of the model compounds.

This thesis showed for the first time that the roots of *H. procumbens* possessed *in vitro* antiplasmodial activity. Although the isolated compounds are known, they have not previously been isolated from *H. procumbens* and are not known to possess selective antiplasmodial activity. Furthermore, the plant-derived compounds have different structural features to any of the current antimalarial drugs. It is hoped that these biologically privileged structures will serve as scaffolds for a new class of antimalarial drugs. Only a small fraction of South Africa's biodiversity has been investigated and it can be assumed that indigenous plants will continue to offer models for novel therapeutic agents. This is particularly relevant to diseases in Southern Africa that lack effective chemotherapeutic agents.

Chapter 7

Materials and Methods

7. Materials and Methods

7.1 Plant Material

The initial sample of *H. procumbens* roots (20g) was obtained from Botswana and little is known about its growing conditions or time of harvest. Two separate batches (I and II) of dried *H. procumbens* roots (3kgs in total) were sourced from the Sunflower Health Shop (Long Market Street, Cape Town). These dried cut root sections originated from wild harvested material in the Namibian region and were collected towards the end of the rainy season (early autumn). Additional *H. procumbens* plant material was acquired from the Grassroots Natural Products Group, which grow *H. procumbens* on a commercial scale on a farm in Gouda in the Western Cape. Since the plant does not grow naturally in this area, cuttings of *H. procumbens* were obtained from the Northern Cape, propagated and planted in well-drained sandy mounds. During summer the plants are irrigated once a week from the Berg River and the average daily temperature exceeds 30°C. Initially two whole plants, including root sections, aerial parts and fruits were investigated for activity. Since the antiplasmodial components were concentrated in the root sections an additional 10kgs of powdered *H. procumbens* roots were obtained. This composite root material was collected towards the end of July from 3-year-old plants. Voucher specimens containing flowers, aerial parts and fruits of these plants were deposited in the Bolus Herbarium, Department of Botany, University of Cape Town.

7.2 Preparation of the Plant Extracts

The first batch of dried *H. procumbens* roots (batch I) was chopped into small pieces (*ca* 0.5cm^3) and extracted with water (H_20), petroleum ether (PE) and methanol (MeOH). For the H_2O and sequential organic (PE followed by MeOH) extraction, 500g of root material was put into a flat-bottomed flask and extracted by vigorous shaking with 500ml of solvent (H_2O, PE and MeOH) for 24 hours. The extracts were filtered and the remaining plant material was placed in a soxhlet for 10 hours. The filtrates for the hot and cold H_2O extractions were combined and concentrated by freeze drying. Similarly, the hot and cold PE extracts were pooled and evaporated under vacuum, as were the hot and cold MeOH extracts. The concentrated extracts were then transferred to pre-weighed vials and stored

at 4°C. The second batch of *H. procumbens* roots (batch II) was only extracted with cold and hot PE.

Two whole *H. procumbens* plants were obtained from the Grassroots Natural Products Group. The aerial sections (leaves and stems) were left at room temperature (25°C) for a week to dry and were then ground into a fine powder with a laboratory blender (Waring). The characteristic hooked fruit of *H. procumbens* was opened with a pair of pliers and the seeds were removed, ground into a powder using a mortar and pestle and were left to dry at room temperature for a week. The roots tubers (*ca* 10 – 20 cm in length) were washed, cut into smaller pieces, dried at room temperature and ground into a fine powder with a laboratory blender. Samples of the powdered aerial sections, seeds and roots were shaken with cold PE for 24hrs and the extracts were filtered and concentrated by rotary vacuum evaporation. Since the roots showed the greatest activity, an additional 10kgs of dried powdered *H. procumbens* roots were obtained from Grassroots. The fresh cut roots were washed, chopped into smaller pieces, dried at 37°C in well-ventilated ovens and ground to a fine powder using an industrial scale dry mill. Several kilograms of this powdered root material were exhaustively extracted with cold PE and concentrated under reduced pressure.

7.3 Flash Chromatography (FC)

7.3.1 FC of the PE extract of *H. procumbens* roots (batch I)

The active crude PE extract of *H. procumbens* (batch I) was separated by flash chromatography on type H silica gel 10 - 40μ (Sigma) in a 10.5 x 9.0cm column, eluting with a step gradient of increasing polarity from PE to ethyl acetate (EtOAc) to MeOH, at 100ml per fraction. Full details of the FC of *H. procumbens* (batch I) are given in Table 7.3.1. The profile of each fraction was monitored using TLC and viewed under UV light (λ 254/365nm) and similar fractions were pooled, concentrated and stored in pre-weighed vials at 4°C. The fractions were tested for *in vitro* antiplasmodial activity and the most active fraction was purified further by HPLC. Scheme 7.3.1 illustrates the isolation and purification of the active component **H5a** from the *H. procumbens* roots (batch I).

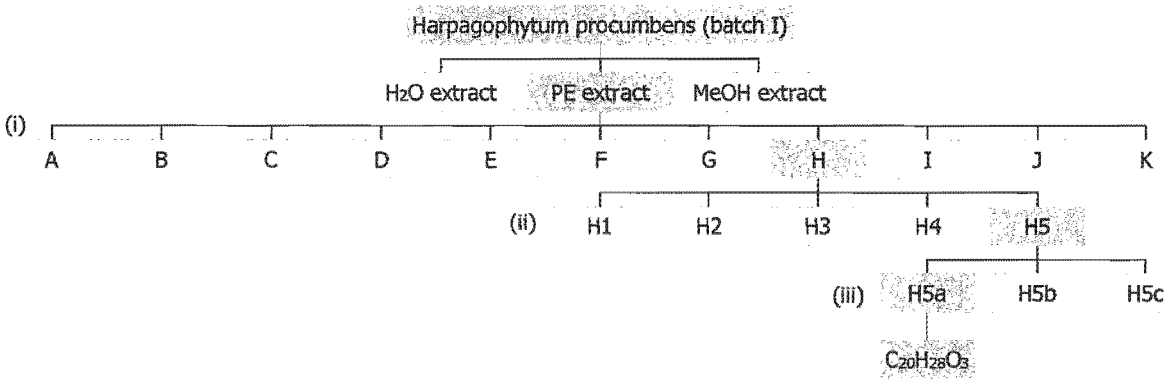

Scheme 7.3.1. Fractionation of the active component **H5a** from *H. procumbens* roots (batch I). (i) FC, Silica gel (PE-EtOAc-MeOH); (ii) HPLC, C_{18} (H_2O: MeOH); (iii) HPLC, C_{18} (H_2O: MeOH)

7.3.2 FC of the PE extract of *H. procumbens* roots (batch II)

The PE extract of *H. procumbens* roots (batch II) was chromatographed using FC. The FC conditions were the same as those described for batch I. Full details of the FC of batch II are given in Table 7.3.2.

Table 7.3.1. Flash chromatography on the PE extract of *H. procumbens* roots (batch I)

FC solvent system			Number of fractions	TLC solvent system	R_f values	Combined fraction	% Yield of combined fraction
PE	EtOAc	MeOH					
100	-	-	9	PE: EtOAc (4:1)	0.95	A	3.5
95	5	-	3	PE: EtOAc (4:1)	0.95	A	-
95	5	-	6	PE: EtOAc (4:1)	0.94, 0.92	B	5.0
95	5	-	60	PE: EtOAc (4:1)	0.94, 0.92, 0.61, 0.55, 0.43	C	32.0
90	10	-	6	PE: EtOAc (4:1)	0.94, 0.92, 0.61, 0.55, 0.43	C	-
85	15	-	6	PE: EtOAc (4:1)	0.94, 0.92, 0.61, 0.55, 0.43	C	-
80	20	-	6	PE: EtOAc (4:1)	0.94, 0.92, 0.61, 0.55, 0.43	C	-
75	25	-	6	PE: EtOAc (4:1)	0.94, 0.92, 0.61, 0.55, 0.43	C	-
70	30	-	18	PE: EtOAc (4:1)	0.66, 0.60, 0.44, 0.36	D	3.5
65	35	-	18	PE: EtOAc (4:1)	0.19	E	4.5
60	40	-	6	PE: EtOAc (4:1)	0.19	E	-
50	50	-	6	PE: EtOAc (4:1)	0.17, 0.06	F	3.5
-	100	-	12	PE: EtOAc (1:1)	0.17, 0.06	F	-
-	80	20	5	EtOAc: MeOH (7:3)	0.98, 0.89, 0.75, 0.56	G	1.5
-	80	20	4	EtOAc: MeOH (7:3)	0.40, 0.04	H	1.5
-	60	40	6	EtOAc: MeOH (1:1)	0.98, 0.82, 0.16	I	3.0
-	40	60	6	EtOAc: MeOH (1:1)	0.98, 0.93, 0.77	J	1.0
-	20	80	6	EtOAc: MeOH (1:1)	0.98, 0.93, 0.77	J	-
-	-	100	6	EtOAc: MeOH (1:1)	0.98, 0.93, 0.77	K	2.5

Table 7.3.2. Flash chromatography on the PE extract of *H. procumbens* roots (batch II)

FC solvent system			Number of fractions	TLC solvent system	R_f values	Combined fraction
PE	EtOAc	MeOH				
100	-	-	5	PE: EA (1:1)	0.95, 0.94	A
80	20	-	7	PE: EA (1:1)	0.95, 0.94, 0.45, 0.33	B
80	20	-	3	PE: EA (1:1)	0.96, 0.93, 0.75, 0.66, 0.59, 0.47	C
80	20	-	8	PE: EA (1:1)	0.98, 0.76, 0.67, 0.42	D
60	40	-	4	PE: EA (1:1)	0.98, 0.95, 0.64, 0.48, 0.33, 0.28	E
60	40	-	5	PE: EA (1:1)	O.98, 0.95, 0.33, 0.28	F
40	60	-	5	PE: EA (1:1)	0.96, 0.90, 0.35	G
40	60		5	PE: EA (1:1)	0.96, 0.90, 0.21	H
20	80	-	3	EA: MeOH (9:1)	0.97, 0.20, 0.12	I
20	80	-	5	EA: MeOH (9:1)	0.97, 0.12	J
5	95	-	10	EA	0.98, 0.29	K
-	100	-	10	EA: MeOH (1:1)	0.98, 0.91, 0.82, 0.75	L
-	95	5	5	EA: MeOH (1:1)	0.96, 0.79, 0.74	M
-	95	5	5	EA: MeOH (1:1)	0.79, 0.74	N
-	95	5	5	EA: MeOH (1:1)	0.79, 0.74, 0.43	O
-	90	10	10	EA: MeOH (1:1)	0.90, 0.62, 0.56	P
-	85	15	15	EA: MeOH (1:1)	0.99, 0.91, 0.80, 0.71, 0.43	Q
-	80	20	10	EA: MeOH (1:1)	0.93, 0.77, 0.61, 0.45, 0.29	R

Table 7.3.2. (Continued) Flash chromatography on the PE extract of *H. procumbens* roots (batch II)

FC solvent system			Number of fractions	TLC solvent system	R_f values	Combined fraction
PE	EtOAc	MeOH				
-	75	25	10	EA: MeOH (1:1)	0.88, 0.29, 0.16	S
-	70	30	10	EA: MeOH (1:1)	0.92, 0.78, 0.70, 0.47	T
-	60	40	10	EA: MeOH (1:1)	0.92, 0.77, 0.42, 0.26	U
-	40	60	10	EA: MeOH (1:4)	0.92, 0.61	V
-	80	20	10	MeOH	0.89, 0.84, 0.77	W
-	-	100	10	MeOH	0.89, 0.83, 0.75	X

7.4 Solid Phase Extraction (SPE)

The crude PE extract of the *H. procumbens* roots (batch III – Grassroots) was separated by SPE on a C_{18} ISOLUTE (Anatech) cartridge (70ml column), eluting with a step gradient of decreasing polarity (water: acetonitrile). The eluant passed through the cartridge under a weak vacuum and was collected in a flask, concentrated and transferred to a pre-weighed vial. Since the collected fractions contained water and acetonitrile (ACN), the ACN was first removed by rotary vacuum evaporation and the remaining water was displaced by freeze drying.

7.4.1 Establishing the SPE conditions for the PE extract

An initial stock solution of 20mg/ml of the PE extract in ACN was diluted with water to a 5mg/ml solution in 25% ACN. Prior to applying this sample to the column, the cartridge was conditioned with 2 volumes (2 x 50mls) of MeOH followed by 2 vols of a H_2O: ACN (25: 75) solution. A 50ml aliquot of the 5mg/ml PE extract solution was then applied to the cartridge and eluted under vacuum. The unretained material was rinsed from the cartridge with 100ml of water (water wash), collected and concentrated. The extract was separated on the cartridge using 100ml volumes of a step gradient of H_2O: ACN in the ratios of 75: 25, 50: 50, 25: 75 and 0: 100. The final 100% ACN mobile phase was followed by 100ml of acetone (organic wash) to rinse any remaining material off the cartridge. The collected fractions were tested for *in vitro* antiplasmodial activity and the results showed that the active components were being eluted with the 75% ACN mobile phase. SPE was then performed again using 5% increments of ACN in the range of 55 – 80% ACN. The antiplasmodial activity of these fractions is summarised in Figure 7.4.1.

Since the active compounds were eluted with the 60% and 65% ACN solutions, the SPE purification was fine tuned further by eluting with 1% increments of ACN in the range 59 – 66% ACN. For this SPE procedure the 100ml water rinse was followed by 100ml of 55% ACN and then the 59-66% ACN mobile phases. The results from these fractions (Chapter 4, Figure 4.2.2.1b) showed that the active compounds were eluted with 60% and 61% ACN. The HPLC profiles of the 60% and 61% ACN fractions revealed that they contained a prominent peak with common minor peaks on either side. In an attempt to optimise separation between adjacent SPE fractions and generate purer samples, 200mls of the 59

– 65% ACN mobile phases were used as opposed to the 100ml volumes. The activity of the 200ml elution fractions was compared to that of the 100ml fractions (Figure 7.4.1.1).

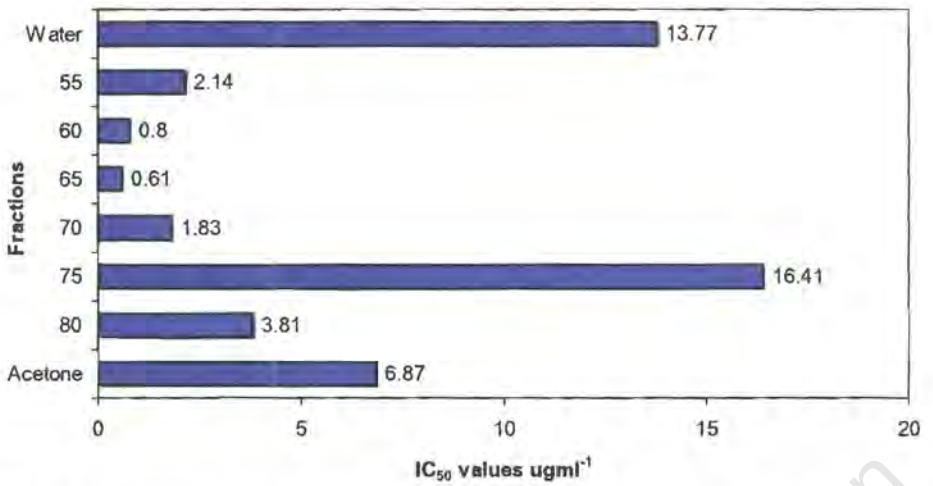

Figure 7.4.1. Summary of the IC_{50} values of the fractions eluted with 55-80% ACN, and the water and acetone washes. The values represent the mean IC_{50} value of two independent experiments each performed in duplicate

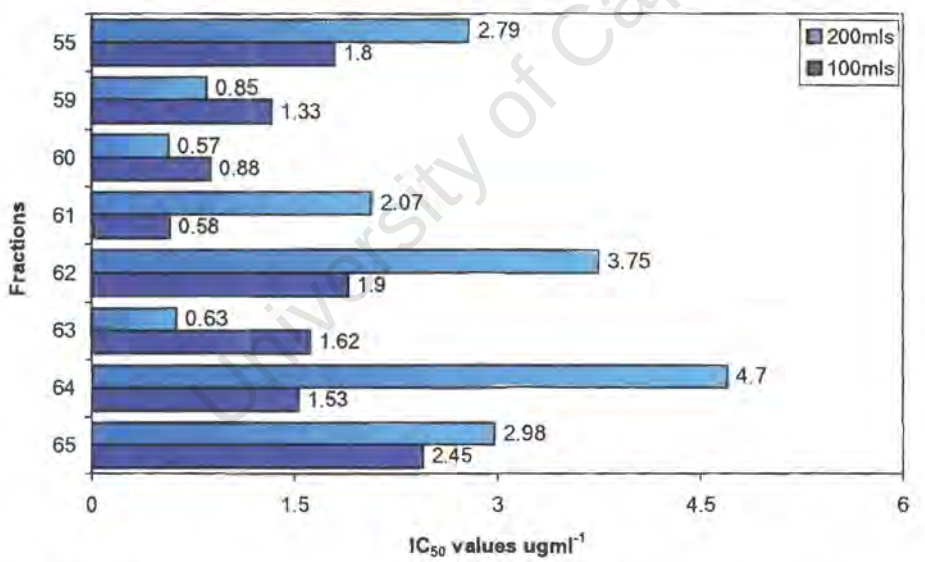

Figure 7.4.1.1. Comparison of the IC_{50} values of the 55-65% ACN SPE fractions eluted with 100mls and 200mls of mobile phase. The values represent the mean IC_{50} value of two independent experiments each performed in duplicate

For the 100ml elution volumes the 60% and 61% ACN fractions were the most active, whereas for the 200ml samples the activity was observed in the 59% and 60% fractions. The HPLC retention time and UV absorbance of the prominent peak in the 60% ACN (100mls) fraction corresponded to the main peak in the 59% ACN (200ml) fraction.

Similarly, the main constituent in the 61% ACN (100ml) sample was identical to the major component in the 60% ACN (200ml) fraction. By doubling the elution volume the active compounds were eluted at a lower percentage of ACN and carry-over between SPE fractions was minimised. To further purify the active 59% and 60% ACN (200ml) fractions, additional 56% and 57% ACN washes were introduced to remove any unwanted material before the 59% ACN elution. The introduction of these two washes changed the HPLC profile of the 59% ACN fraction considerably. It was found that a 55% wash (200ml) followed by a 56% ACN (200ml), 59% ACN (200ml) and 60% ACN (200ml) elution resulted in a single prominent peak for the 56% ACN sample, two main peaks for the 59% ACN and a single prominent peak for the 60% ACN sample (Figure 7.4.1.2). By comparing the HPLC retention times and UV absorbance, the 59% ACN sample appeared to contain the main constituent in the 56% (**56**) and 60% (**60**) ACN fractions. This was confirmed by HREIMS analysis of the 59% ACN fraction, which showed that it contained the molecular ions of both **56** and **60**. Furthermore, all three fractions displayed similar antiplasmodial activity. The introduction of additional 57% and 58% ACN mobile phases appeared to spread out **56** and **60** amongst the 57%, 58% and 59% ACN fractions.

Thus, the final SPE purification procedure that provided optimum separation of the active components **56** and **60** consisted of a C_{18} ISOLUTE cartridge and 200ml volumes of H_2O: ACN mobile phases in the ratio of 45: 55, 44: 56, 41: 59, 40: 60, 39: 61. Several grams of the PE extract were purified by SPE to obtain sufficient quantities of **56** and **60** for structure elucidation and *in vitro* testing. The HPLC profiles of SPE fractions from different runs confirmed that the separation procedure was reproducible and that the level of purity was consistent. Scheme 7.4.1 illustrates the isolation and purification of the active components **56** and **60** from the *H. procumbens* roots (batch III).

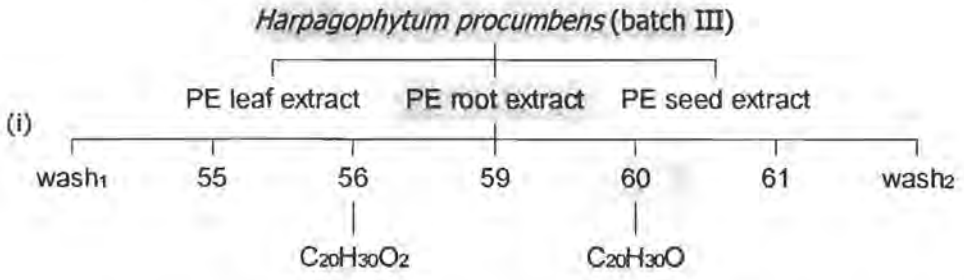

Scheme 7.4.1. SPE purification of the active compounds **56** and **60** from *H. procumbens* (batch III). (i) SPE C_{18}, (H_2O: ACN)

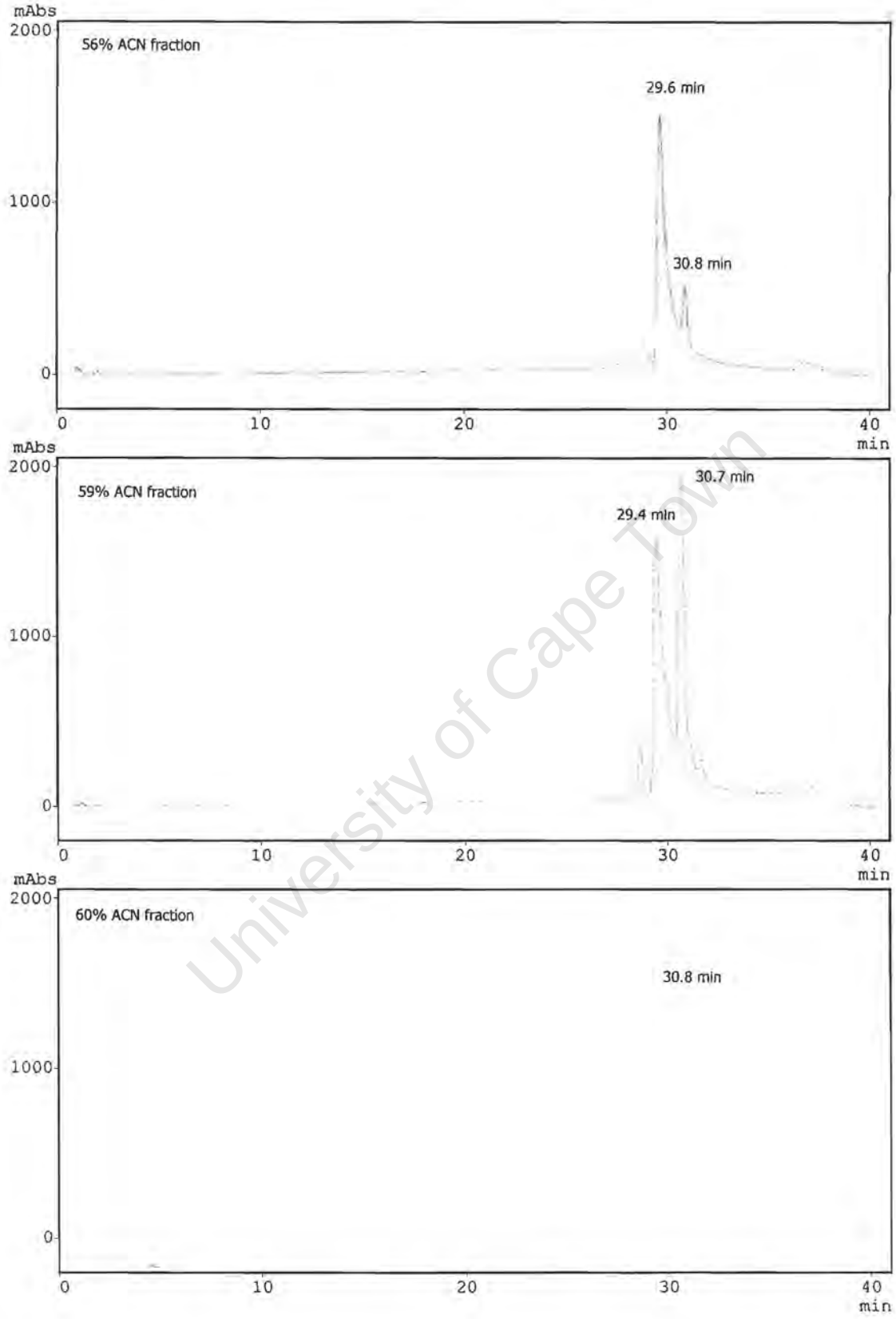

Figure 7.4.1.2. HPLC profiles of the fractions eluted with 200ml of 56%, 59% and 60% ACN

7.5 High Pressure Liquid Chromatography (HPLC)

HPLC analyses were performed using a Shimadzu LC10AS high pressure gradient system controlled through a desktop PC running Shimadzu control software via a Shimadzu CBM10A communication bus module. The HPLC instrument consisted of an automatic sample injector, two solvent delivery systems (LC10AS pumps) and a diode array detector (Shimadzu SPDM10A). The diode array detector was set to acquire UV spectra at λ 210nm and 280nm. HPLC grade methanol (Scharlau) and acetonitrile (Sharlau) were used with purified deionised water (Millipore, Milli-Q Water System).

7.5.1 Analytical HPLC conditions

All of the analytical HPLC separations were made using a pre-packed Higgens HAISIL 100 C_{18} 5μ (150 x 4.6mm) column with a C_{18} 40μm (Bondesil) guard column (Anatech), except for compound **3**, which was separated on a Phenomenex Bondclone 10 Silica 10μ (150 x 3.90mm) column. The column flow rate was set to 1.0ml/min and the injection volumes were 20μl. A 1mg/ml stock solution of the samples was made up in MeOH (FC fractions) or ACN (SPE fractions, totarol and compound **3**), sonicated for 10 minutes and centrifuged in a microcentrifuge at 10 000rpm for 5 mins to pellet any undissolved material.

The SPE fractions and totarol were run in a H_2O: ACN mobile phase. Following an initial hold at 20% ACN for 10 mins, samples were separated using a gradient of 20% to 100% ACN in 30 mins, with a hold at 100% ACN for 2 mins. The equilibration time between analyses was 5 mins. Compound **3** was separated using a 97% ACN: H_2O isocratic gradient over 10mins. The FC fractions were run in a H_2O: MeOH gradient. The column was conditioned at 40% MeOH for 10 mins and the samples were separated using a gradient of 40% to 100% MeOH in 40 mins with a hold at 100% MeOH for 2 mins. The equilibration time between analyses was 5 mins. The HPLC conditions described provided optimum separation for the large range of SPE and FC fractions analysed. HPLC analysis was used to monitor the purity of the totarol, compound **3** and the SPE and FC fractions. The percentage purity was determined by integrating the area under the peak and dividing that by the total area under the spectra curve. HPLC was also used to purify and isolate individual compounds from the FC fractions. The analytical HPLC conditions for the active FC fractions were scaled up for preparative HPLC.

7.5.2 Preparative HPLC conditions

Preparative HPLC separations were achieved for the FC fractions using a pre-packed Higgens HAISIL 100 C_{18} 5μm (250 x 10mm) column with a C_{18} 40μm (Bondesil) guard column (Anatech). The gradient was the same as described for the analytical FC fraction analysis. The flow rate was set to 2ml/min and 200μl of a 5mg/ml stock solution made up in MeOH was injected. Once an HPLC chromatograph was obtained, fractions were delineated for collection. Repeat injections of the sample were then run and the fractions were collected manually, concentrated and tested for activity. Since the collected fractions contained MeOH and water, the MeOH was first removed using a centrifuge sample concentrator at 50°C and the water was displaced by freeze drying.

7.6 Cultivation of Malaria Parasites

Different strains of *P. falciparum* were continuously cultured according to methods described by Trager and Jensen (1976). The CQ^S cloned strain D10 (derived from FCQ-27 from Papua New Guinea) (Ekong *et al.*, 1993) and the CQ^R strain W2 clone (originally from a mixture of Sierra Leone I/CDC and Indochina III/CDC lines) (Oduola *et al.*, 1988b), were donated by Dr A. Cowman, Walter and Eliza Hall Institute of Medicinal Research, Melbourne, Australia. The culture adapted South African CQ^R isolate RSA11 (isolated at Kwazulu Natal) was obtained from Dr. J. Freese, Malaria Research Programme, Medical Research Council of South Africa, Durban, South Africa. Two culture adapted strains, CQ^R K1 (isolated at Kanchnaburi, Thailand) (Thaithong *et al.*, 1981) and CQ^S 3D7 (the geographical origin of this strain is not known) were donated by Dr D. Wallaker, University of Edinburgh, Edinburgh, Scotland.

The parasites were maintained at a 5% haematocrit with RPMI 1640 (Biowhittaker) medium supplemented with Albumax II (lipid rich bovine serum albumin) (GibcoBRL) (25g/L) hypoxanthine (44mg/L), HEPES (N-[2-Hydroxyethyl]-piperazine-N'-[2-Ethansulphonic acid]) (6g/L), sodium bicarbonate (2.1g/L) and gentamycin (50mg/L). The medium reagents were all purchased from Sigma-Aldrich, South Africa, with the exception of the RPMI and Albumax II. The parasitaemia was kept between 5 - 10% by the addition of O^+ RBC (Western Province Blood Transfusion Service, Groote Schuur Hospital, Cape Town, South Africa) that had been washed twice with medium to remove

the buffy coat. Medium was changed daily and the parasitaemia was determined using Giemsa (Sigma) stained blood films of the cultures. The parasites were routinely synchronised by treatment with D-sorbital (Lambros and Vanderberg, 1979). The cultures were contained in flat bottomed flasks ($75cm^3$) in an atmosphere of 93% N_2, 4% CO_2 and 3% O_2 and incubated at 37°C.

7.6.1 Drug preparations and dilutions, and plate design

7.6.1.1 Dose response curves

CQ (Sigma) was used as a positive control to determine the *in vitro* susceptibility of the different *P. falciparum* strains. A 1mg/ml stock solution of CQ was made up in water and serially diluted in medium to the required concentration. The crude plant extracts, SPE and FC fractions as well as the isolated and synthesised compounds were first dissolved in MeOH, sonicated for 10 mins and then sterile water was added to reach a 1mg/ml solution in 13% methanol. The highest concentration of MeOH that the parasites were exposed to was 0.7%, which had no measurable effect on parasite viability in this system. The original CQ stock solution (1mg/ml in water) was aliquoted into multiple tubes and frozen at -80°C until use. Since little is known about the stability of the plant extracts or the isolated and synthesised compounds, fresh stock solutions were made on the day of the experiment.

Microtitration techniques were used to measure the activity of a large number of samples over a range of concentrations. The microtitre plates (Greiner) consisted of 96 wells arranged in a matrix of eight rows (A to H) and 12 columns (1 to 12). At the beginning of the experiment 100µl of drug free medium was dispensed to wells A to H in columns 1, 2 and 4 through to 12, and 200µl of the drug stock solutions (200µg/ml) were added to each of two adjacent wells in column 3. A multi-channel pipette dispenser was used to make two fold serial dilutions across the plate in the concentration range of 200µg/ml to 0.39µg/ml. The starting concentration of CQ was set to 2µg/ml.

Parasitised RBC in the trophozoite stage were adjusted to a 2% parasitaemia and 2% haematocrit, and a 100µl of this suspension was dispensed to all of the wells except those in column 1. To column 1 (blank) was added 100µl of unparasitised RBC at a 2% haematocrit. The final volume in each well was 200µl and the final haematocrit of both

the parasitised and unparasitised RBC was 1%. In summary, rows A to H in column 1 contained unparasitised RBC (blank), column 2 served as a parasite control (parasitised RBC and no drug) and columns 3 to 12 contained parasites and varying concentrations of the drug over a 500-fold range. The microtitre plate was placed in a desiccator cabinet, flushed with a gas mixture consisting of 93% N_2, 4% CO_2 and 3% O_2, sealed and incubated at 37°C for 48 hours.

7.6.1.2 Drug combination studies

The interactions of chloroquine with compounds **56** and **6** were tested *in vitro* against D10 using a technique adapted from Chawira and Warhurst (1987). The IC_{50} values of CQ, **56** and **6** were first determined in D10 using the described dose response assays. Stock solutions were then made up of twice the IC_{50} values for CQ and **56**. In rows A to B of a 98 well microtitre plate, dose responses of CQ and **56** were included as controls. Aliquots of 100µl of medium were then dispensed in column 1 (blank) and 100µl of twice the IC_{50} of CQ was added to wells E to H in column 2. The same volume of twice the IC_{50} of **56** was added to wells E to H in column 12. The wells between columns 2 and 12 (E to H) received 100µl volumes of ratios of 90:10, 80:20, 70:30, 60:40, 50:50, 40:60, 30:70, 20:80, 10:90 of CQ and **56** respectively. Parasitised RBC (PRBC) and uninfected RBC suspensions were prepared as for the dose response curves and 100µl of RBC were dispensed to the wells in column 1, and 100µl of PRBC were added to the rest of the wells. The microtitre plate was then incubated in a desiccator cabinet in an atmosphere of 93% N_2, 4% CO_2 and 3% O_2 at 37°C for 48 hours. This procedure was repeated for CQ and **6**.

7.6.2 Parasite lactate dehydrogenase assay

The parasite lactate dehydrogenase (PLDH) activity was used to measure parasite viability according to the methods described by Makler *et al.*, (1993). This enzymatic assay differentiates between pLDH and host LDH activity by using 3-acetylpyridine adenine dinucleotide (APAD). The pLDH uses APAD as a coenzyme in the conversion of pyruvate to lactate and reduces it to APADH. The formation of APADH can be measured by the subsequent reduction of a yellow nitroblue tetrazolium (NBT) salt to a blue formazan product, the absorbance of which can be monitored on a microplate reader.

The pLDH activity was measured using a 1.96 mM NBT (Sigma) and 0.24 mM phenazine ethosulfate (PES) (Sigma) solution in millipore water, and the Malstat reagent containing triton (1ml/L), APAD (0.33g/L) and TRIS buffer (3.3g/L) in millipore water. At the end of the 48 hr incubation period of the test plate, 100μl of Malstat reagent and 25μl of NBT/PES solution were added to all the wells of another 96-well microtitre plate. The test plate was removed from the desiccator and the parasites were re-suspended in each well and then transferred (15μl) with a multi-channel dispenser to the corresponding wells in the plate containing the Malstat and NBT/PES solution. This plate was placed in a 7520 Microplate Reader (Cambridge Technology), blanked on the wells in column 1 and the absorbance of the blue formazan salt was measured at λ 620nm. Since the amount of formazan produced is proportional to parasite viability, the percentage parasite survival in each well was calculated using the formula:

$$\% \text{ Parasite Viability} = \frac{A_{\lambda 620} \text{ test well (PRBC + drug)}}{A_{\lambda 620} \text{ parasite control well (PRBC + no drug)}} \times 100$$

7.7 Cell Cultures

The initial cytotoxicity tests were performed on Rat-1 cells obtained from the Department of Medical Biochemistry, University of Cape Town. The cytotoxicity of the isolated and synthesised compounds were evaluated against two mammalian cell lines, Chinese hamster ovarian (CHO) and human heptoma (HepG2) cells, which were routinely cultured. The CHO cells were originally obtained from S. Schwager, Department of Medical Biochemistry, University of Cape Town. A starting stock of the HepG2 cell line was donated by L. Davids, Department of Medicine, University of Cape Town. Both of the cells were maintained as adherent monolayers in culture flasks ($75cm^3$) and were incubated in a 5% CO_2-air humidified atmosphere at 37°C. The medium reagents were obtained from Highveld Biological, South Africa, with the exception of the DMEM-Glutamax that was purchased from Gibco Life Technologies, Paisley, Scotland. The CHO cells were cultured in Dulbecos Modified Eagles Medium (DMEM): Hams F-12 medium (1:1) supplemented with 10% heat inactivated fetal calf serum (FCS) and gentamycin (0.04μg/ml). The HepG2 cells were maintained in DMEM with Glutamax-1 (L-Alanyl-L-Glutamine) supplemented with 10 % heat inactivated FCS. The Rat-1 cells were cultured in DMEM with 10% FCS,

penicillin (100 units/ml) and streptomycin (100μg/ml). The culture medium was changed every 2 – 3 days and the cells were subcultured once they had reached confluency. A 1% trypsin solution was used to digest the cellular matrix for subculturing and the cells underwent a maximum of 10 subcultures before fresh stocks were thawed and the cell culture re-initiated.

7.7.1 Drug preparations and dilutions, and plate design

Daunomycin (DN) (Sigma) was used as a positive control in the cytotoxicity assays. An initial DN stock of 2mg/ml in millipore water was prepared and aliquoted into tubes and frozen at -20°C until use. For the isolated and synthesised compounds a 2mg/ml stock solution in 13% MeOH was made up on the day of the experiment. The highest concentration of MeOH that the cells were exposed to was 0.7%, which had no measureable effect on cell viability in this system. The stock solutions of DN and the test compounds were diluted in culture medium to 6 different concentrations to give final concentrations of 100μg/ml to 1ng/ml in the wells.

At the beginning of the experiments, the cells were adjusted to a concentration of 10^5/ml and 100μl of this cell suspension were seeded in all of the wells except in column 1 (blank) in a 96 well culture plate (Costar). The plates were incubated for 24 hours at 37°C in a humidified 5% CO_2-air atmosphere. After the incubation period, the medium was carefully aspirated out of the wells and 100μl of the different drug solutions were added in quadruplicate to columns 3 through to 9. A further 100μl of culture medium was then added to all of the wells containing cells and drugs (columns 3 to 9), and 200μl of medium was dispensed to the wells in column 1 (blank) and column 2 (cells and no drug). The microplate was then incubated at 37°C for 48 hours.

7.7.2 MTT cytotoxicity assay

The MTT (3-[4,5-Dimethylthiazol-2-yl]-2,5-diphenyltetrazolium bromide) assay described by Mosman (1983) was used to measure cell growth and chemosensitivity. This colorimetric assay is based on the ability of viable cells to metabolise a yellow water-soluble tetrazolium salt into a water-insoluble purple formazan product. The amount of

formazan produced can be measured spectrophotometrically and is proportional to the metabolic activity and number of cells in the test plate.

After the 48 hr incubation of the test plate, 25µl of sterile MTT (5mg/ml in PBS) was added to each well and incubation was continued for 4 hrs at 37°C. The plates were then centrifuged at 2050rpm for 10 minutes and the supernatant was carefully aspirated from the wells, ensuring that the formazan crystals were not disturbed. The formazan crystals were dissolved in 100µl of DMSO and the plate was gently shaken for 5 minutes on a microtitre plate shaker. The plate was blanked on the wells in column 1 and the absorbance of the crystals was measured at λ 540nm on a Microtitre Plate Reader (Cambridge Technologies). The cell viability was calculated in each well using the formula:

$$\% \text{ Cell Viability} = \frac{A_{\lambda 540} \text{ test well (cells + drug)}}{A_{\lambda 540} \text{ cell control well (cells + no drug)}} \times 100$$

7.8 Data Analysis

The percentage viability of parasites and cells was calculated and dose response curves were constructed using nonlinear dose response curve fitting analyses with GraphPad Prism v.3.00 software. The concentration of the drug that inhibits 50% of the parasites or cells (IC_{50} values) was established from the dose response curves using GraphPad Prism. The non-parametric Mann-Whitney test was used to compare IC_{50} values obtained from dose response curves and to determine whether the values were significantly different (p-value). The computer program GraphPad Prism was used to calculate the two-tailed p-values at a 95% confidence interval. In the drug combination studies, the percentage viability obtained for the two drugs individually were plotted on two ordinates and joined by a solid line. The 95% confidence intervals for these values were joined by dashed lines to indicate the variability to be expected in values obtained using the fixed ratios. Between these two ordinates the percentage viability using the fixed ratios of the two drugs was plotted.

7.9 Chemistry

7.9.1 General methods

The 1-phenylpiperazine and 1-(2-chlorophenyl)-piperazine monohydrochloride were obtained from Lancaster, B&M Scientific, South Africa and the totarol was purchased from Sequoia Chemicals, Oxford, United Kingdom. The remaining reagents were obtained from Sigma-Aldrich, South Africa and the common solvents were purchased from KIMIX, South Africa. Column chromatography was carried out on Merck Kieselgel silica gel 60 and preparative TLC was performed on silica 60 F_{254} coated plates (20 x 20cm x 0.55 mm) (Merck). All reactions were monitored by TLC, which was carried out on silica 60 F_{254} coated aluminium sheets (Merck). Melting points were measured on a Reichert-Jung Thermovar hot stage microscope and are uncorrected. The infrared spectra were recorded (NaCl) on a Thermo Mattson FTIR spectrometer connected to a desktop PC running EZ OMNIC software version 6.0A. Optical rotations were measured in $CHCl_3$ on an ADP220 Polarimeter. High-resolution mass spectra (HREIMS) were obtained on a VG-70-SEQ mass spectrometer operating at 70eV. All NMR spectra were measured in $CDCl_3$ with TMS as an internal reference. The ^1H and ^{13}C NMR spectroscopic data for totarol and the synthesised compounds **1** to **6** were recorded on a Varian 400MHz (VXR 400) and the HSQC, HMBC and COSY experiments were recorded on a Varian 300MHz (VXR 300) instrument (University of Cape Town). The ^1H and ^{13}C NMR data for compound **56** was recorded on a Varian 600MHz (VXR 600) machine (University of Stellenbosh, South Africa). The ^1H and ^{13}C NMR spectra of compound **60** as well as the HSQC, HMBC, COSY and NOESY spectroscopic data of **56** and **60** were recorded on Varian 500MHz (VXR 500) or Varian 400MHz (VXR 400) instruments (University of Barcelona, Spain).

7.9.2 Preparation of amines

Diethylamine (amine **2**) and 1-phenylpiperazine (amine **4**) were available commercially. The amines 1-(2-ethoxyphenyl)-piperazine (amine **6**) and 1-(2-chlorophenyl)-piperazine (amine **5**) existed as amine hydrochloride salts and were neutralised using a ~~polymer~~ supported tetraalkylammonium carbonate; macroporous triethylammonium methylpolystyrene carbonate (MP-carbonate) (Argonaut Technologies). Neutralisation of 1-(2-chlorophenyl)-piperazine monohydrochloride (237.12mg, 1.02mmol) with MP-carbonate (1.55mg, 4.08mmol) in MeOH (3ml) at 20°C for 7hrs yielded amine **5**. Reaction

of 1-(2-ethoxyphenyl)-piperazine monohydrochloride (235.39mg, 0.97mmol) with MP-Carbonate (1.47mg, 3.88mmol) in MeOH (3ml) at 20°C for 7hrs gave amine **6**. The resins were removed by filtration, washed twice with MeOH and the resulting filtrate was concentrated under reduced pressure to yield the neutralised amines. Amine **3** was not available commercially and was synthesised by condensation of 4,7-dichloroquinoline with piperazine (Biot *et al.*, 1997). A mixture of piperazine (10.875mg, 126.45mmol), potassium carbonate (1.047g, 7.58mmol), triethylamine (5.28ml, 37.88mmol) and 4,7-dichloroquinoline (5.00g, 25.25mmol) was stirred in N-methyl-2-pyrrolidinone (17.7ml) under nitrogen at 135°C for 2hrs and after cooling to room temperature was diluted with CH_2Cl_2 (200ml). The reaction mixture was washed with brine (2 x 50ml), dried ($MgSO_4$) and concentrated under reduced pressure. The resulting oil was purified by column chromatography on silica gel using CH_2Cl_2/MeOH (4:1) as the eluant and gave amine **3** (5.433g, 87.5%): mp 113 - 115°C; ^{1}H NMR ($CDCl_3$, 300MHz) δ 8.72 (1H, d, J=5.0Hz, H-2), δ 8.04 (1H, d, J=2.1Hz, H-8), δ 7.96 (1H, d, J=9.0Hz, H-5), δ 7.42 (1H, dd, J=9.0Hz and 2.1Hz, H-6), δ 6.84 (1H, d, J=5.0Hz, H-3), δ 3.18 (4H, m, H-2′, H-3′, H-5′ and H-6′), δ 1.65 (1H, s, H-4′); ^{13}C NMR ($CDCl_3$, 300MHz) δ 151.9 (C-2), δ 150.2 (C-4), δ 134.9 (C-7), δ 128.9 (C-8), δ 126.1 (C-6), δ 125.2 (C-5), δ 121.9 (C-4a), δ 108.9 (C-3), δ 53.6 (C-2′ and C-6′), δ 46.1 (C-3′ and C-5′). The ^{1}H, ^{13}C and HSQC NMR spectra of **3** can be found in Appendix 2 (A2.11).

7.9.3 Synthesis of compounds 1 to 6

Synthesis of the β-amino alcohols (**1** – **6**) involved the generation of a phenoxide anion of totarol, followed by a nucleophillic substitution reaction with epichlorohydrin to give an epoxide intermediate that was reacted with the appropriate amine. The HREIMS data, NMR spectral data, IR measurements, optical rotations and melting points for totarol and compounds **1** – **6** are in Chapter 5.

Epoxide intermediate (**1**), Epichlorohydrin (1.88μl, 2.4mmol) was stirred in a solution of sodium hydride (60%, 77mg, 1.92mmol) and totarol (0.274g, 0.96mmol) in DMF (3ml) at 0°C under nitrogen. The suspension was allowed to warm to room temperature (20°C), heated to 50°C and stirred for 16 hours. Excess epichlorohydrin was removed *in vacuo* and the resulting product was extracted into ethyl acetate, washed with water, dried ($MgSO_4$) and concentrated under reduced pressure. Purification of 18mg of the product (254.3mg, 77.6%) on preparative TLC using hexane: EtO_2 (9.5: 0.5); R_f (0.35) gave **1**.

The amine (1.05 eq.) was added to a stirred solution of the epoxide (1.0 eq.) in MeOH (5ml for 0.10mmol scale of epoxide). The resulting mixture was stirred for 16hrs at 65°C, concentrated under reduced pressure and purified using preparative TLC.

Compound ***2*** (0.109mmol scale), 17mg, 35.3%, R_f (0.17); Et_2O

Compound ***3*** (0.218mmol scale), 30.7mg, 20.0%, R_f (0.60); Et_2O: EtOAc (1:1)

Compound ***4*** (0.109mmol scale), 29.8mg, 51.0%, R_f (0.29); Et2O: Hex (1:1)

Compound ***5*** (0.109mmol scale), 23.6mg, 37.8%, R_f (0.25); Et_2O: Hex (1:1)

Compound ***6*** (0.109mmol scale, 34.3mg, 53.9%,R_f (0.39); Et_2O: Hex (1:1)

Since the reactions were relatively clean, the low yields could be attributed to the loss of product in the purification procedure. The assumption that the epoxide intermediate was pure would influence the calculated theoretical yields and subsequent percentage yields. All of the synthesised compounds were shown to be consistent with their expected structures (Chapter 5).

7.9.4 Phenol-sulphuric acid reaction test for the detection of sugars

The white crystalline substance that precipitated out of the cold MeOH extract of *H. procumbens* (batch I) was filtered off using a Büchner funnel and washed twice with MeOH. Since the *H. procumbens* roots are rich in sugars (van Wyk *et al.*, 1997), the crystals were tested for sugars using the phenol-sulphuric acid reaction (Rao *et al.*, 1989). This colorimetric test involves the dehydration of saccharides with potential (or free) aldehydic or keto groups to furfural derivatives, which condense with phenols to form colored complexes.

Purified deionised water served as a negative control, and a 50mg/ml solution of glucose (positive control) and a 50mg/ml solution of the isolated crystals were made up in purified water. To 1ml aliquots of the water, glucose and crystal solutions, 3.0ml of sulphuric acid was added and vortexed. The solutions were cooled in ice to 15-20°C and then 0.05ml of 80% phenol was added, mixed and left to stand at room temperature for 30 minutes

before the colour intensity was recorded. The colour of the glucose and crystal solutions turned a dark transparent orange, while the water remained a pale orange. These qualitative results suggested that the crystals were sugars, but no attempt was made to determine the exact composition of the sugar.

Bibliography

Bibliography

Aboul-Ela, M.A. and El-Lakany, A. (2000). Abietane diterpenes from the roots of *Salvia lanigera.* Alex. J. Pharm. Sci. 14(1): 57 -61

Achenbach, H., Waibel, R., Nkunya, M.H.H. and Weenen, H. (1992). Antimalarial compounds from *Hoslundia opposita*. Phytochemistry. 31(11): 3781 - 3784

Baghdikian, B., Guiraud-Dauriac, H., Ollivier, E., N'Guyer, A., Dumenil, G. and Balansard, G. (1999). Formation of nitrogen-containing metabolites from the main iridoids of *Harpagophytum procumbens* and *H. zeyheri* by human intestinal bacteria. Planta Medica. 65(2): 164-166

Baleta, A. (1998). South Africa to bring traditional healers into mainstream medicine. The Lancet. 352: 554

Barltrop,J.A. and Rogers, N.A.J. (1958). Experiments on the synthesis of diterpenes: Total synthesis of (±)-totarol. Journal. Chem. Soc: 2566-2572

Bélaiche, P. (1982). Étude clinique de 630 cas d'arthrose traité par nébulisat aqueux d' *Harpagophytum procumbens* (Radix). Phytotérapy. 1: 22 - 28

Bendall, J.G. and Cambie, R.C. (1995). Invited review. Totarol: a non-conventional diterpenoid. Australian Journal of Chemistry. 48: 883 - 917

Bhattacharya, A. and Bhattacharya, S.K. (1998). Anti-oxidant activity of *Harpagophytum procumbens* (Devil's Claw). British Journal of Phytotherapy. 5(2): 68-71

Biot, C., Glorian, G., Maciejewski, L.A. and Brocard, J.S., Domarle, O., Blampain, G., Millet, P., Georges, A.J., abessolo, H., Dive, D., and Lebibi, J. (1997). Synthesis and antimalarial activity *in vitro* and *in vivo* of a new ferrocene-chloroquine analogue. J. Med. Chem. 40: 3715 - 3718

Bradley, P.R. (1992). British Herbal Commendium (1). British Herbal Medicine Association. Bournemouth.

Bray, P.G., Howells, R.E. and Ward, S.A. (1992). Vacuolar acidification and chloroquine sensitivity in *Plasmodium falciparum*. Biochemical Pharmacology. 44: 1317 – 1324

Bray, P.G., Howells, R.E., Ritchie, G.Y. and Ward, S.A. (1992). Rapid efflux phenotype in both chloroquine-sensitive and chloroquine-resistant *Plasmodium falciparum*. Biochemical Pharmacology. 44 (7): 1317 – 1324

Bray, P.G., Mungthin, M., Ridley, R.G. and Ward, S.A. (1998). Access to hematin: the basis of chloroquine resistance. Mol. Pharmacol. 54: 170 - 179

Bray, P.G. and Ward, S.A. (1998). A comparison of the phenomenology and genetics of multidrug resistance in cancer cells and quinoline resistance in *Plasmodium falciparum*. Pharmacol. Ther. 77(1): 1 - 28

Brieskorn, C.H., Fuchs, A., Bredenberg, J.B., McChesney, J.D. and Wenkert, E. (1964). The structure of carnosol. Journal of Organic Chemistry. 29: 2293 - 2298

Brown, S.B., Dean T.C. and Jones, P. (1970). Aggregation of ferrihaem. Dimerization and protolytic equilibria of protoferrihaem and deuterferrihaem in aqueous solution. J. Biochem. 117: 733 – 739

Buckingham, J., Ya Cai, Munasinghe, V.R.N., Pattenden, C.F., Rhodes, P.H and Roberts, A.D.C. (1994). Dictionary of Natural Products. Volume 7. Chapman and Hall, London.

Burnell, R.H., Jean, M. and Marceau, S. (1988). Synthesis of matenoquinone. Canadian Journal of Chemistry. 66: 227-230

Cambie, R.C., Hayward, R.C. and Palmer, B.D. (1982). Chemistry of the *Podocarpaceae*. LXIII. Ring-C oxidation of totarol. Australian Journal of Chemistry. 35: 1679 - 1697

Cambie, R.C. and Mander, L.N. (1962). Chemistry of the *Podocarpaceae* – VI: Constituents of the heartwood of *Podocarpus totara* G. Benn. Tetrahedron. 18: 465 - 475

Chawira, A.N. and Warhurst, D.C. (1987). The effect of artemisinin combined with standard antimalarials against chloroquine-sensitive and chloroquine-resistant strains of *Plasmodium falciparum in vitro*. Journal of Tropical Medicine and Hygiene. 90: 1 - 8

Chevallier, A. (1996). The Encyclopedia of Medicinal Plants. Dorling Kindersley Limited, London.

Circosta, C. Occhiuto, F., Ragusa, S., Trovato, A., Tumino, G., Briguglio, F. and Costa De Pasquale, A. (1984). A drug used in traditional medicine: *Harpagophytum procumbens* DC. II. Cardiovascular activity. Journal of Ethnopharmacology. 11(3): 259 - 274

Cocks, M. and Møller, V. (2002). Use of indigenous and indigenised medicines to enhance personal well-being: A South African case study. Social Science and Medicine. 54: 387 – 397

Cowman, A.F., Karcz, S., Galatis, D. and Culvenor, J. G. (1991). A P-glycoprotein homologue of *Plasmodium falciparum* is localized on the digestive vacuole. The Journal of Cell Biology. 113 (5): 1033 – 1047

Cowman, A.F. (1995). Mechanisms of drug resistance in malaria. Aust NZ J Med. 25: 837 - 844

Cragg, G. and Newman, D. (2001). Nature's bounty. Chemistry in Britain. 37 (1): 22 – 26

Cruickshank, P.A. and Fishman, M. (1969). Studies in Alkylation. II. Reactions of epoxyalkyl bromides. The Journal of Organic Chemistry. 34(12): 4060 - 4065

Cumming, J.N., Ploypradith, P. and Posner, G. (1996). Antimalarial activity of artemisinin (qinghaosu) and related trioxanes: Mechanism(s) of action. Adv Pharmacol. 37: 253 - 297

De Smet, P.A.G.M. (1997). The role of plant-derived drugs and herbal medicines in healthcare. Drugs. 54(6): 801 – 840

De, D., Krogstad, F.M., Cogswell, F.B. and Krogstad, D.J. (1996). Aminoquinolines that circumvent resistance in *Plasmodium falciparum in vitro*. Am. J. Trop. Med. Hyg. 55: 579 - 583

Dhar, R., Zhang, K., Talwar, G.P., Garg, S. and Kumar, N. (1998). Inhibition of the growth and development of asexual and sexual stages of drug-sensitive and resistant strains of the human malaria parasite *Plasmodium falciparum* by Neem (*Azadirachta indica*) fractions. Journal of Ethnopharmacology. 61: 31 - 39

Diggens, S.M., Gutteridge, W.E. and Trigg, P.I. (1970). An altered dihydrofolate reductase associated with pyrimethamine resistant *P.berghei* produced in a single step. Nature. 228: 579 – 580

Dorn, A., Sudha, R.V., Hugues, M., Jaquet, C., Vennerstrom, J.L. and Ridley, R.G. 1998. An Assessment of drug-haematin binding as a mechanism for inhibition of haematin polymersiation by quinoline antimalarials. Biochemical Pharmacology. 55: 727-736

Dzekunov, S.M., Uros, L.M.B. and Roepe, P.D. (2000). Digestive vacuolar pH of intact intraerythrocytic *P. falciparum* either sensitive or resistant to chloroquine. Molecular and Biochemical Parasitology. 110 (1): 107-124

Easterfield, T.H. and McDowell. (1911). Trans. New Zealand Inst. 43: 55

Easterfield, T.H. and McDowell. (1915). Trans. New Zealand. Inst. 48: 578

Edinburg, T.L. (1998). Traditional medicines in South Africa. The Pharmaceutical Journal. 261: 242- 261

Edwards, S.D. (1986). Traditional and modern medicine in South Africa: A research study. Social Science and Medicine. 22 (11): 1273 – 1276

Egan, T.J., Ross, D.C. and Adams, P.A. (1994). Quinoline antimalarial drugs inhibit spontaneous formation of beta-haematin (malaria pigment). FEBS letter. 352: 54 – 57

Egan,T.J., Hunter, R., Kaschula, C.H., Marques, H.M., Misplon, A. and Walden, J. (2000). Structure-function relationships in aminoquinolines: effect of amino chloro groups on quinoline-hematin complex formation, inhibition of β-hematin formation, and antiplasmodial activity. Journal of Medicinal Chemistry. 43: 283 - 291

Eichler,O. and Koch, C. (1970). Über die antiphlogistische, analgetische und spasmolytische wirksamkeit von *Harpagophytum procumbens*. Arzneimittel-Forsch/Drug Res. 20: 107-109

Ekong, R.M., Robson, K.J.H., Baker, D.A. and Warhurst, D.C. (1993). Transcripts of the multidrug resistance genes in chloroquine-sensitive and chloroquine-resistant *Plasmodium falciparum*. Parasitology. 106: 107 - 115

Elford, B.C., Roberts, M.F., Phillipson, J.D. and Wilson, R.J.M. (1987). Potentiation of the antimalarial activity of qinhaosu by methoxylated flavones. Transactions of the Royal Society of Tropical Medicine and Hygiene. 81: 434-436

Elmore, N.F. and King, T.J. (1961). The synthesis of 8-isopropylpodocarpane-6,7diol (6-hydroxy-totarol) and of 7,8-dimethoxypodocarpane. Journal of the Chemical Society. 4425 –4429

Eloff, J.N. (1998). Which extractant should be used for the screening and isolation of antimicrobial components from plants? Journal of Ethnopharmacology. 60: 1 - 8

Enomoto, H., Yoshikuni, Y., Yasutomi, Y., Ohata, K., Sempuku, K., Kitaguchi, K., Fujita Y. and Mori, T. (1977). Hypocholesterolemic action of tricyclic diterpenoids in rats. Chem. Pharm. Bull. 25(3): 507 - 510

Enzell, C.R. (1967). Mass spectrometric studies of diterpenes. 2. Deuterium labelling of podocarpa-8,11,13-trienes. Arkiv För Kemi. 26: 87 - 100

Erdoes, A. Fontaine, R., Friehe, H., Durand, R. and Poeppinghaus, T. (1978). Pharmakologie und toxikologie verschiedener extrakte, sowie des harpagosids aus *Harpagophytum procumbens* DC. Planta Medica. 34: 97-108

Evans, G.B. and Furneaux, R.H. (2000). The synthesis and antibacterial activity of totarol derivatives. Part 2: Modifications at C-12 and O-13. Bioorganic & Medicinal Chemistry. 8: 1653-1662

Evans, G.B., Furneaux, R.H., Gainsford, G.J. and Murphy, M.P. (2000). The synthesis and antibacterial activity of totarol derivatives. Part 3: Modification of Ring-B. Bioorganic & Medicinal Chemistry. 8 : 1663 - 1675

Evans, G.B., Furneaux, R.H., Gravestock, M.B., Lynch, G.P. and Scott, G.K. (1999). The synthesis and antibacterial activity of totarol derivatives. Part 1: Modifications of ring-C and pro-drugs. Bioorganic & Medicinal Chemistry. 7: 1953-1964

Farnsworth, N.R. and Soejarto, D.D. (1991). In: Global importance of medicinal plants. Conservation of Medicinal Plants. Cambridge University Press, Cambridge. 25 - 51

Farnsworth, N.R. (1984). The role of medicinal plants in drug development. In: Natural Products and Drug Development. Baillière, Tindal and Cox, London. 8 - 98

Fidock, D.A., Nomura, T., Talley, A.K., Cooper, R.A., Dzekunov, S.M., Ferdig, M.T., Ursos, L.M.B. bir Singh Sidhu, A., Naude, B., Deitsch, K.W., Su, X.Z., Wootton, J.C., Roepe, P.D. and Wellems, T.E. (2000). Mutations in the *P. falciparum* digestive vacuole transmembrane protein PfCRT and evidence for their role in chloroquine resistance. Mol. Cell. 6: 861 - 871

Fishman, M. and Cruickshank, P.A. (1968). Studies in Alkylation. I. Synthesis and reactions of spiro(oxirane-2,4'-piperidines). Journal of Heterocycl. Chem. 5: 467 - 469

Fitch, C.D. (1970). *Plasmodium falciparum* in owl monkeys: drug resistance and chloroquine binding capacity. Science. 169: 289 - 298

Fojo, A., Akiyama, S., Gottesman, M.M. and Patsan, I. (1985). Reduced drug accumulation in multiple drug-resistant human KB carcinoma cell lines. Cancer Research. 45: 3002 – 3007

Foote, S.J., Thompson, J.K., Cowman, A.F. and Kemp, D.J. (1989). Amplification of the multidrug resistance gene in some chloroquine-resistant isolates of *Plasmodium falciparum*. Cell. 57: 921 - 930

Ford, J.M. (1996). Experimental reversal of P-glycoprotein mediated multidrug resistance by pharmacological chemosensitisers. Eur. J. Biochem. 32A: 991 - 1001

Francis, S., Sullivan, D.J. and Goldberg, D. (1997). Hemoglobin metabolism in the malaria parasite *Plasmodium falciparum*. Annu. Rev. Microbiol. 51: 97 - 123

François, G., Bringmann, G., Phillipson, J.D., Aké Assi, L., Dochez, C., Rübenacker, M., Schneider, C., Wéry, M., Warhurst, D.C. and Kirby, G.C. (1994). Activity of extracts and naphthylisoquinoline alkaloids from *Triphyophyllum peltatum*, *Ancistrocladus abbreviatus* and *A. barteri* against *Plasmodium falciparum in vitro*. Phytochemistry. 35(6): 1461 - 1464

Geissman, T.A. and Crout, D.H.G. (1969). In: Organic chemistry of secondary plant metabolism. Freeman Cooper and Company, San Francisco. 298

George, J., Laing, M.D. and Drewes, S.E. (2001). Phytochemical research in South Africa. South African Journal of Science. 97: 93 – 105

Ginsburg, H., Famin, O., Zhang, J. and Krugliak, M. (1998). Inhibition of Glutathione-dependant degradation of haem by chloroquine and amodiaquine as a possible basis for their antimalarial mode of action. Biochemical Pharmacology. 56: 1305 – 1313

Goldberg, D.E., Slater, A.F.G., Cerami, A. and Henderson, G.B. (1990). Hemoglobin degradation in the malaria parasite *Plasmodium falciparum*: an ordered process in a unique organelle. Proceedings of the National Academy of Science USA. 87: 2931 – 2935

González, A., Aguiar, Z.E., Grillo, T.A. and Luis, J. (1992). Diterpenes and diterpene quinones from the roots of *Salvia apiana*. Phytochemistry. 31(5): 1691-1695

Grahame, R. and Robinson, B.V. (1981). Devil's Claw (*Harpagophytum procumbens*): Pharmacological and clinical studies. Annals of Rheumatic Disease. 40(6): 632

Gutteridge, W.E. and Trigy, P.I. (1971). Action of pyrimethamine and related drugs against *Plasmodium knowlesi in vitro*. Parasitology. 62: 431 - 444

Haraguchi, H., Oike, S., Muroi, H. and Kubo, I. (1996). Mode of action of totarol, a diterpene from *Podocarpus nagi*. Planta Medica. 62(2): 122 - 125

Harrison, L.J. and Asakawa, Y. (1987). 18-Oxoferruginol from the leaf of *Torreya nucifera*. Phytochemistry. 26 (4): 1211 – 1212

Harvey, A.L. (1999). Medicines from nature: are natural products still relevant to drug discovery? Trends in Pharmacological Sciences. 20: 196 - 198

Hayashi, Y., Takahashi, S., Ona, H. and Sakan, T. (1968). Structures of nagilactones A, B, C and D, novel nor- and bisnorditerpenoids. Tetrahedron Letters. 9: 2071-2076

Hayashi, Y., Takeo, S., Yoshio, S. and Tazuko, T. (1975). Antitumour activity of nagilactones. Gann. 66(5): 587 - 588

He, K., Zeng, L., Shi, G. Zhao, G., Kolzlowski, J.F. and Mclaughlin, J.L. (1997). Bioactive compounds from *Taiwania cryptomerioides*. Journal of Natural Products. 60: 38 - 40

Hein, T.T. and White, N.J. (1993). Drug Profiles – Qinghaosu. The Lancet. 341: 603 - 608.

Hitokato, H., Morozumi, S., wauke, T., Saiki, S. and Kurata, H. (1980). Inhibitory effects of spices on growth and toxin production of toxigenic fungi. App. Envir. Microbiol. 39: 818

Hostettman, K., Wolfender, J.L., Rodriguez, S. and Marston, A. (1996). Strategy in the search for bioactive plant constituents. Proceedings of the first international IOCD-symposium, Victoria Falls, Zimbabwe. 21- 42

Hyde,J.E. (2002). Mechanisms of resistance of *Plasmodium falciparum* to antimalarial drugs. Microbes and Infection. 4: 165 - 174

Inselburg, J. (1985). Induction and Isolation of artemisinin-resistant mutants of *Plasmodium falciparum*. Am. J. Trop. Med. Hyg. 34: 417 - 418

Iwu, M. (1993). Handbook of African Medicinal Plants. CRC Press Inc, Florida. 188 - 189

Johnson, A.W., King, T.J. and Martin, R.J. (1961). Maytenone. Part 1. Isolation and structural studies. Journal of the Chemical Society. 4420 – 4424

Kale, R. (1995). Traditional healers in South Africa: a parallel health care system. British Medical Journal. 310: 1182 - 1185

Kalemba, D. (1999). Antibacterial and antifungal properties of essential oils. Postepy Mikrobiologii. 38(2): 185-203

Kirby,G.C. (1996). Medicinal plants and the control of parasites. Transactions of the Royal Society of Tropical Medicine and Hygiene. 90: 605 – 609

Kirby,G.C., Noamesi, B.K., Paine, A., Warhurst, D.C. and Phillipson, J.D. (1995a). *In vitro* and *in vivo* antimalarial activity of cryptolepine, a plant-derived indoloquinoline. Phytotherapy Research. 9: 359- 363

Kobayashi, K., Kuroda, K., Shinomiya, T., Nishino, C., Ohya, J. and Sato, S. (1989). Effect of pisiferic acid and its derivatives on cytotoxicity, macromolecular synthesis and DNA polymerase alpha of HeLa cells. International Journal of Biochemistry. 21(5): 463 –463

Kobayashi, K., Nishino, C., Fukushima, M., Shiobara, Y. and Kodama, M. (1988). Antibacterial activity of pisiferic acid and its derivatives against Gram-negative and -positive bacteria. Agric. Biol. Chem. 52(1): 77 - 83

Krogstad, D.J., Gluzman, I.Y, Kyle, D.E. and Oduola, A.M.J. (1987). Efflux of Chloroquine from *Plasmodium falciparum*: mechanism of chloroquine resistance. Science. 236: 1283 – 1285.

Krogstad, D.J., Gluzman, I.Y., Herwaldt, B.L., Schlesinger, P.H. and Wellems, T.E. (1992). Energy dependence of chloroquine accumulation and chloroquine efflux in *Plasmodium falciparum*. Biochemical Parmacology. 43(1): 57 – 62

Krungkrai, S.R. and Yuthvong, Y. (1987). The antimalarial action of qinghaosu and artesunate in combination with agents that modulate oxidant stress. Transactions of the Royal Society of Tropical Medicine and Hygiene. 81: 710 - 714

Kubo,I., Muroi, H. and Himejima, M. (1992). Antibacterial activity of totarol and its potentiation. Journal of Natural Products. 55(10): 1436 - 1440

Lambros, C. and Vanderberg, J.P. (1979). Synchronization of *Plasmodium falciparum* erythrocytic stages in culture. Journal of Parasitology. 65(3): 41 - 420

Lanhers, M.C., Fleurentin, J., Mortier, F., Vinache, A. and Younos, C. (1992). Anti-inflammatory and analgesic effects of an aqueous extract of *Harpagophytum procumbens*. Planta Medica. 58(2): 117 – 123

Lipinski, C.A., Lombardo, F., Dominy, B.W. and Feeney, P.J. (1997). Experimental and computational approaches to estimate solubility and permeability in drug discovery and developmental settings. Advanced Drug Delivery Reviews. 23: 3 - 25

Litchi, H. and von Wartburg, A. (1964). Constitution of harpagoside. Tetrahedron Letters. 15: 835-34

Makler,M.T., Ries, J.M., Williams, J.A., Bancroft J.E., Piper, R.C., Gibbins, B.L. and Hinrichs, D.J. (1995). Parasite lactate dehydrogenase as an assay for *Plasmodium falciparum* drug sensitivity. Am. J. Trop. Med. Hyg. 48 (6): 739 - 741

Malenicic, D., Gasic, O., Popovic, M. and Boza, P. (2000). Screening for antioxidant properties of *Salvia reflexa hornem*. Phytotherapy Research. 14(7): 546 - 548

Mander, M. (1998). In: Marketing of Indigenous Medicinal Plants in South Africa: A Case Study in Kwazulu-Natal. FAO of the UN. Rome.

Martin, J.D. (1973). New diterpenoids extractives of *Maytenus dispermus*. Tetrahedron. 29: 2553 - 2559

Martin, S.K., Oduoro, A.M.J. and Milhous, W.K. (1987). Reversal of chloroquine resistance in *Plasmodium falciparum* by verapamil. Science. 235: 899 – 901

Martinez-Vazquez, M, Miranda, P., Valencia, N.A., Torres, M.L., Miranda, R., Cardenas, J. and Salmon, M. (1998). Antimicrobial diterpenes from *Salvia reptans*. Pharmaceutical Biology. 36(2): 77-80

Mateo, C.R., Prieto, M., Micol, V., Shapiro, S. and Villalaín, J. A fluorescence study of the interaction and location of (+)-totarol, a diterpenoid bioactive molecule, in model membranes. Biochimica et Biophysica Acta. 1509: 167 – 175

Matsabisa, M. (2001). The antimalarial activity of *D. anomala* and the chloroquine resistance reversing effects of *S. birrea* in *P. falciparum in vitro*. University of Cape Town, South Africa. Unpublished PhD thesis.

Matsumoto, T. and Suetsugu, A. (1979). The total synthesis of (+)-totarol and (+)-podototarin. Bulletin of the Chemical Society of Japan. 52(5): 1450 - 1453

Matsumoto, T. and Ohmura, T. (1977). Synthesis of (±)-matenonquinone, (±)-dispermol, and (±)-dispermone. Chemical Letters. 4: 335 - 358

Matsumoto, T. and Usui, S. (1978). The revised structure of dispermol and total synthesis of (-)-dispermone, (+)-dispermone, and (+)-maytenonquinone. Chemical Letters. 8: 897 - 900

Meshnick, S.R., Yang, Y.Z., Lima, V., Kuypers, F., Kamchowongpaisan, S. and Yuthavong, Y. (1993). Iron-dependant free radical generation and the antimalarials artemisinin (*qinghaosu*). Antimicrobial Agents and Chemotherapy. 37: 1108 – 1114

Meshnick, SR. (1994). The mode of action of antimalarial endoperoxides. Transactions of the Royal Society of Tropical Medicine and Hygiene. 88(1): 31 – 32.

Mosman, T. (1983). Rapid colorimetric assay for cellular growth and survival: application to proliferation and cytotoxicity assays. J. Immunol Methods. 65: 55 - 63

Mueller, M.S., Karhagomba, I.B., Hirt, H.M. and Wemakor, E. (2000). The potential of *Artemisia annua L.* as a locally produced remedy for malaria in the tropics: agricultural, chemical and clinical aspects. Journal of Ethnopharmacology. 73: 487 - 493

Nakanishi, T, Miyasaka, H., Nasu, M., Hashimoto, H. and Yoneda, K. (1983). Production of cryptotanshinone and ferruginol in cultured cells of *Salvia miltiorrhiza*. Phytochemistry. 22(3): 721 - 722

Nicolson, K., Evans, G. and O'Toole, P.W. (1999). Potentiation of methicillin activity against methicillin-resistant *Staphylococcus aureus* by diterpenes. FEMS Microbiology Letters. 179 : 233 - 239

Nielsen, D. and Skovsgaard, T. (1992). P-glycoprotein as a multidrug transporter: a critical review of current multidrug cell lines. Biochem. Biophys. Acta. 1139: 169 – 183

O'Neill, M.J., Bray, D.H., Boardman, P., Phillipson, J.D., Warhurst, D.C., Peters, W. and Suffness, M. (1986). Plants as sources of antimalarial drugs: *In vitro* antimalarial activities of some quassinoids. Antimicrobial Agents and Chemotherapy.30 (1): 101 - 104

Occhiuto, F., Circosta, C., Ragusa, S., Ficarra, P. and Costa De Pasquale, R. (1985). A drug used in traditional medicine: *Harpagophytum procumbens* DC. IV. Effects on some isolated muscle preparations. Journal of Ethnopharmacology. 13(2): 201-201

Oduola, A.M.J., Weatherly, N.F., Bowdre, J.H and Dejardins, R.E. (1988). *Plasmodium falciparum*: cloning by single-erythrocyte micromanipulation and heterogeneity *in vitro*. Experimental Parasitology. 66: 86 – 95

Olliaro,P.L., Haynes, R.K., Meunier, B. and Yuthavong, Y. (2001). Possible modes of action of the artemisinin-type compounds. TRENDS in Parasitology. 17 (3): 122 - 126

Orjih, A.U., Ryerse, J. S. and Fitch, C.D. (1994). Hemoglobin catabolism and the killing of intraerythrocytic *Plasmodium falciparum* by chloroquine. Experimenta. 50:34-38

Parker,F.S. and Irvin, J.I. (1952). Interaction of chloroquine with nucleic acids and nucleophiles. J. Biol. Chem. 199: 897 – 909

Paulo, A., Gomes, E.T., Steele, J., Warhurst, D.C. and Houghton, P.J. (2000). Antiplasmodial activity of *Cryptolepis sanguinolenta* alkaloids from leaves and roots. Planta Medica. 66: 30 - 34

Peters, W. and Robinson, B.L. (1999). The chemotherapy of rodent malaria. LVI. Studies on the development of resistance to natural and synthetic endoperoxides. Ann Trop Med Parasitol. 93(4): 325 – 339

Phillipson, J.D. (1994). Natural products as drugs. Transactions of the Royal Society of Tropical Medicine and Hygiene. 88(1): 17-19

Phillipson, J.D. (1995). Review article: A matter of some sensitivity. Phytochemistry. 38 (6): 1319 - 1343

Phillipson, J.D., Wright, C.W, Kirby, G.C. and Warhurst, D.C. (1993). Tropical plants as sources of antiprotozoal agents. Recent Advances in Phytochemistry. 27: 1 - 40

Phillipson, J.D. and Wright, C.W. (1991). Medicinal plants in tropical medicine 1. Medicinal plants against protozoal diseases. Transactions of the Royal Society of Tropical Medicine and Hygiene. 85: 18 - 21

Plowe, C., Kublin, J.G. and Doumbo, O.K. (1998). *P. falciparum* dihydrofolate reductase and dihydropteroate synthetase mutations: epidemiology and role of clinical resistance to antifolates. Drug Resistance Updates.1: 389 - 396

Prescott, L.M., Harley, J.P. and Klein, D.A. (1993). Microbiology, Second Edition. Wm. C. Brown Publishers, Dubuque, Iowa.

Prozesky, E.A., Meyer, J.J.M. and Louw, A.I. (2001). *In vitro* antiplasmodial activity and cytotoxicity of ethnobotanically selected South African plants. Journal of Ethnopharmacology. 76: 239 – 245

Rao, P. and Pattabiraman, T.N. (1989). Re-evaluation of the phenol-sulphuric acid reaction for the estimation of hexoses and pentoses. Analytical Biochemistry. 1881: 18 - 22

Reed,M.B., Saliba, K.J., Caruana, S.R., Kirk, K. and Cowman, A. F. (2000). Pgh1 modulates sensitivity and resistance to multiple antimalarials in *Plasmodium falciparum*. Nature. 403: 906 – 909

Riordan, J.R., Deuchars, K., Kartner, N., Alon, N., Trent, J. and Ling, V. (1985) Amplification of P-glycoprotein genes in multidrug-resistant mammalian cell lines. Nature. 316: 817 - 819

Sachs, J. and Malaney, P. (2002). The economic and social burden of malaria. Nature. 415: 680-685

Sairafianpour, M., Christensen, J., Stærk, D., Budnik, B., Kharazmi, A., Bagherzadeh, K. and Jaroszewski, J.W. (2001). Leishmanicidal, antiplasmodial and cytotoxic activity of novel diterpenoid 1,2-quinones from *Perovskia abrotanoides*: a new source of tanshinones. Journal of Natural Products. 64: 1398 - 1403

Sanchez, C.P., Wünsch, S. and Lanzer, M. (1997). Identification of a chloroquine importer in *Plasmodium falciparum*. Journal of Biological Chemistry. 272(5): 2652 – 2658

Schellenberg, K.A. and Coatney, G.R. (1961). The influence of antimalarials drugs on nuclei acid synthesis in *Plasmodium gallinaceum* and *Plasmodium berghei.* Biochem Pharmacol. 6: 143 - 152

Sharp, H., Latif, Z., Bartholomew, B., Bright, C., Jones, C.D. and Sarker, S. (2001). Totarol, totaradiol and ferruginol: three diterpenes from *Thuja plicata* (*Cupressaceae*). Biochemical Systematics and Ecology. 29: 215 - 217

Sharp, B.L. and le Sueur, D. (1996). Malaria in South Africa – the past, the present and selected implications for the future. South African Medical Journal. 86(1): 83-89

Short, W.F., Wang, H. and Goulden, J.D.S. (1951). Totarol II. Journal. Chem. Soc. 2979 - 2987

Silverman, R.B. (1992). The Organic Chemistry of Drug Design and Drug Action. Academic Press, Inc., San Diego.

Soulimani, R. Younos, C., Mortier, F. and Derrieu, C. (1994). The role of stomachal digestion on the pharmacological activity of plant extracts, using as an example extracts of *Harpagophytum procumbens*. Can J Physiol Pharmacol. 72(12): 1532 - 1536

Sullivan, D.J., Matile, H., Ridley, R.G. and Goldberg, D.E. (1998). A common mechanism for blockade of heme polymerization by antimalarial quinolines. J. Biol. Chem. 273: 31103 – 31107

Surolia, N. and Padmanaban, G. (1991). Chloroquine inhibits heme-dependant protein synthesis in *Plasmodium falciparum*. Proc. Natl. Acad. Sci. USA. 88(11): 4786-4790

Tada,M., Okuno, K., Chiba, K., Ohnishi, E. and Yoshii, T. (1994). Antiviral diterpenes from *Salvia officinalis*. Phytochemistry. 35(2): 539 - 541

Takaya, Y., Tasaka, H., Chiba, T., Uwai, K., Tanitsu, M., Kim, H., Wataya, Y., Miura, M., Takeshita, M. and Oshima, Y. (1999). New type of febrifugine analogues, bearing a quinolizidine moiety, show potent antimalarial activity against *Plasmodium* malaria parasites. 42: 3163 – 3166

Terret, N.K., Gardner, M., Gordon, D.W., Kobylecki, R.J. and Steele, J. (1995). Combinatorial synthesis - the design of compound libraries and their application to drug discovery. Tetrahedron. 51(30): 8135 - 8173

Thaithong, S. and Beale, G.H. (1981). Resistance of ten Thai isolates of *Plasmodium flaciparum* to chloroquine and pyrimethamine by *in vitro* tests. Transactions of the Royal Society of Tropical Medicine and Hygiene. 75: 271

Trager,W. and Jensen, J.B. (1976). Human malaria parasites in continuous culture. Science. 193: 673 - 675

Tunmann, P. and Stierstorfer, N. (1964). Constituents of *Harpagophytum procumbens* root. III. A third Glycoside. Tetrahedron Letter. 25-26: 1697 – 1699

Ulubelen, A., Topcu, G., Tan, N., Lin, L.J. and Cordell, G.A. (1992). Microstegiol, a rearranged diterpene from *Salvia microstegia*. Phytochemistry. 31: 2419 - 2121

Ulubelen, A. Öksüz, S., Kolak, U., Birman, H., C. and Voelter, W. (2000). Cardioactive terpenoids and a new rearranged diterpene from *Salvia syriaca*. Planta Medica. 66: 627 – 629

Ulubelen, A., Evren, N., Tuziaci, E. and Bozok-Johansson, C. (1988). Diterpenoids from the roots of *Salvia hypargeia*. Journal of Natural Products. 51(6): 1178 – 1183

Ulubelen, A., Öksüz, S., Kolak, U., Bozok-Johansson, C., Çelik, C. and Voelter, W. (2000). Antibacterial diterpenes from the roots of *Salvia viridis*. Planta Medica. 66: 458 – 462

Ulubelen, A., Topcu, G., Eris, C., Sönmez, U., Kartal, M., Kurucu, S. and Bozok-Johansson, C. (1994). Terpenoids from *Salvia sclarea*. Phytochemistry. 36(4): 971 - 974

Ulubelen, A., Topcu, G. and Tan, N. (1992). Rearranged abietane diterpenes from *Salvia candidissima*. Phytochemistry. 31(10): 3637 - 3638

van Agtmael, M.A., Eggelte, T.A. and van Boxtel, C.J. (1999). Artemisinin drugs in the treatment of malaria: from medicinal herb to registered medication. Trends in Pharmacological Sciences. 20: 199 - 204

van Wyk, B.E. and Gericke, N. (2000). People's Plants; A Guide to Useful Plants of Southern Africa. Briza Publications, Pretoria.

van Wyk, B.E., van Oudtshoorn, B. and Gericke, N. (1997). Medicinal Plants of South Africa. Briza Publications, Pretoria.

Vander Jagt, D.L., Hunsaker, L.A. and Campos, N.M. (1986). Characterisation of a haemoglobin-degrading, low molecular weight protease from *Plasmodium falciparum.* Mol Biochem Parasitol. 18(3): 389 - 400

Wang, P., Lee, C.S., Bayoumi, R., Djimde, A., Doumbo, O., Swedberg G., Dao, L.D., Mshinda, H., Tanner, M., Watkins, W.M., Sims, P.F. and Hyde, J.E. (1997). Resistance to antifolates in *Plasmodium falciparum* monitored by sequence analysis of dihydropteroate synthetase and dihydrofolate reductase alleles in a large number of field samples of diverse origins. Mol Biochem Parasitol. 89 (2): 161 - 177

Wang, P., Read, M. Sims, P.F.G. and Hyde, J.E. (1997). Sulfadoxine resistance in the human malaria parasite *Plasmodium falciparum* is determined by mutations in dihydropteroate synthetase and an additional factor associated with folate utilization. Mol. Microbiol. 23: 979 – 986

Watt, J.M. and Breyer-Brandwijk, M.G. (1962). The Medicinal and Poisonous Plants of Southern Africa. E&S Livingstone Ltd., London.

Wegener, T. (2000). Devil's Claw: From African traditional remedy to modern analgesic and anti-inflammatory. Herbalgram - The Journal of the American Botanical Council and Herb Research Foundation. 50: 47-54

Wellems, T.E., Panton, L.J., Gluzman, I.Y. and do Rosario, V.E. (1990). Chloroquine resistance not linked to *mdr* -like genes in *Plasmodium falciparum* cross. Nature. 345: 253 – 255

Wenkert, E. and Jackson, B.G. (1958). Re-arrangements and oxidations of tricarbocyclic diterpenes. American Chemical Society Journal. 80: 211 - 217

Wenkert, E. Clouse, A.O., Cochran, D.W. and Doddrell, D. (1969). Carbon-13 nuclear magnetic spectroscopy of naturally occurring substances. I. Direct analysis on nonprotonated carbon centres. J. Am. Chem. Soc. 91(24): 6879 - 6880

Wess, G., Urmann, M. and Sickenberger, B. (2001). Medicinal chemistry: challenges and opportunities. Angewante Chemie International Edition in English. 40(18): 3341-3350

Whitehouse, L.W., Znamirowska, M. and Paul, C.P. (1983). Devil's Claw (*Harpagophytum procumbens*): no evidence for anti-inflammatory activity in the treatment of arthritic disease. Can Med assoc J. 129(3): 249-251

WHO, World Health Organisation Fact Sheet No. 94. Revised Oct. 1998. WHO information. http://www.int/inf~fs/en/fact094.html

WHO, World Health Organisation. (1998). Regulatory situation of herbal medicines, a worldwide review. http://www.WHO/TRM/98.1

Wille, N. (2001). Department of Health, South Africa – Malaria Notification Data 2001

Yang, Y.Z., Aswamamhasakda, W. and Meshnick, S.R. (1993). Alkylation of human albumin by the antimalarials artemisinin. Biochemical Pharmacology. 46: 336 – 339

Yang,Z., Kitano, Y., Chiba, K., Shibata, N., Kurokawa, H., Doi, Y., Arakawa, Y. and Tada, M. (2001). Synthesis of variously oxidized abietane diterpenes and their antibacterial activities against MRSA and VRE. Bioorganic & Medicinal Chemistry. 9: 347 - 356

Yayon, A., Cabantchik, Z.I. and Ginsburg, H. (1984). Identification of the acidic compartment of *Plasmodium falciparum* infected human erythrocytes as the target of the antimalarial drug chloroquine. The EMBO Journal. 3(11): 2695 – 2700

Ying, B. and Kubo, I. (1991). Complete ^{1}H and ^{13}C NMR assignments of totarol and its derivatives. Phytochemistry. 30 (6): 1951 - 19

Zhang, Y. and Meshnick, S.R. (1991). Inhibition of *Plasmodium falciparum* dihydropteroate synthetase and growth *in vitro* by sulfa drugs. Antimicrob. Agents Chemother. 35: 267 – 271

Zhang, Y., Gosser, D. and Meshnick, S.R. (1992). Hemin-catalysed decomposition of artemisinin (*qinghaosu*). Biochemical Pharmacology. 43: 1805 - 1809

Zorn, B. (1985). Uber die antiarthritische wirkung der *Harpagophytum* - wurzel. Z. Rheumaforsch. 17: 134-138

Appendix 1

In vitro Antiplasmodial and Cytotoxicity Dose Response Curves

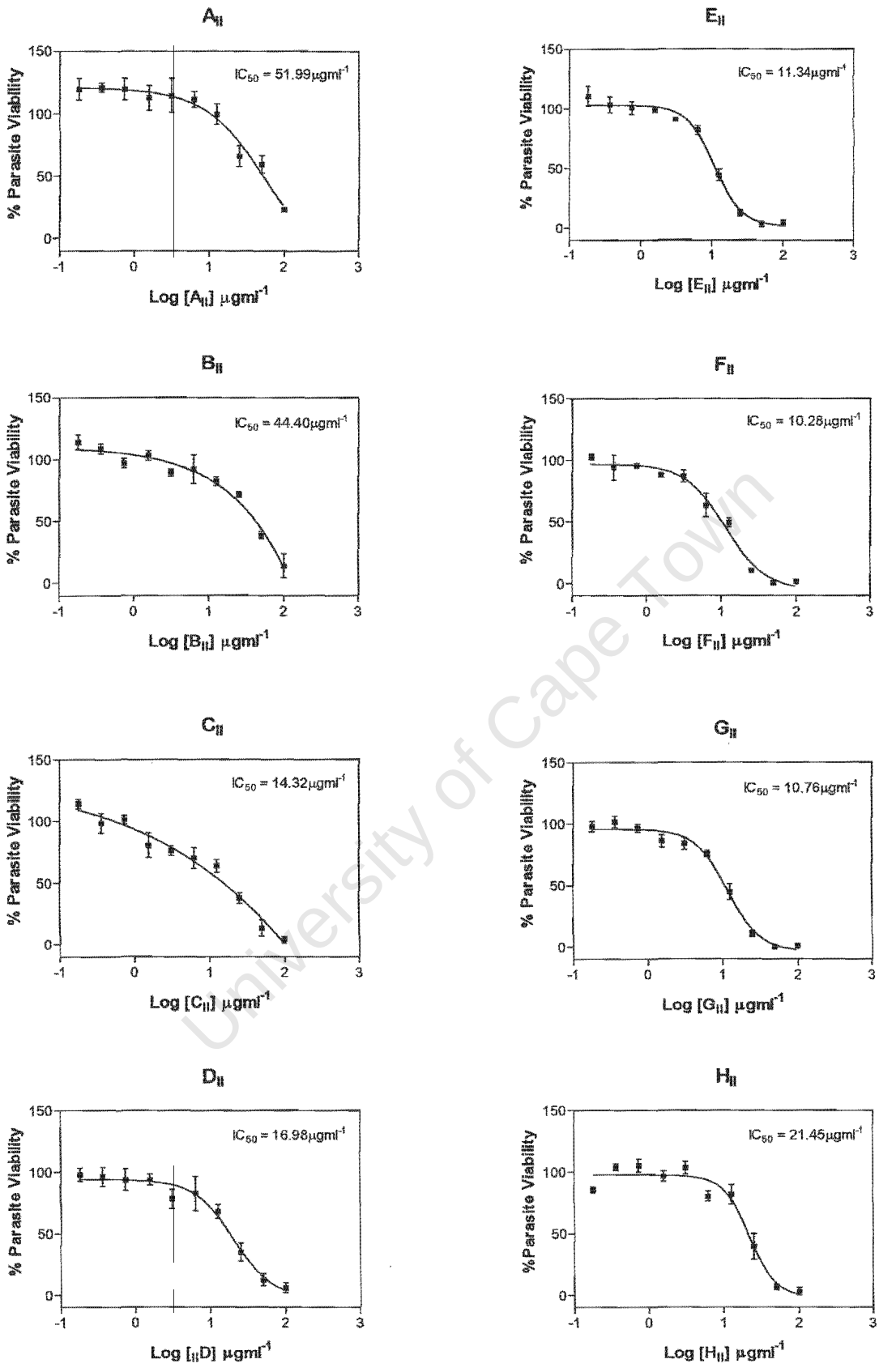

Figure 3.2.6.1. Dose response curves of the fractions $(A\text{-}H)_{II}$ generated by flash chromatography on the PE extract of *H. procumbens* (batch II). Each point represents the mean of 2 independent experiments each performed in duplicate

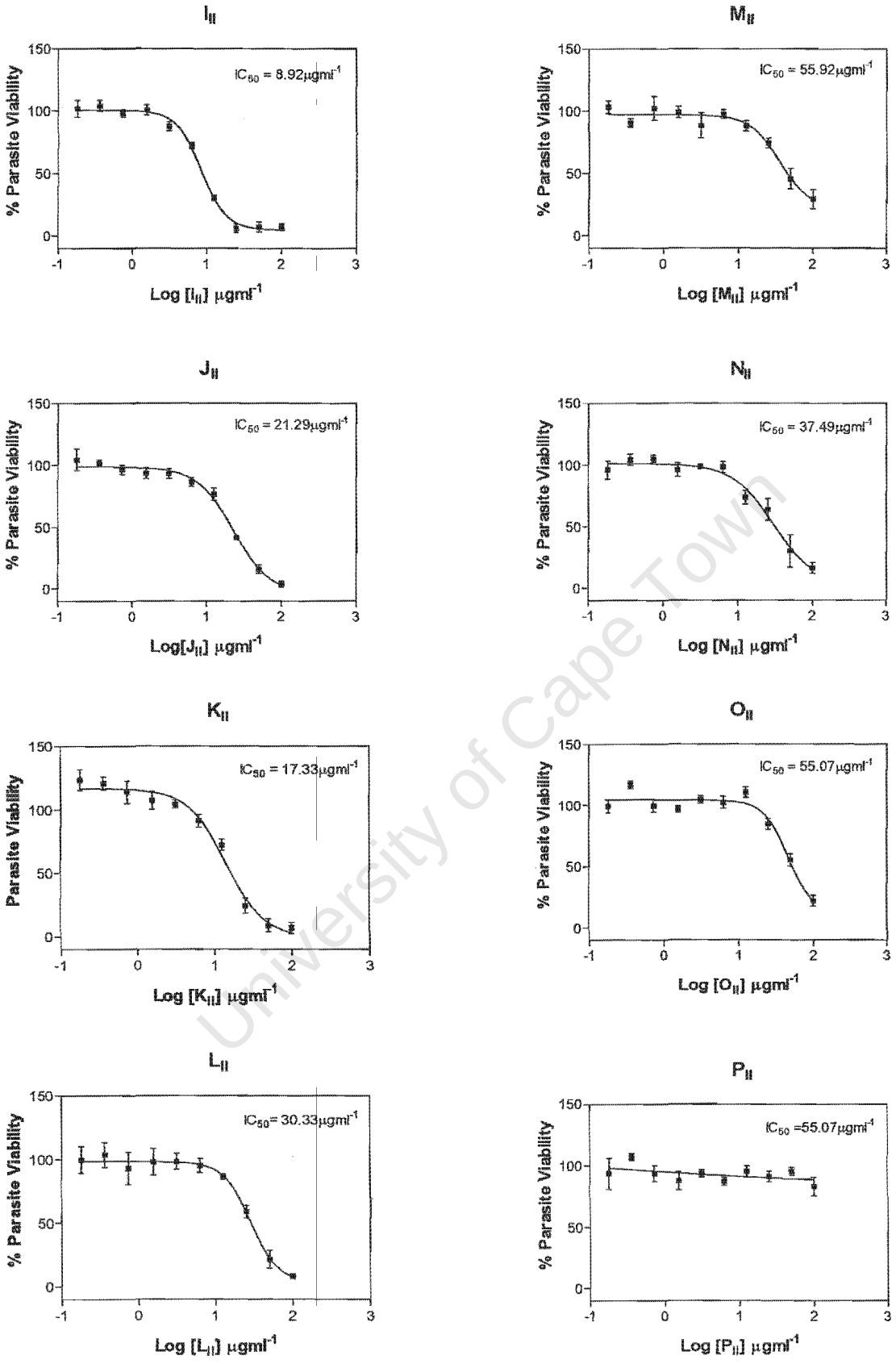

Figure 3.2.6.1. (Continued) Dose response curves of the fractions $(I\text{-}P)_{II}$ generated by flash chromatography on the PE extract of *H. procumbens* (batch II). Each point represents the mean of 2 independent experiments each performed in duplicate

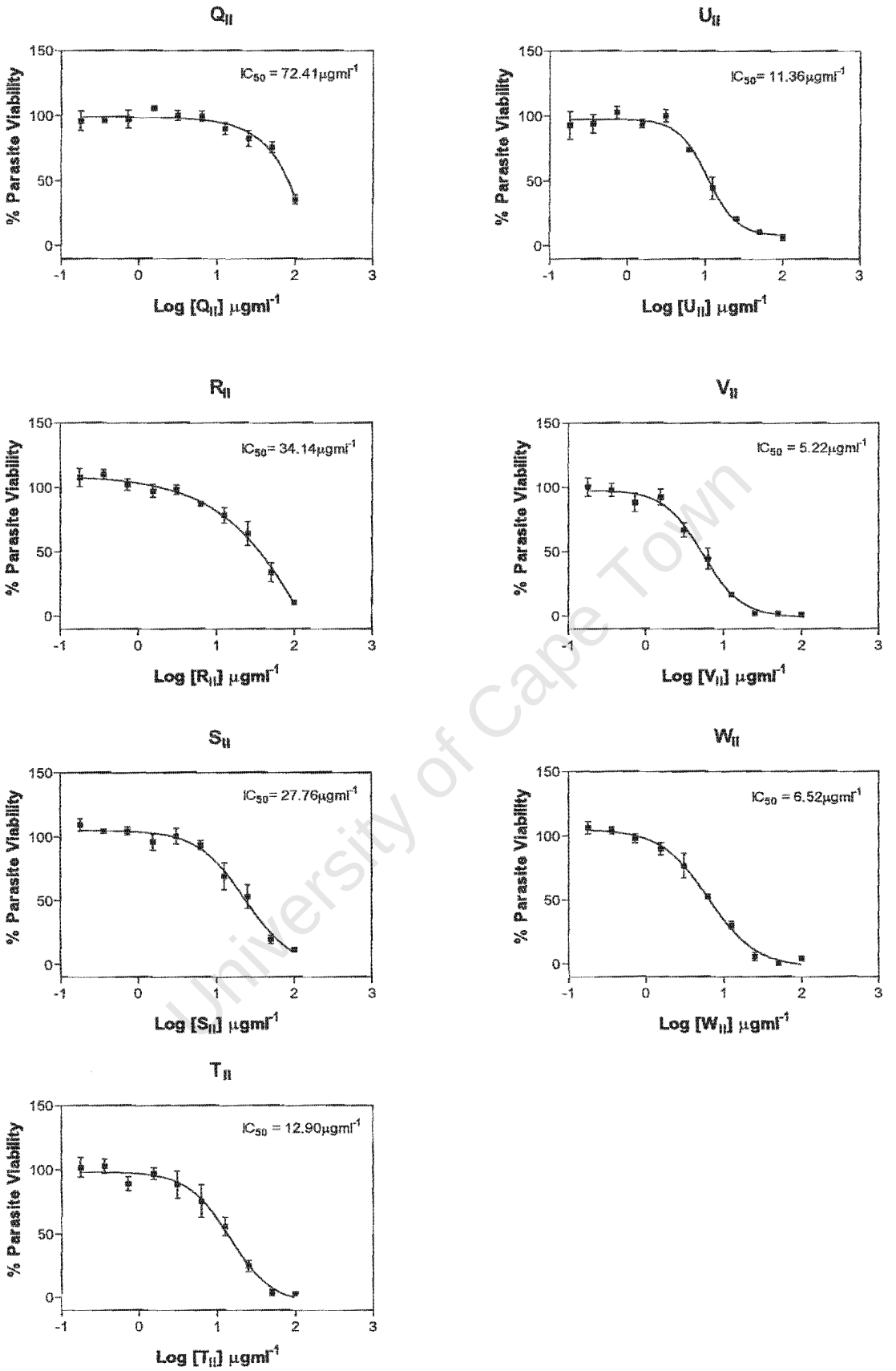

Figure 3.2.6.1. (Continued) Dose response curves of the fractions $(Q\text{-}W)_{II}$ generated by flash chromatography on the PE extract of *H. procumbens* (batch II). Each point represents the mean of 2 independent experiments each performed in duplicate

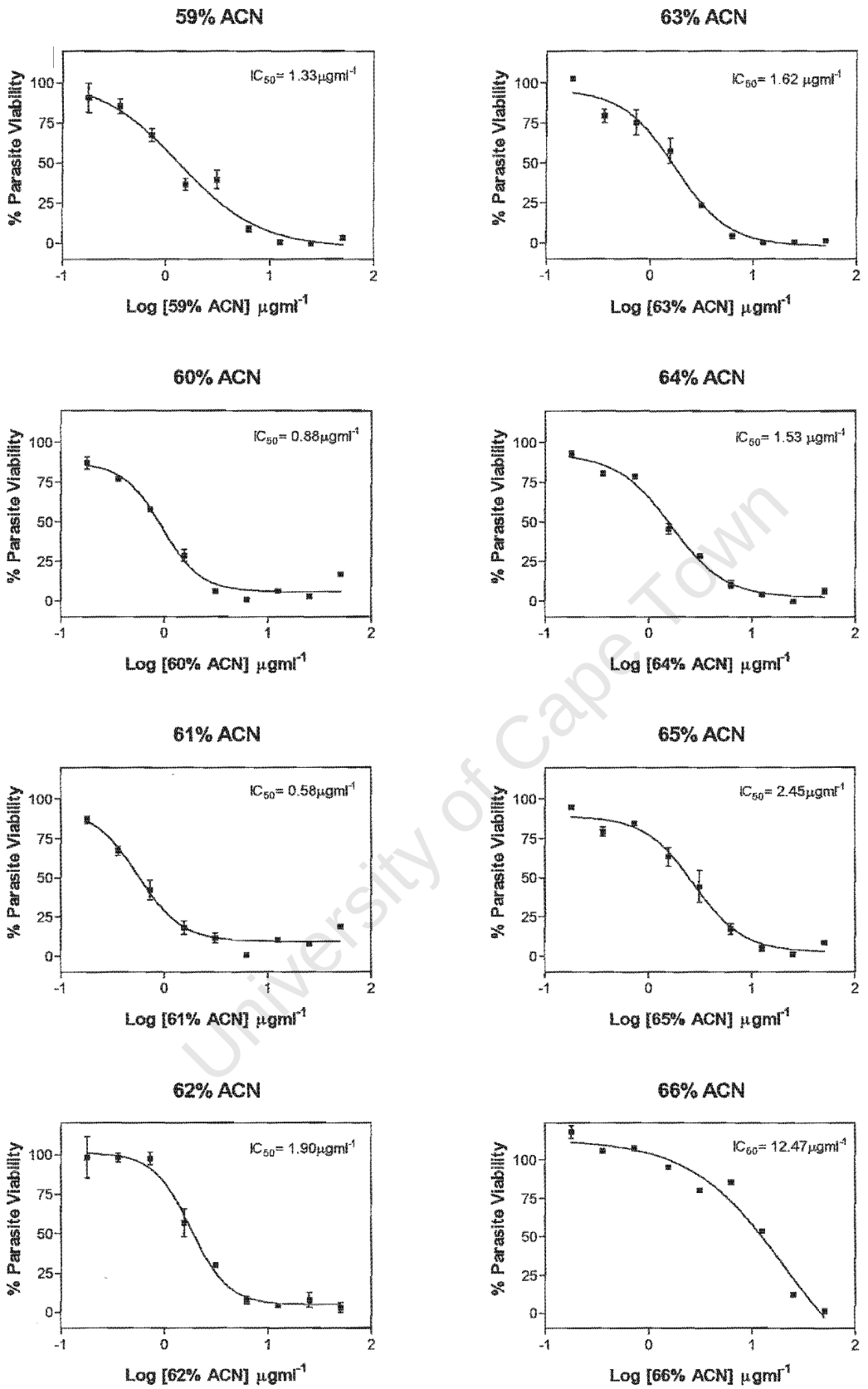

Figure 4.2.2.1a. Dose response curves of the fractions 59% - 66% ACN generated by SPE on the PE extract of *H. procumbens* (batch III). Each point represents the mean of 2 independent experiments each performed in duplicate

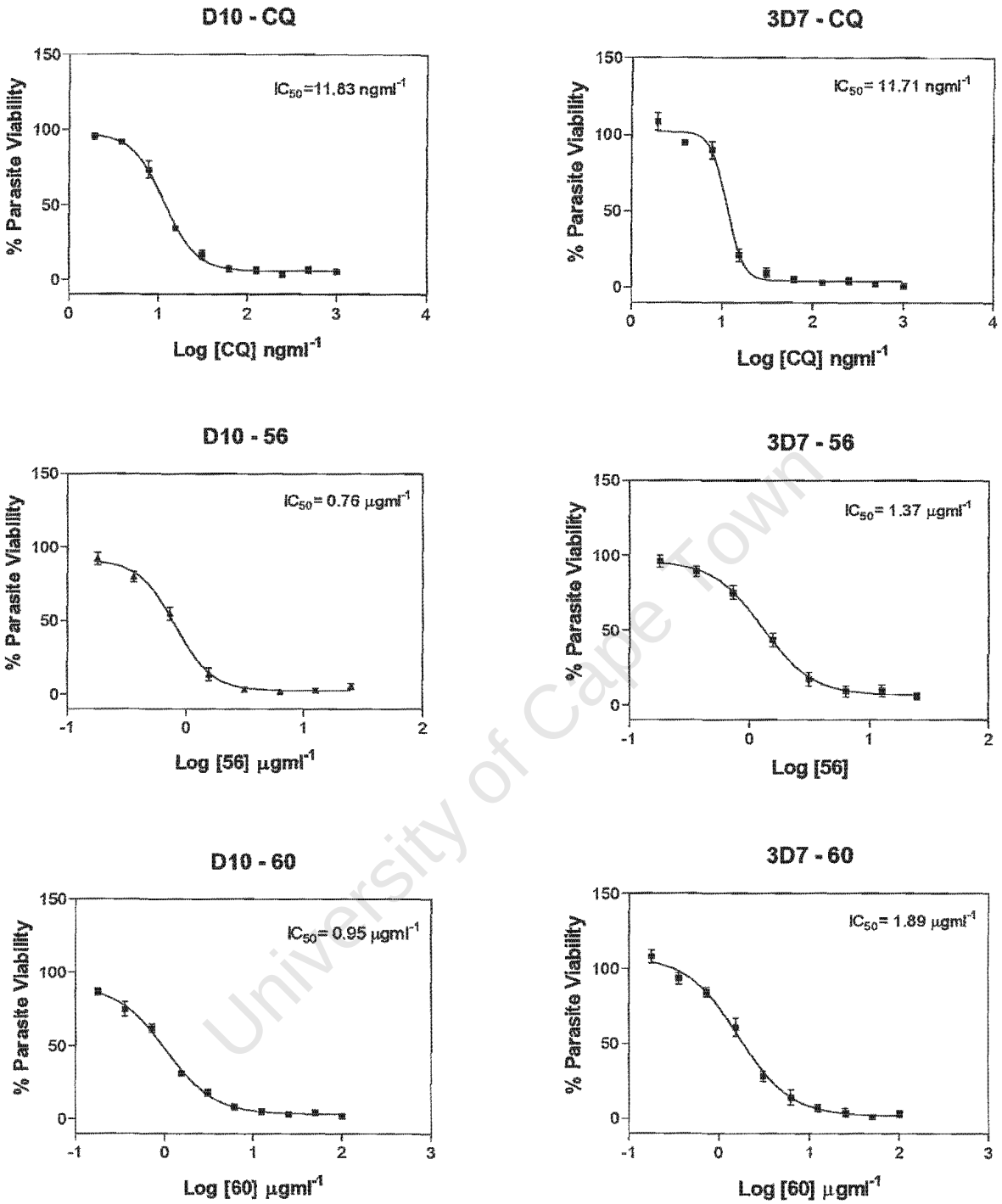

Figure 4.2.4.1. Dose response curves of CQ and compounds **56** and **60** on *P. falciparum* D10 and 3D7 strains. Each point represents the mean of 3 independent experiments each performed in duplicate

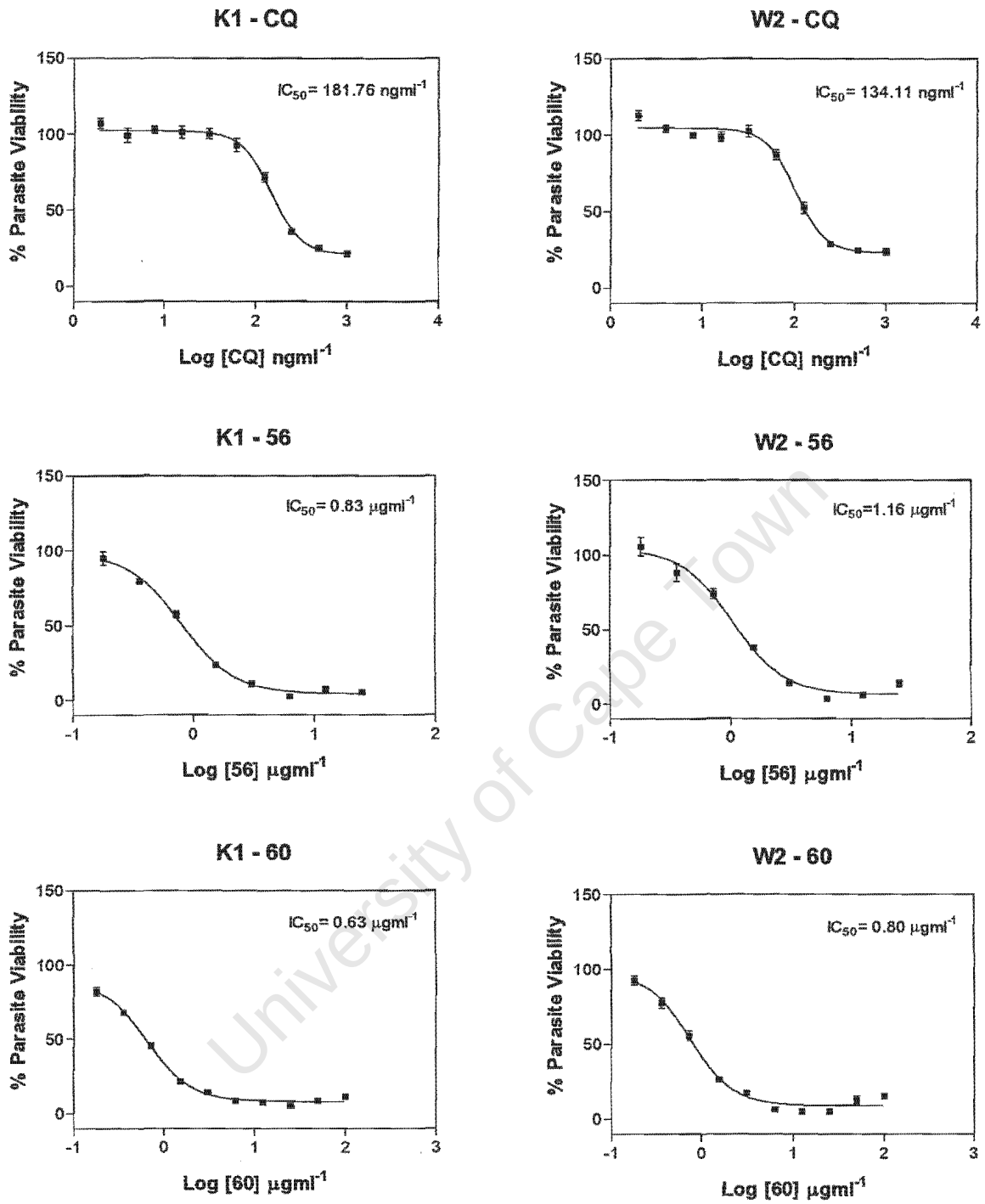

Figure 4.2.4.1. (Continued) Dose response curves of CQ and compounds **56** and **60** on *P. falciparum* K1 and W2 strains. Each point represents the mean of 3 independent experiments each performed in duplicate

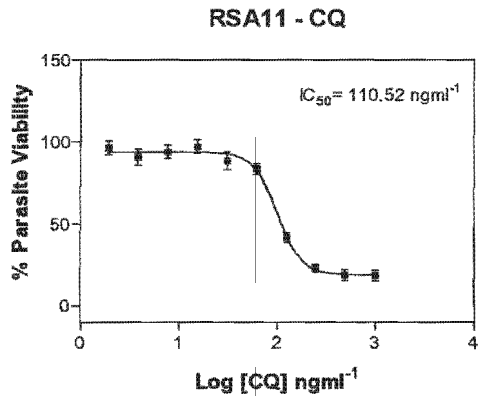

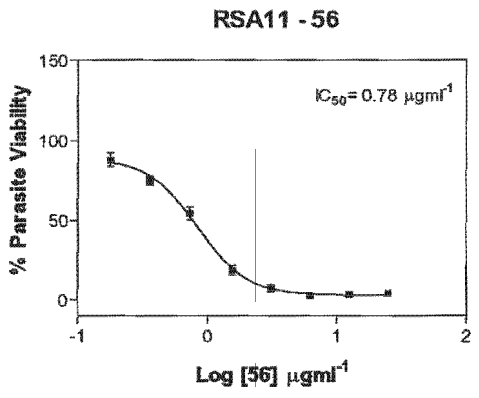

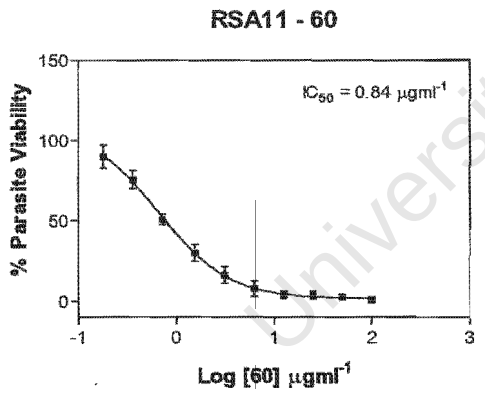

Figure 4.2.4.1. (Continued) Dose response curves of CQ and compounds **56** and **60** on *P. falciparum* RSA11 strain. Each point represents the mean of 3 independent experiments each performed in duplicate

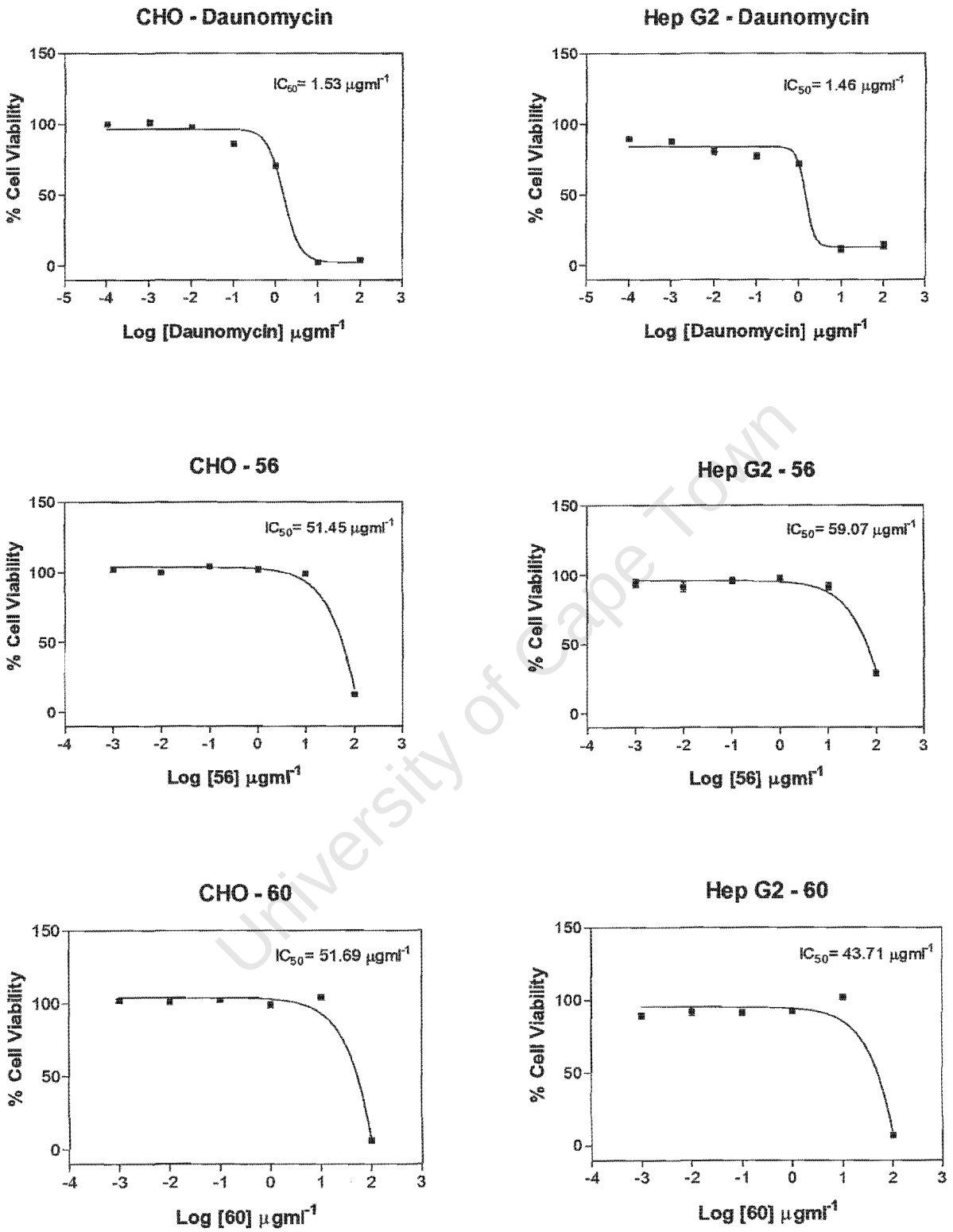

Figure 4.2.4.2. Dose response curves of daunomycin and compounds **56** and **60** on Chinese hamster ovarian (CHO) and Heptoma (HepG2) cells. Each point represents the mean of 3 independent experiments each performed in quadruplicate

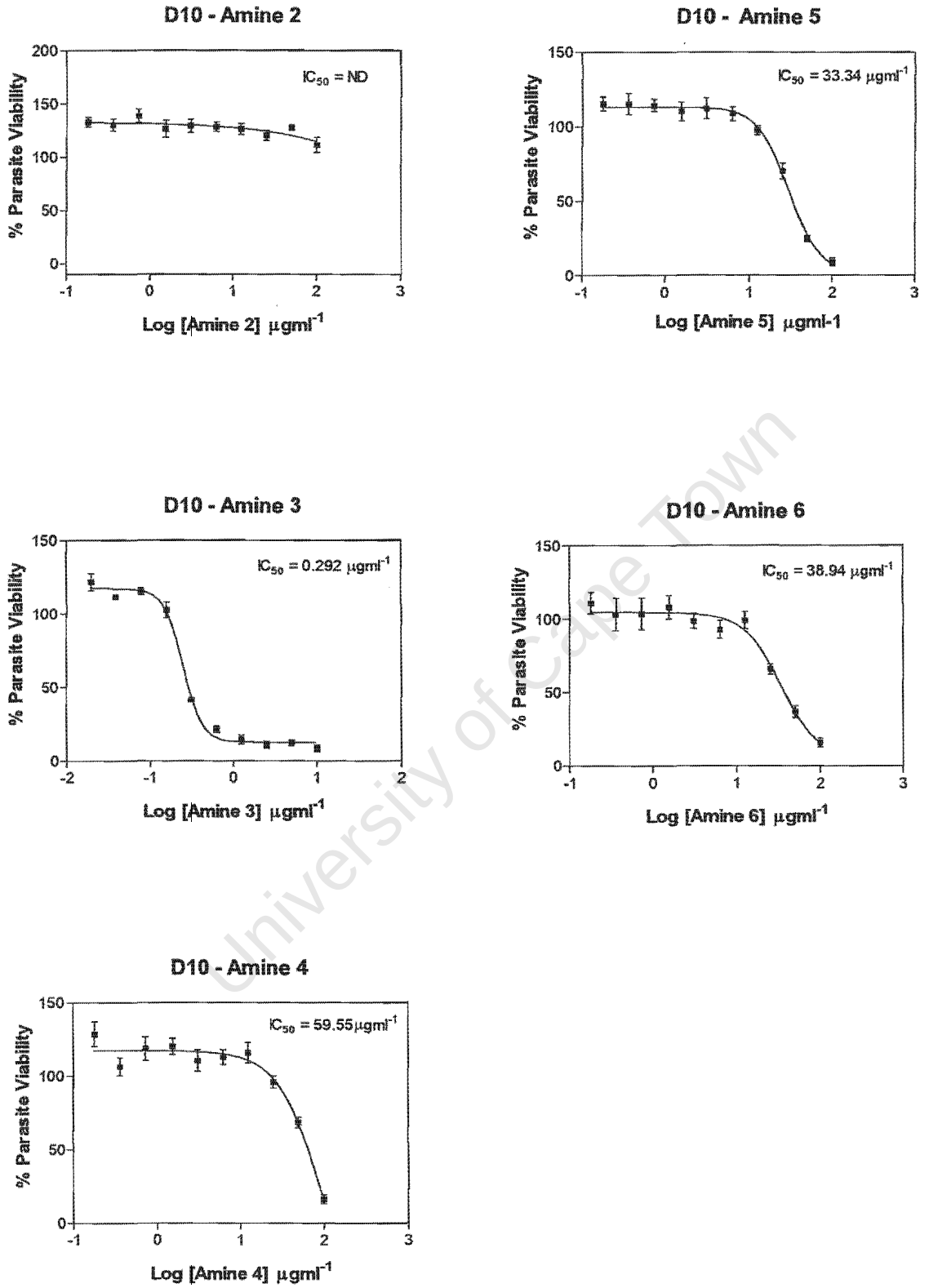

Figure 5.3.3. Dose response curves of the amines **2** to **6** against *P. falciparum* D10. Each point represents the mean of 3 independent experiments each performed in triplicate

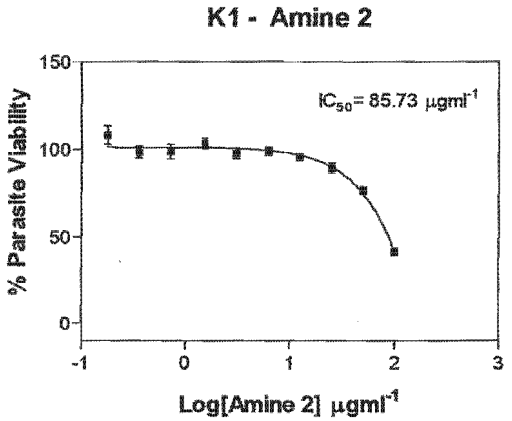

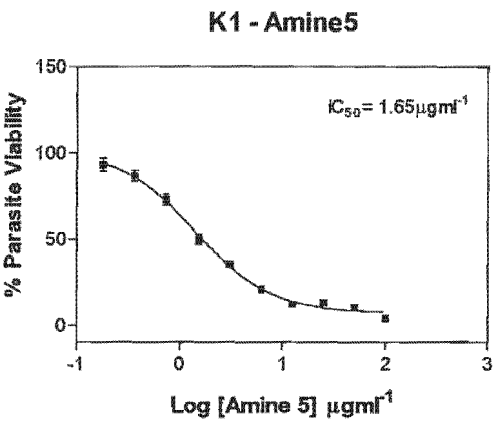

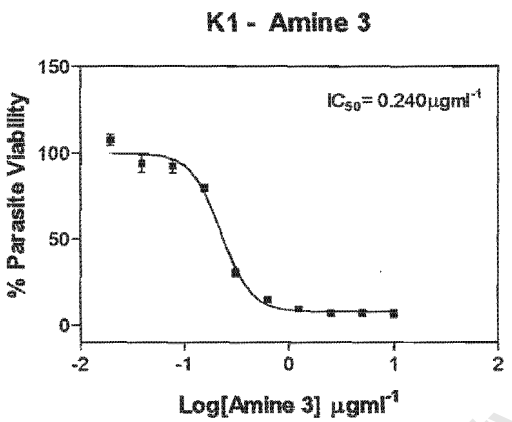

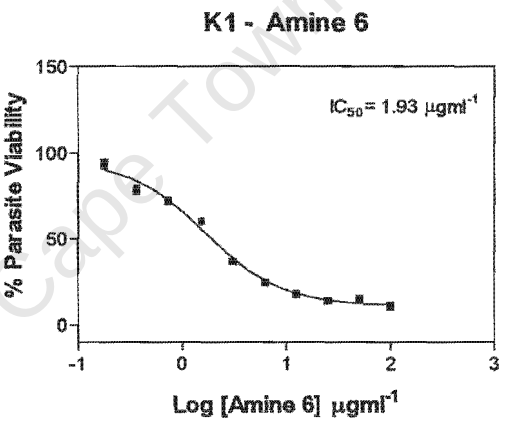

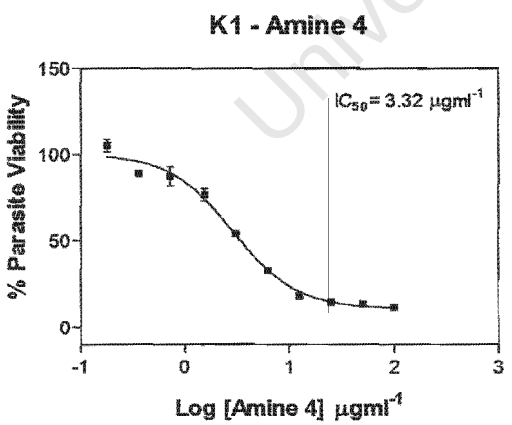

Figure 5.3.3. (Continued) Dose response curves of the amines **2** to **6** against *P. falciparum* K1. Each point represents the mean of 3 independent experiments each performed in triplicate

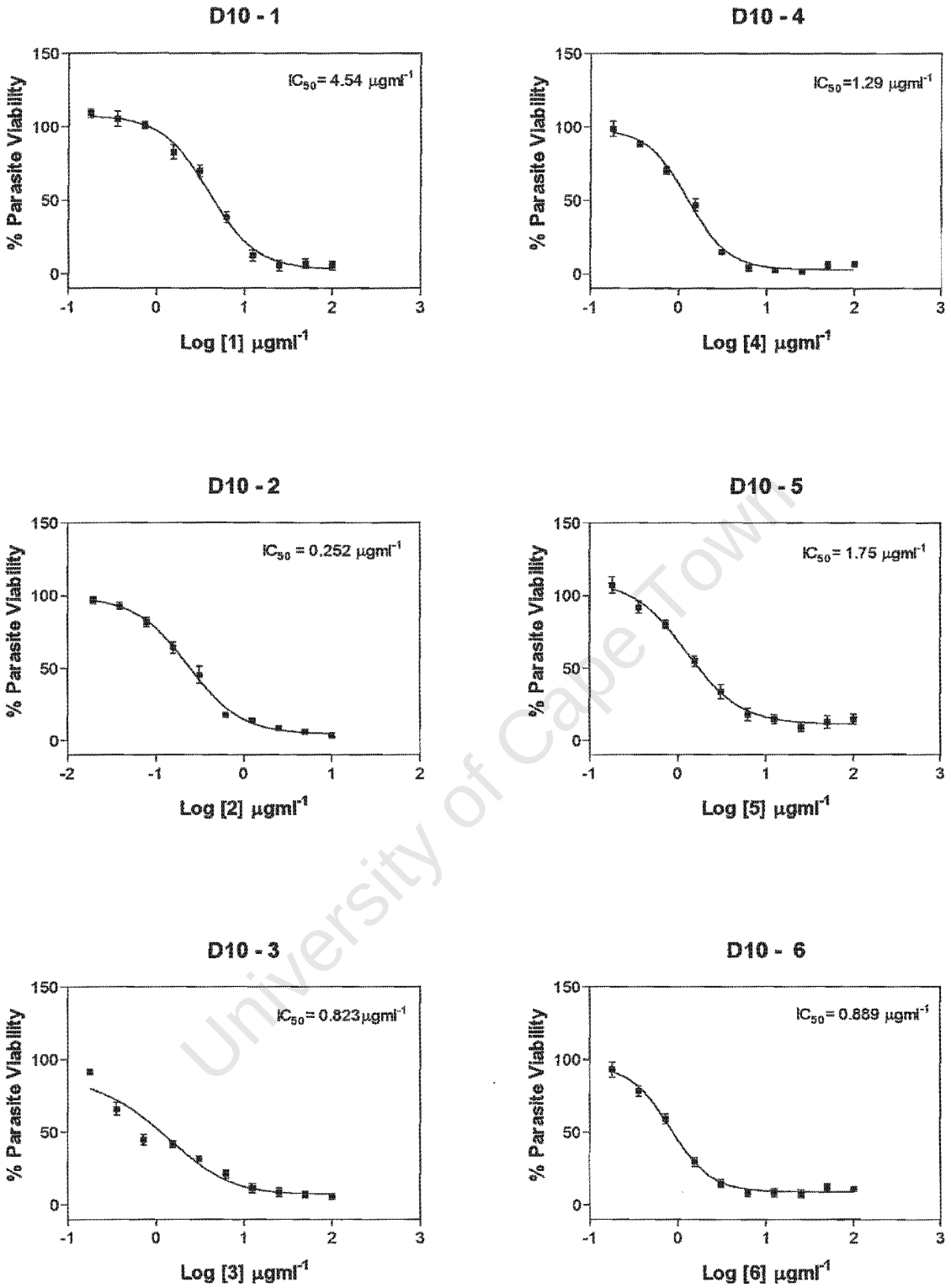

Figure 5.3.3. (Continued) Dose response curves of the epoxide **1** and the β-amino alcohols **2** to **6** against *P. falciparum* D10. Each point represents the mean of 3 independent experiments each performed in triplicate

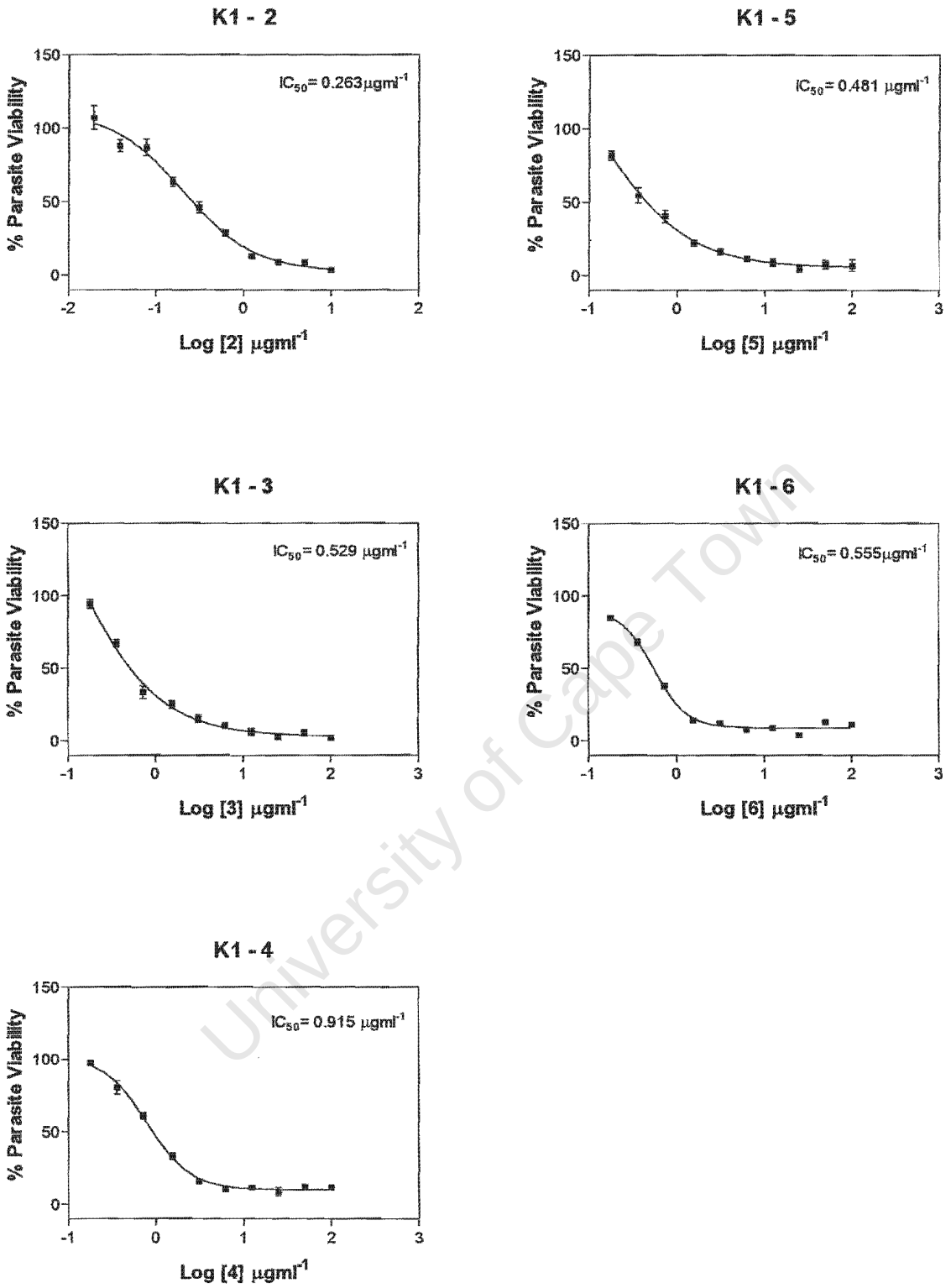

Figure 5.3.3. (Continued) Dose response curves of the epoxide **1** and the β-amino alcohols **2** to **6** against *P. falciparum* K1. Each point represents the mean of 3 independent experiments each performed in triplicate

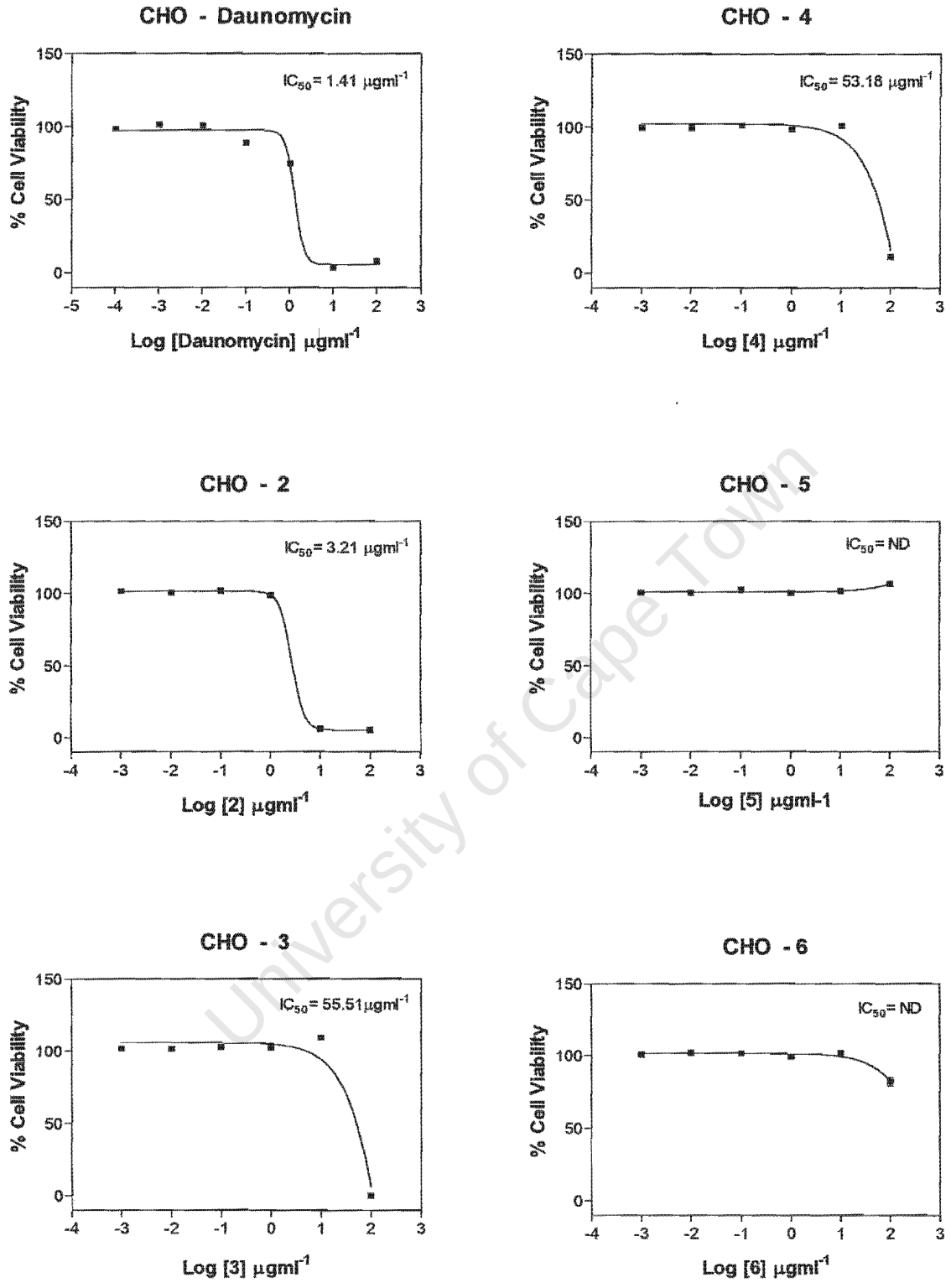

Figure 5.3.3. (Continued) Dose response curves of the epoxide **1** and the β-amino alcohols **2** to **6** against Chinese hamster ovarian (CHO) cells . Each point represents the mean of 3 independent experiments each performed in quadruplicate

Appendix 2

HPLC, UV, IR and NMR spectra

A2.1 Compound H5a

List of spectra:

- HPLC profile
- UV
- HREIMS

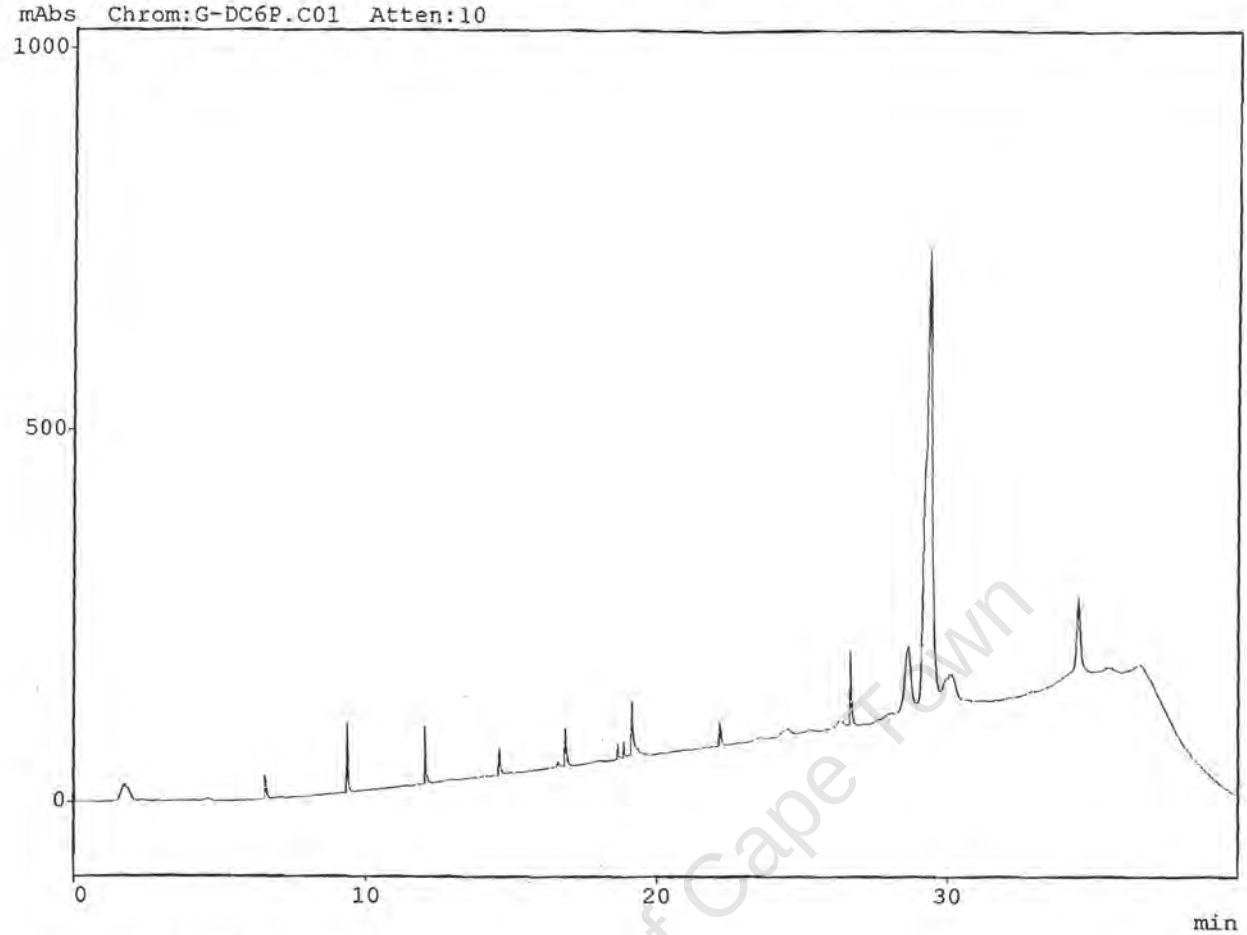

Figure A2.1.1 HPLC chromatogram of **H5a**

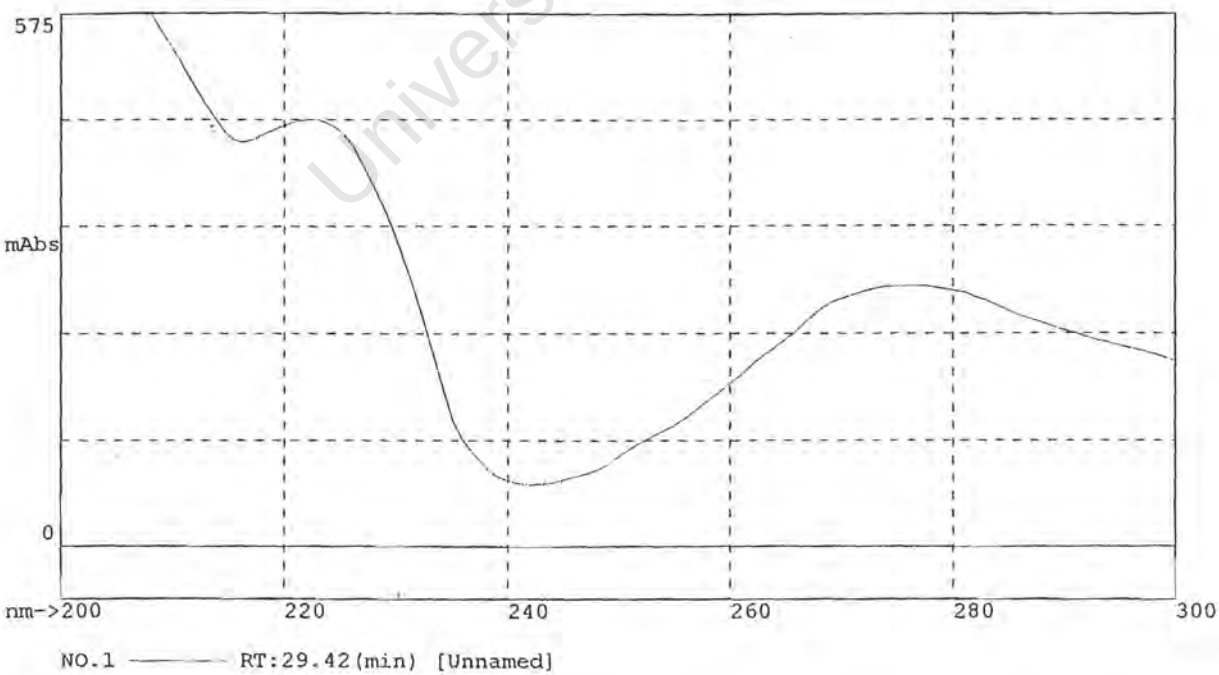

Figure A2.1.2 UV spectrum of **H5a**

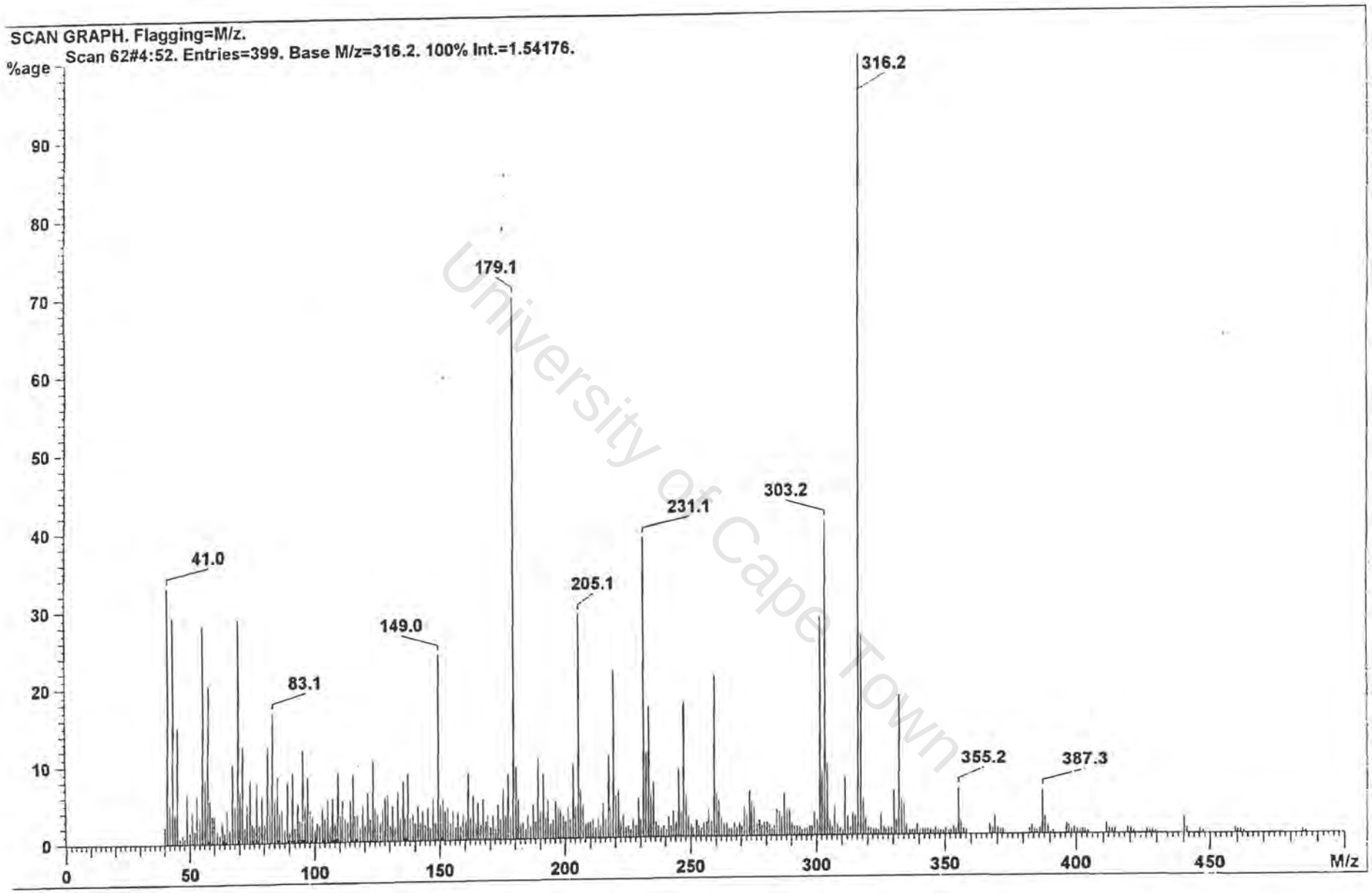

Figure A2.1.3 HREIMS spectrum of **H5a**

A2.2 Compound 56

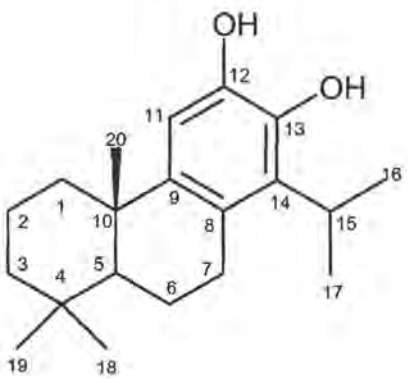

8,11,13-Totaratriene-12-13-diol (56)

IUPAC [Isopropyl-4b,8,8-trimethyl-4b,5,6,7,8,8a,9,10-octahydro-phenanthrene-2,3-diol]

List of spectra:

- HPLC profile
- UV absorbance
- IR
- HREIMS
- ^{1}H NMR (600MHz, CD_3OD)
- ^{13}C NMR (600MHz, CD_3OD)
- HSQC (500MHz, CD_3OD)
- HMBC (500MHz, CD_3OD)
- COSY (500MHz, CD_3OD)
- NOESY (500MHz, CD_3OD)

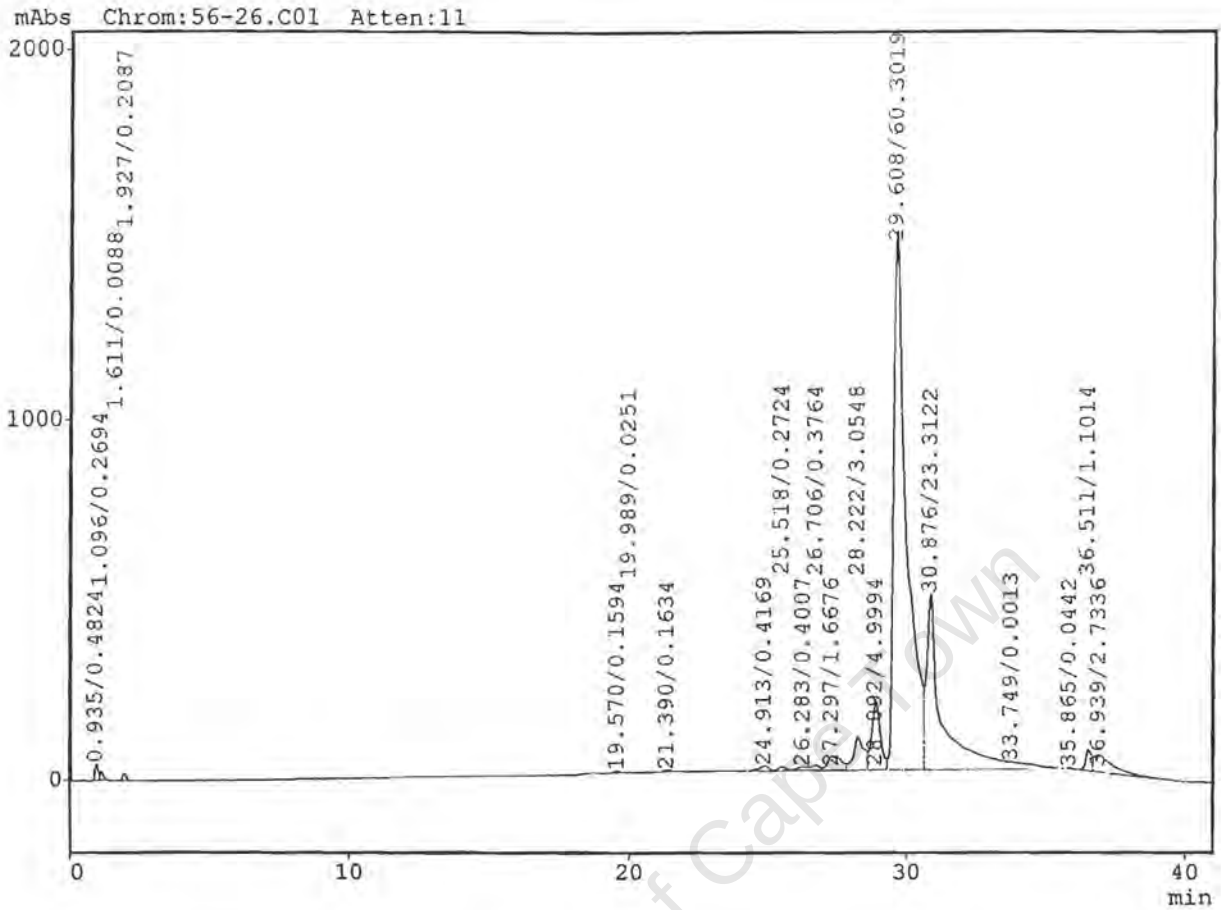

Figure A2.2.1 HPLC profile of **56** (H_2O: ACN)

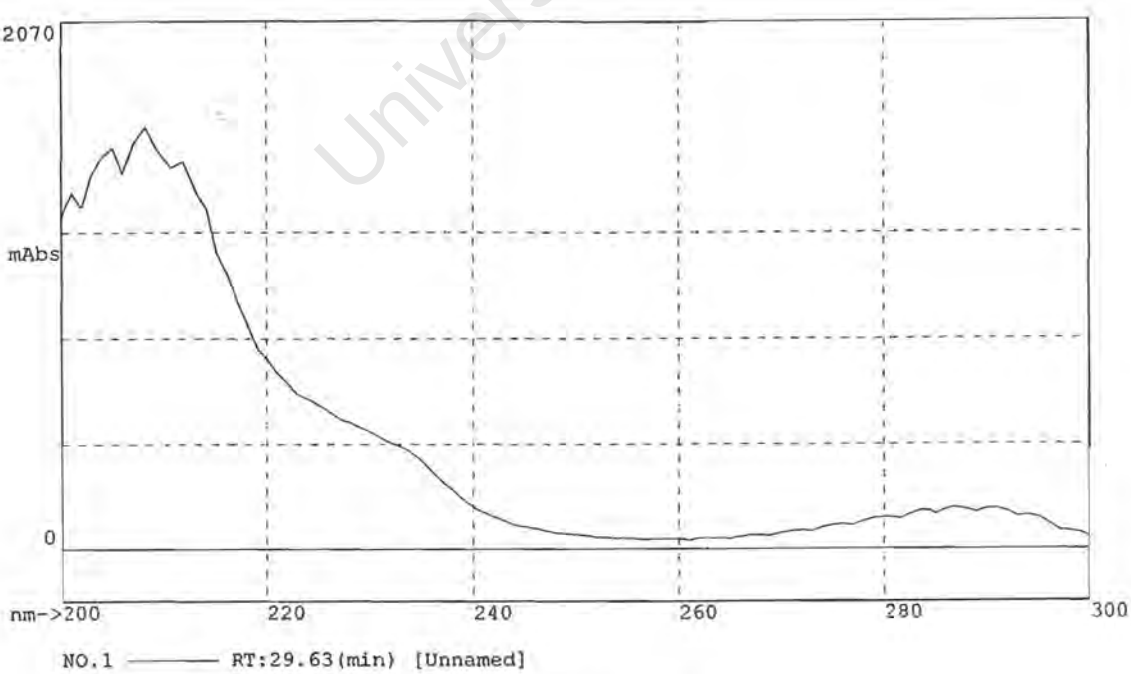

Figure A2.2.2 UV absorbance of **56** (H_2O: ACN)

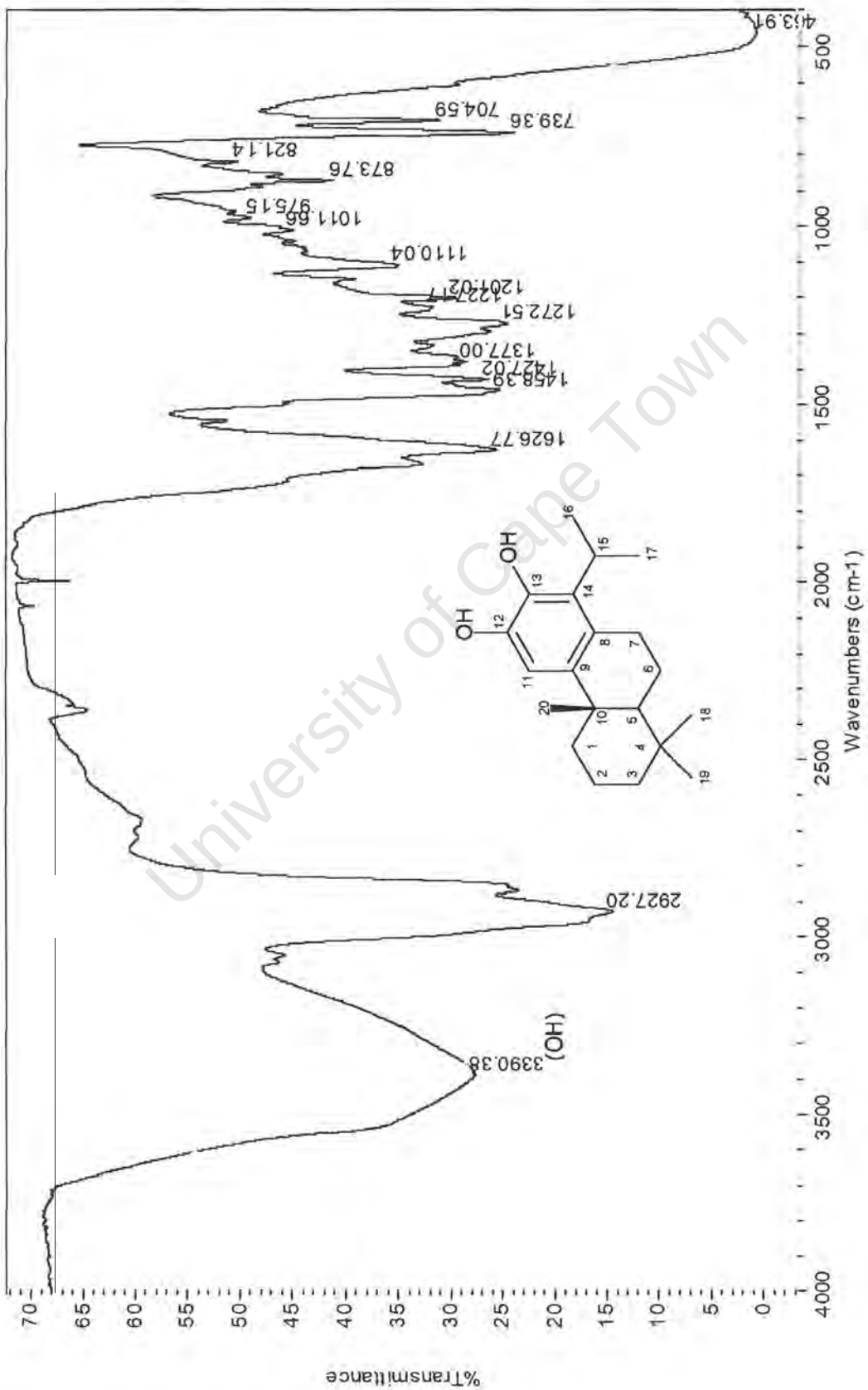

Figure A2.2.3 IR spectrum of **56**

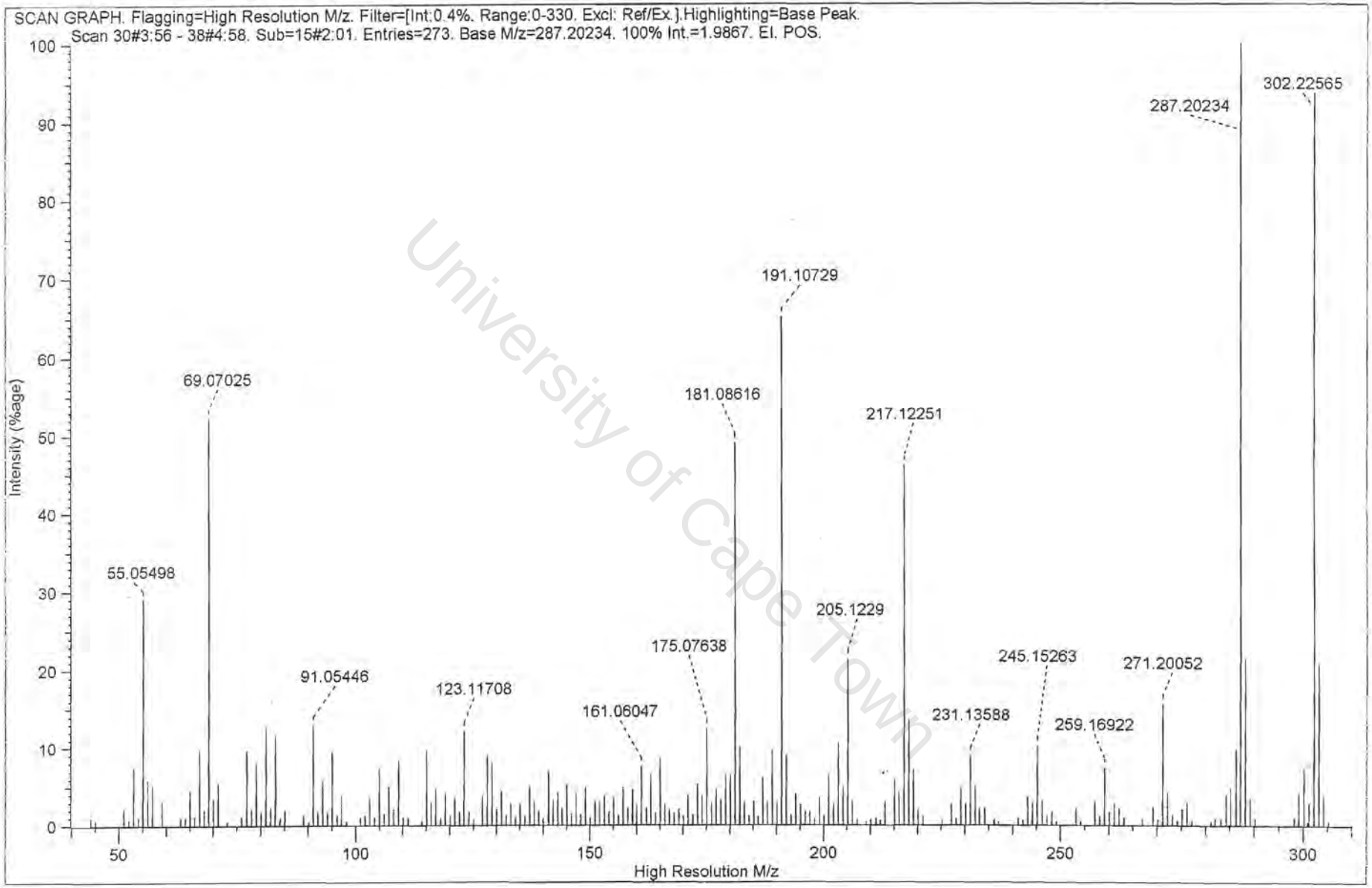

Figure A2.2.4 HREIMS spectrum of **56**

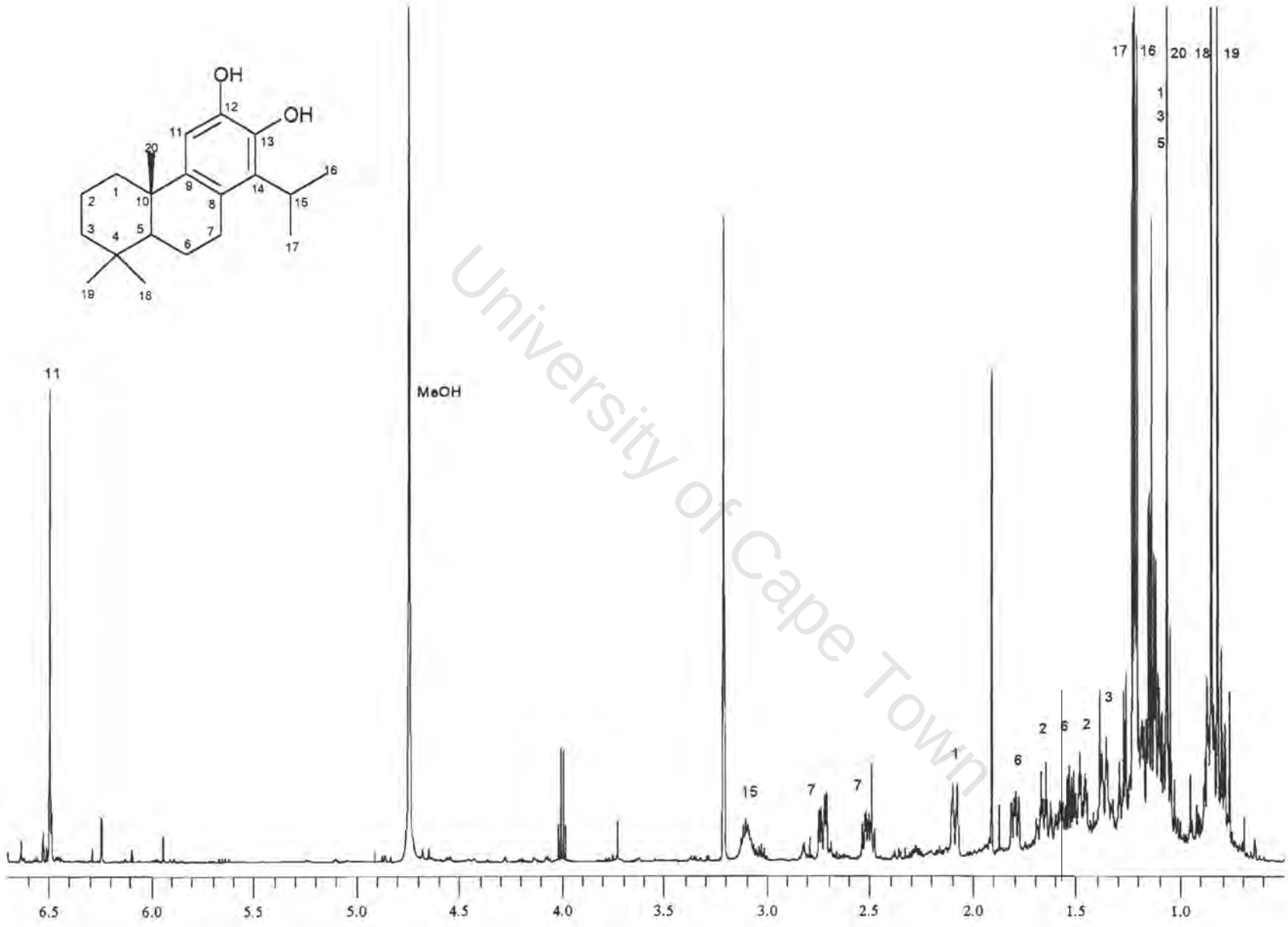

Figure A2.2.5 ^{1}H NMR spectrum of **56** in CD_3OD, 600MHz

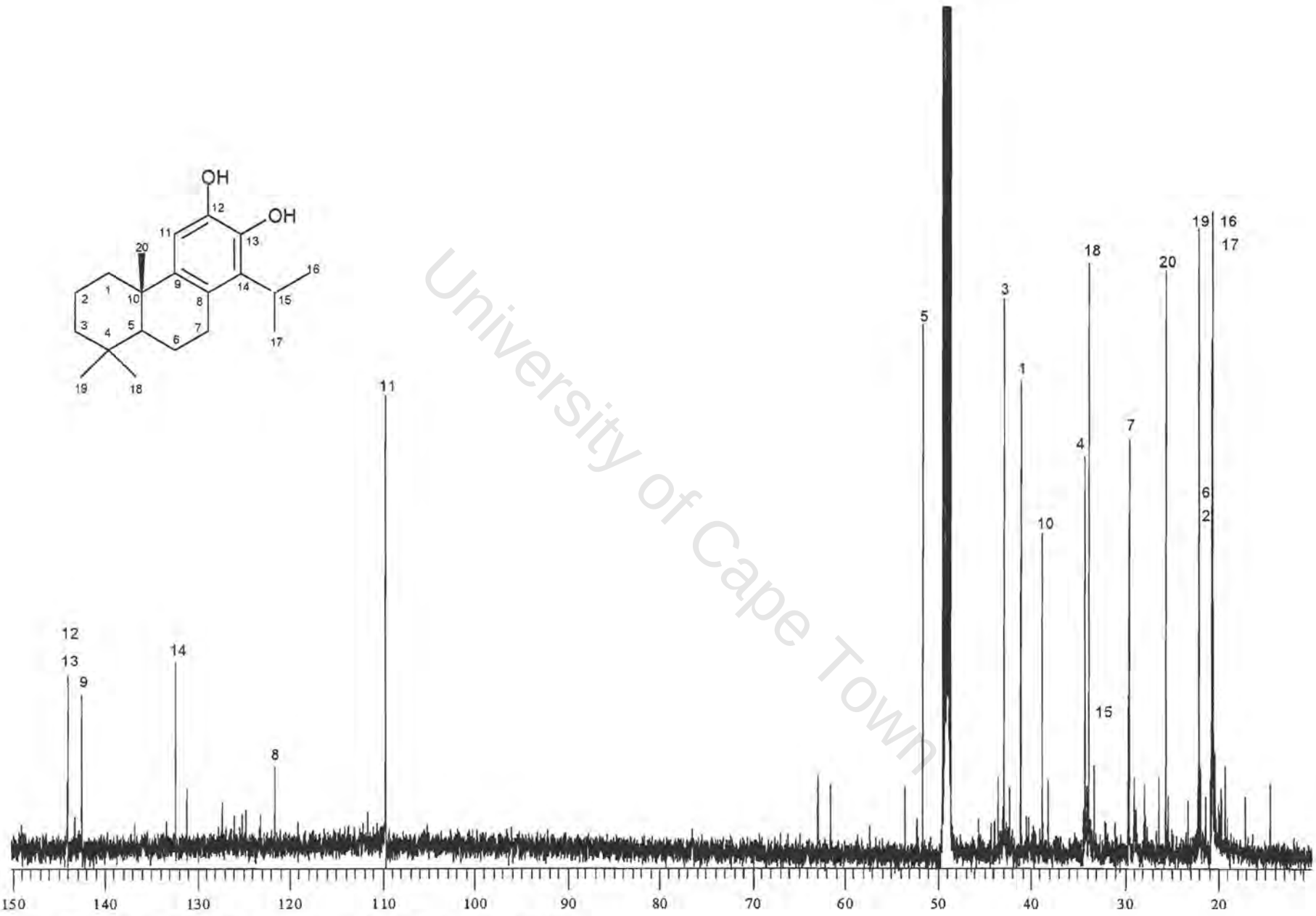

Figure A2.2.6 ^{13}C NMR spectrum of **56** in CD_3OD, 600MHz

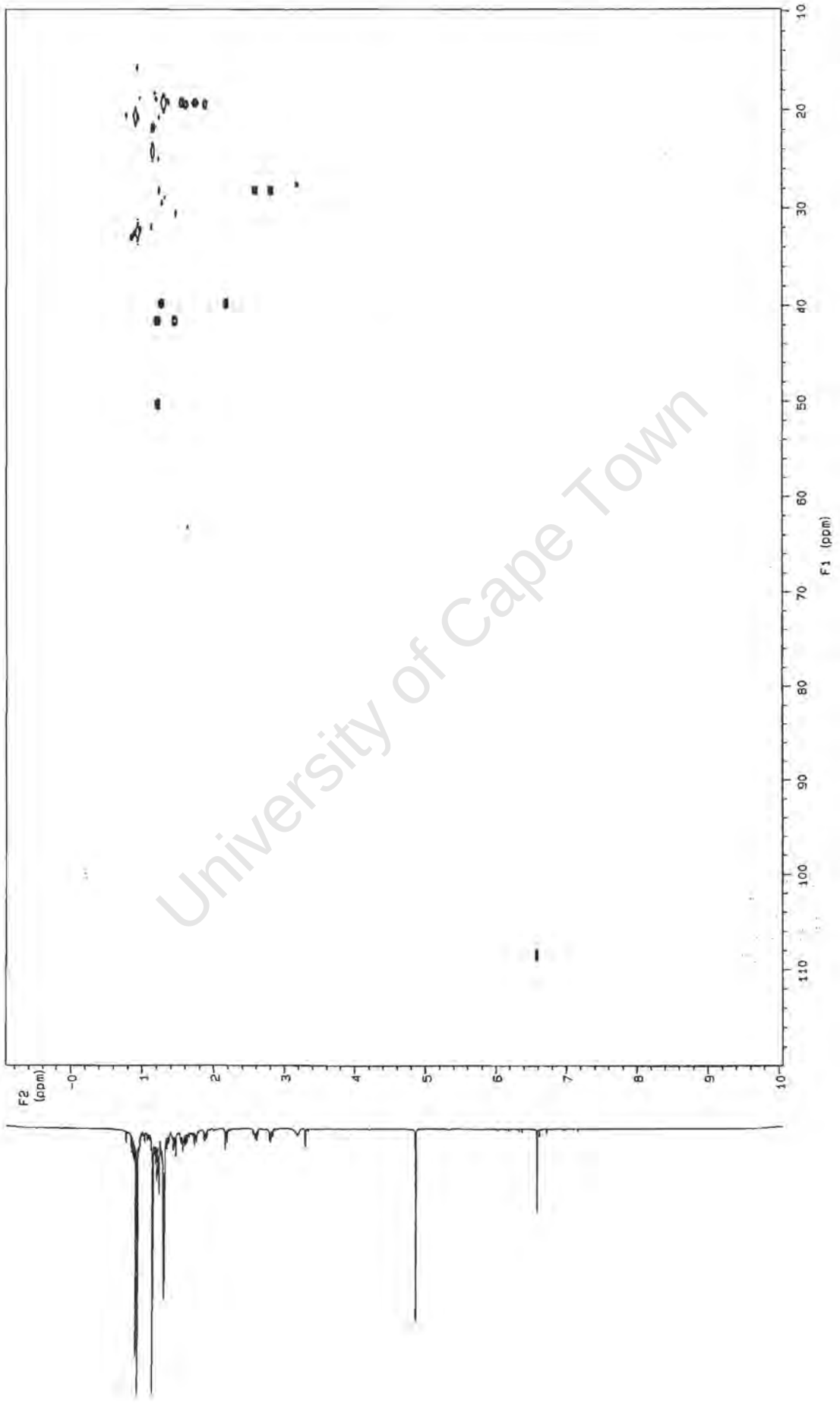

Figure A2.2.7 HSQC spectrum of **56** in CD_3OD, 500MHz

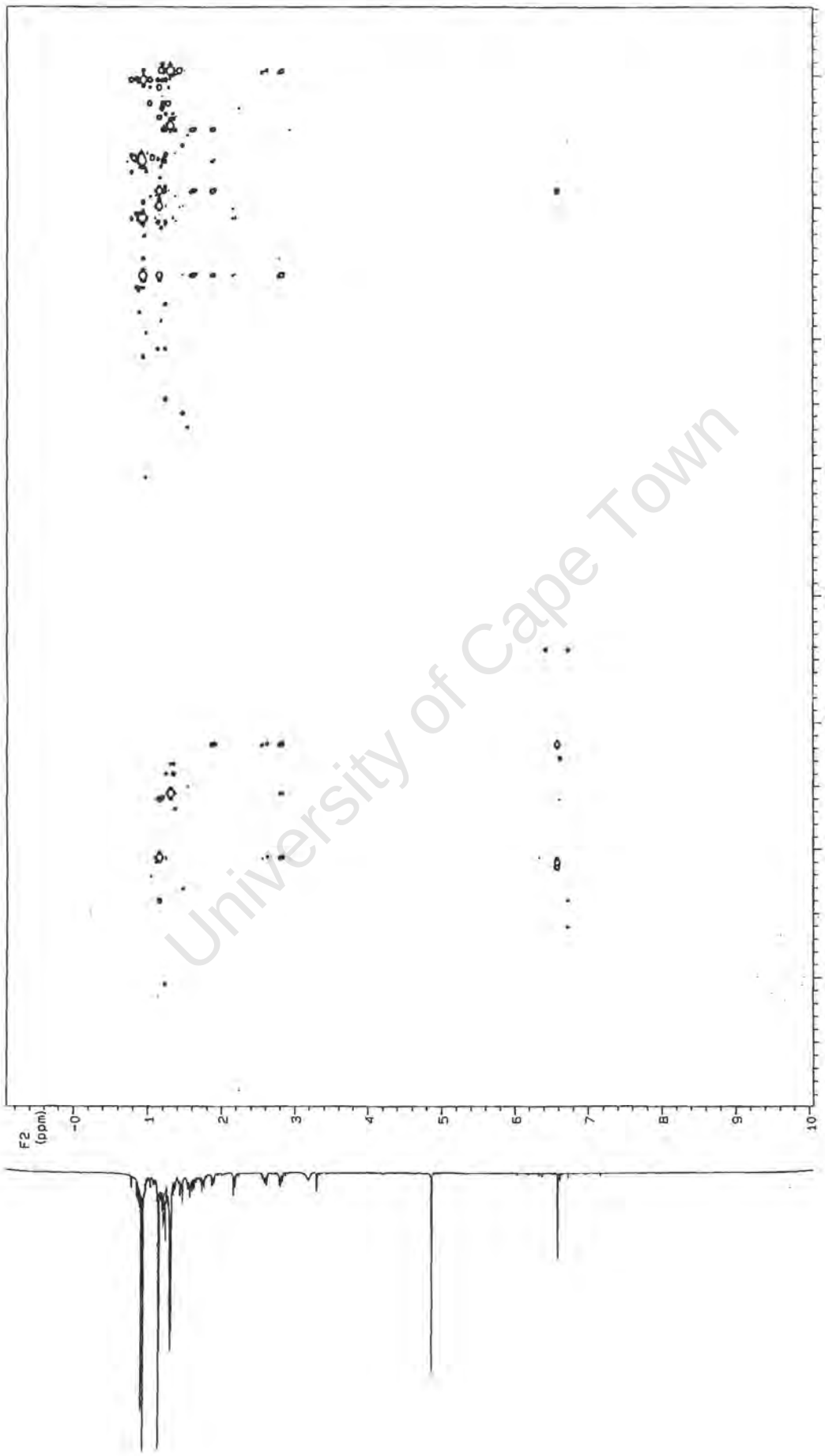

Figure A2.2.8 HMBC spectrum of **56** in CD_3OD, 500MHz

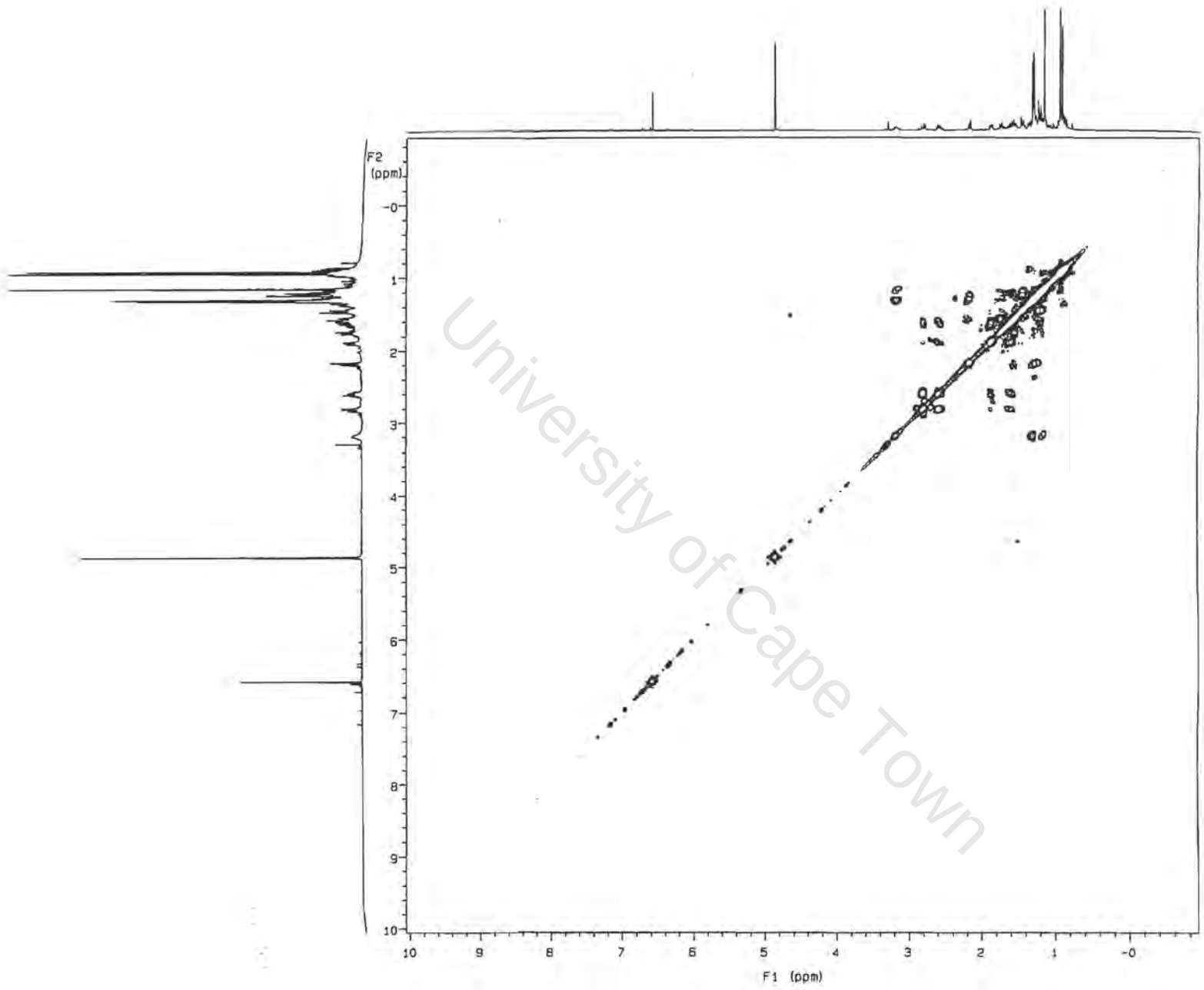

Figure A2.2.9 COSY spectrum of **56** in CD_3OD, 500MHz

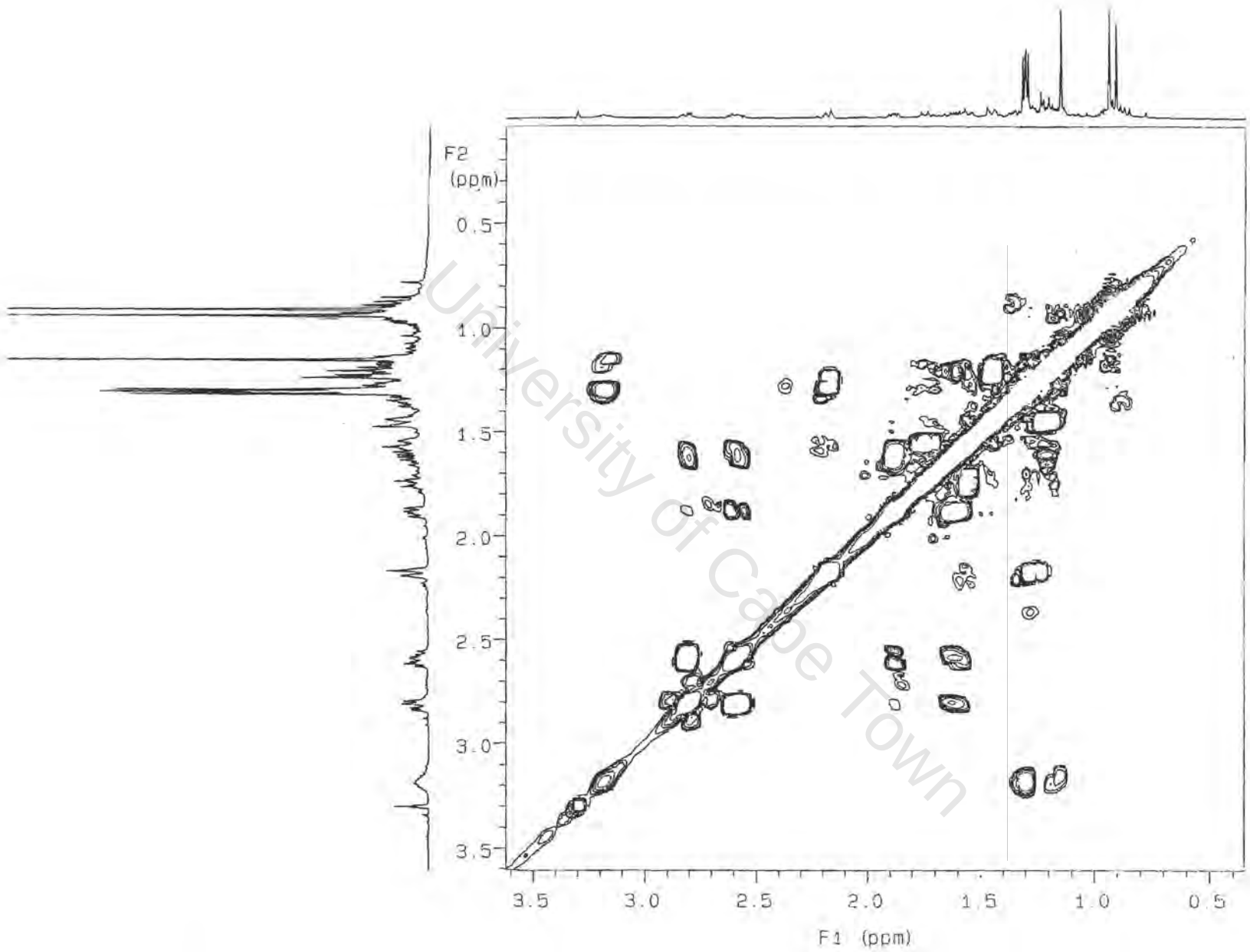

Figure A2.2.9.1 Expansion of COSY spectrum of **56** in CD_3OD, 500MHz

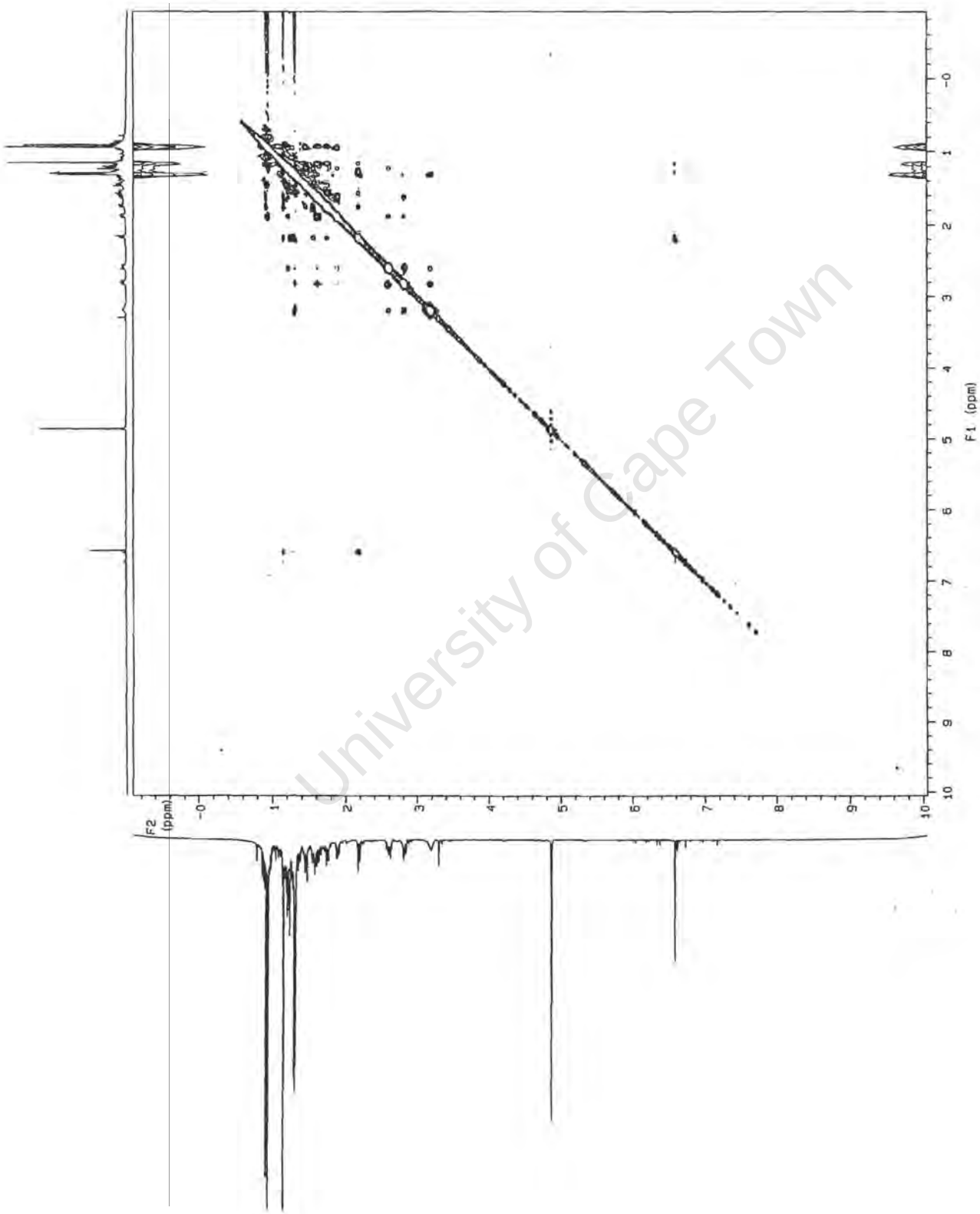

Figure A2.2.10 NOESY spectrum of **56** in CD_3OD, 500MHz

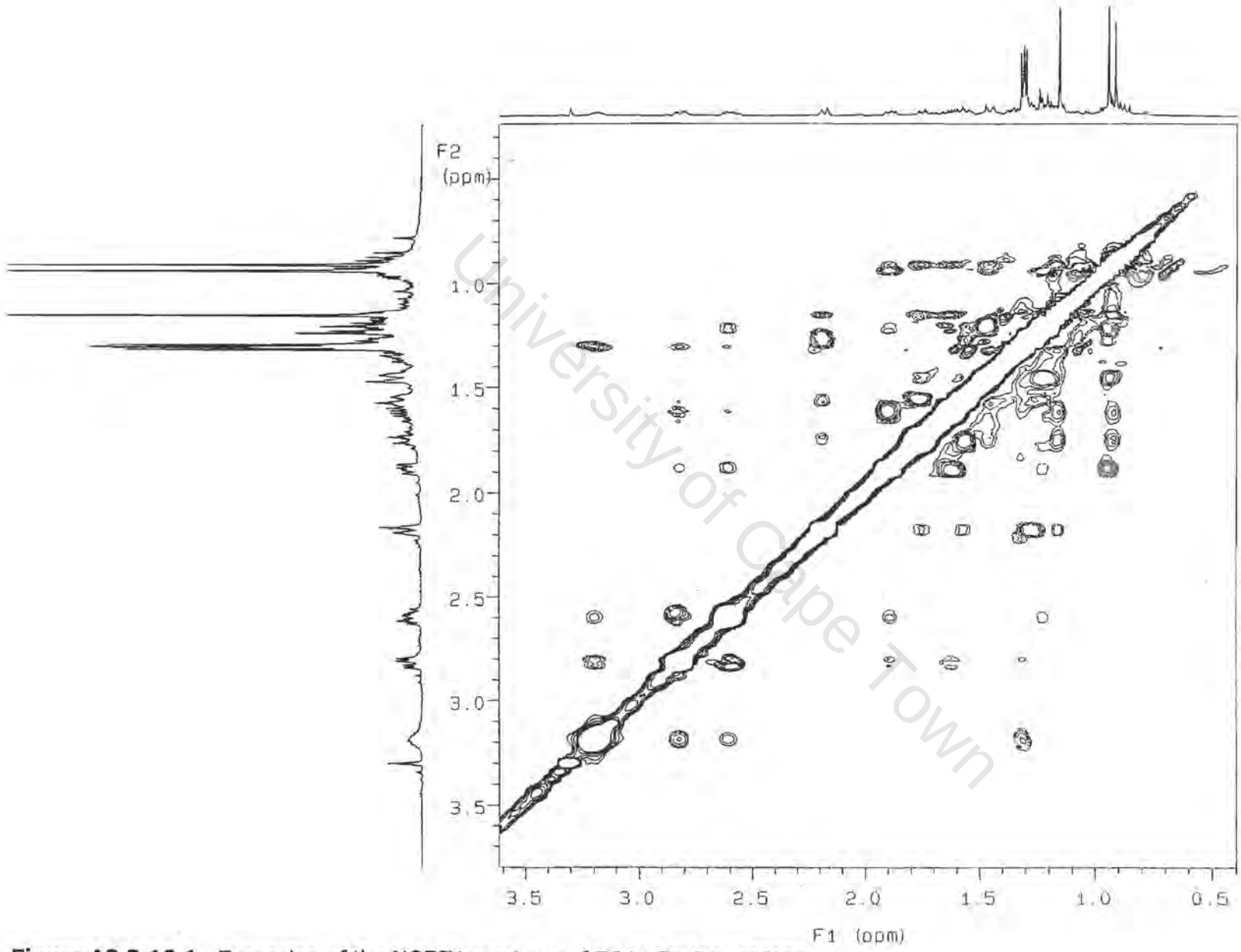

Figure A2.2.10.1 Expansion of the NOESY spectrum of **56** in CD_3OD, 500MHz

A2.3 Compound 60

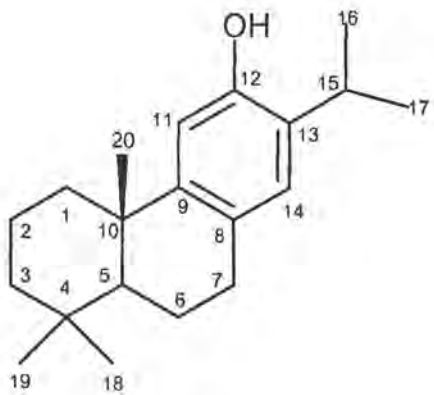

8,11,13-Abietatrien-12-ol (60)

IUPAC [14-Isopropyl-4b,8,8-trimethyl-4b,5,6,7,8,8a,9,10-octahydro-phenanthrene-3-ol]

List of spectra:

- HPLC profile
- UV absorbance
- IR
- HREIMS
- ^{1}H NMR (400MHz, $CDCl_3$)
- ^{13}C NMR (400MHz, $CDCl_3$)
- HSQC (300MHz, $CDCl_3$)
- HMBC (300MHz, $CDCl_3$)
- COSY (500MHz, $CDCl_3$)
- NOESY (500MHz, $CDCl_3$)

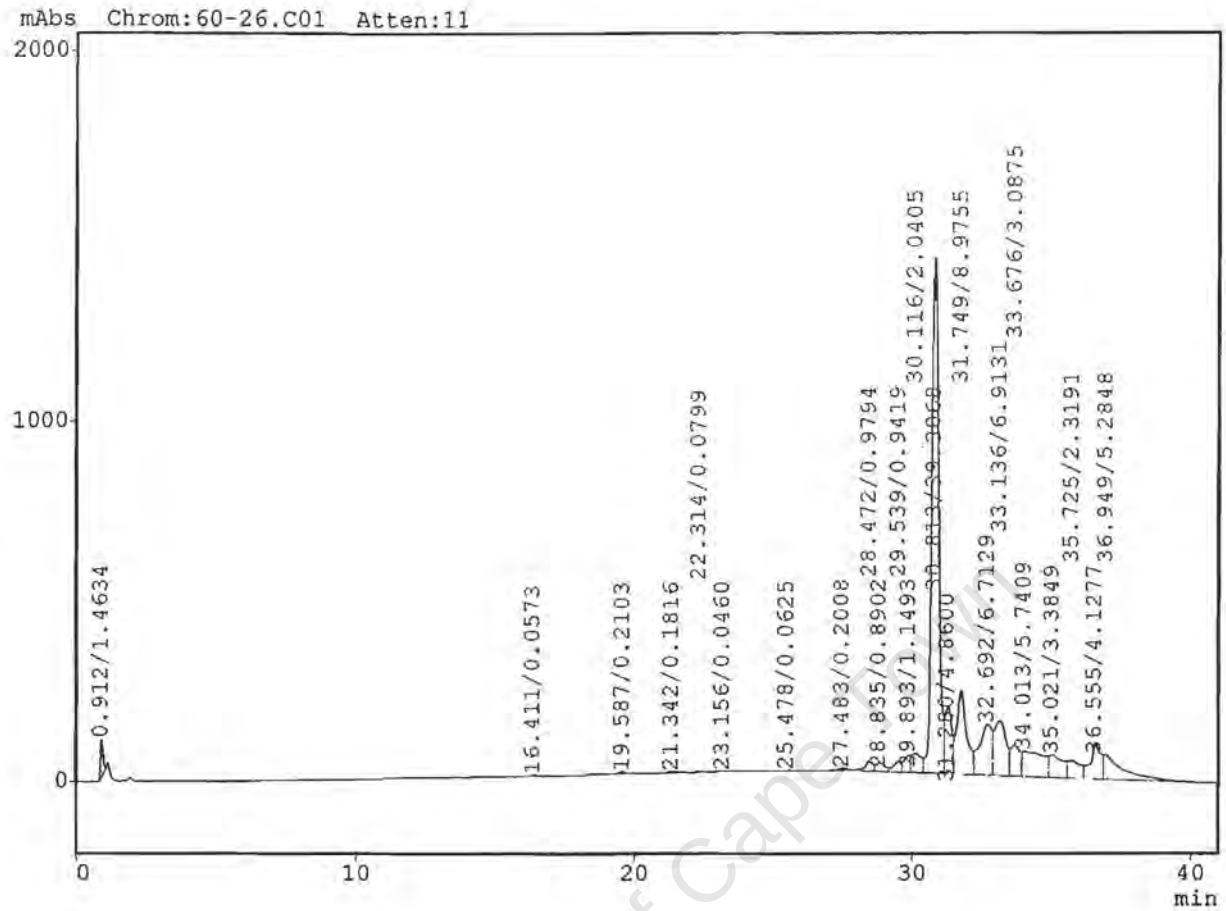

Figure A2.3.1 HPLC profile of **60** (H_2O: ACN)

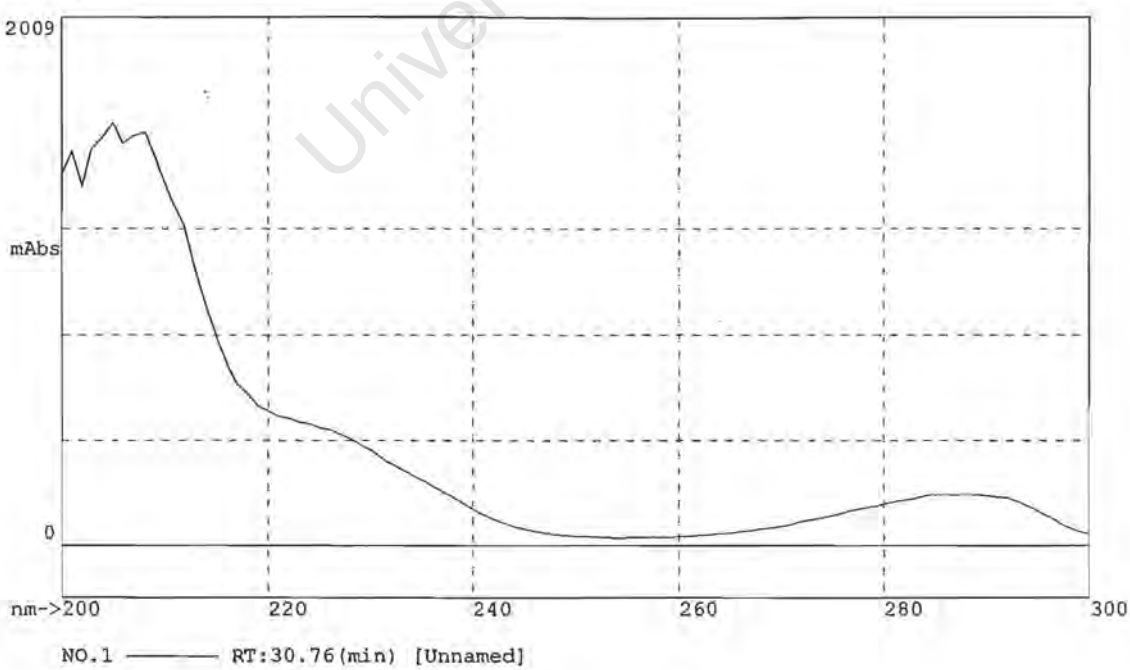

Figure A2.3.2 UV absorbance of **60** (H_2O: ACN)

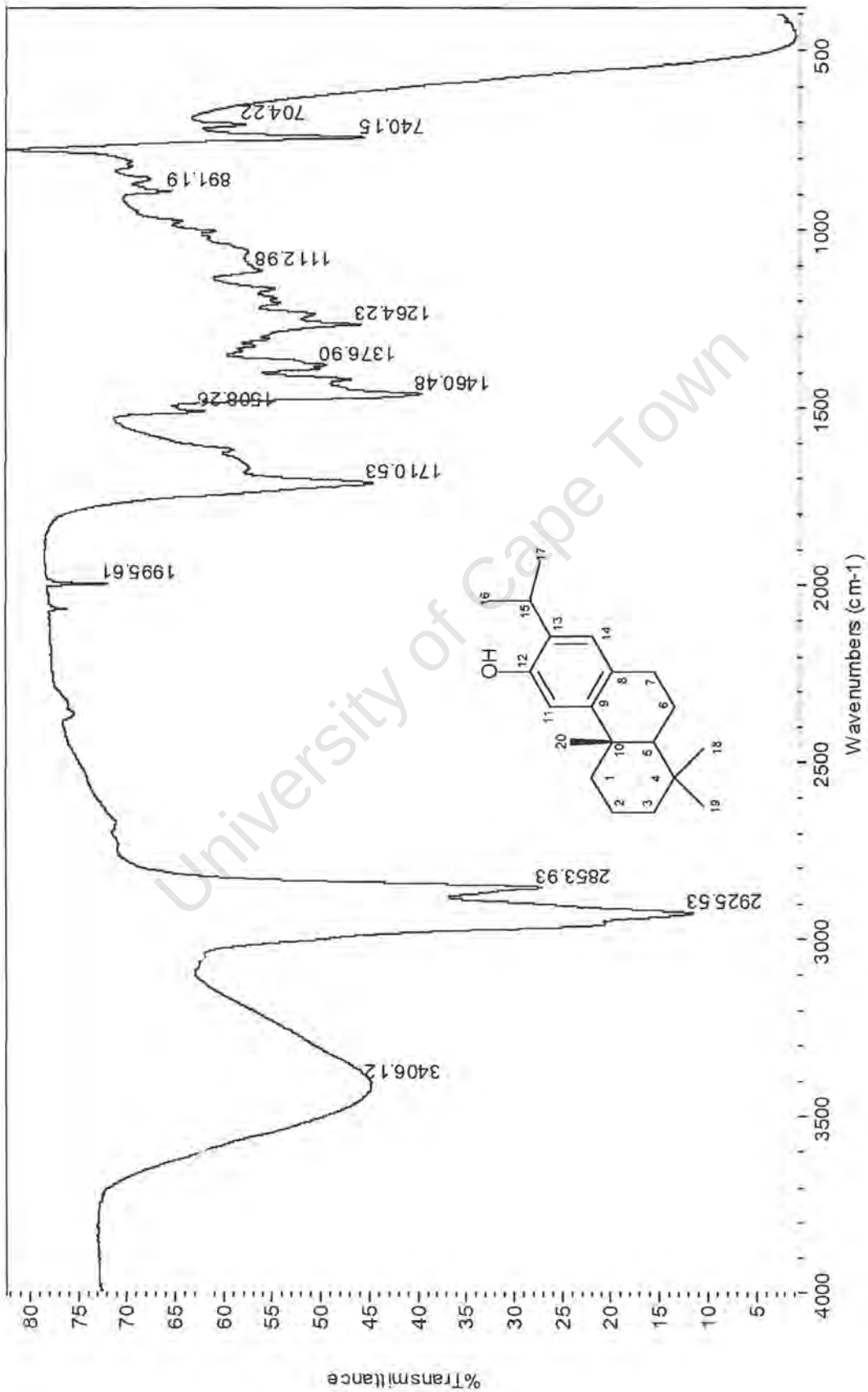

Figure A2.3.3 UV spectrum of **60**

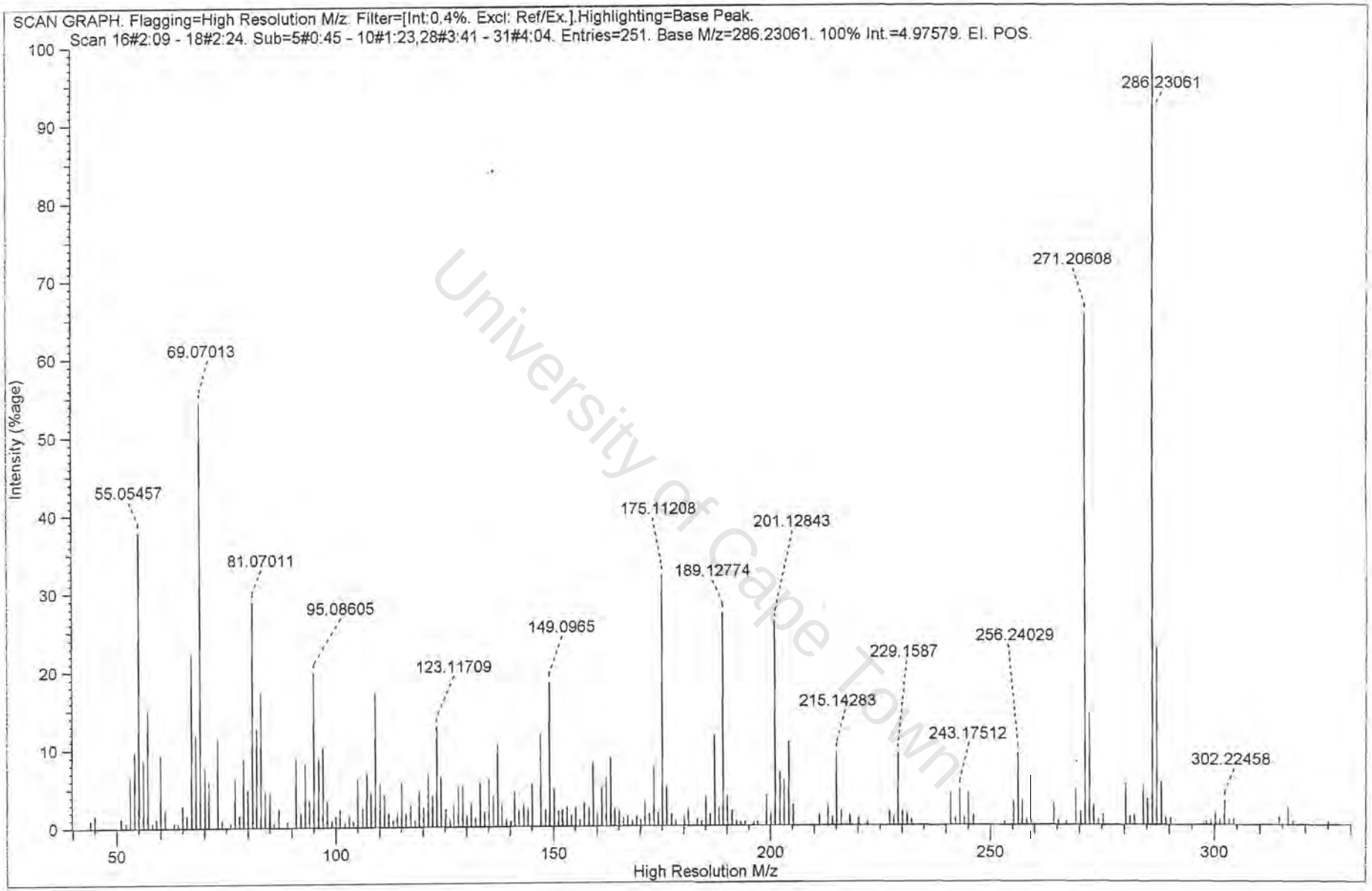

Figure A2.3.4 HREIMS spectrum of **60**

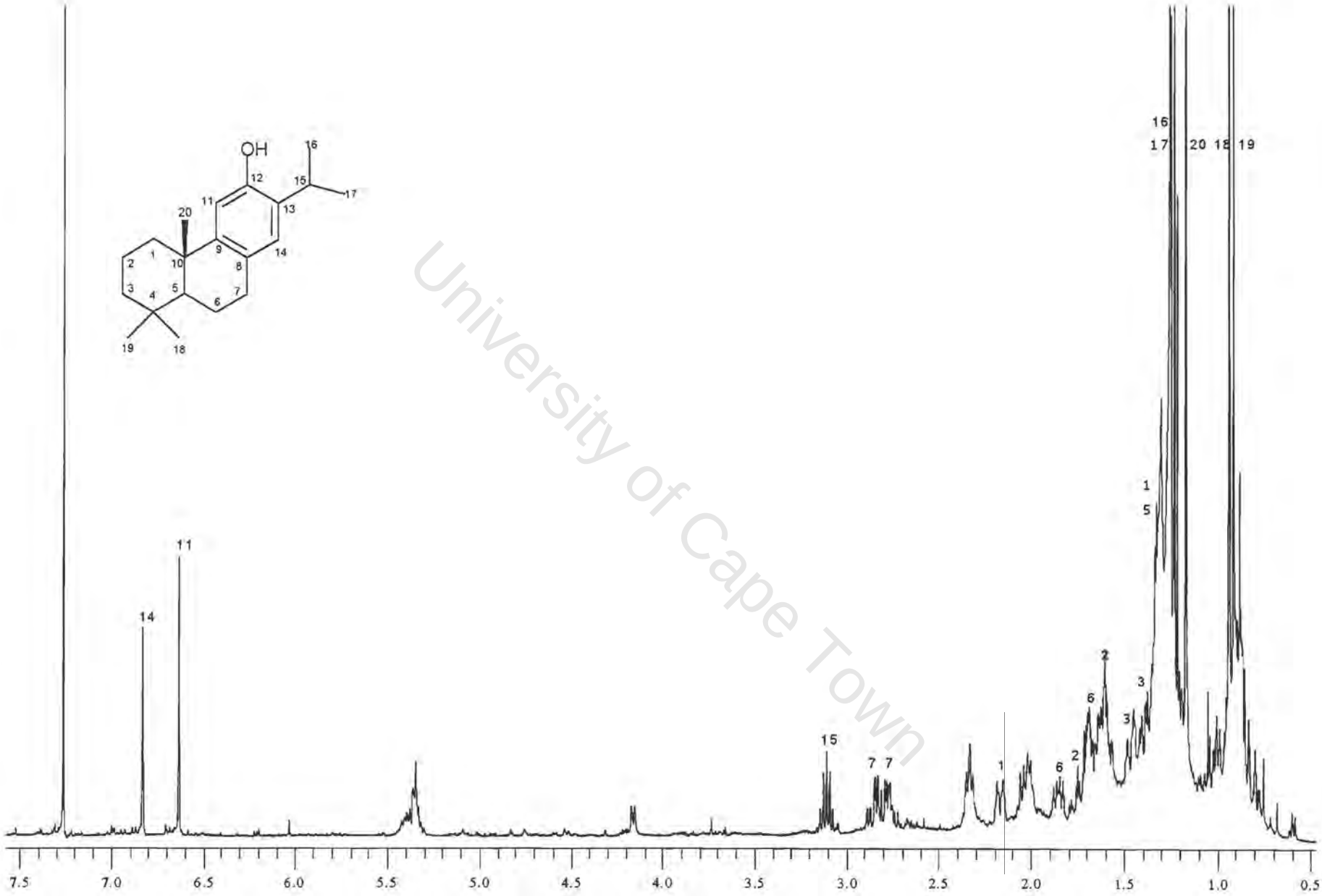

Figure A2.3.5 ^{1}H NMR spectrum of **60** in $CDCl_3$, 400MHz

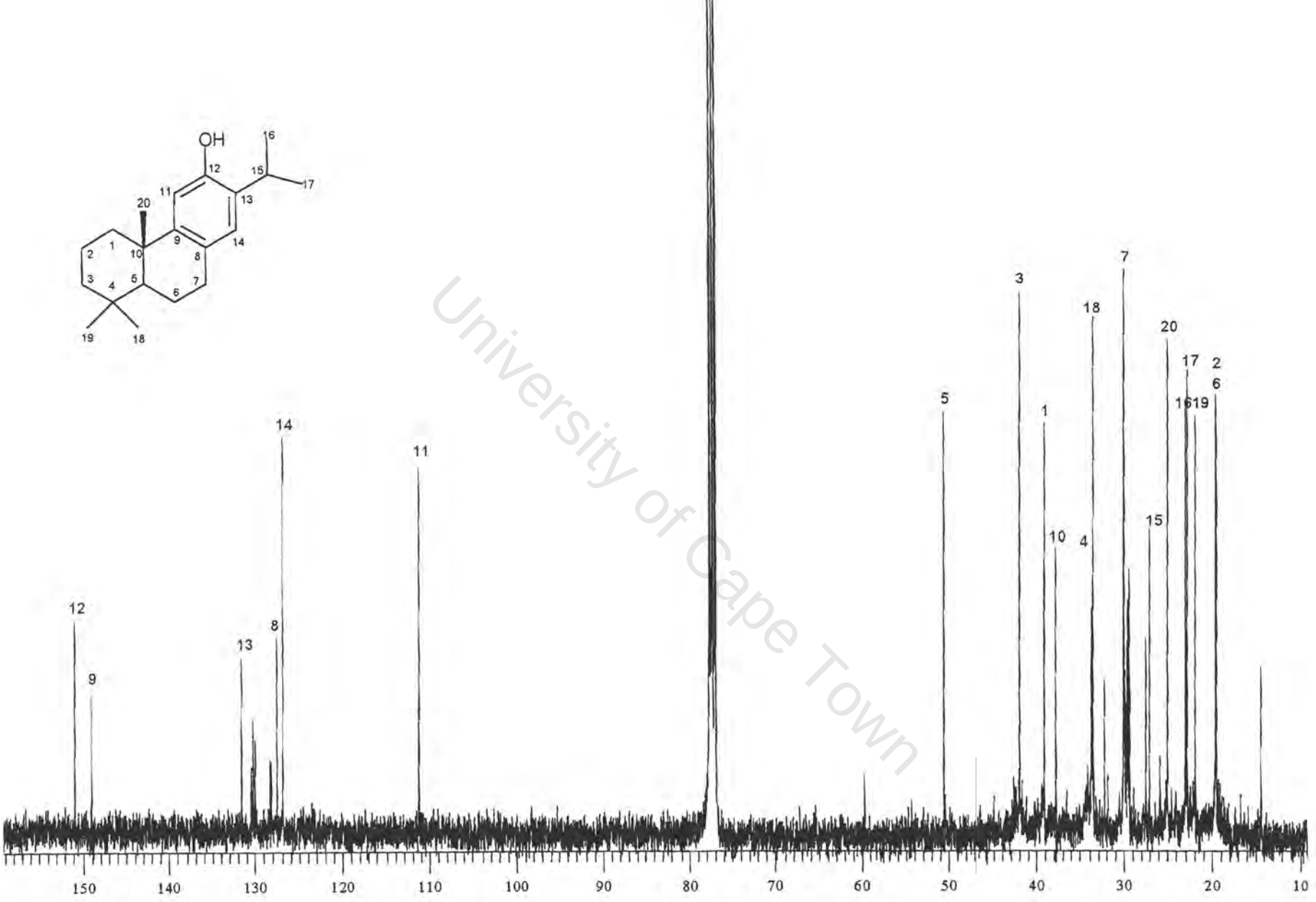

Figure A2.3.6 ^{13}C NMR spectrum of **60** in $CDCl_3$, 400MHz

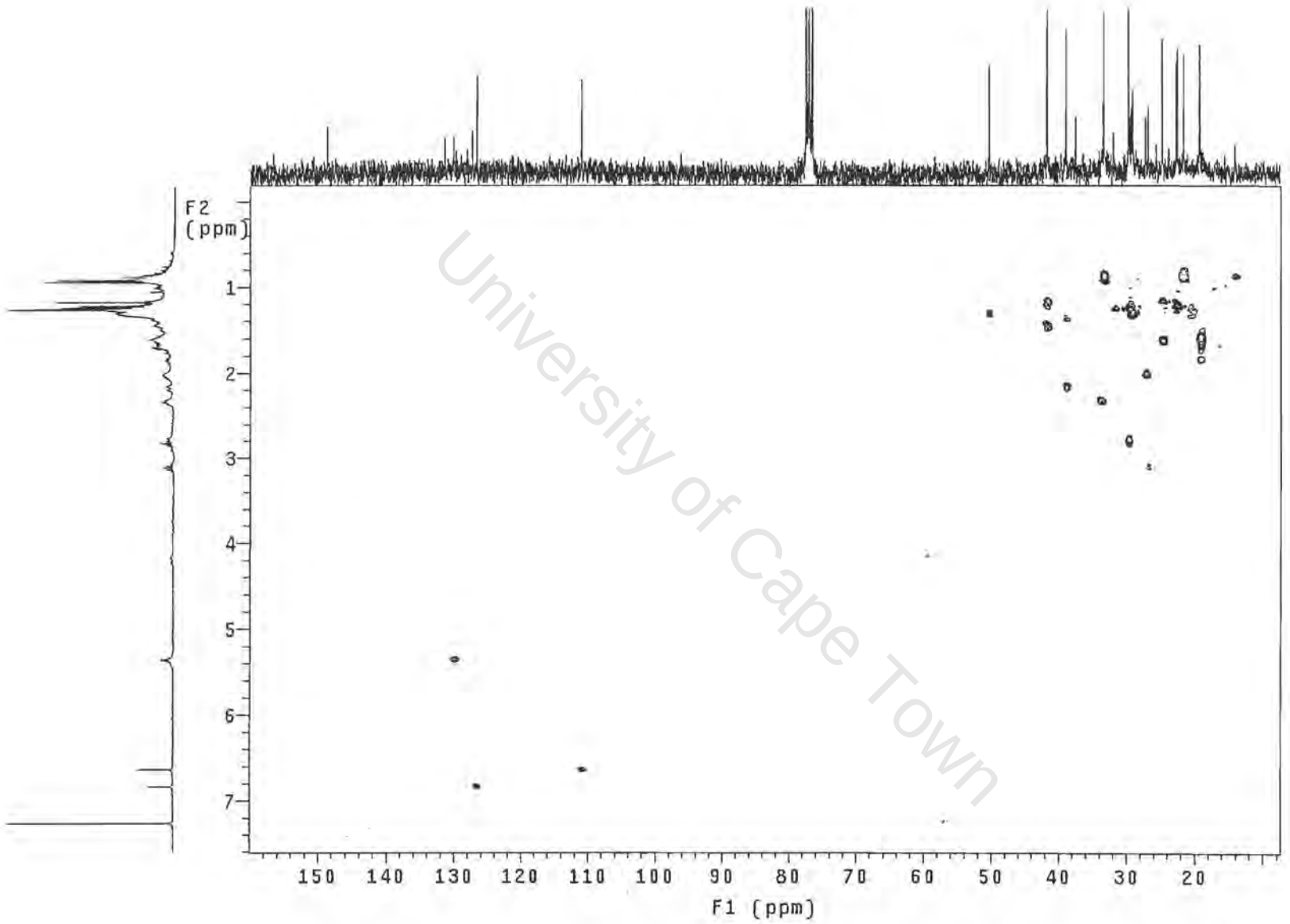

Figure A2.3.7 HSQC spectrum of **60** in $CDCl_3$, 300MHz

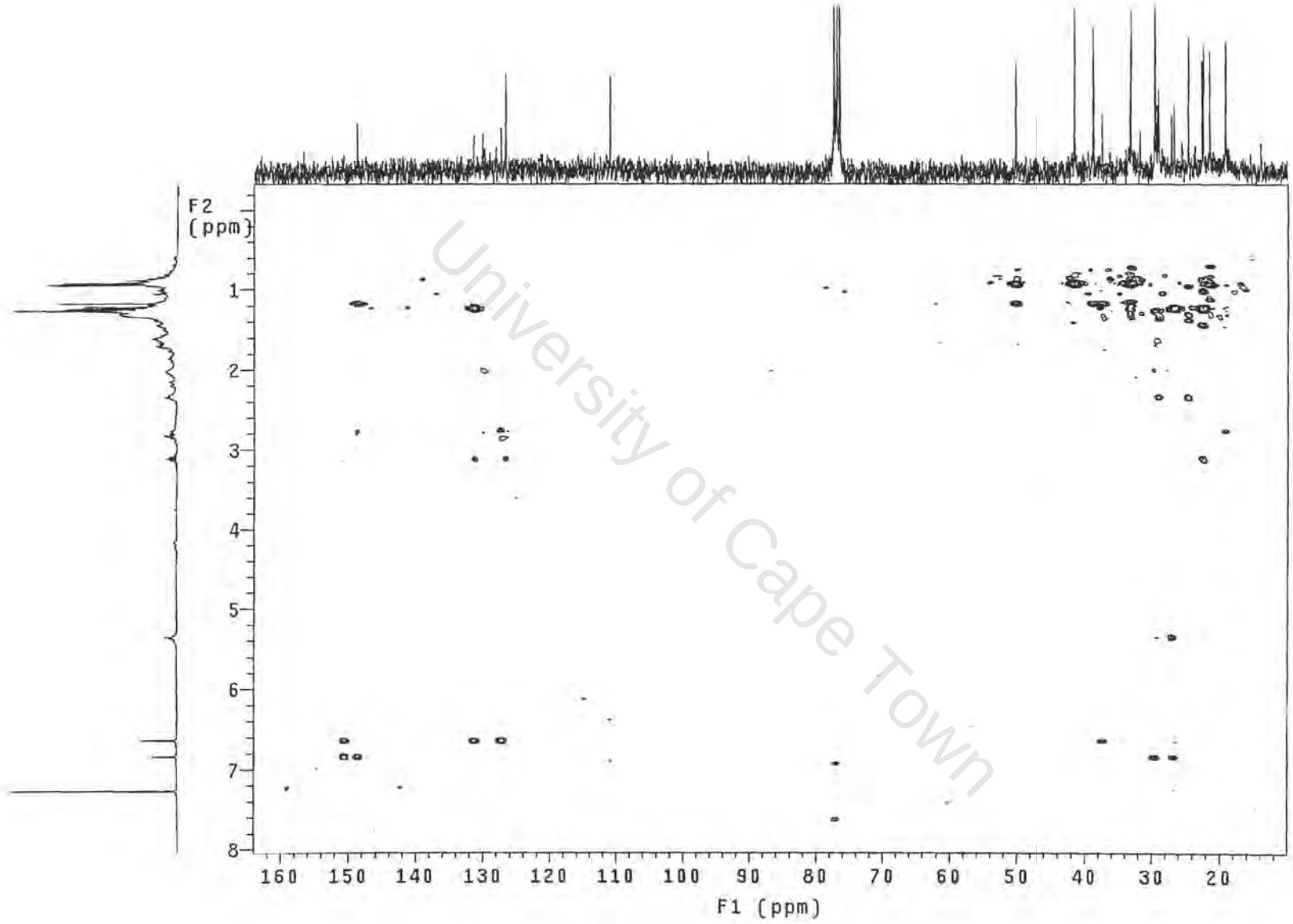

Figure A2.3.8 HMBC spectrum of **60** in $CDCl_3$, 300MHz

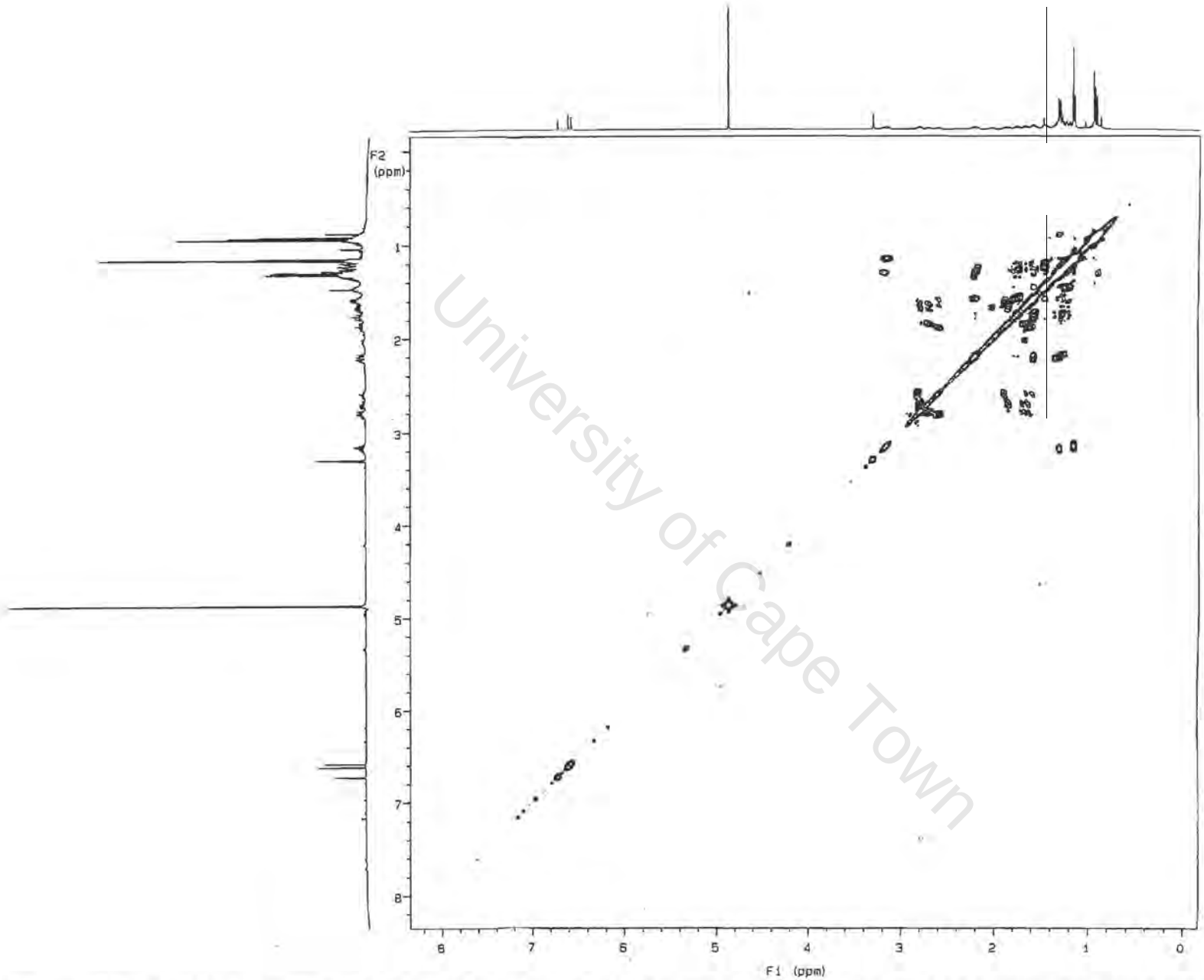

Figure A2.3.9 COSY spectrum of **60** in $CDCl_3$, 500MHz (The sample of **60** used for the COSY experiment was not as pure as the one for the 1D NMR, however the impurities can easily be identified by comparing the 1D and COSY spectra)

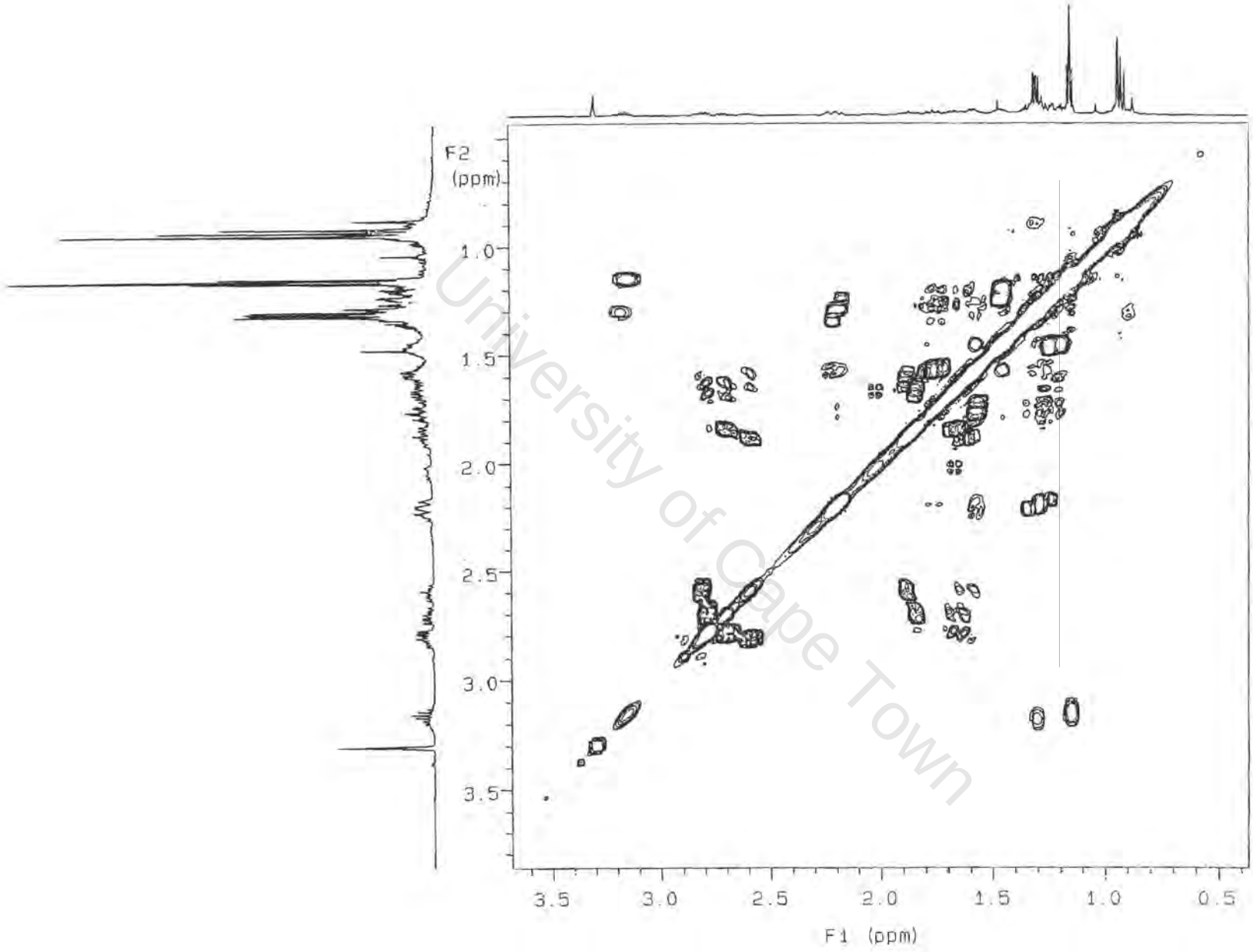

Figure A2.3.9.1 Expansion of the COSY spectrum of **60** in $CDCl_3$, 500MHz

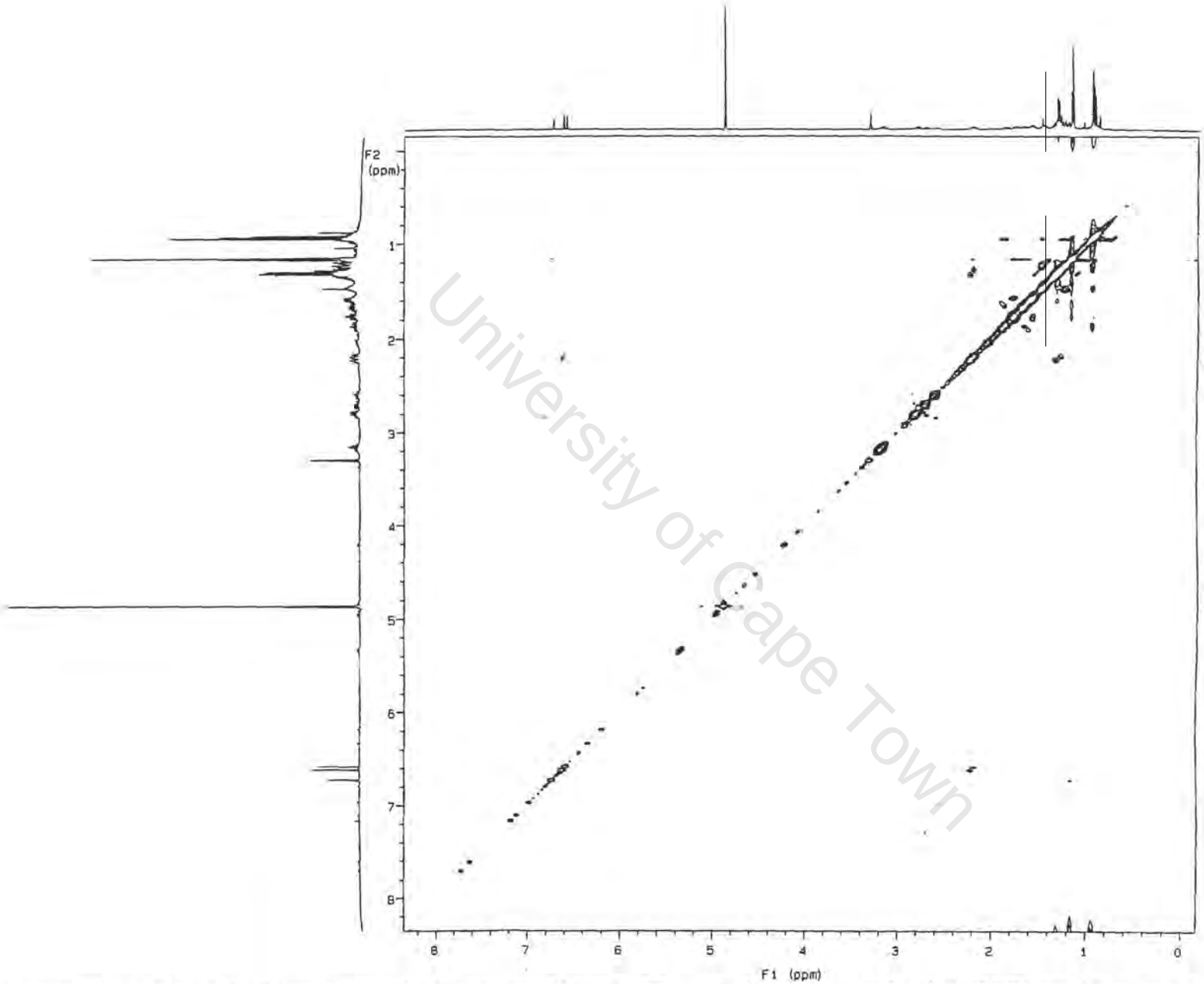

Figure A2.3.10 NOESY spectrum of **60** in $CDCl_3$, 500MHz. (The sample of **60** used for the NOESY spectrum was not as pure as the one used for the 1D NMR, however the impurities can easily be identified by comparing the 1D and COSY spectra)

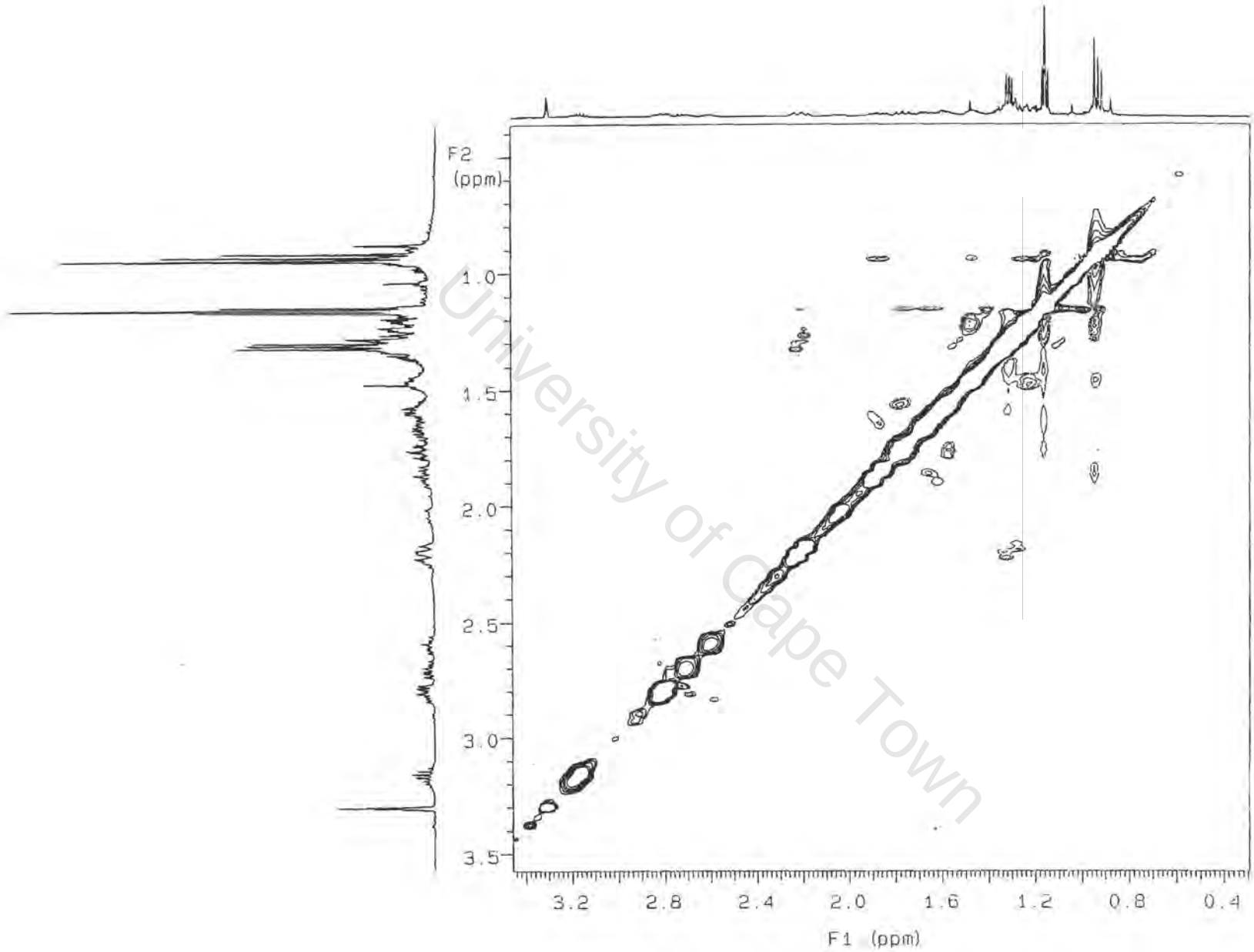

Figure A2.3.10.1 Expansion of the NOESY spectrum of **60** in $CDCl_3$, 500MHz

A2.4 Totarol

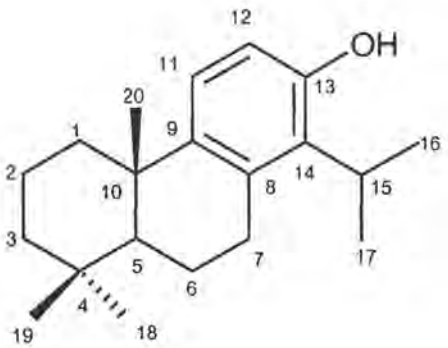

8,11,13-Totaratrien-13-ol (Totarol)

IUPAC [14-Isopropyl-4b,8,8-trimethyl-4b,5,6,7,8,8a,9,10-octahydro-phenanthrene-2-ol]

List of spectra:

- HPLC profile
- IR
- ^{1}H NMR (400MHz, $CDCl_3$)
- ^{13}C NMR (400MHz, $CDCl_3$)
- HSQC (400MHz, $CDCl_3$)
- COSY (400MHz, $CDCl_3$)
- NOESY (400MHz, $CDCl_3$)

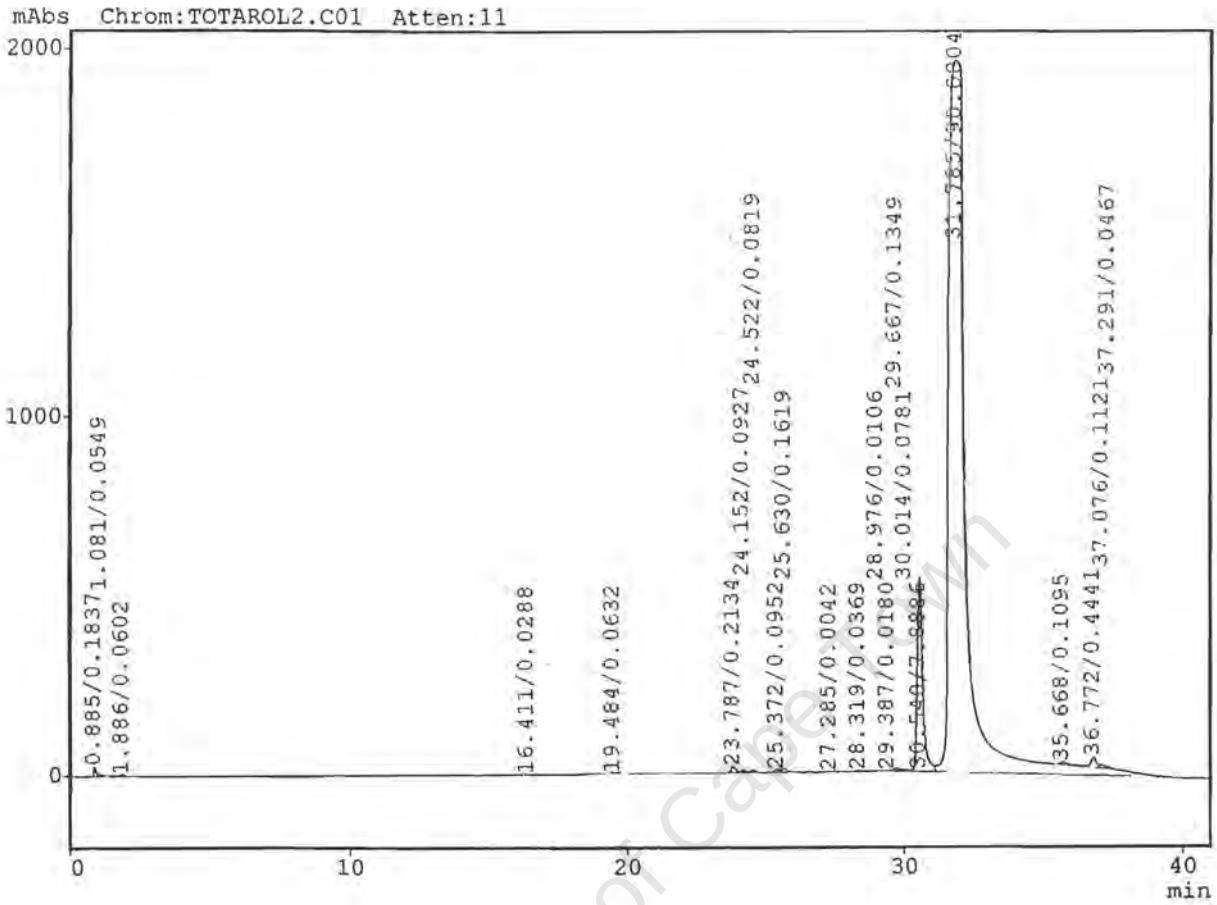

Figure A2.4.1 HPLC profile of totarol (H_2O: ACN)

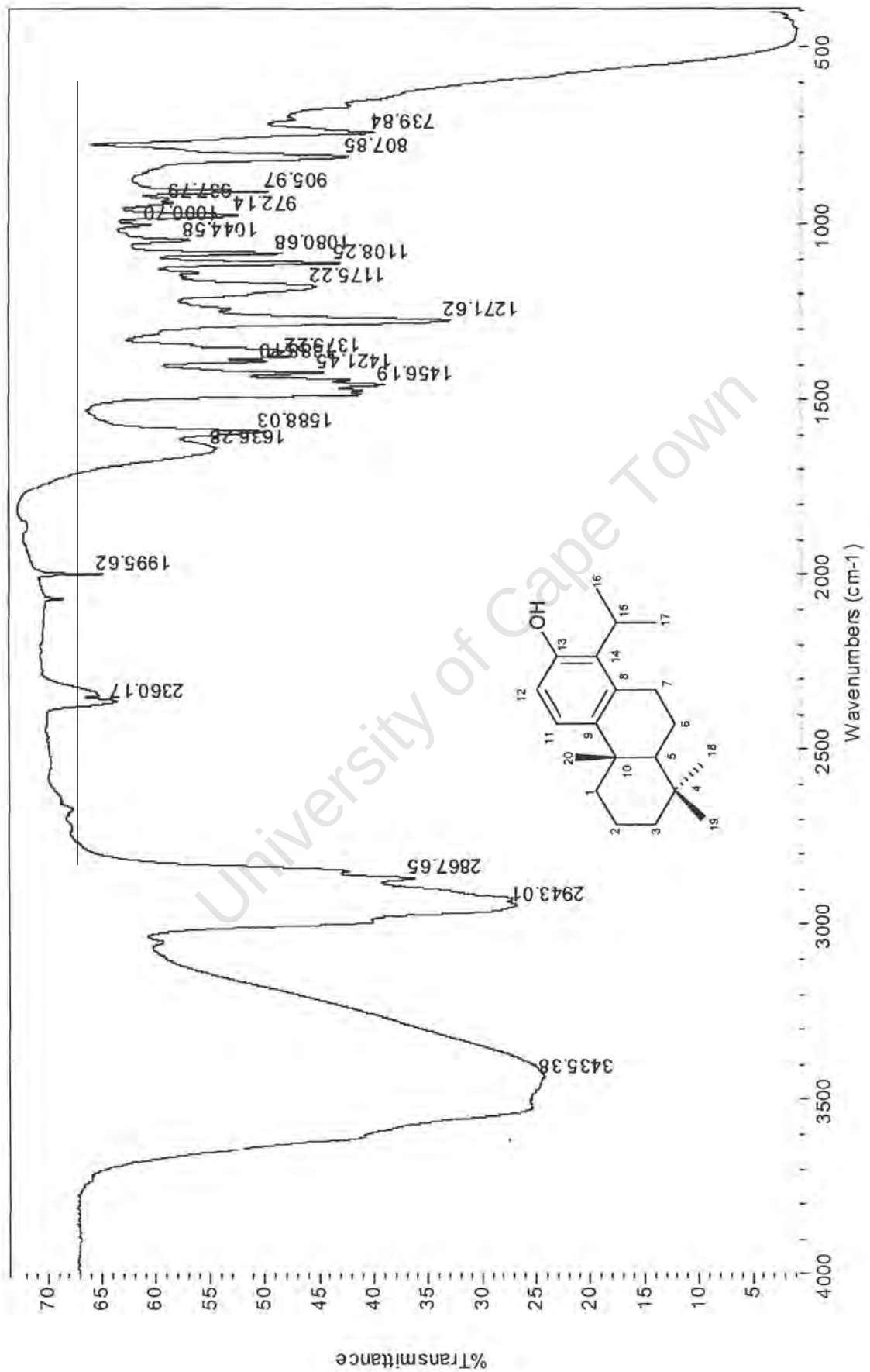

Figure A2.4.2 IR spectrum of totarol

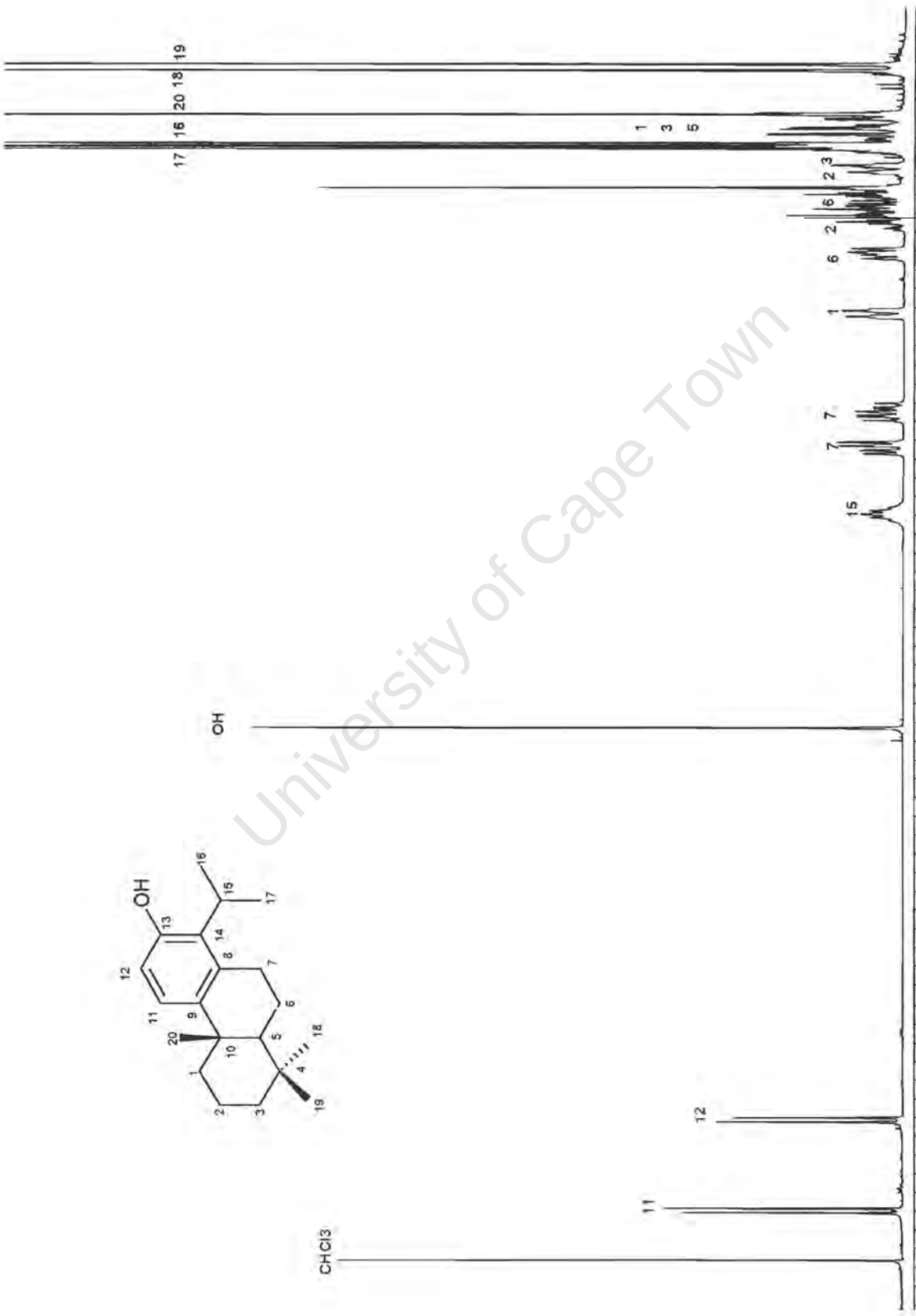

Figure A2.4.3 ^{1}H NMR spectrum of totarol in $CDCl_3$, 400MHz

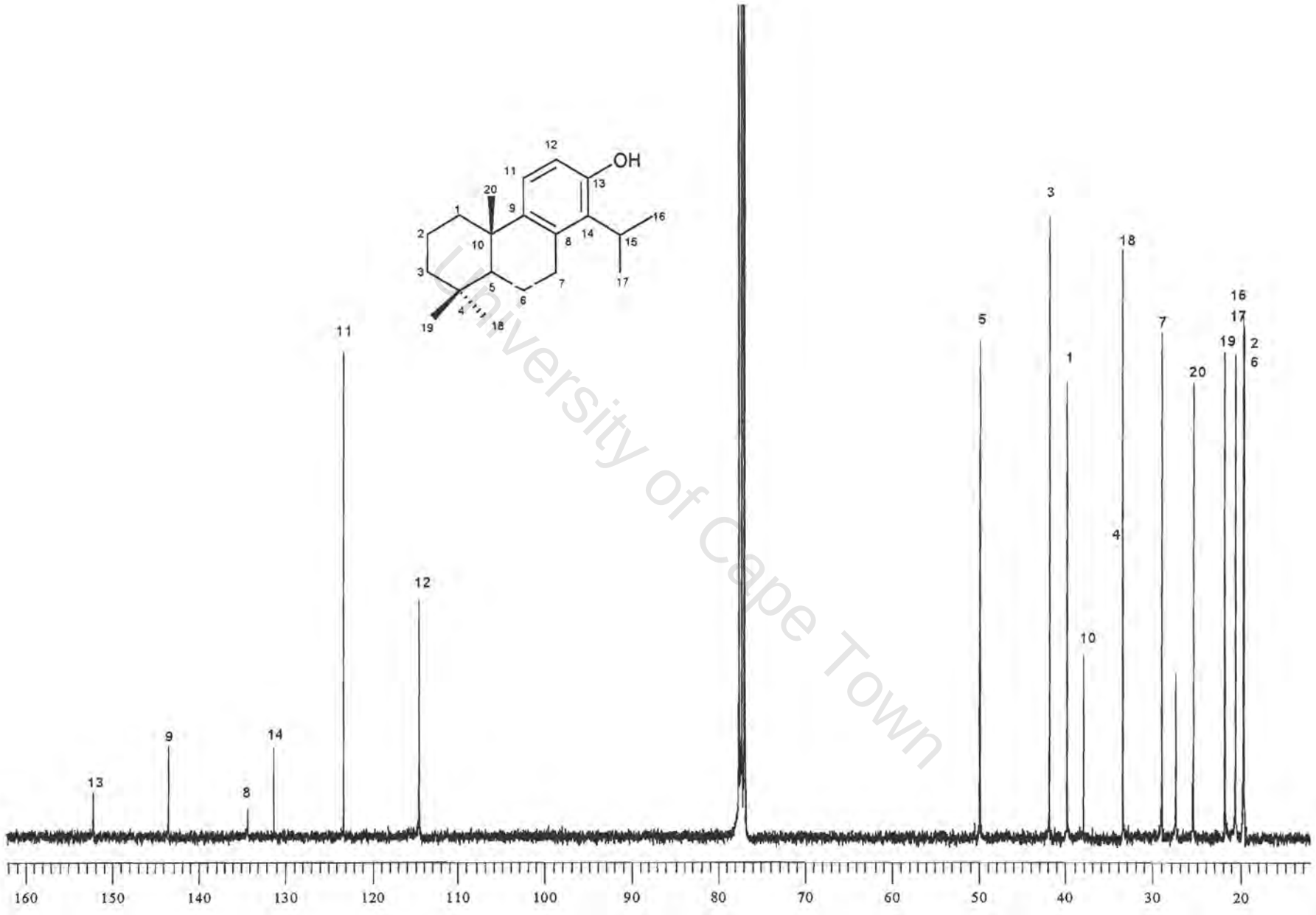

Figure A2.4.4 ^{13}C NMR spectrum of totarol in $CDCl_3$, 400MHz

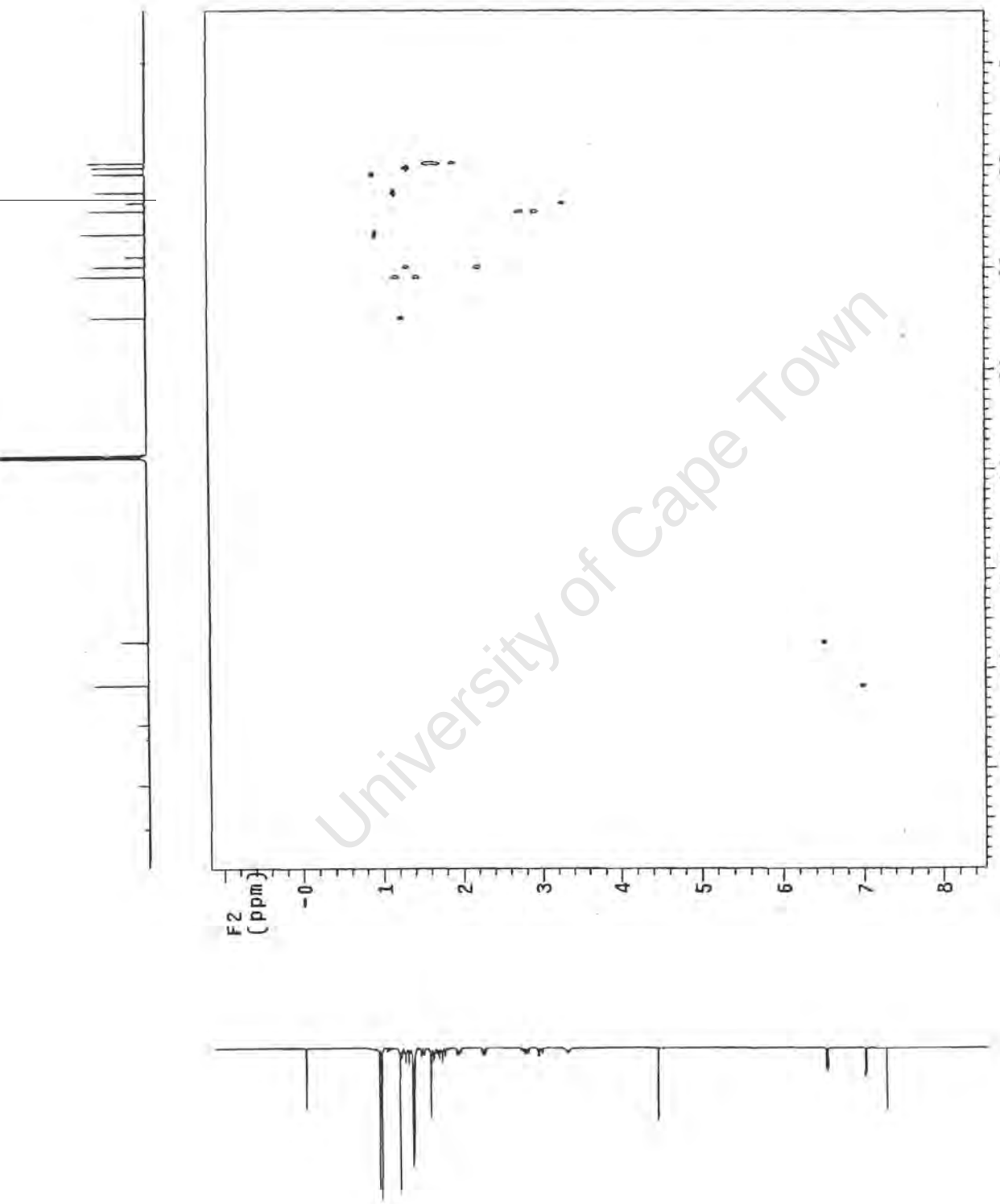

Figure A2.4.5 HSQC spectrum of totarol in $CDCl_3$, 400MHz

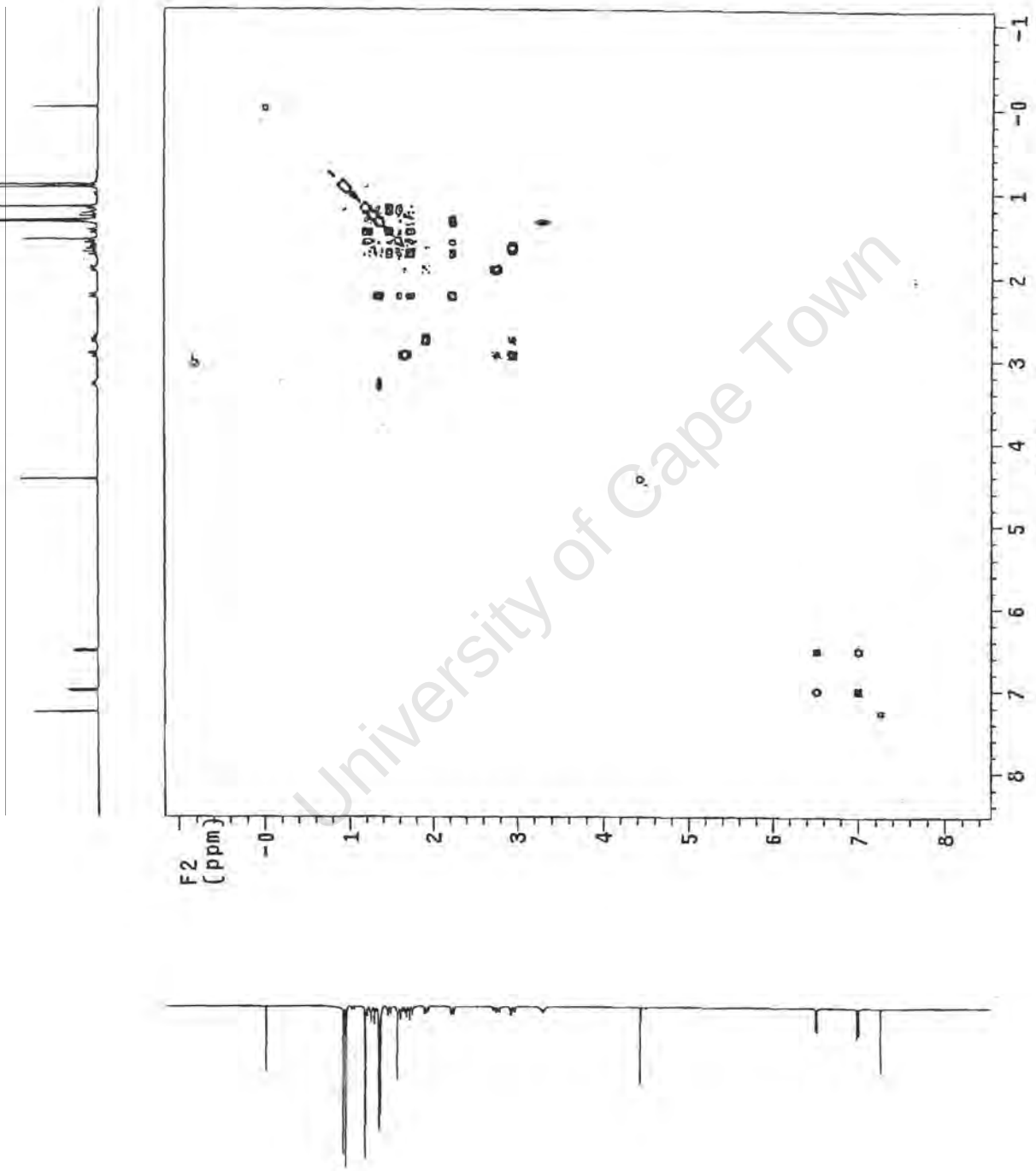

Figure A2.4.6 COSY spectrum of totarol in $CDCl_3$

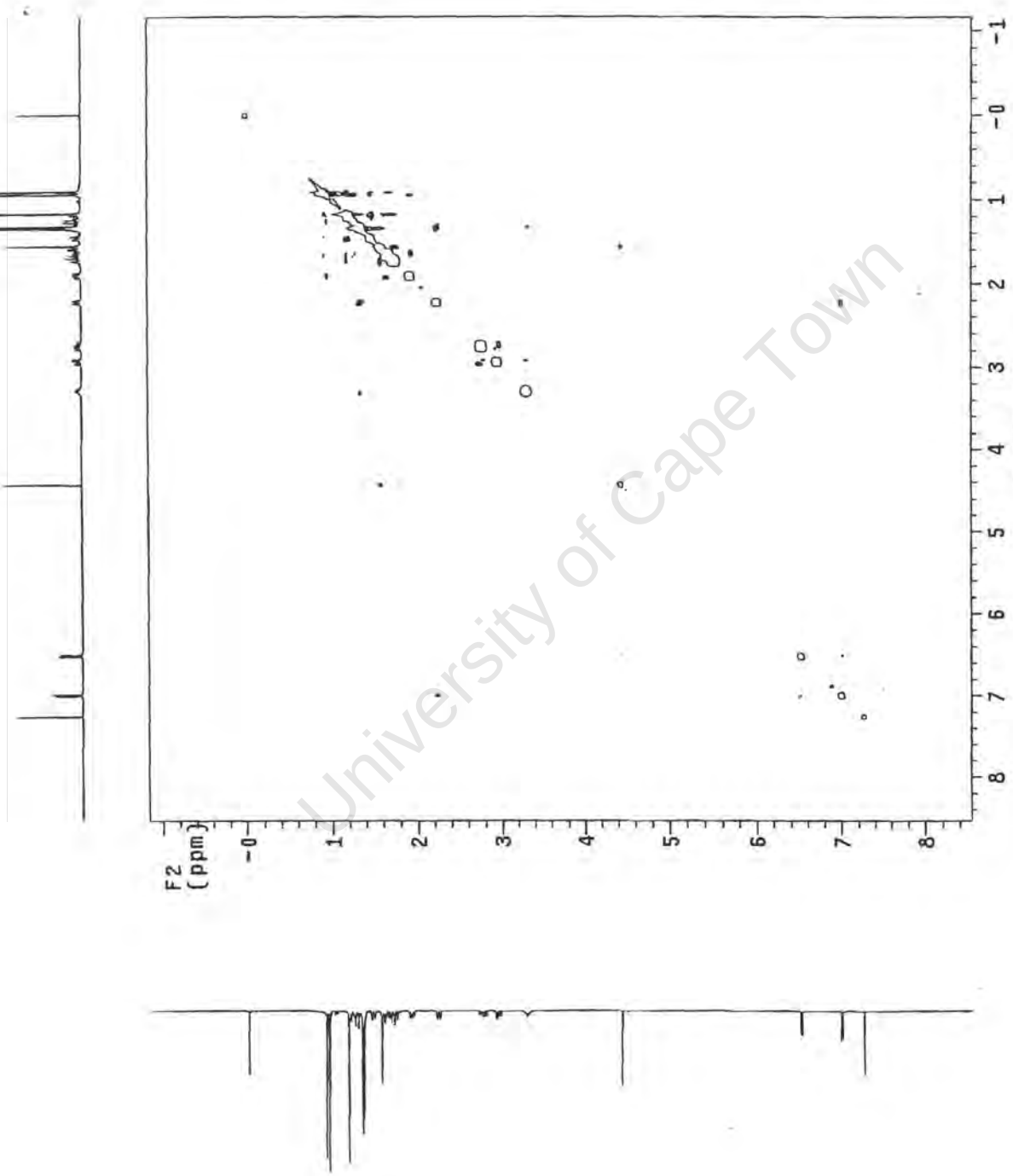

Figure A2.4.7 NOESY spectrum of totarol in $CDCl_3$, 400MHz

A2.5 Epoxide intermediate (1)

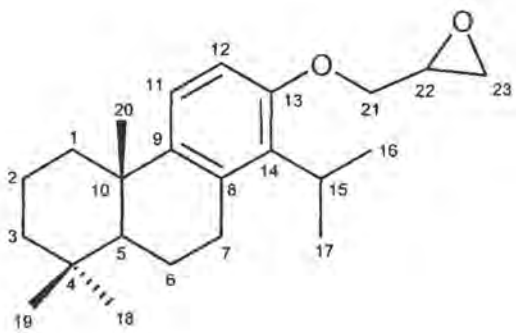

Epoxide intermediate (1)

IUPAC [2-(1-Isopropyl-4b,8,8,-trimethyl-4b,5,6,7,8,8a,9,10-octahydro-phenanthren-2-yloxymethyl-oxirane]

List of spectra:

- HREIMS
- ^{1}H NMR (400MHz, $CDCl_3$)
- ^{13}C NMR (400MHz, $CDCl_3$)
- HSQC (300MHz, $CDCl_3$)
- HMBC (300MHz, $CDCl_3$)
- COSY (300MHz, $CDCl_3$)

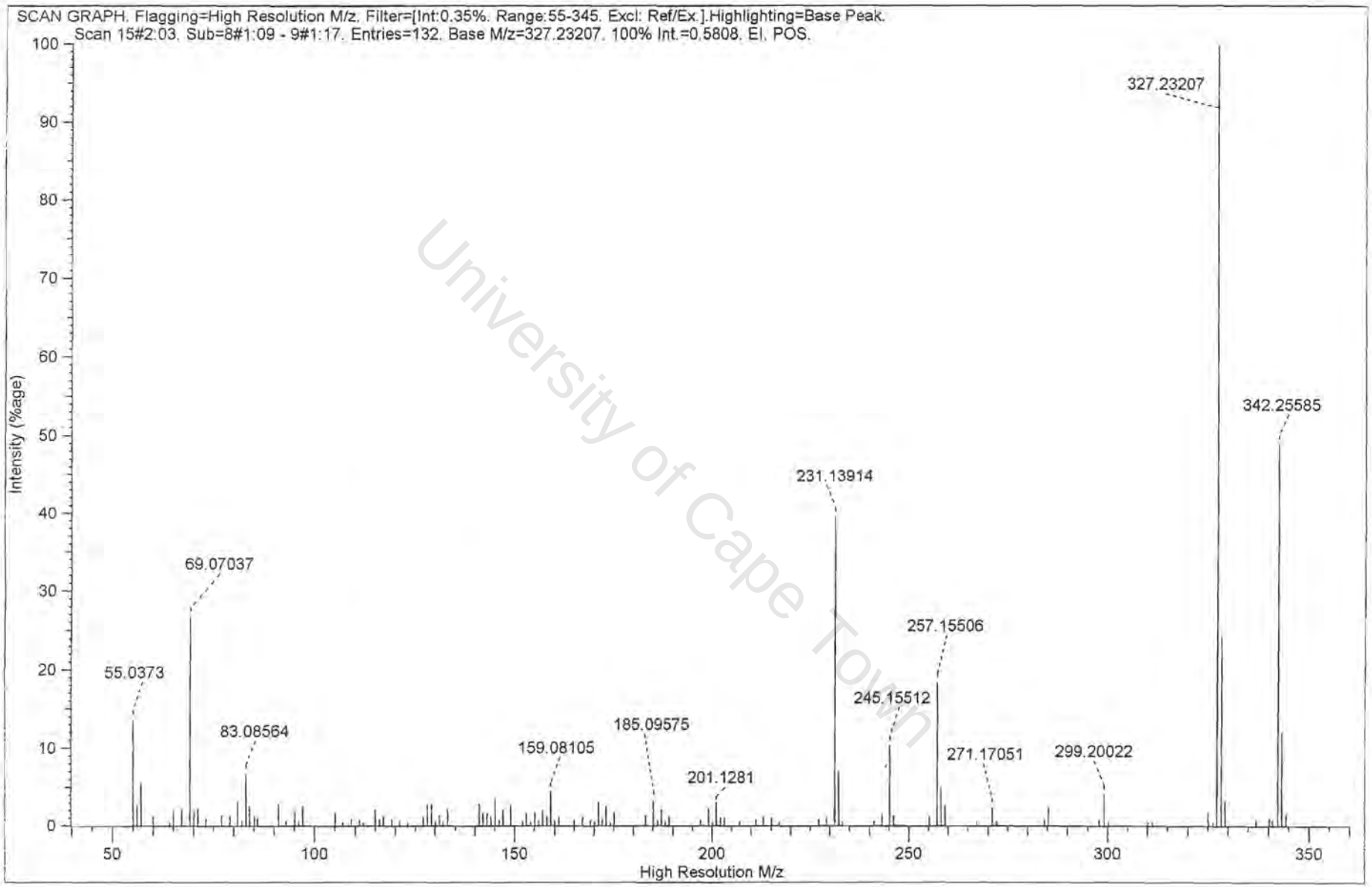

Figure A2.5.1 HREIMS spectrum of the epoxide (**1**)

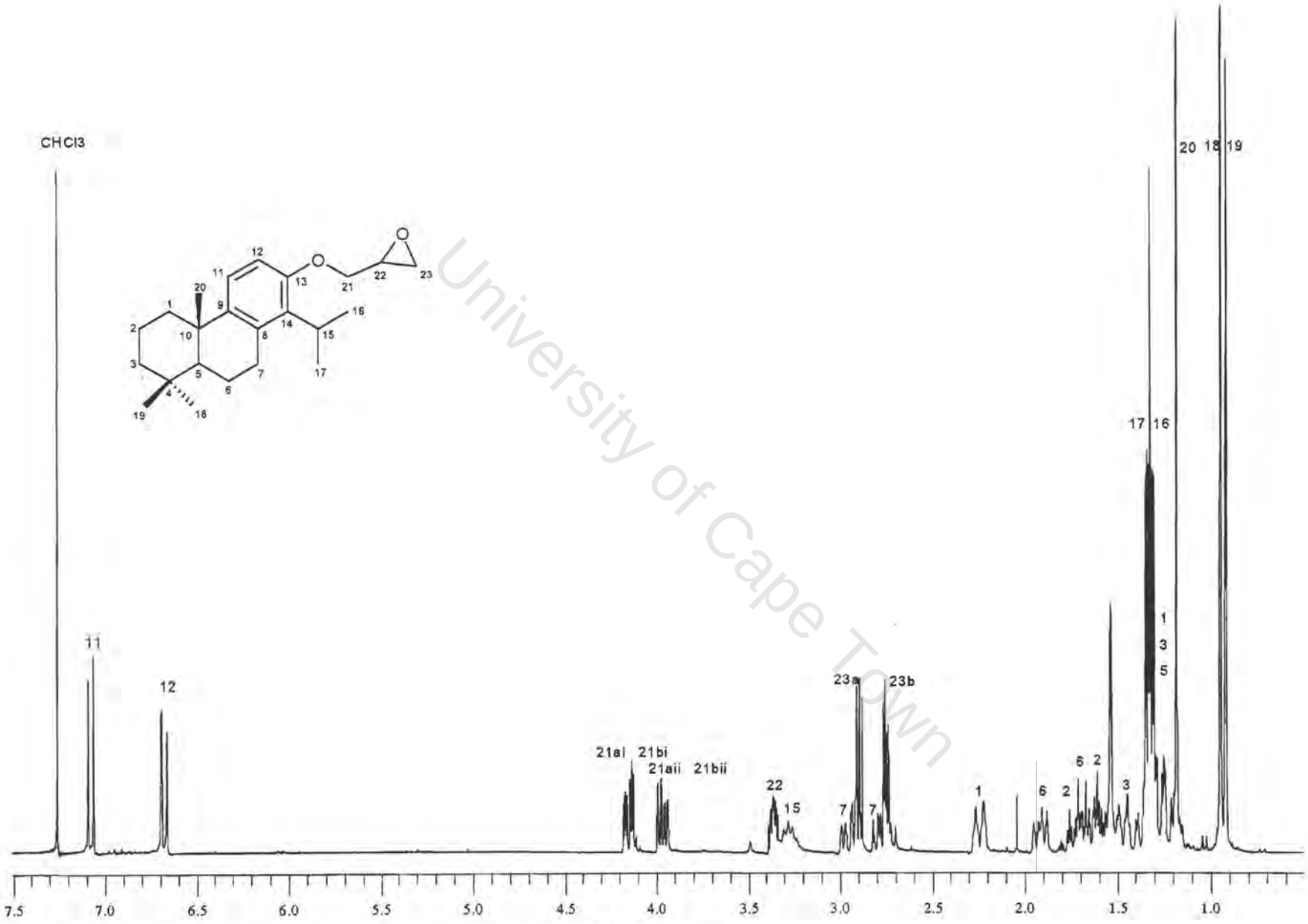

Figure A2.5.2 ^{1}H NMR spectrum of the epoxide (**1**) in $CDCl_3$, 400MHz

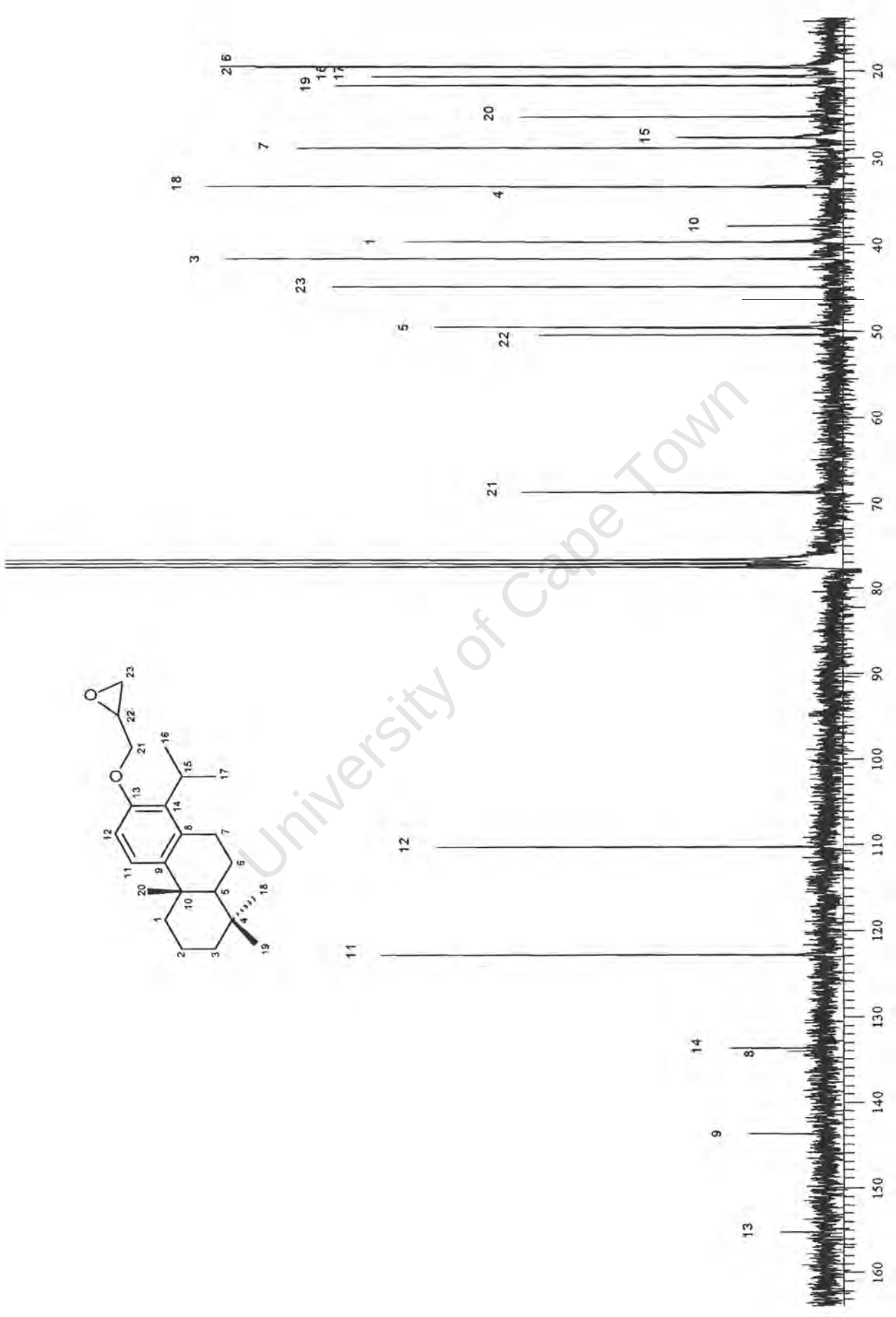

Figure A2.5.3 ^{13}C NMR spectrum of the epoxide (**1**)

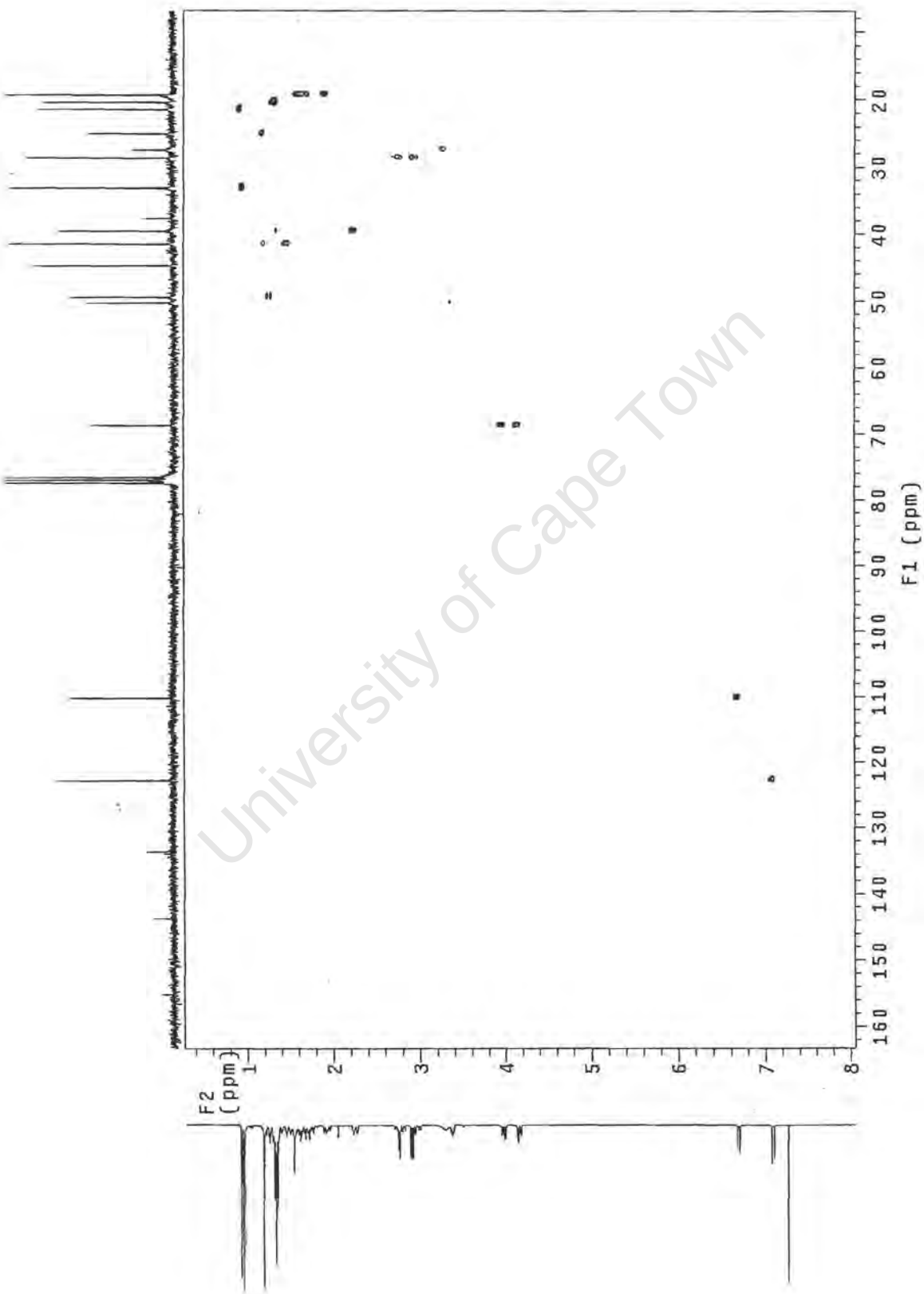

Figure A2.5.4 HSQC spectrum of the epoxide (**1**) in $CDCl_3$, 300MHz

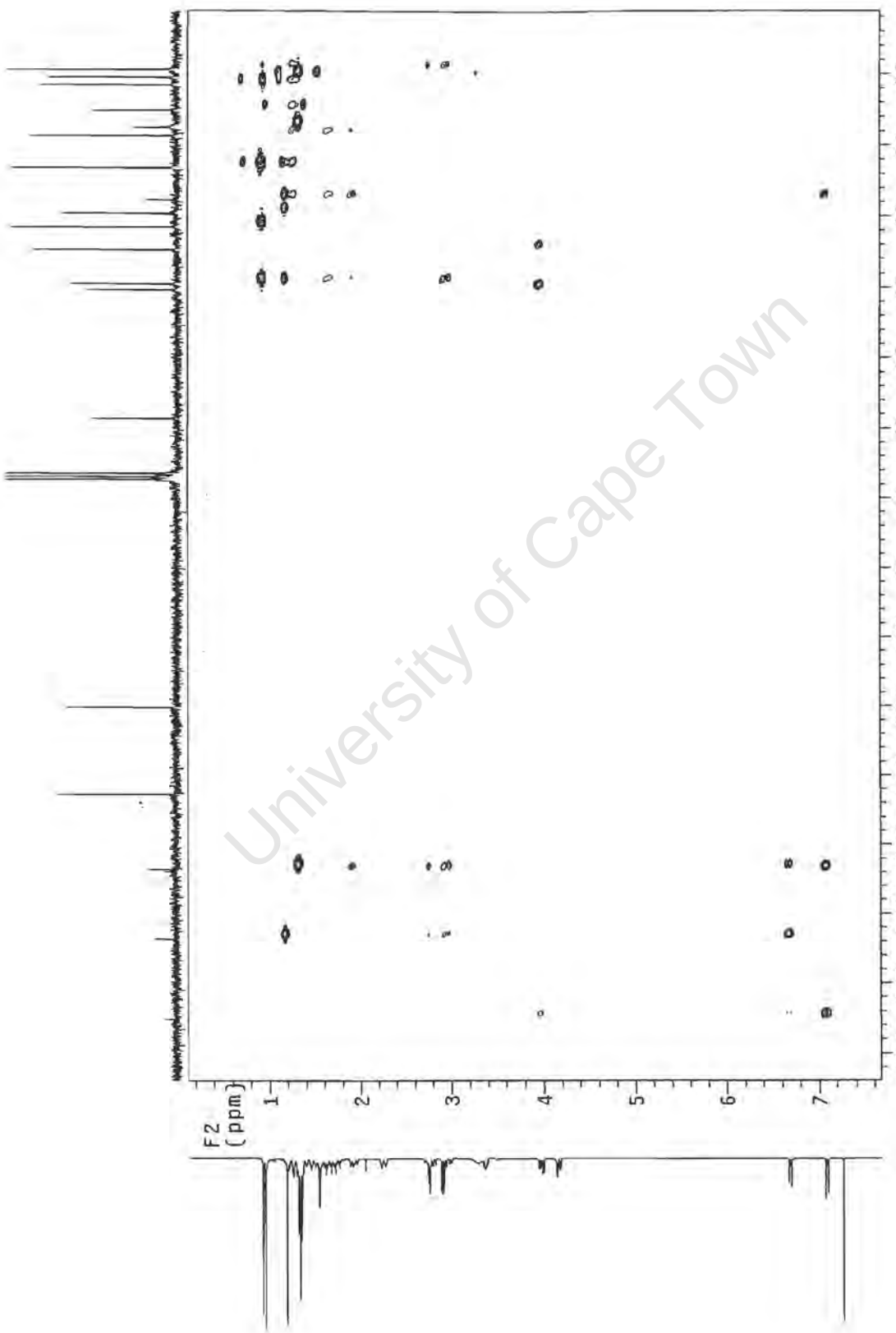

Figure A2.5.5 HMBC spectrum of the epoxide (1) in $CDCl_3$, 300MHz

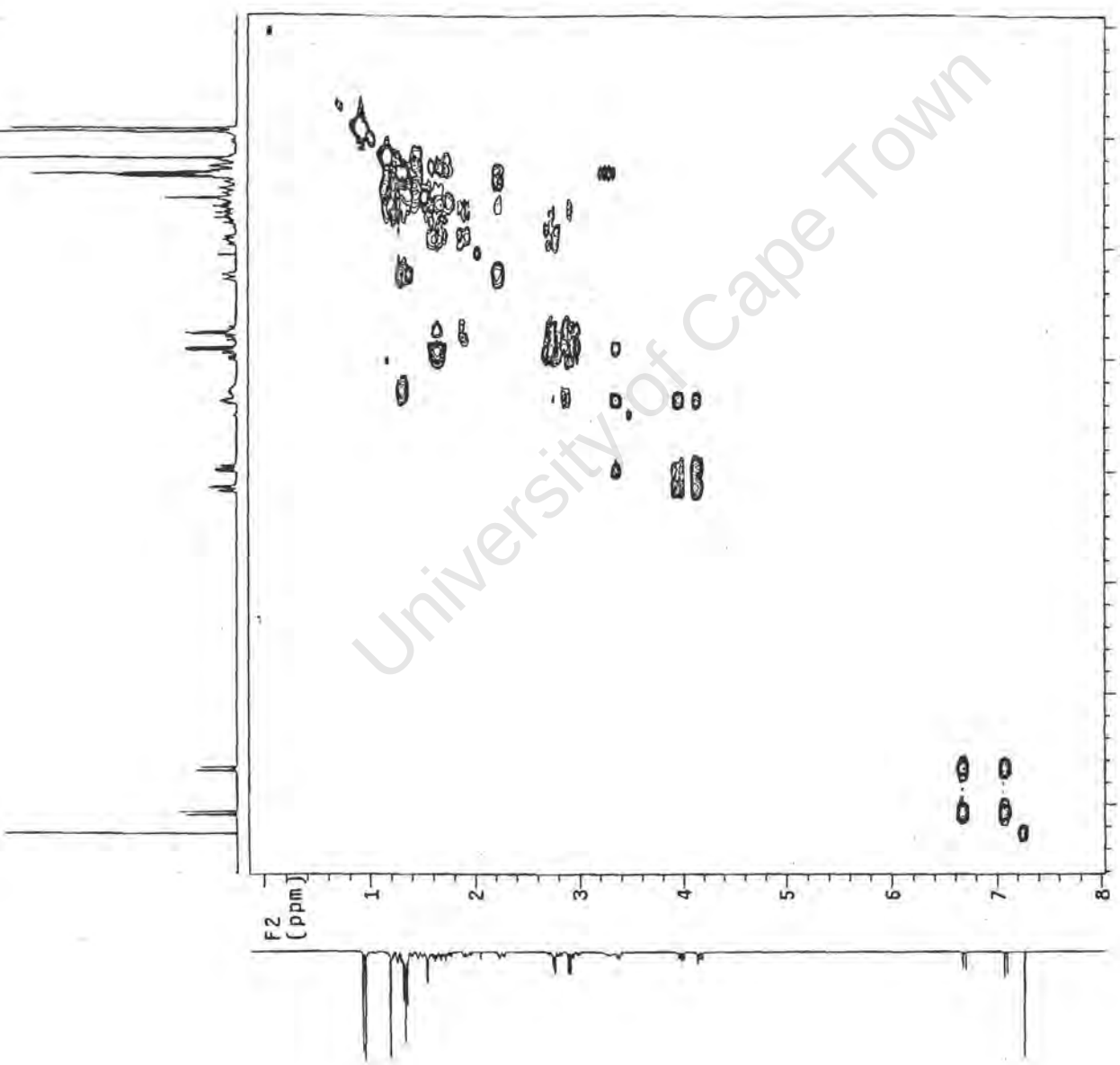

Figure A2.5.6 COSY spectrum of the epoxide (**1**) in $CDCl_3$, 300MHz

A2.6 Compound 2

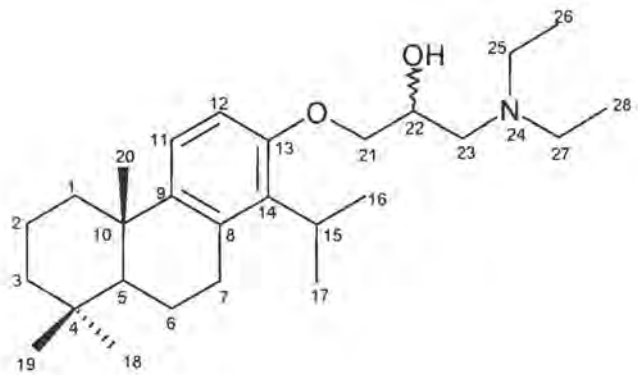

Compound 2

IUPAC [1-Diethylamino-3-(1-isopropyl-4b,8,8-trimethyl-4b,5,6,7,8,8a,9,10-octahydro-phenanthren-2-yloxy)-propan-2-ol]

List of spectra:

- IR
- HREIMS
- ^{1}H NMR (400MHz, $CDCl_3$)
- ^{13}C NMR (400MHz, $CDCl_3$)
- HSQC (300MHz, $CDCl_3$)
- HMBC (300MHz, $CDCl_3$)
- COSY (300MHz, $CDCl_3$)

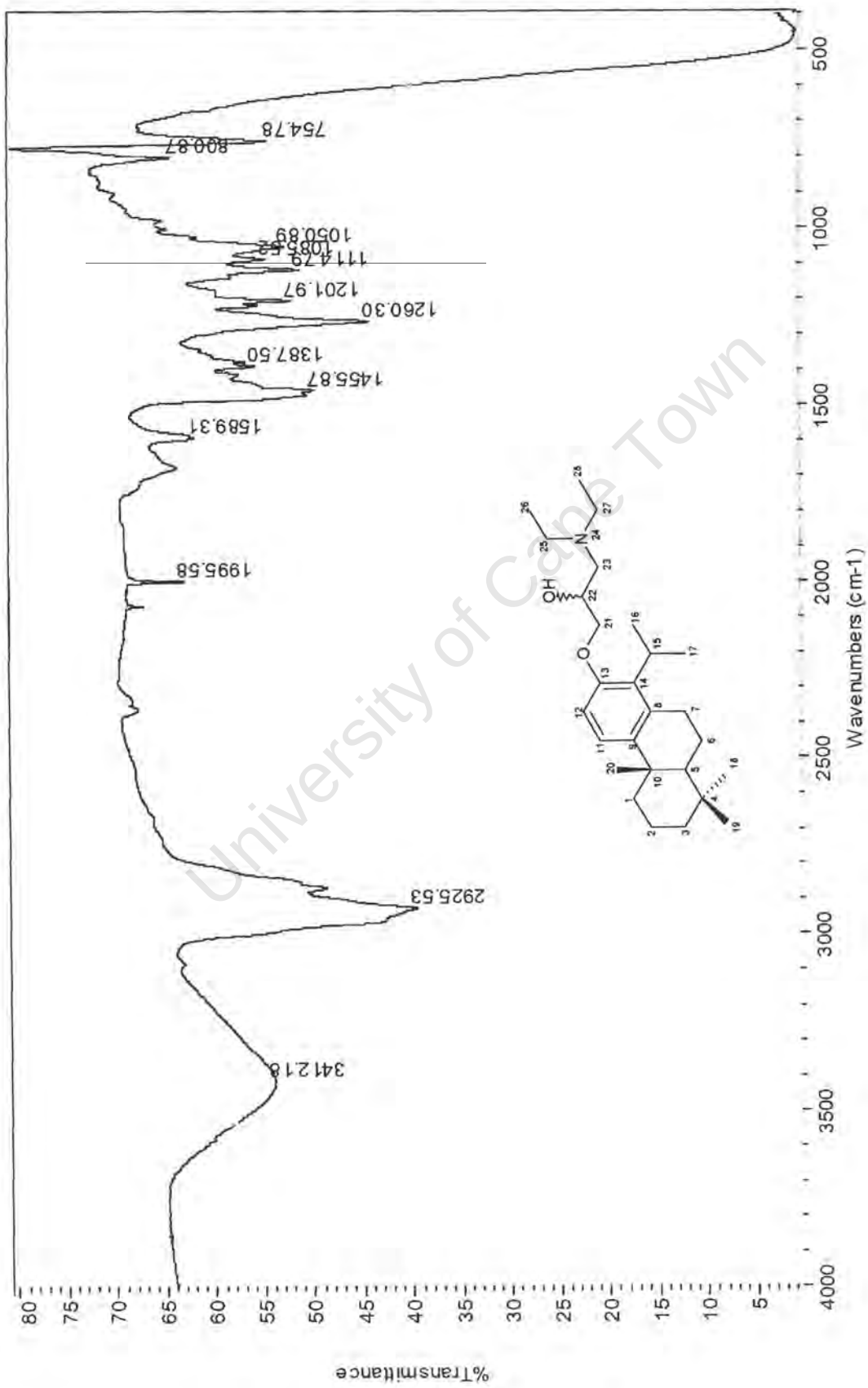

Figure A2.6.1 IR spectrum of compound **2**

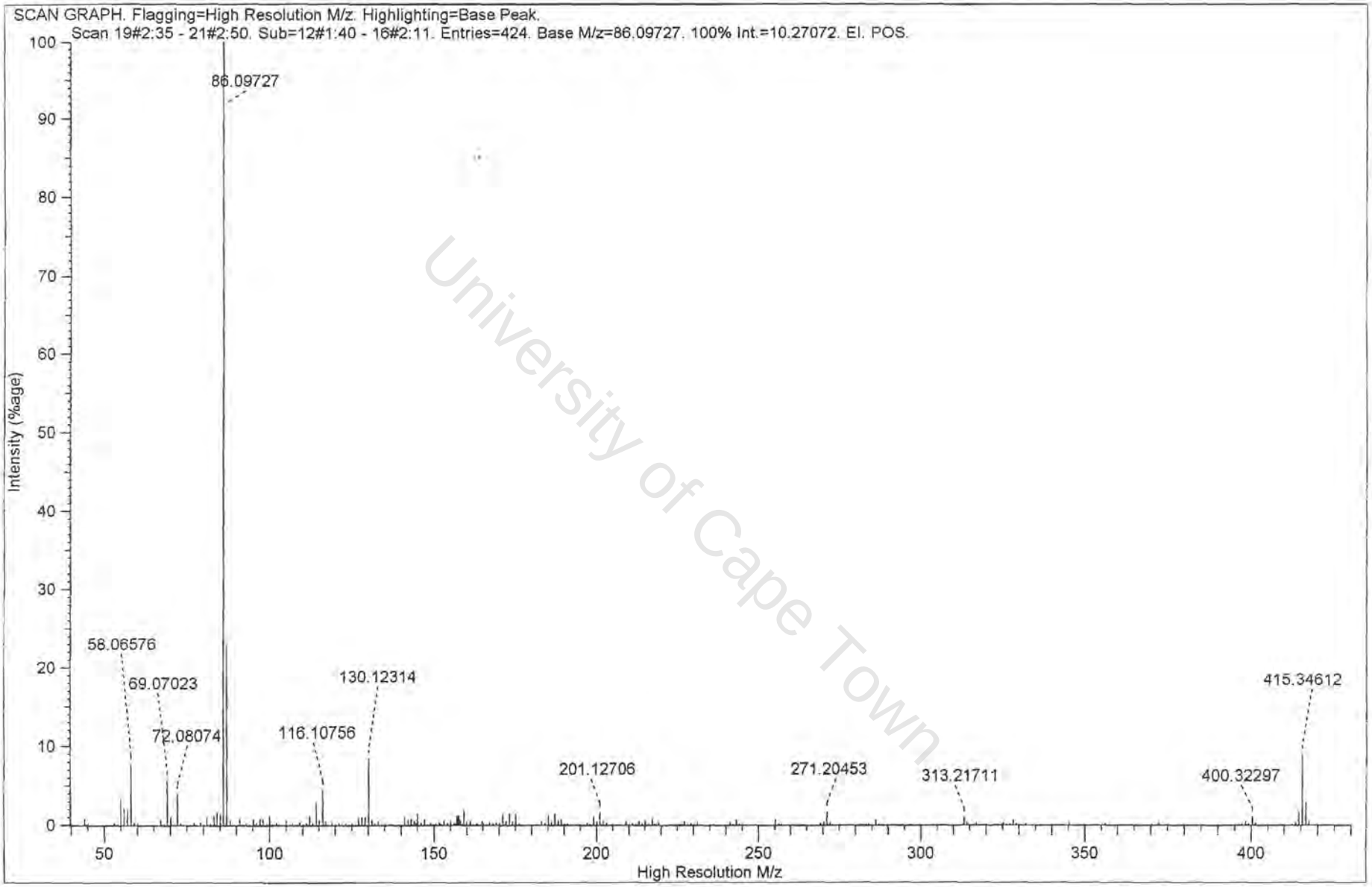

Figure A2.6.2 HREIMS spectrum of compound **2**

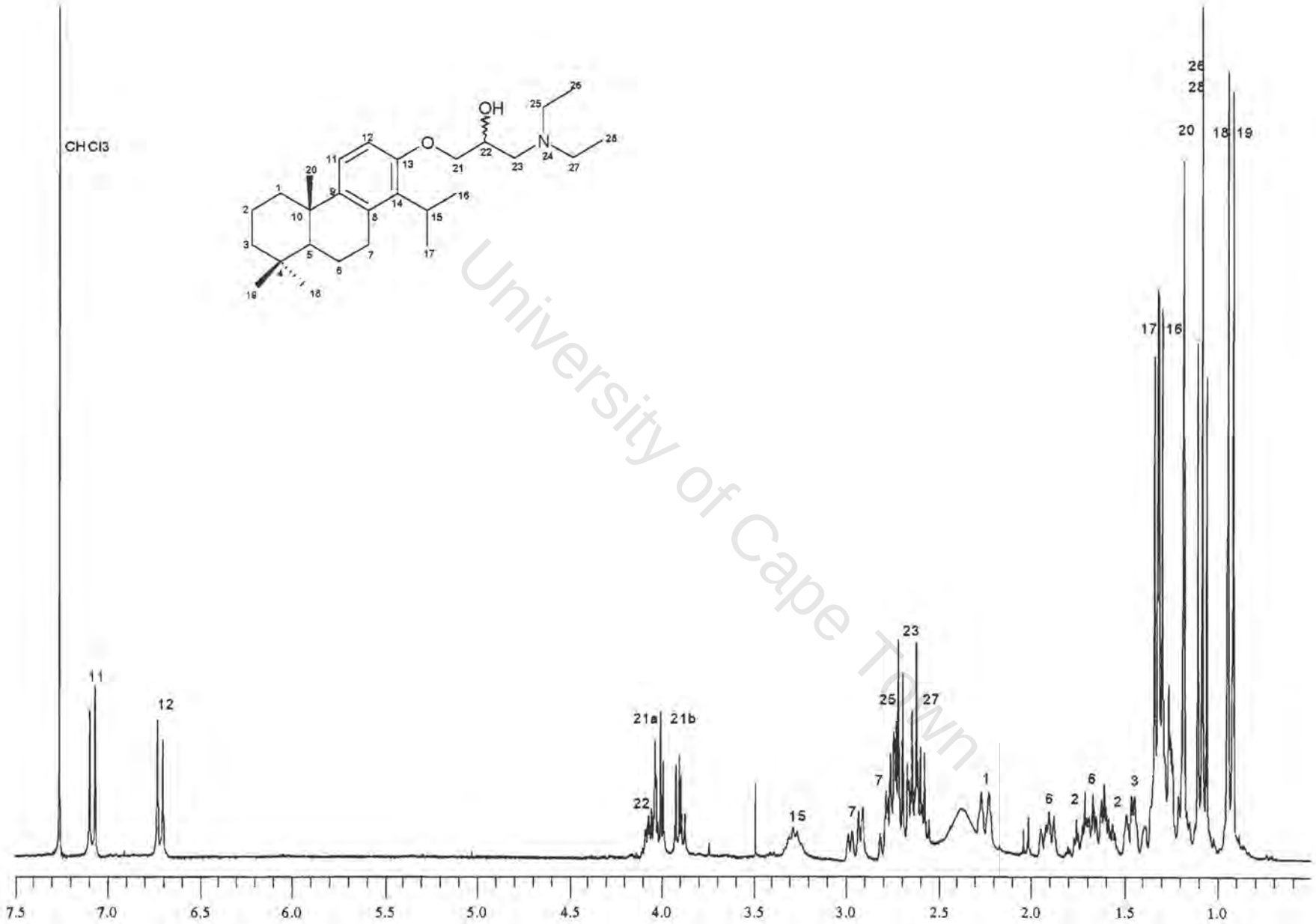

Figure A2.6.3 ^{1}H NMR spectrum of compound **2** in $CDCl_3$, 400MHz

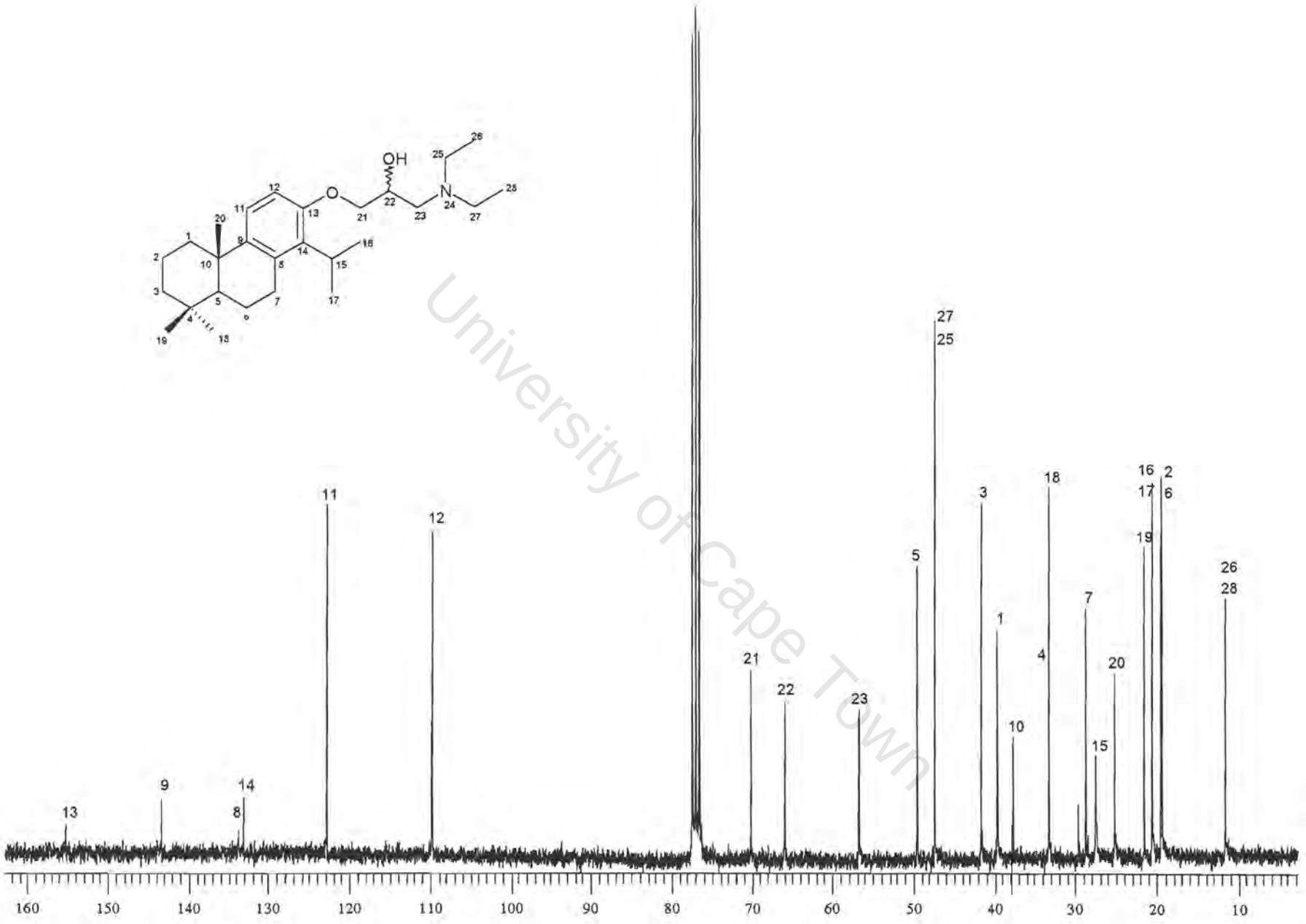

Figure A2.6.4 ^{13}C NMR spectrum of compound **2** in $CDCl_3$, 400MHz

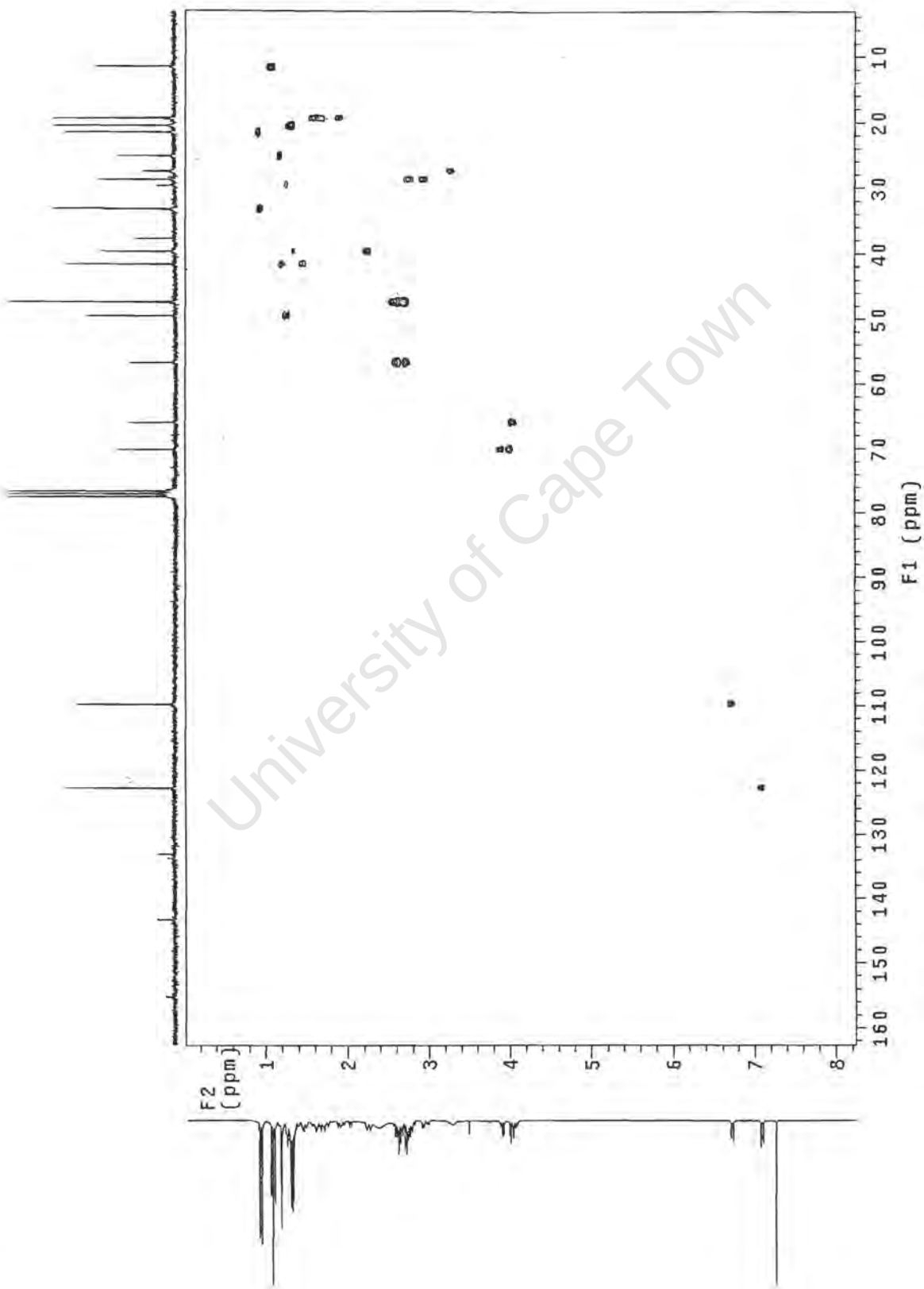

Figure A2.6.5 HSQC spectrum of compound **2** in $CDCl_3$, 300MHz

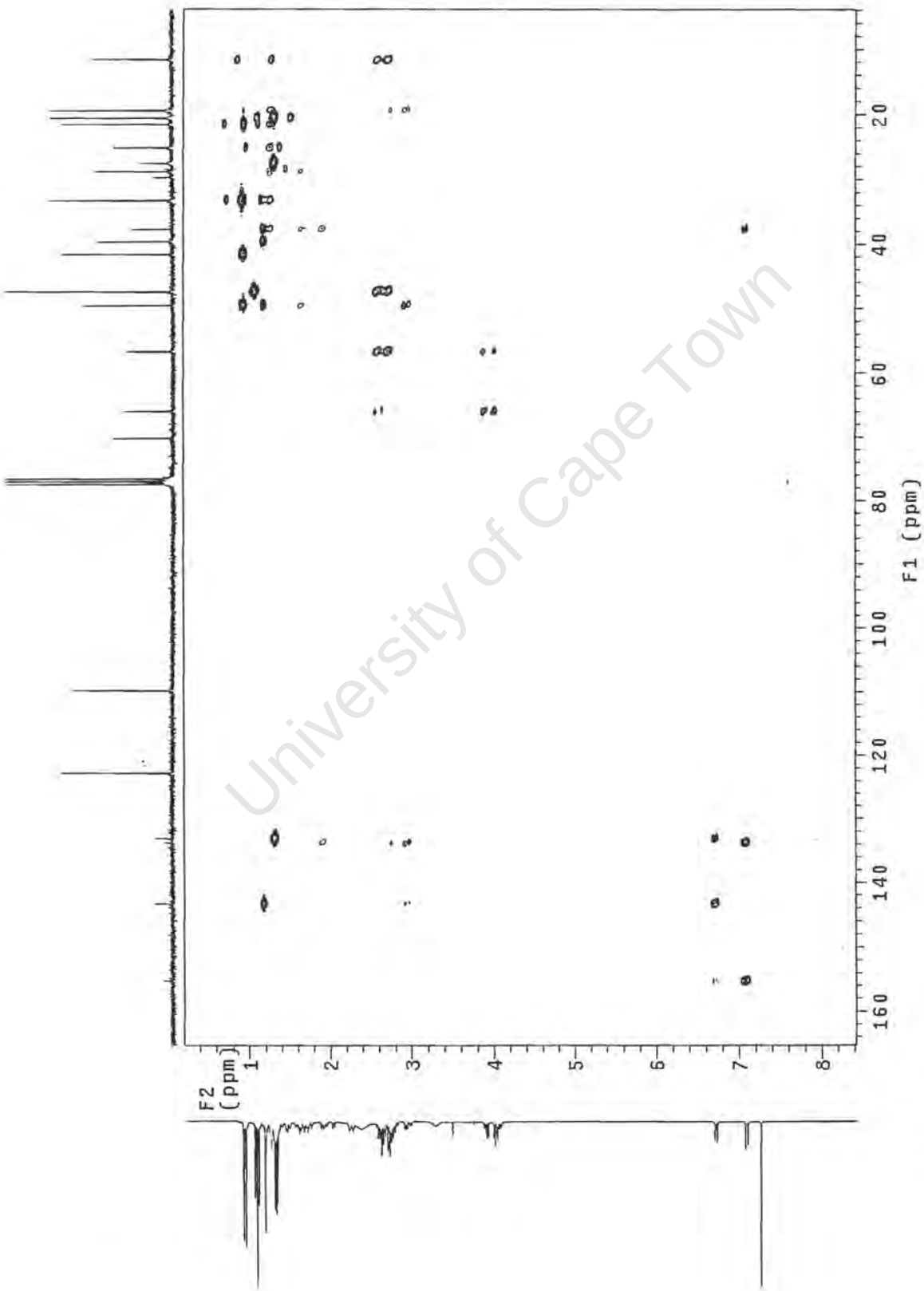

Figure A2.6.6 HMBC spectrum of compound **2** in $CDCl_3$, 300MHz

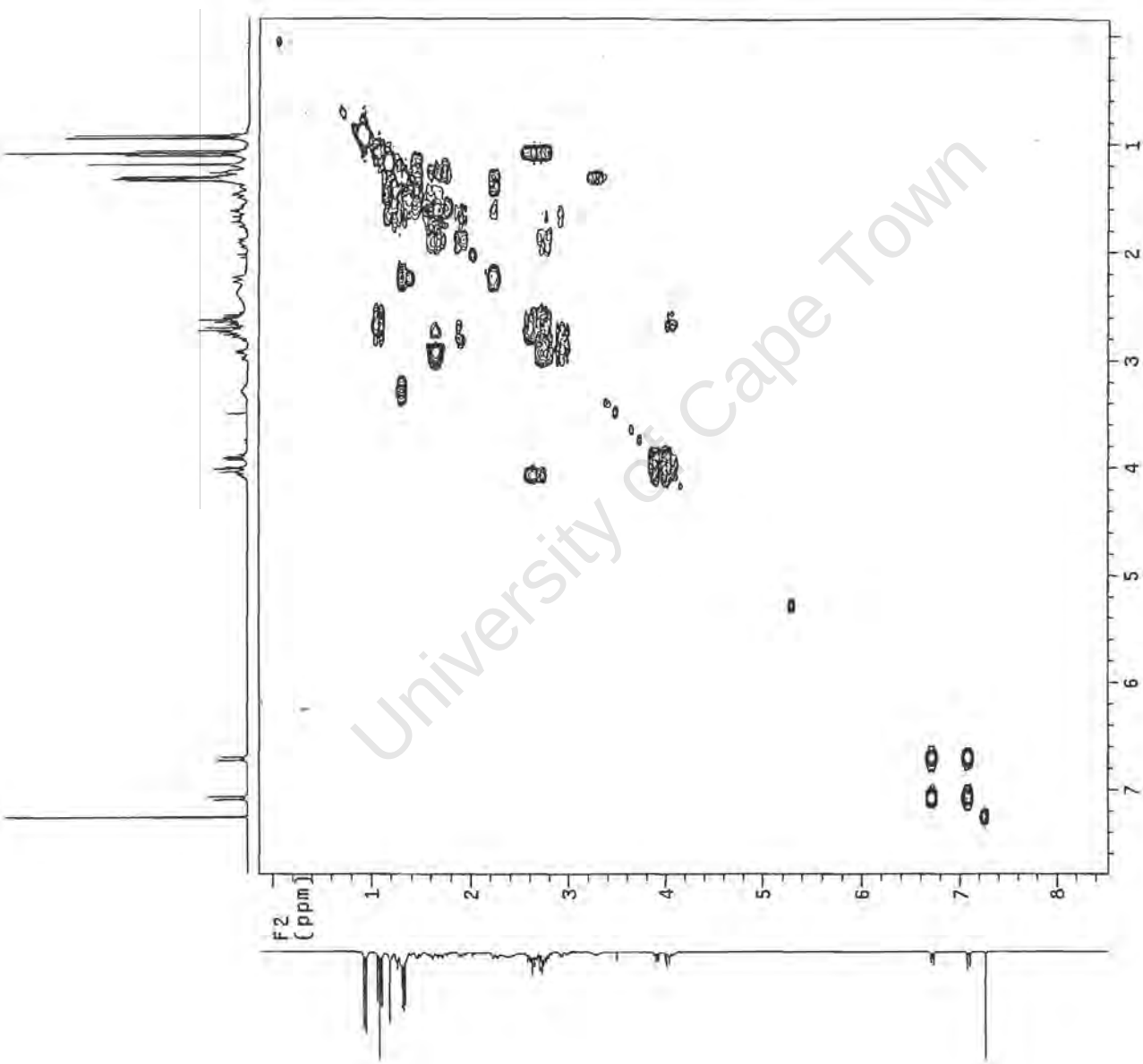

Figure A2.6.7 COSY spectrum of compound **2** in $CDCl_3$

A2.7 Compound 3

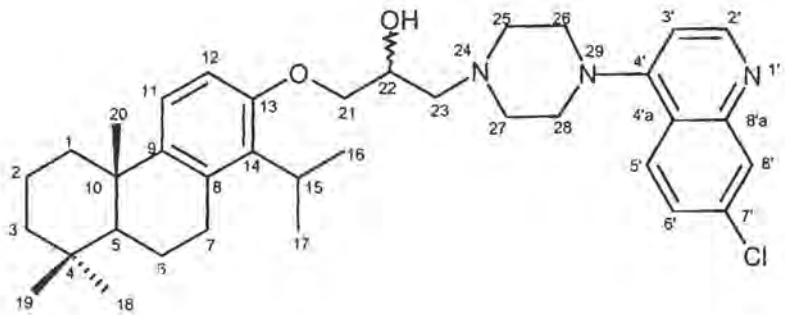

Compound 3

IUPAC [1-(1-Isopropyl-4b,8,8-trimethyl-4b,5,6,7,8,8a,9,10-octahydro-phenanthren-2-yloxy)-3-(7-chloroquinolin-4-yl-piperazine)-1-yl-propan-2-ol]

List of spectra:

- HPLC profile
- UV absorbance
- IR
- HREIMS
- ^{1}H NMR (400MHz, $CDCl_3$)
- ^{13}C NMR (400MHz, $CDCl_3$)
- HSQC (300MHz, $CDCl_3$)
- HMBC (300MHz, $CDCl_3$)
- COSY(300MHz, $CDCl_3$)

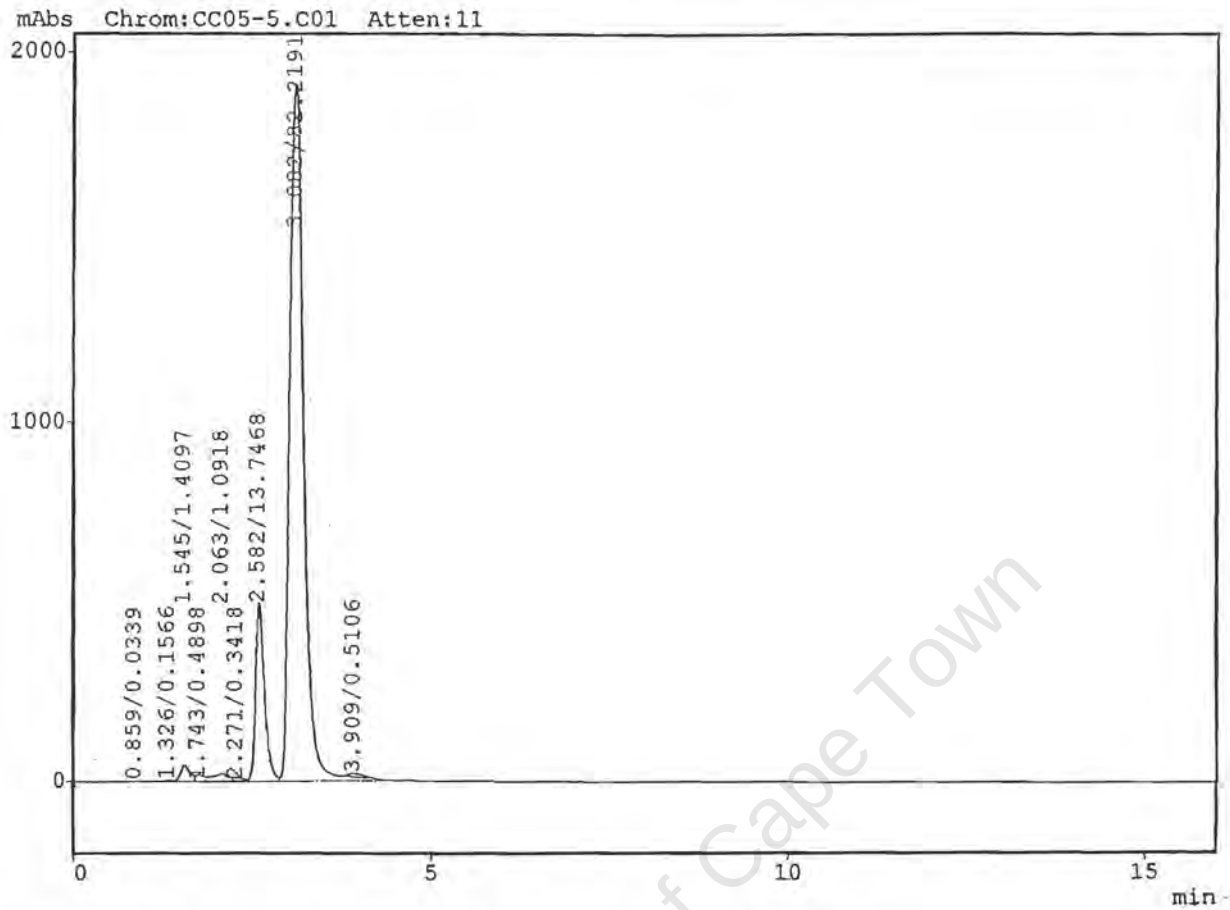

Figure A2.7.1 HPLC profile of compound **3** (H_2O: ACN)

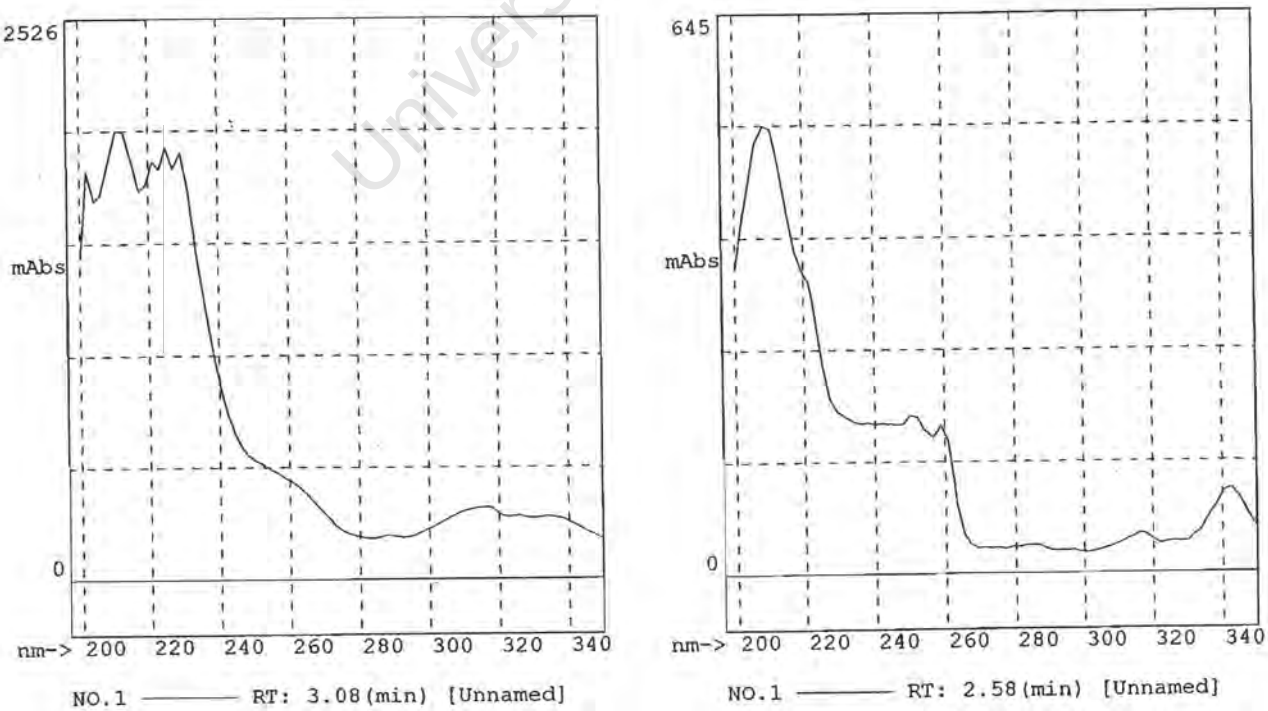

Figure A2.7.2 UV absorbance of compound **3** (R_t=3.08) and the minor impurity (R_t=2.58)

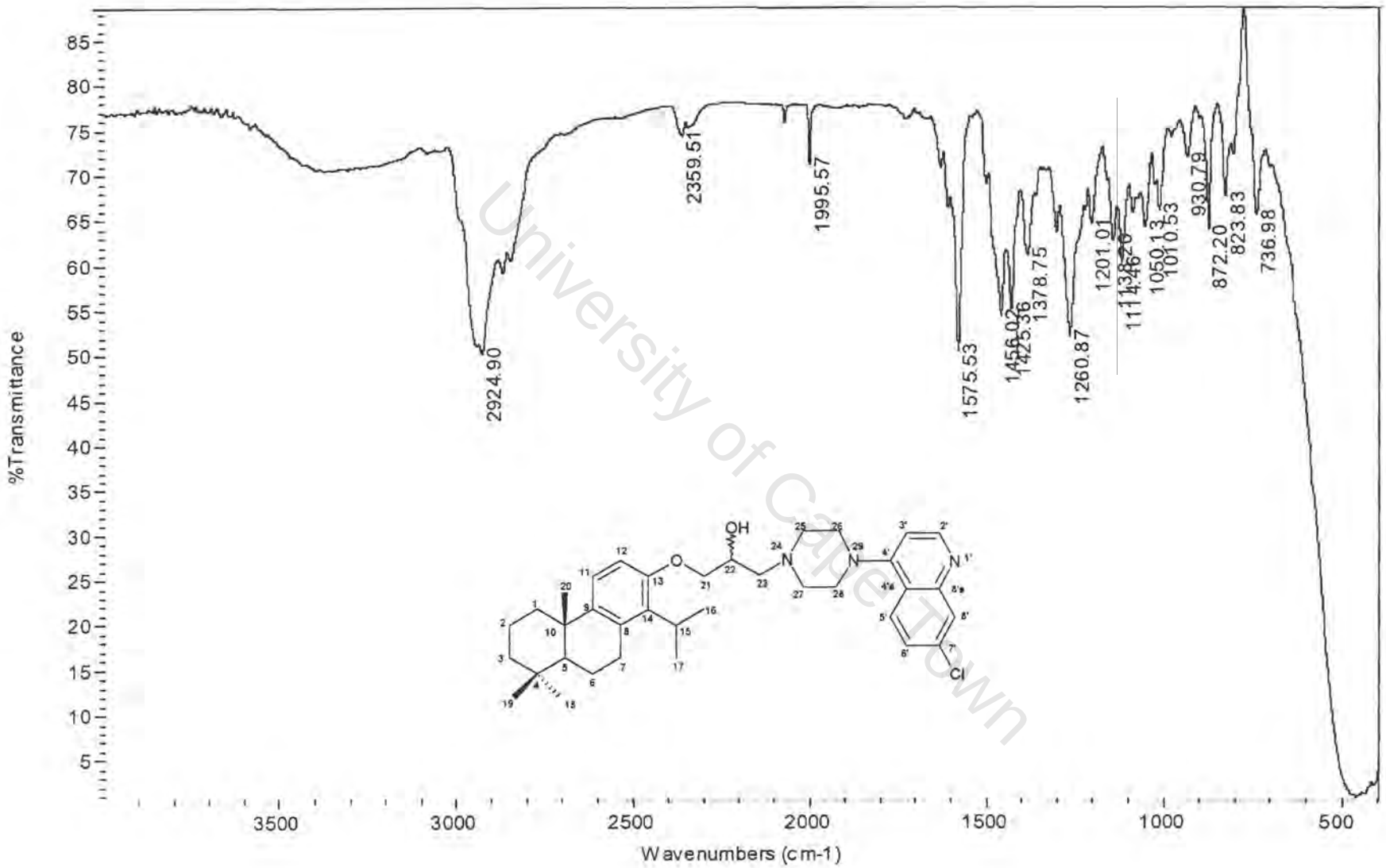

Figure A2.7.3 IR spectrum of compound **3**

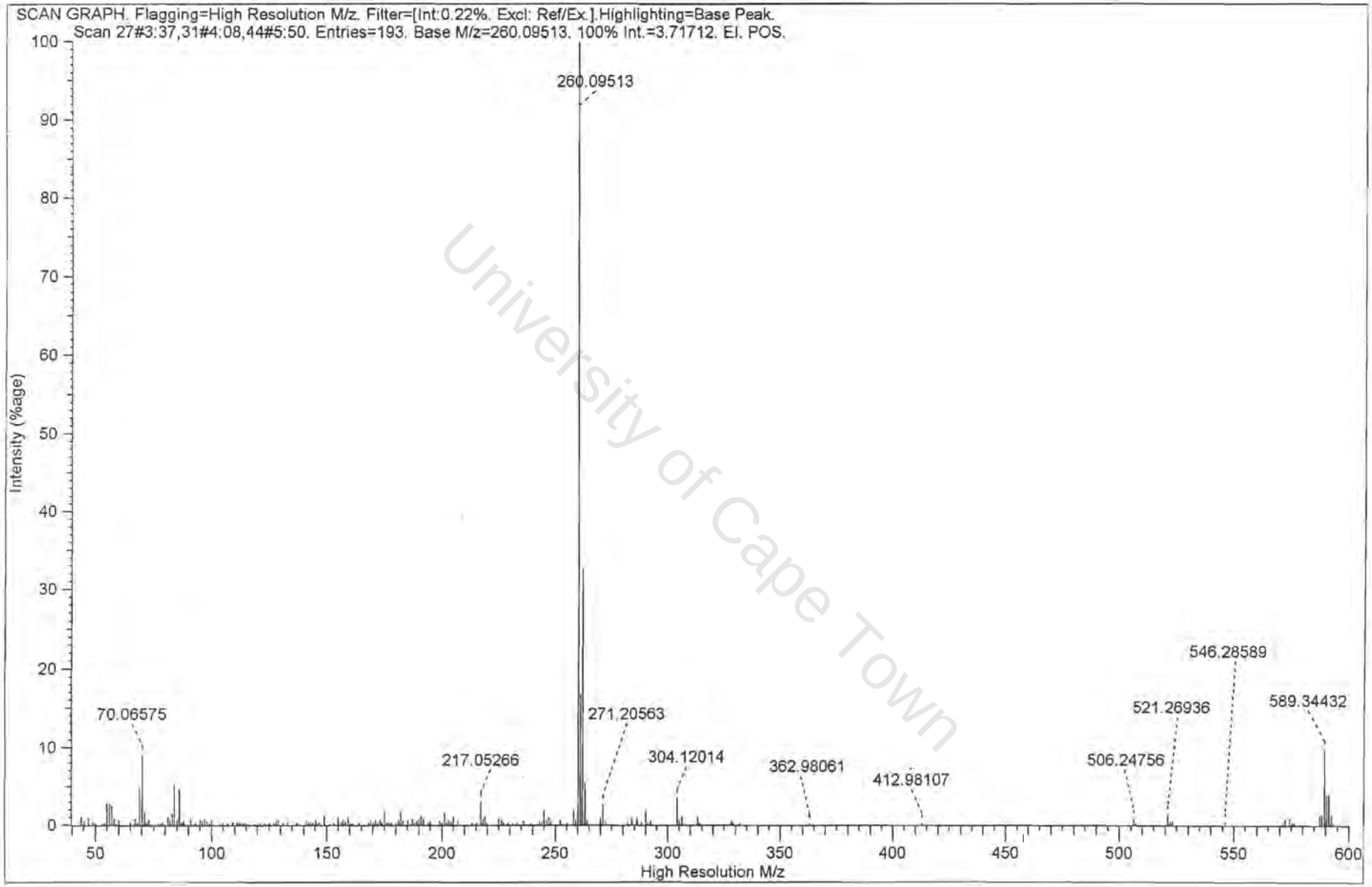

Figure A2.7.4 HREIMS spectrum of compound **3**

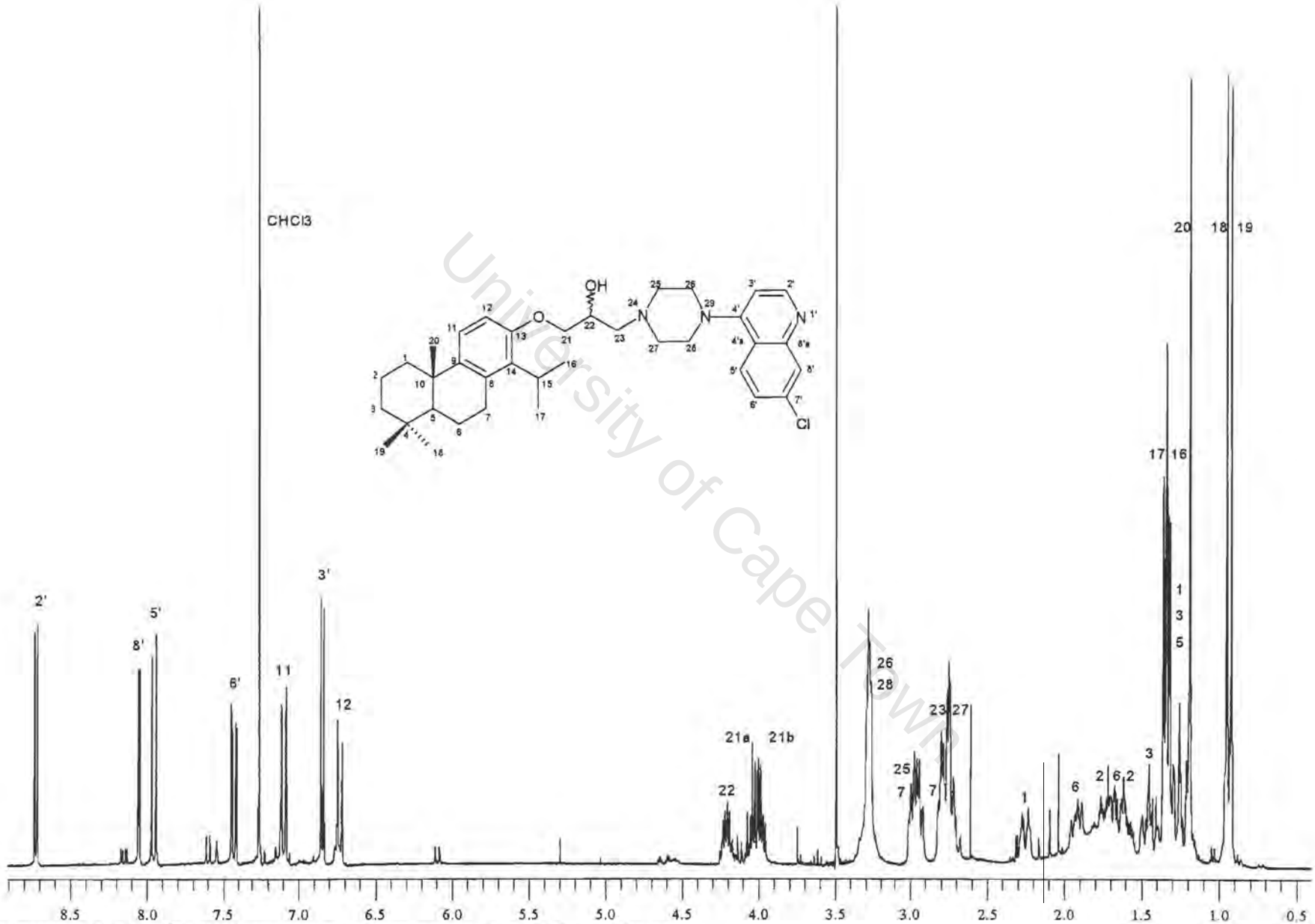

Figure A2.7.5 ^{1}H NMR spectrum of compound **3** in $CDCl_3$, 400MHz

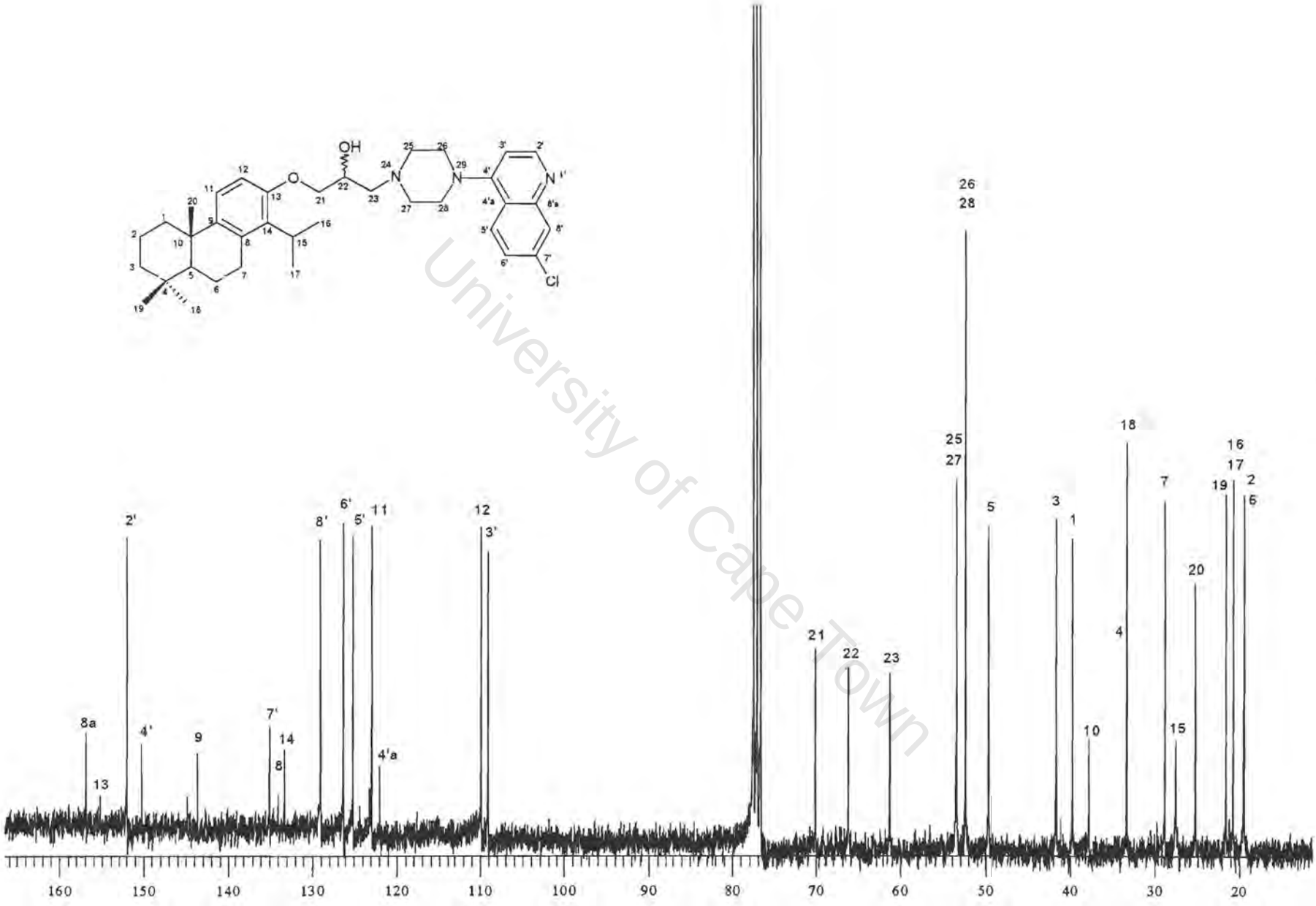

Figure A2.7.6 ^{13}C NMR spectrum of compound **3** in $CDCl_3$, 400MHz

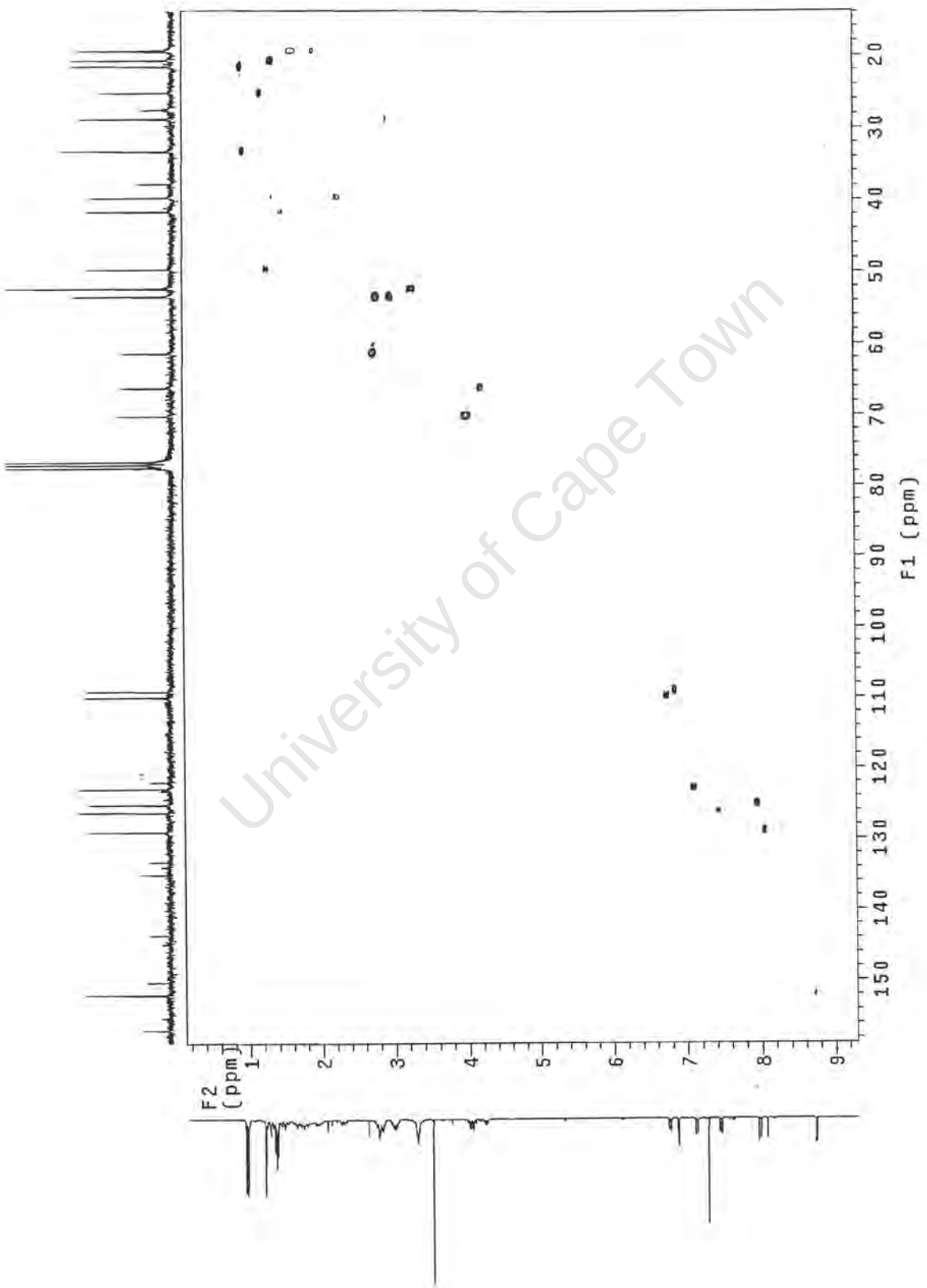

Figure A2.7.7 HSQC spectrum of compound **3** in $CDCl_3$, 300MHz

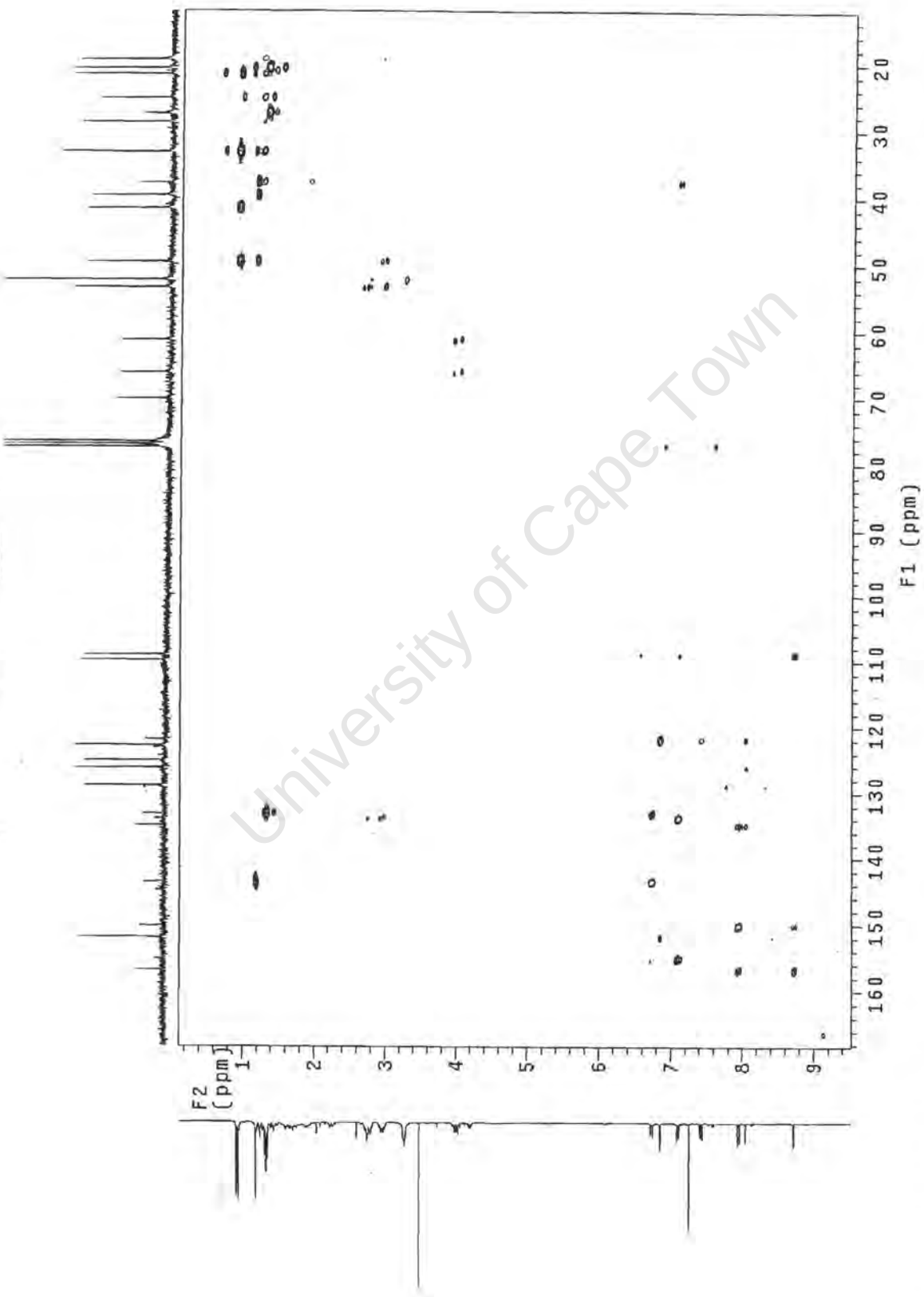

Figure A2.7.8 HMBC spectrum of compound **3** in $CDCl_3$, 300MHz

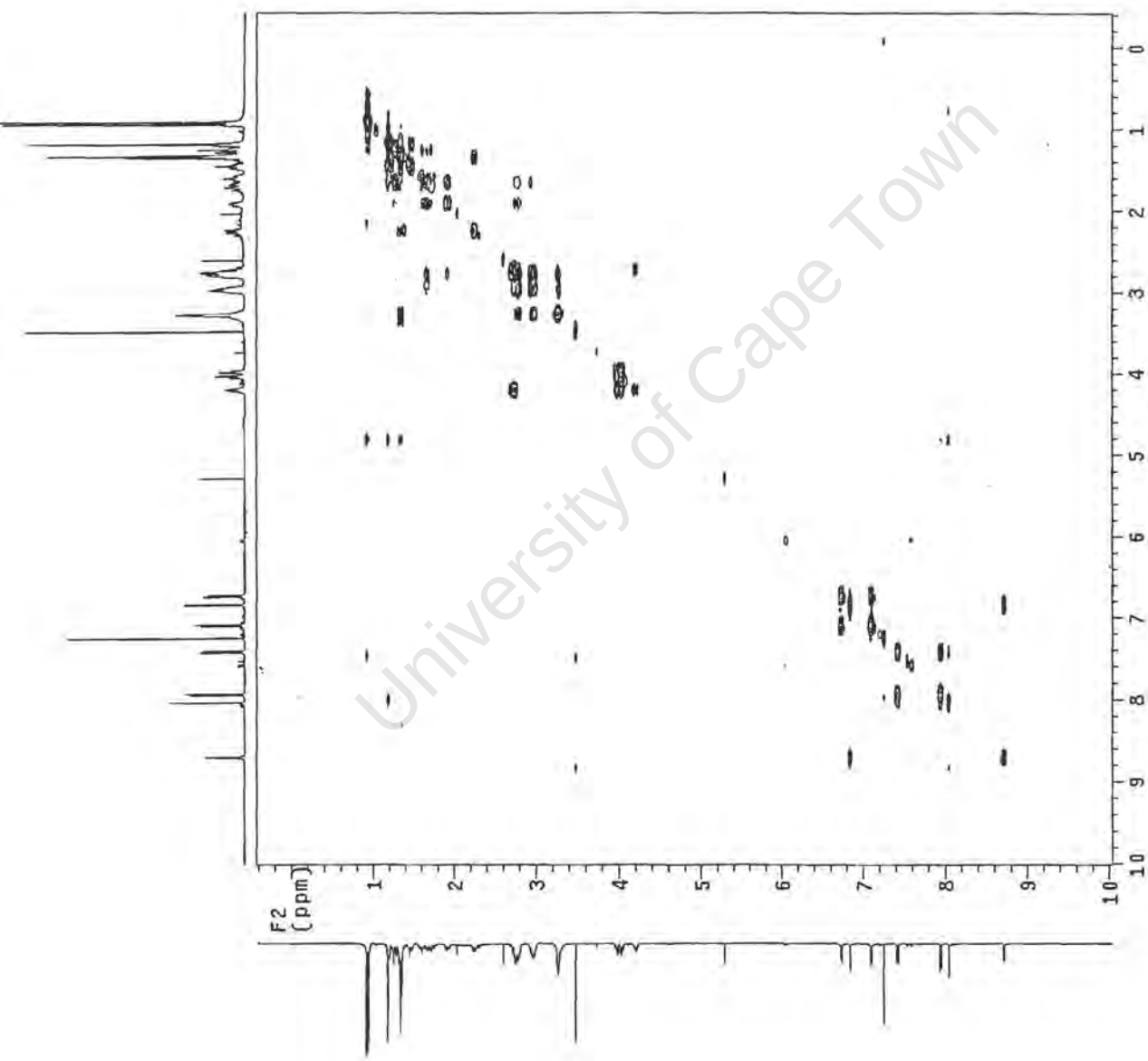

Figure A2.7.9 COSY spectrum of compound **3** in $CDCl_3$, 300MHz

A2.8 Compound 4

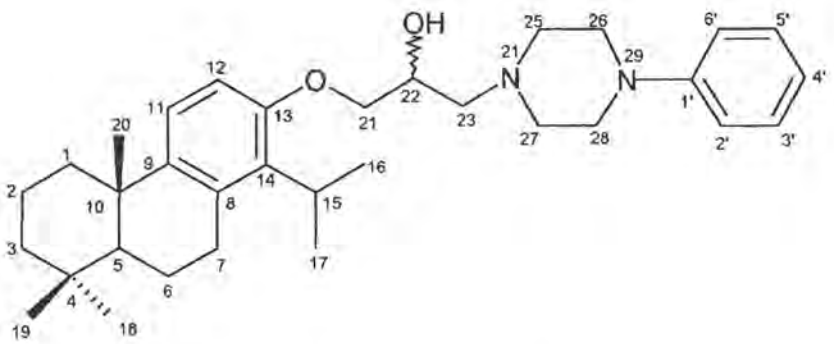

Compound 4

IUPAC [1-(1-Isopropyl-4b,8,8-trimethyl-4b,5,6,7,8,8a,9,10-octahydro-phenanthren-2-yloxy)-3-(phenylpiperazine)-1-yl-propan-2-ol]

List of spectra:

- IR
- HREIMS
- ^{1}H NMR (400MHz, $CDCl_3$)
- ^{13}C NMR (400MHz, $CDCl_3$)
- COSY (300MHz, $CDCl_3$)

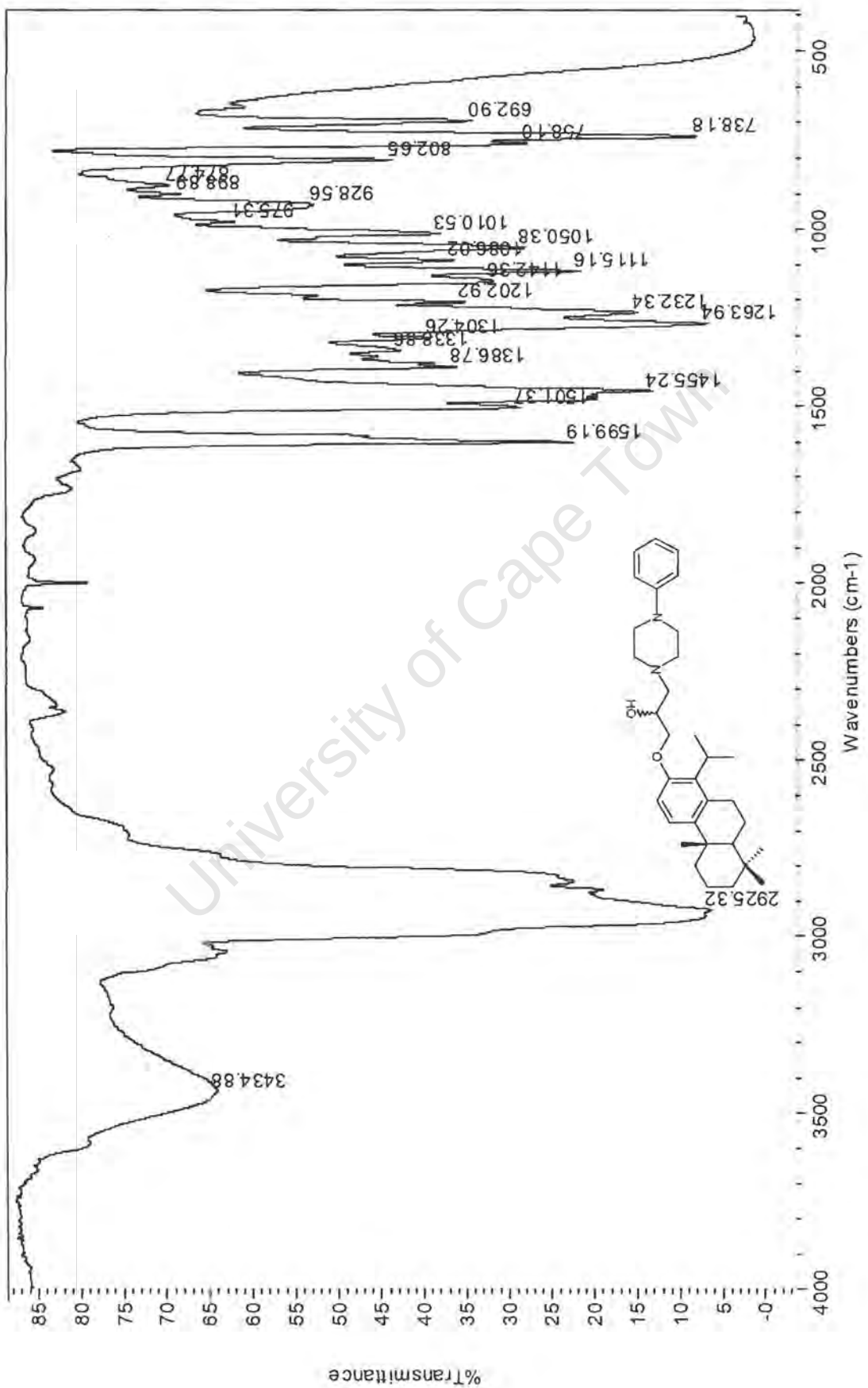

Figure A2.8.1 IR spectrum of compound **4**

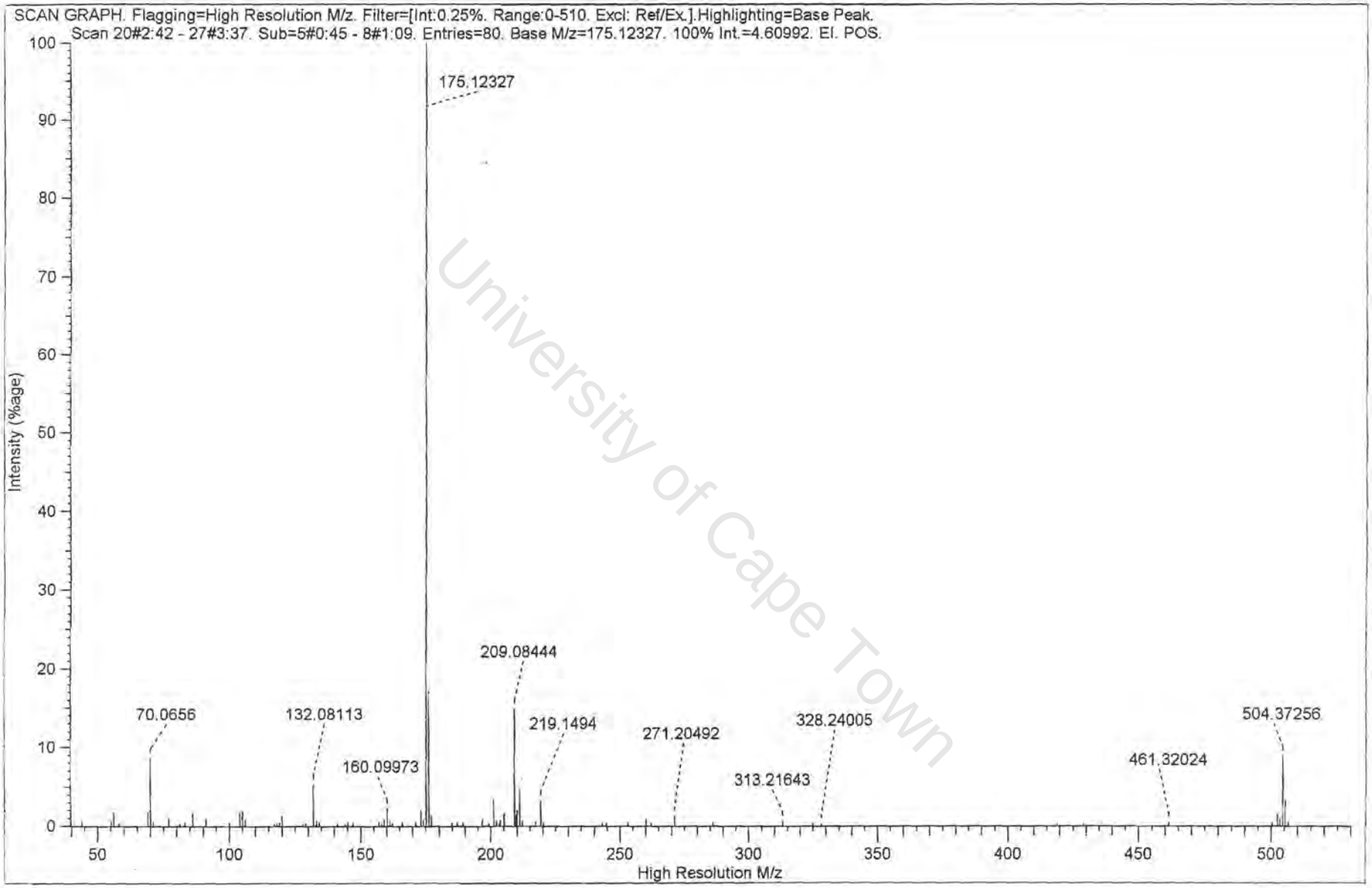

Figure A2.8.2 HREIMS spectrum of compound **4**

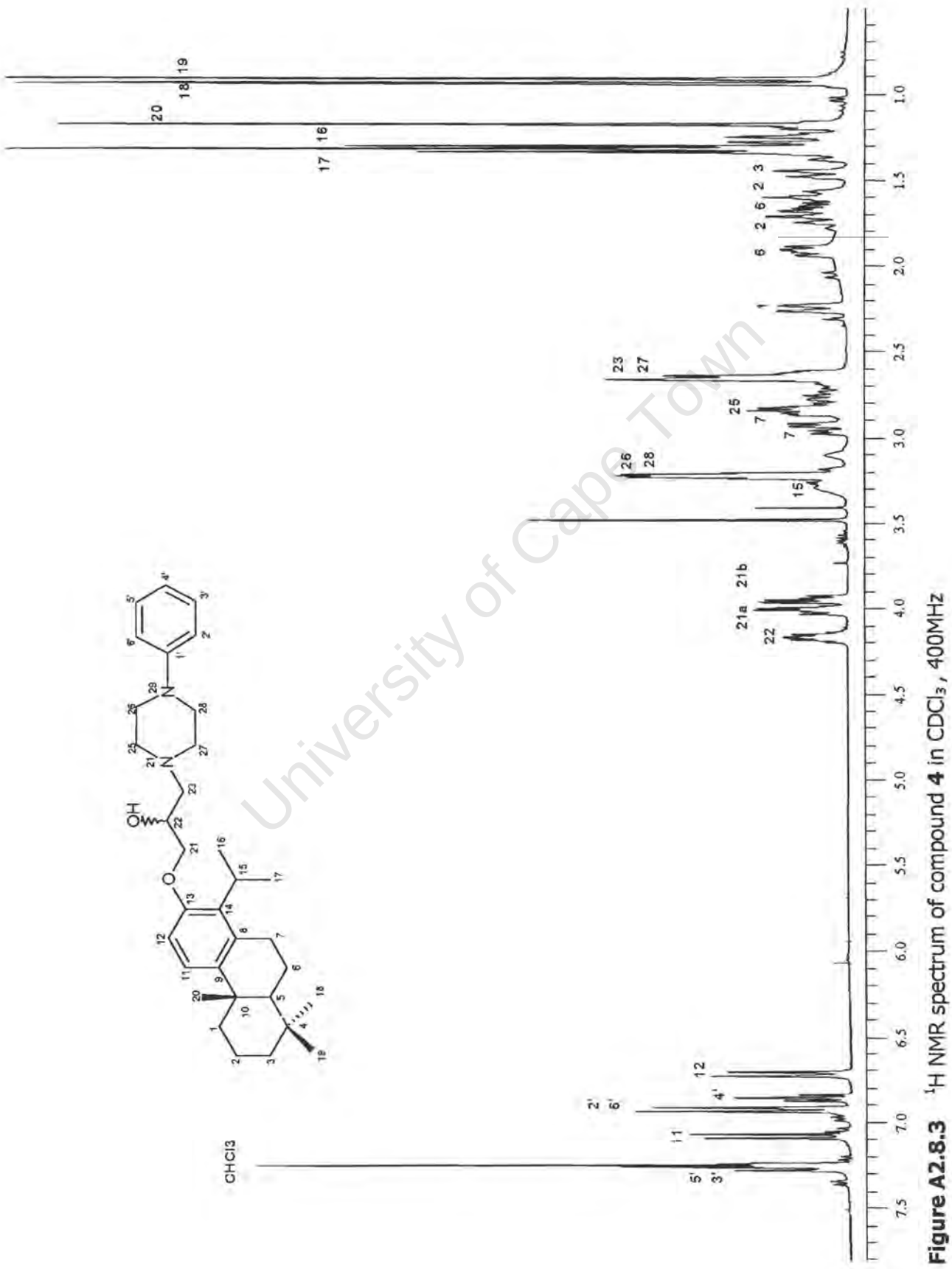

Figure A2.8.3 ^{1}H NMR spectrum of compound **4** in $CDCl_3$, 400MHz

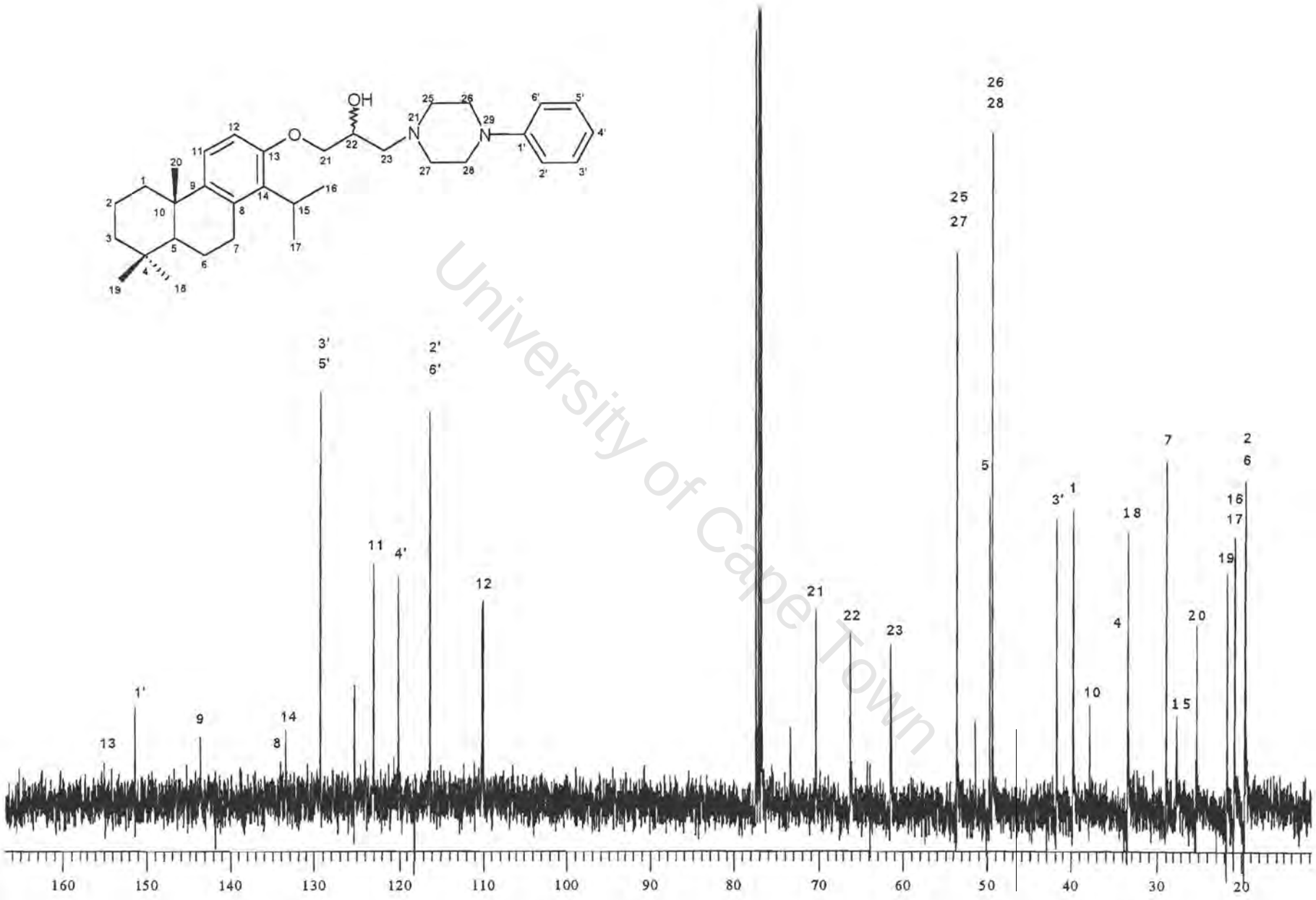

Figure A2.8.4 ^{13}C NMR spectrum of compound **4** in $CDCl_3$, 400MHz

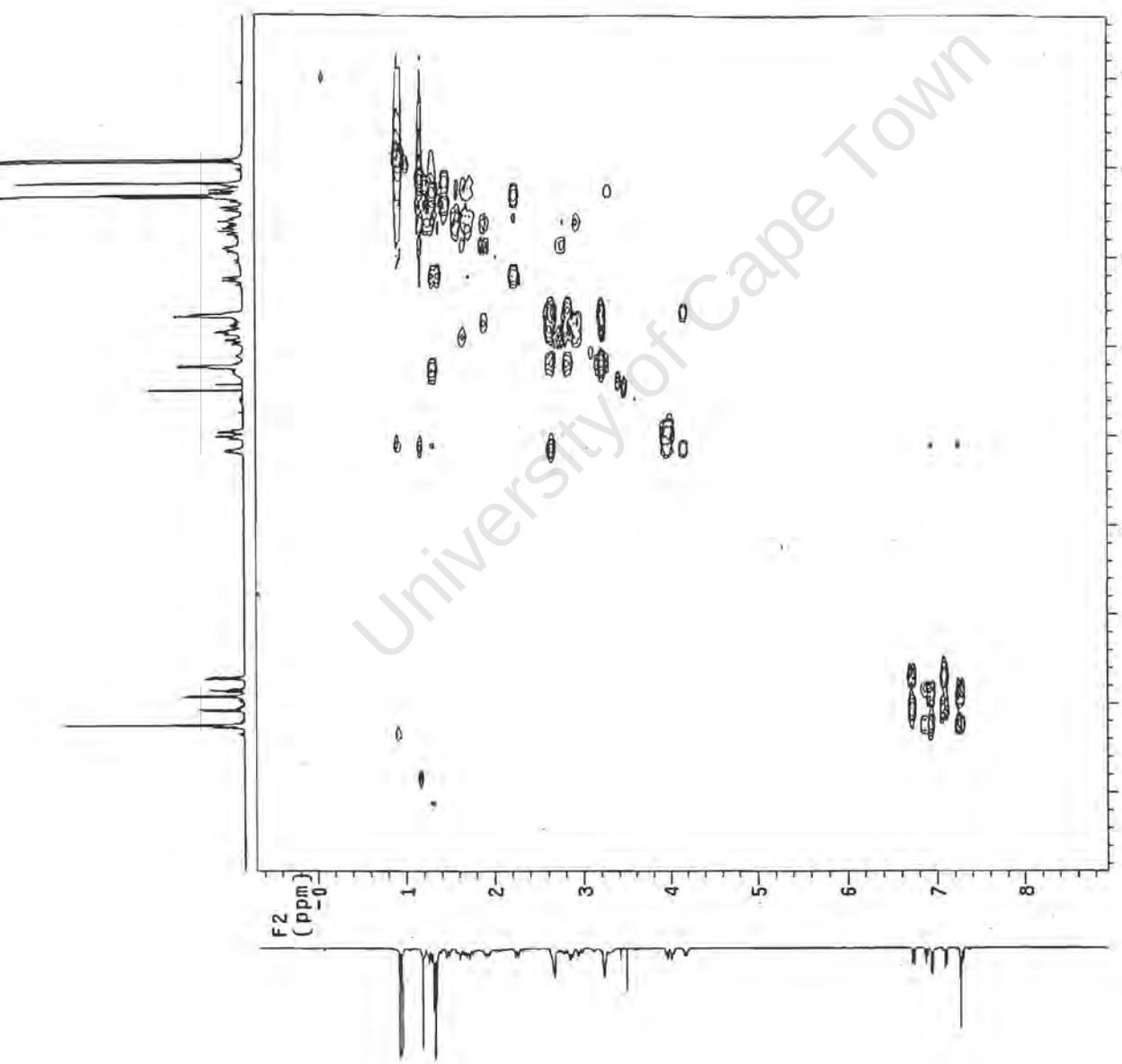

Figure A2.8.5 COSY spectrum of compound **4** in $CDCl_3$, 300MHz

A2.9 Compound 5

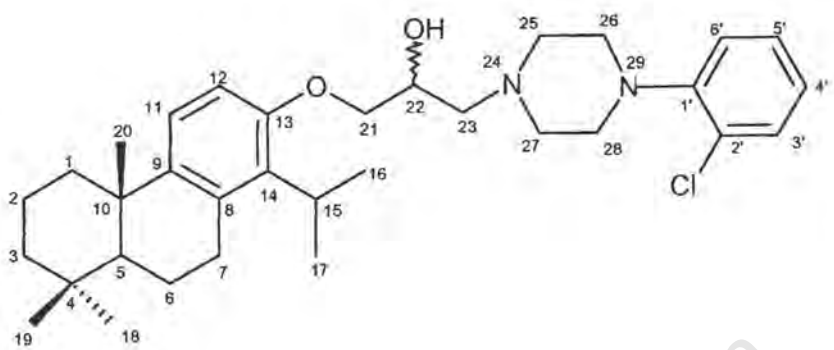

Compound 5

IUPAC [1-(1-Isopropyl-4b,8,8-trimethyl-4b,5,6,7,8,8a,9,10-octahydro-phenanthren-2-yloxy)-3-(2-chloroquinolin-4-yl-piperazine)-1-yl-propan-2-ol]

List of spectra:

- IR
- HREIMS
- ^{1}H NMR (400MHz, $CDCl_3$)
- ^{13}C NMR (400MHz, $CDCl_3$)
- HSQC (300MHz, $CDCl_3$)
- HMBC (300MHz, $CDCl_3$)
- COSY (300MHz, $CDCl_3$)

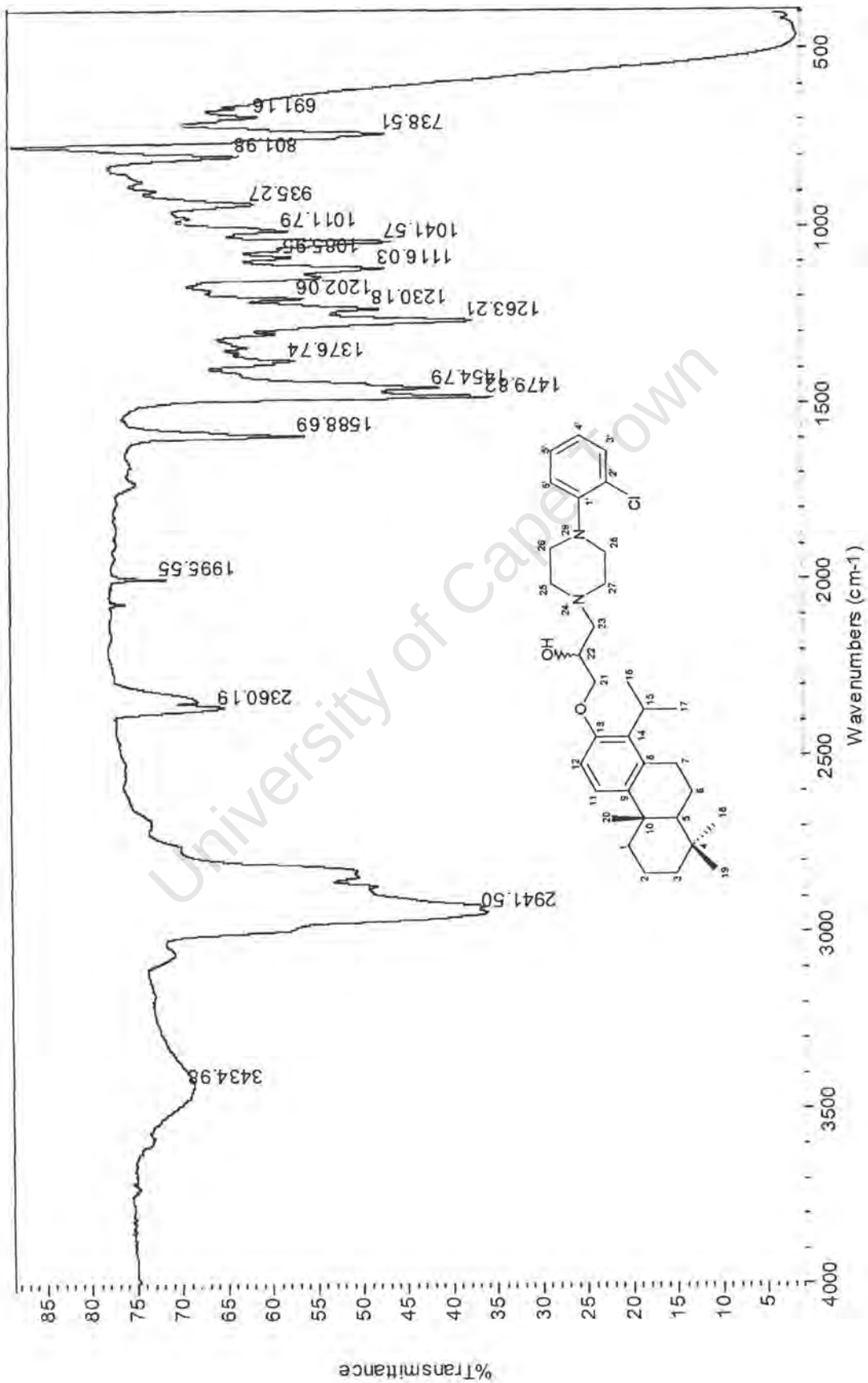

Figure A2.9.1 IR spectrum of compound **5**

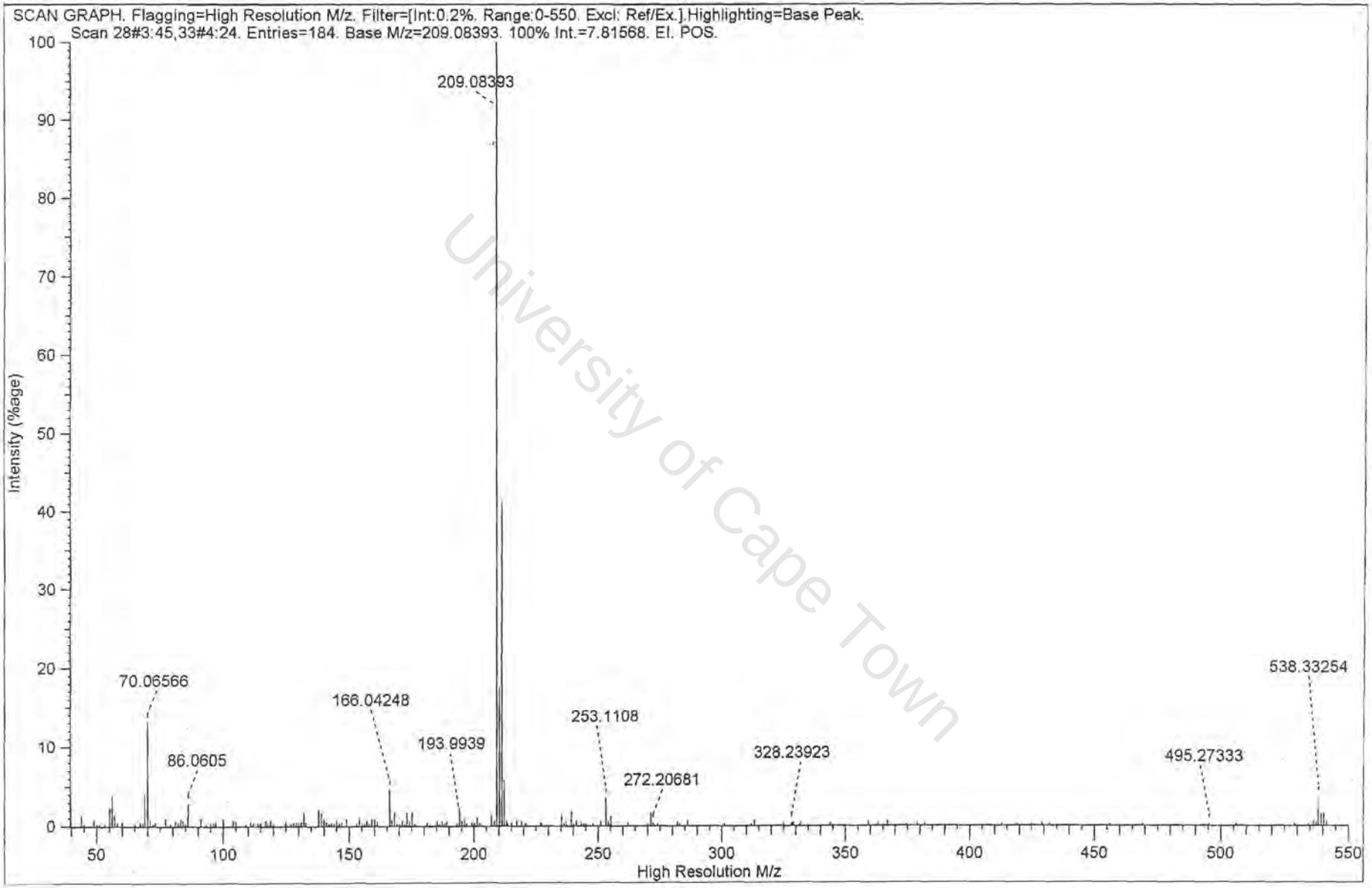

Figure A2.9.2 HREIMS spectrum of compound **5**

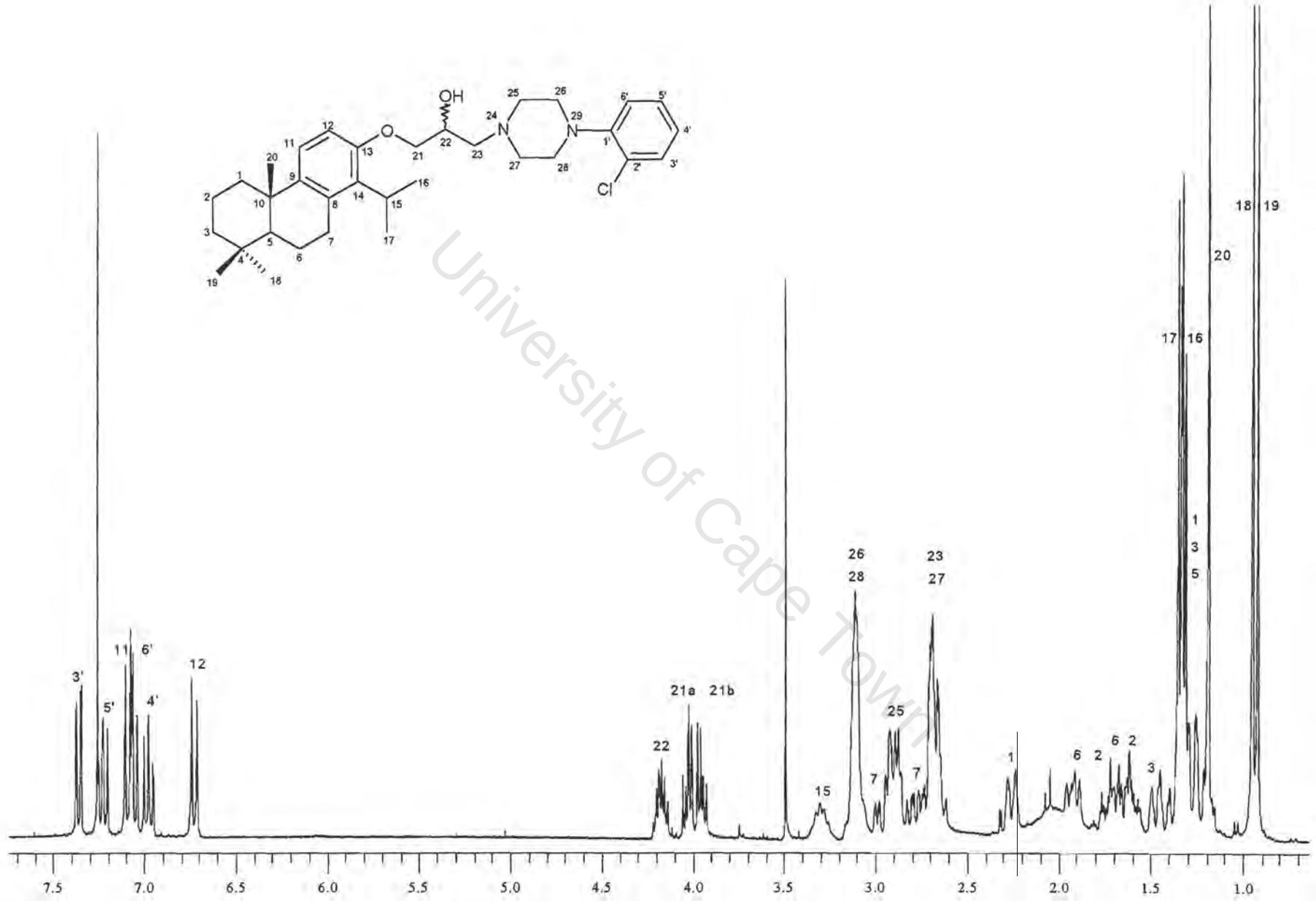

Figure A2.9.3 ^{1}H NMR spectrum of compound **5** in $CDCl_3$, 400MHz

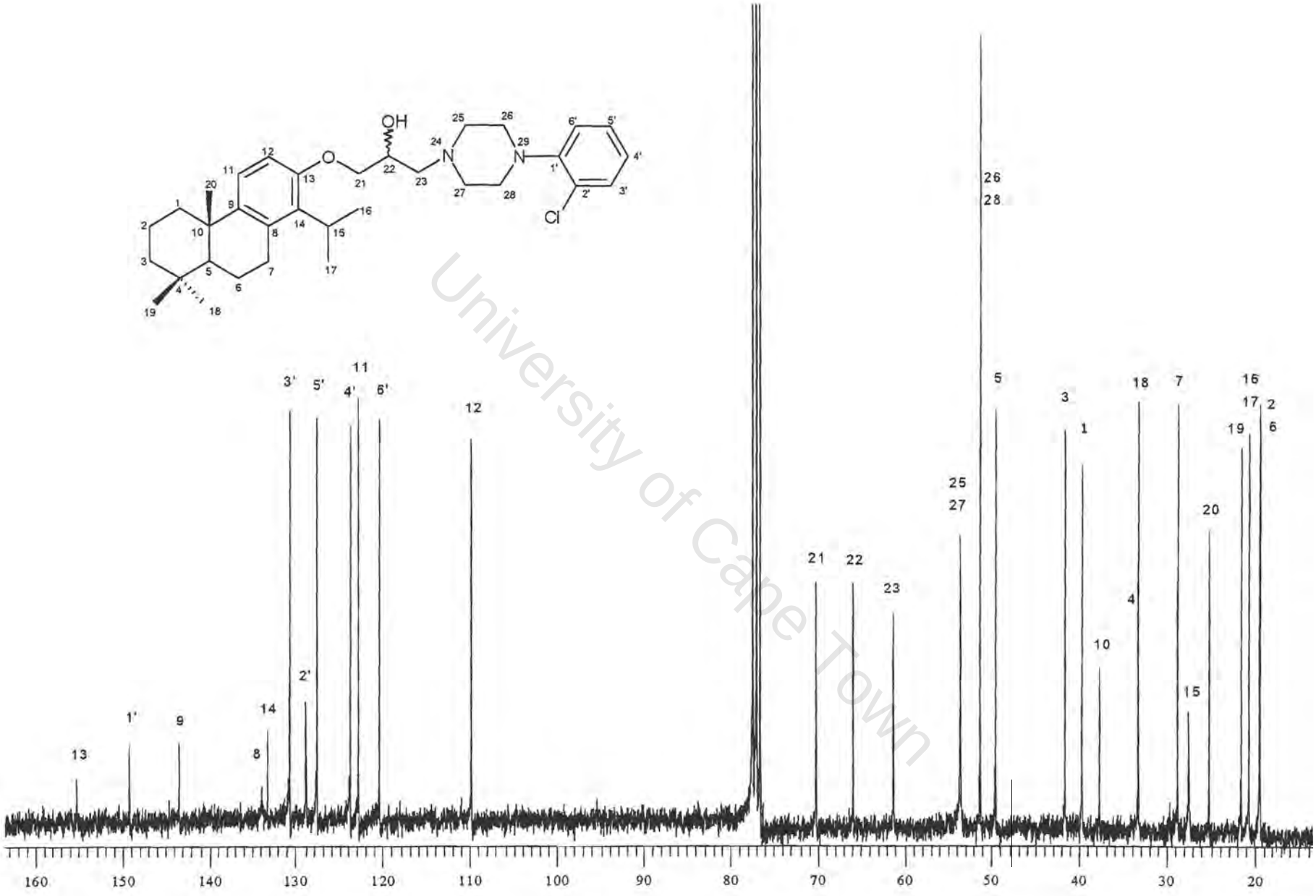

Figure A2.9.4 ^{13}C NMR spectrum of compound **5** in $CDCl_3$, 400MHz

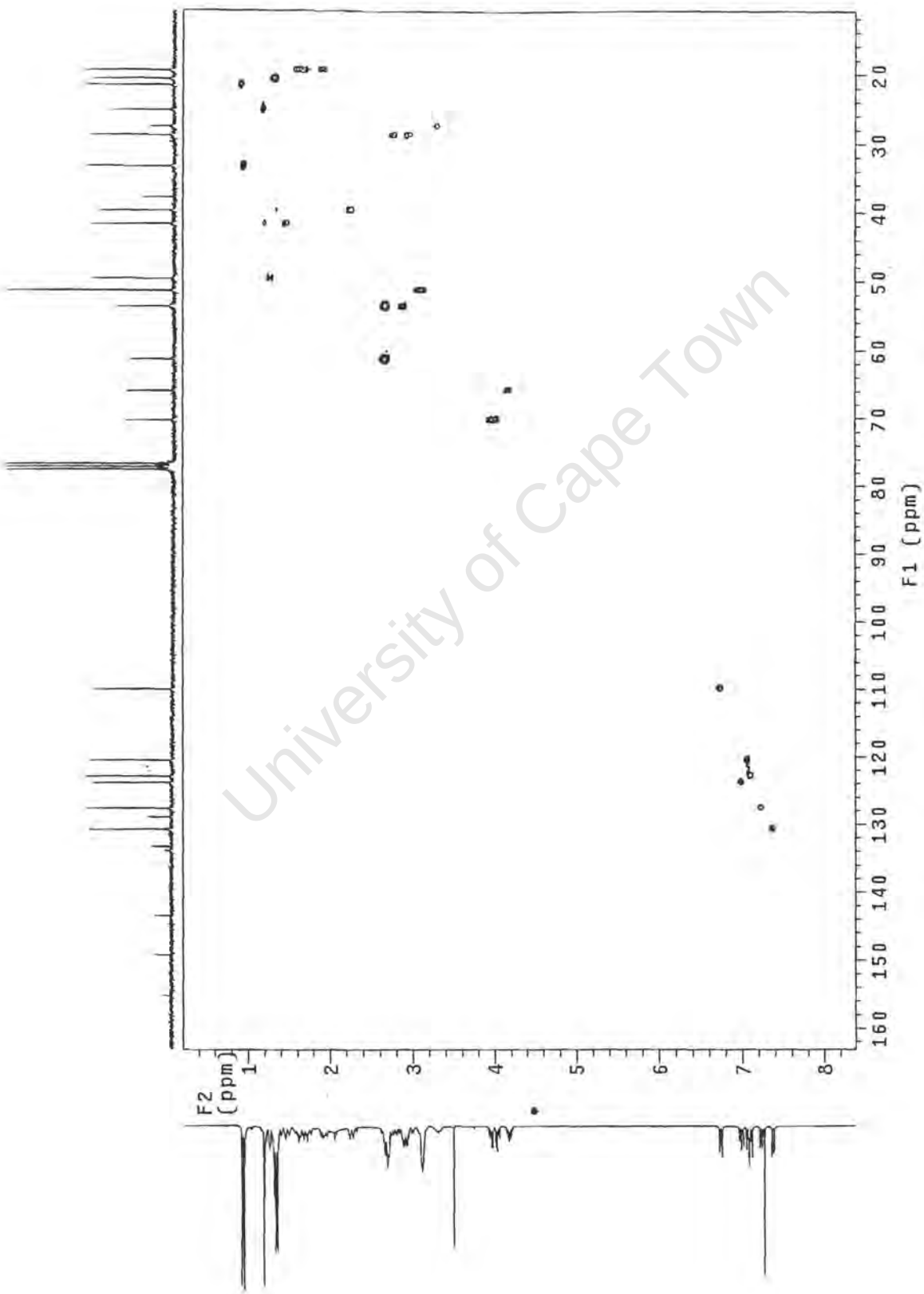

Figure A2.9.5 HSQC spectrum of compound **5** in $CDCl_3$, 300MHz

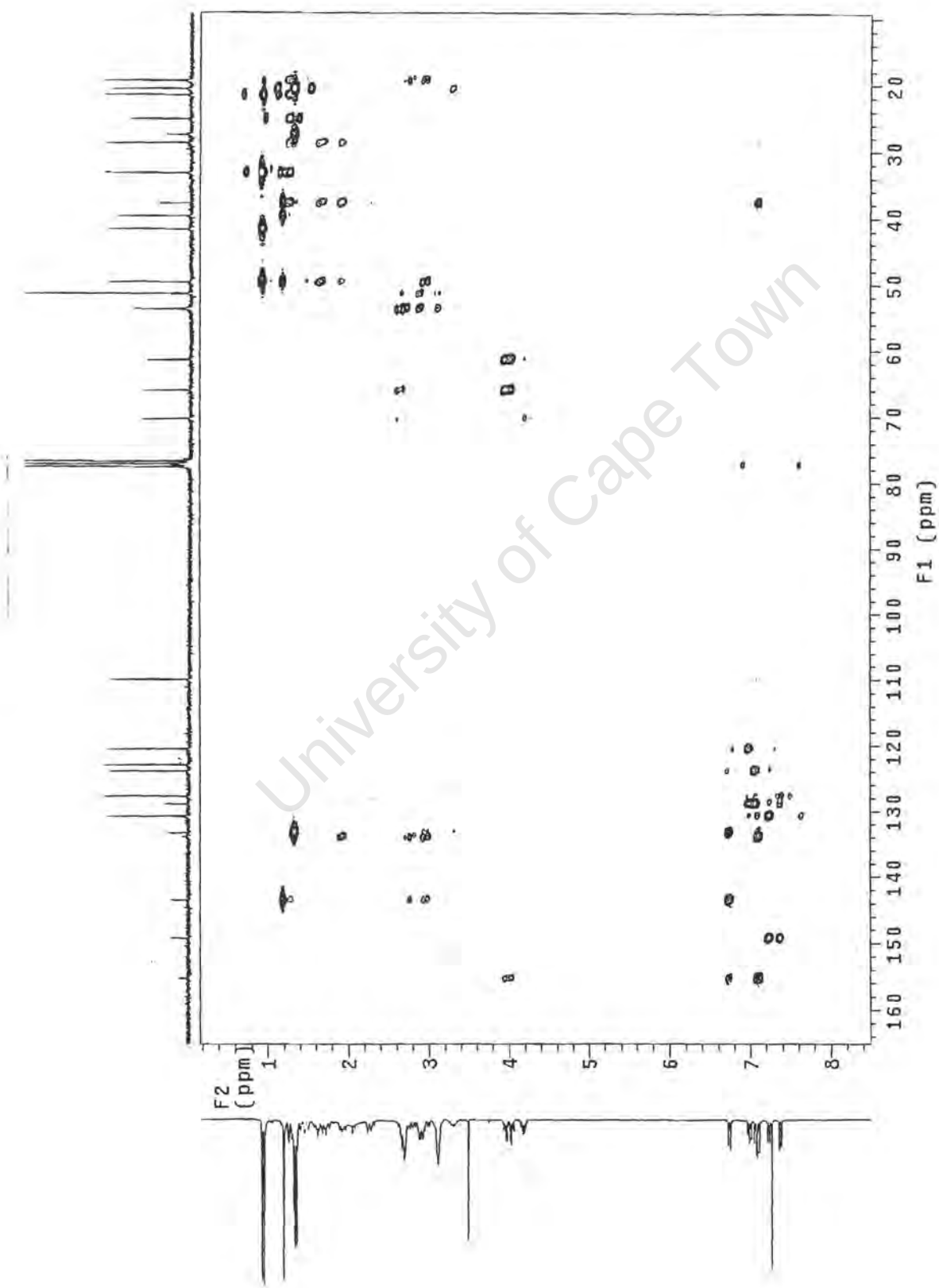

Figure A2.9.6 HMBC spectrum of compound **5** in $CDCl_3$, 300MHz

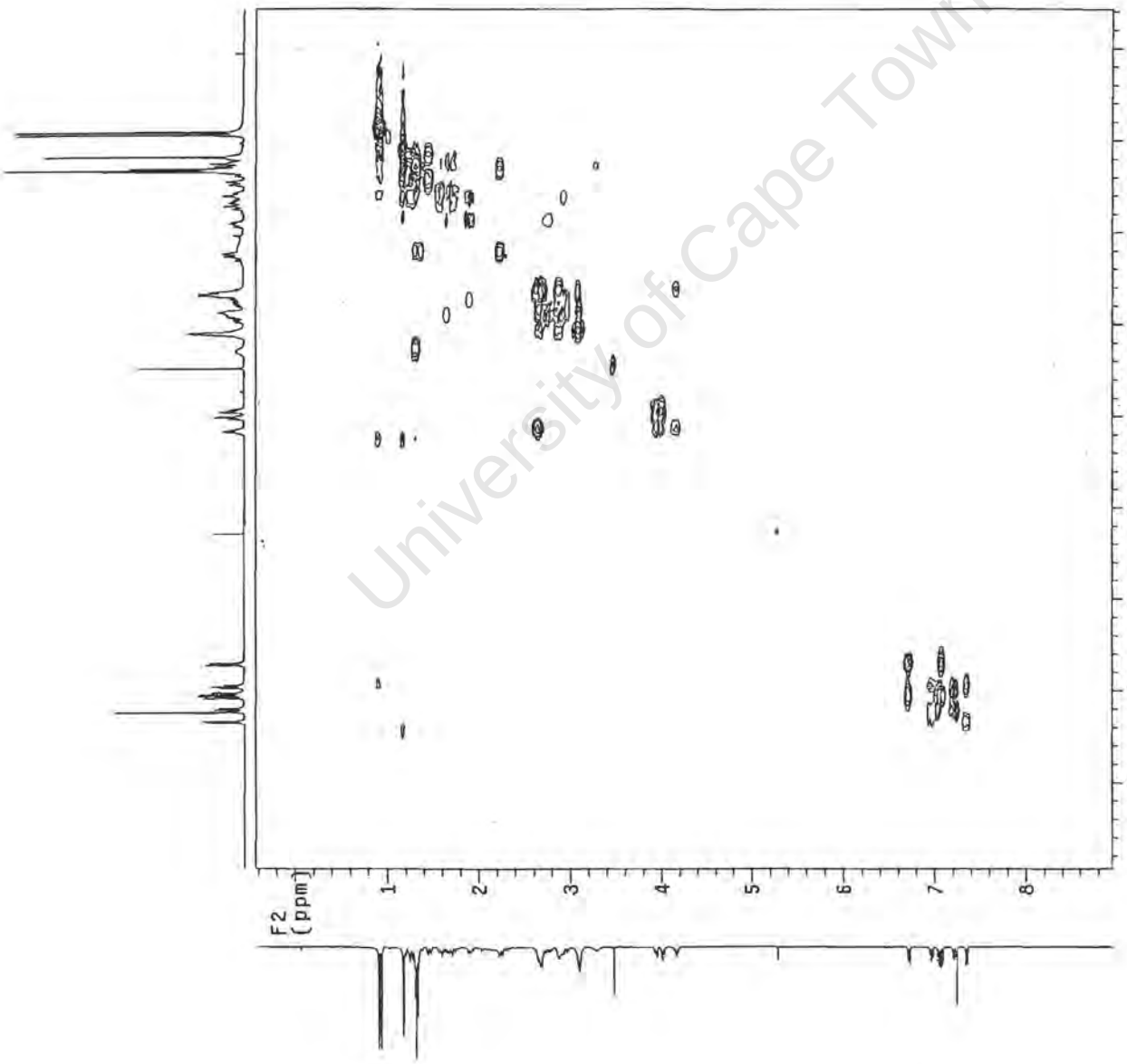

Figure A2.9.7 COSY spectrum of compound **5** in $CDCl_3$, 300MHz

A2.10 Compound 6

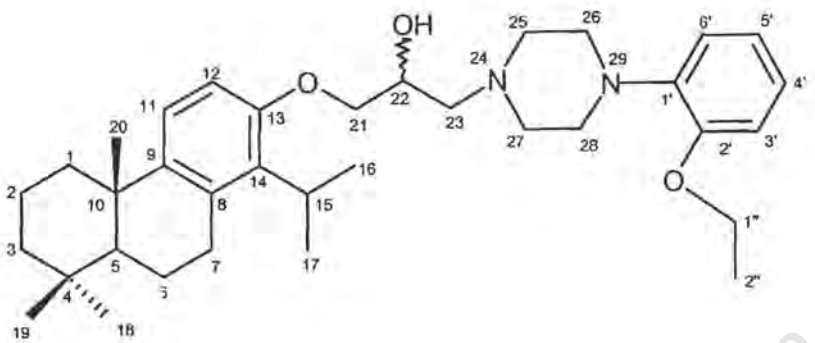

Compound 6

IUPAC [1-(1-Isopropyl-4b,8,8-trimethyl-4b,5,6,7,8,8a,9,10-octahydro-phenanthren-2-yloxy)-3-(2-ethoxyphenyl-piperazine)-1-yl-propan-2-ol]

List of spectra:

- IR
- HREIMS
- ^{1}H NMR (400MHz, $CDCl_3$)
- ^{13}C NMR (400MHz, $CDCl_3$)
- HSQC (300MHz, $CDCl_3$)
- HMBC (300MHz, $CDCl_3$)
- COSY (300MHz, $CDCl_3$)

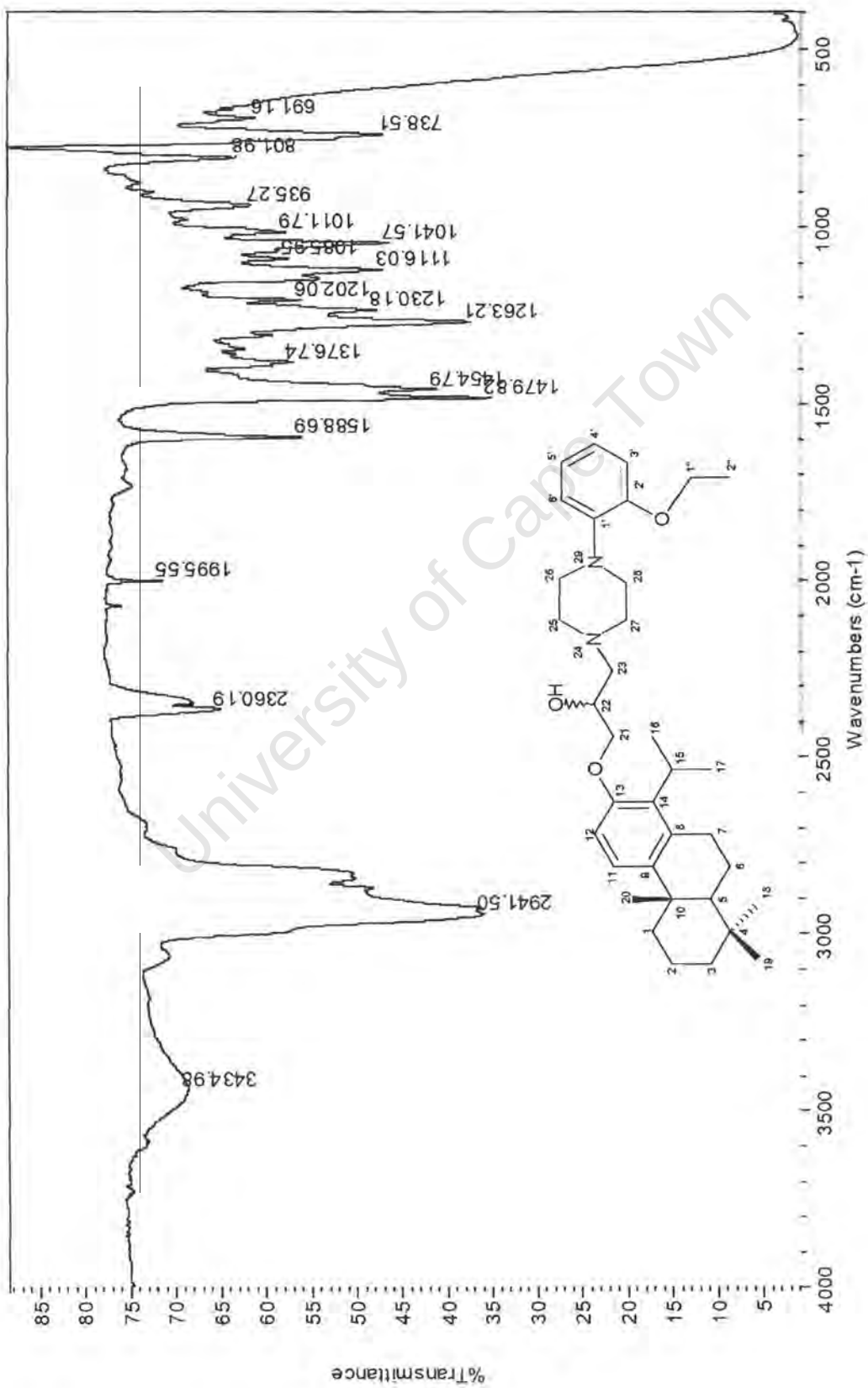

Figure A2.10.1 IR spectrum of compound **6**

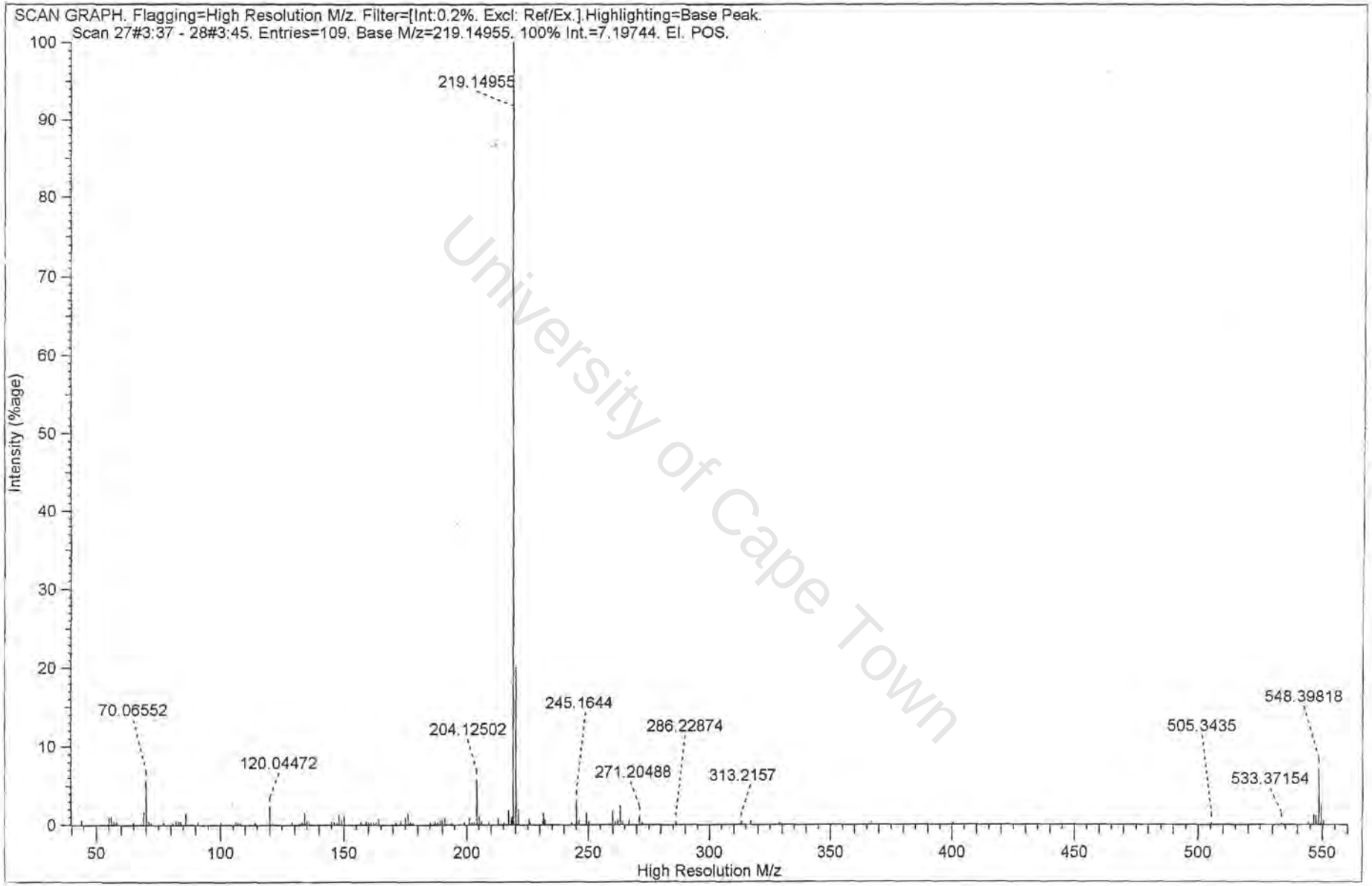

Figure A2.10.2 HREIMS spectrum of compound **6**

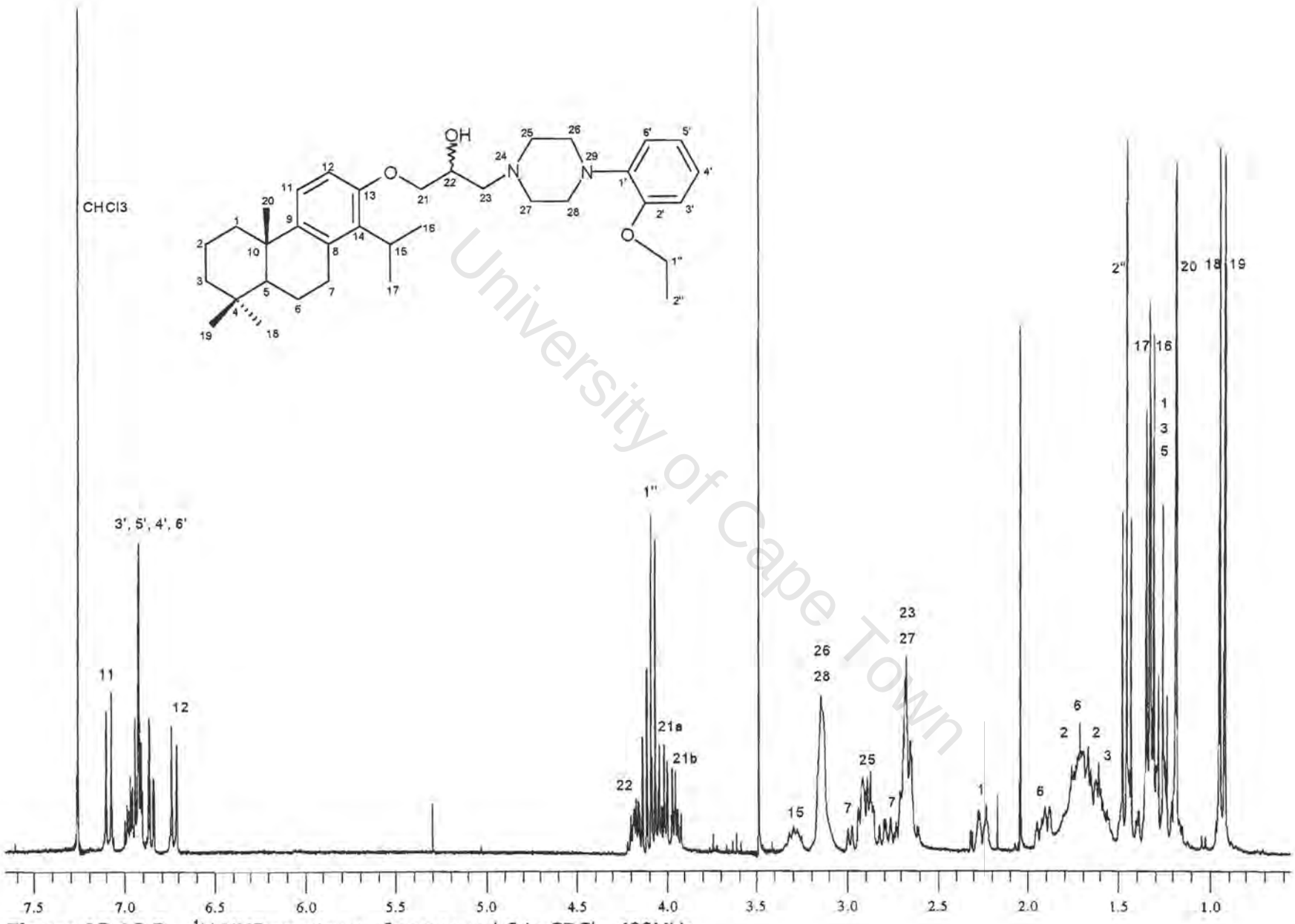

Figure A2.10.3 ^{1}H NMR spectrum of compound **6** in $CDCl_3$, 400MHz

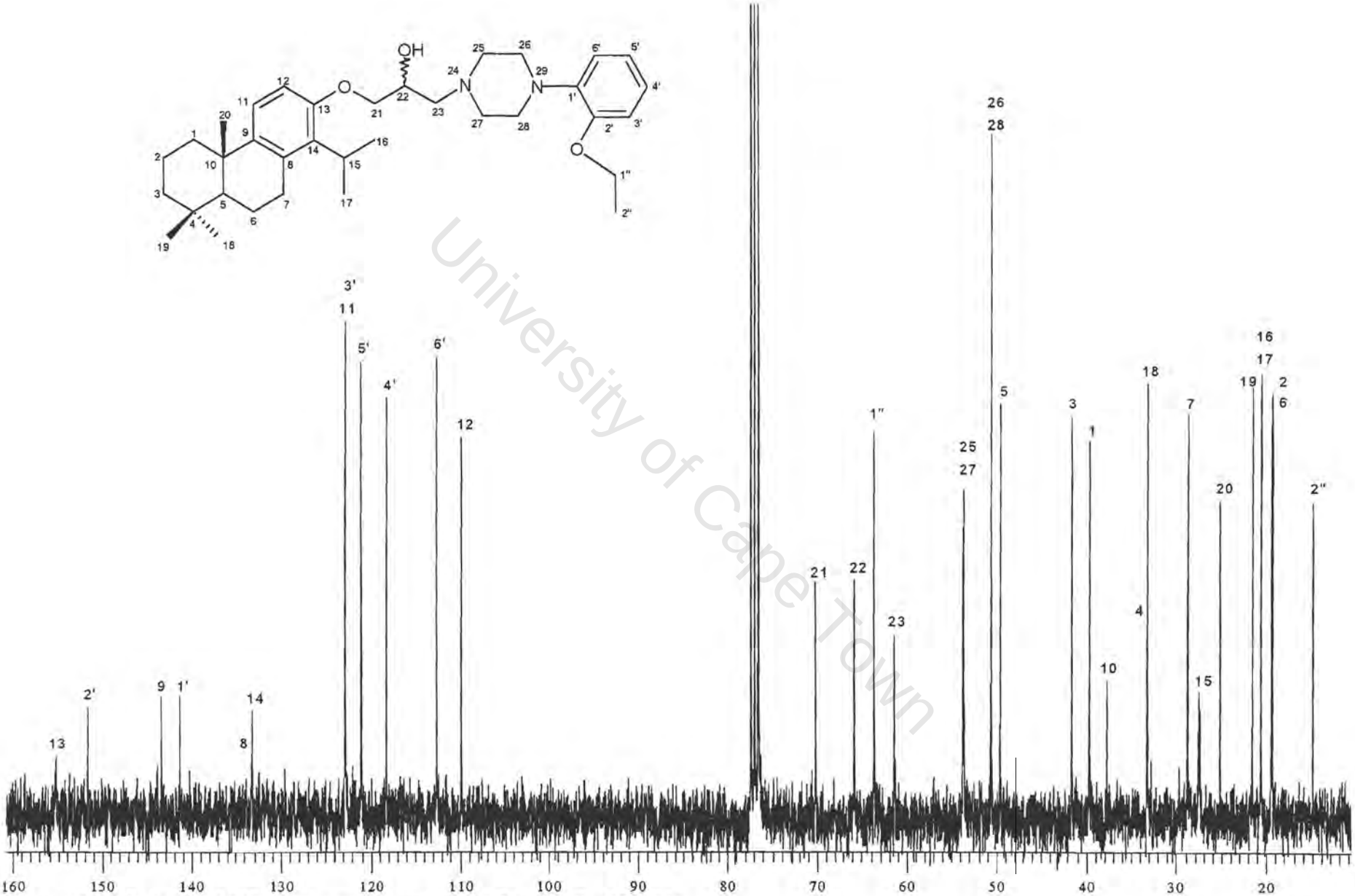

Figure A2.10.4 ^{13}C NMR spectrum of compound **6** in $CDCl_3$, 400MHz

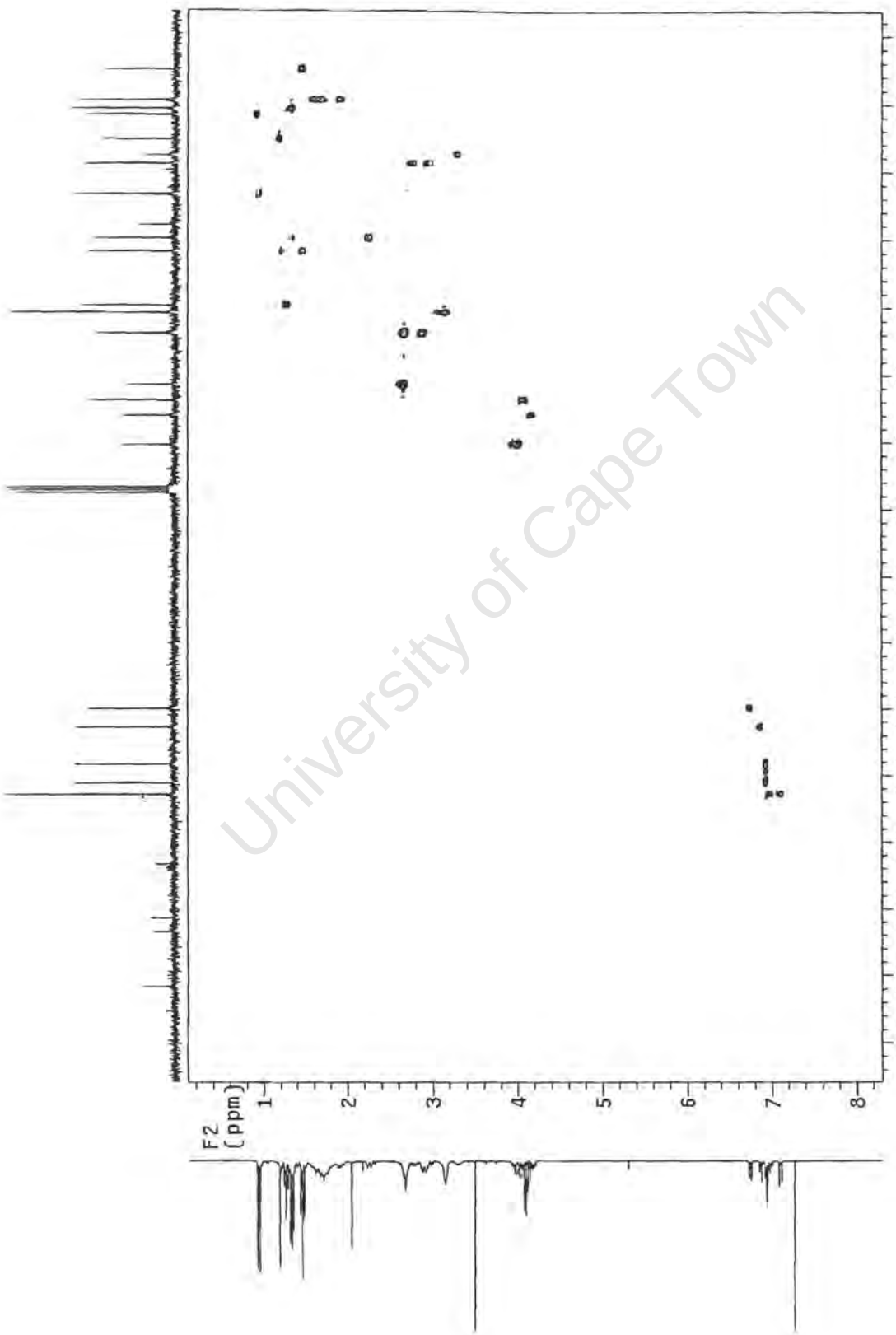

Figure A2.10.5 HSQC spectrum of compound **6** in $CDCl_3$, 300MHz

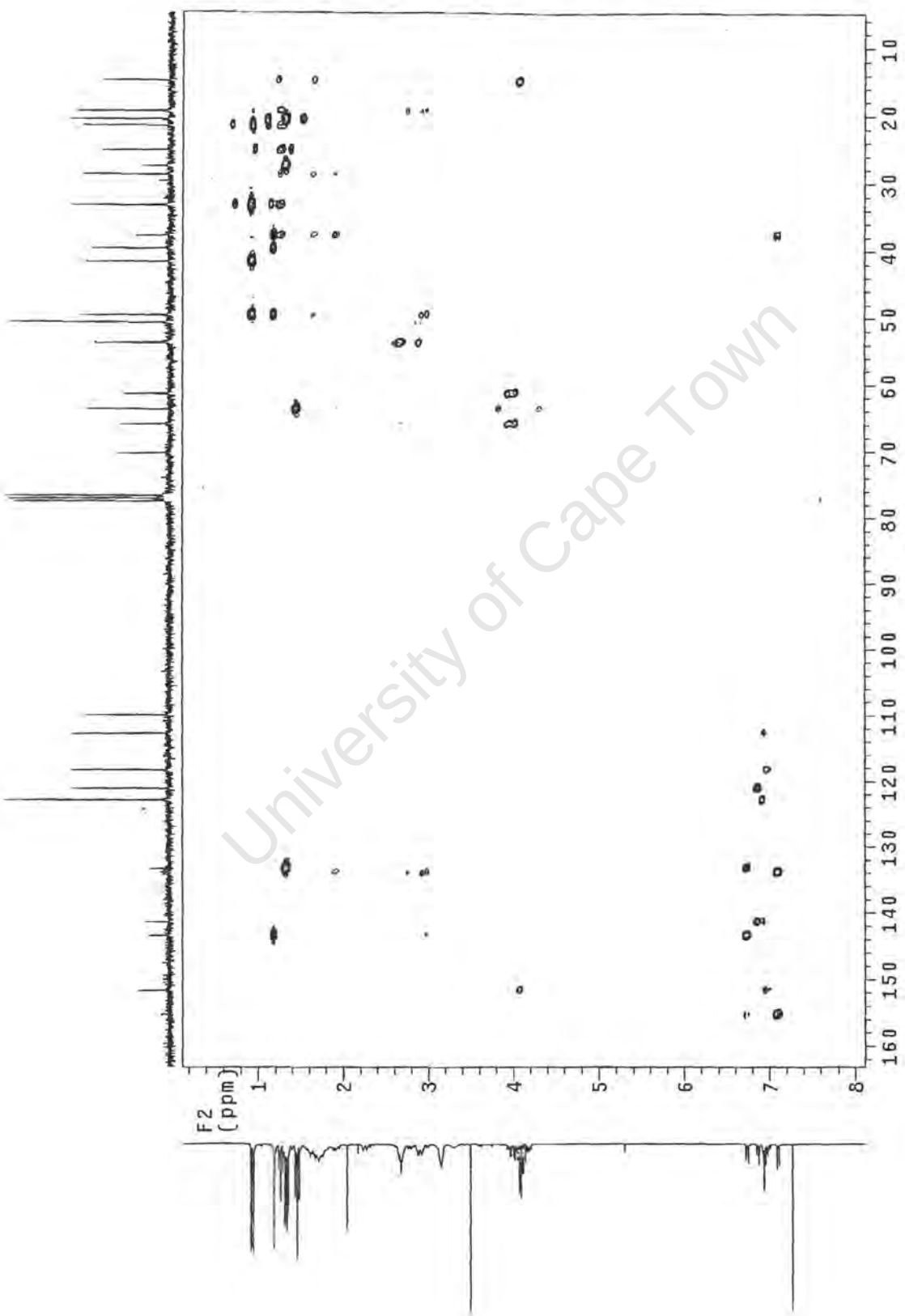

Figure A2.10.6 HMBC spectrum of compound **6** in $CDCl_3$, 300MHz

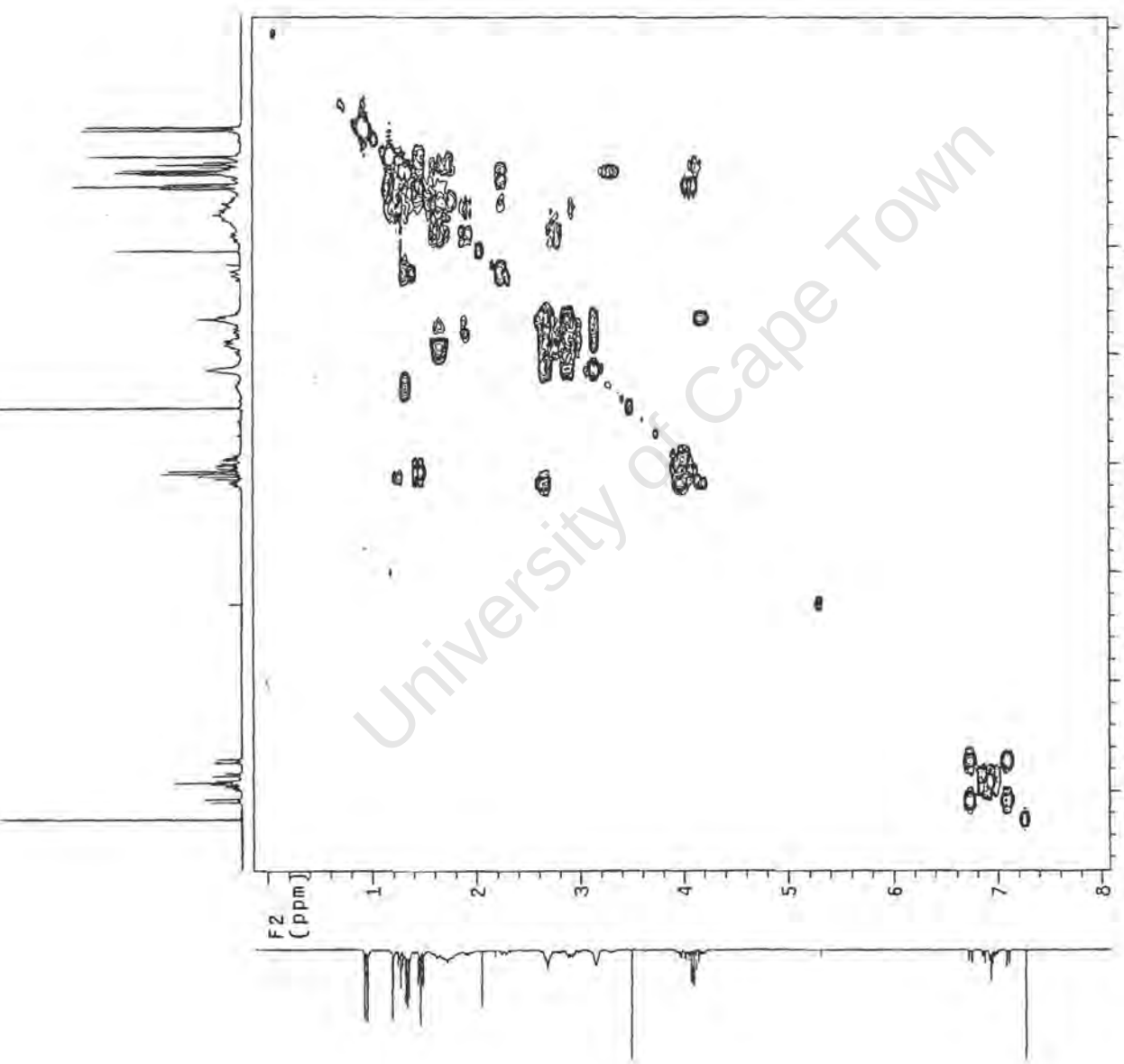

Figure A2.10.7 COSY spectrum of compound **6** in $CDCl_3$, 300MHz

A2.11 Amine 3

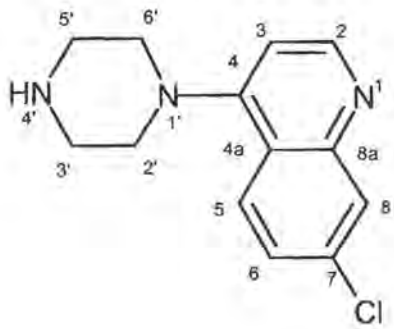

Amine 3

IUPAC [(7-chloroquinolin-4-yl)-piperazine]

List of spectra:

- ^{1}H NMR (300MHz, $CDCl_3$)
- ^{13}C NMR (300MHz, $CDCl_3$)
- HSQC (300MHz, $CDCl_3$)

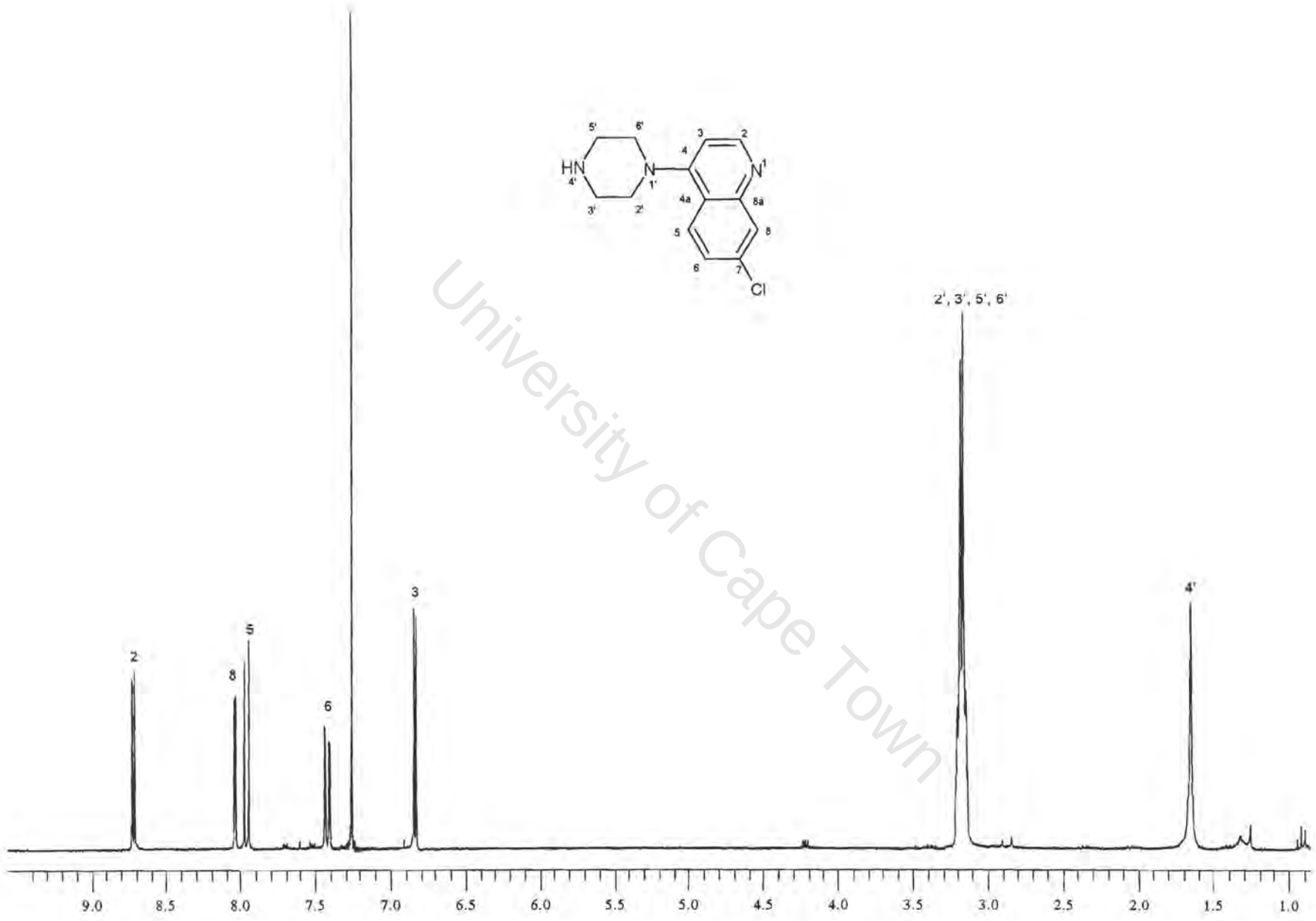

Figure A2.11.1 ^{1}H NMR spectrum of amine 3 in $CDCl_3$, 300MHz

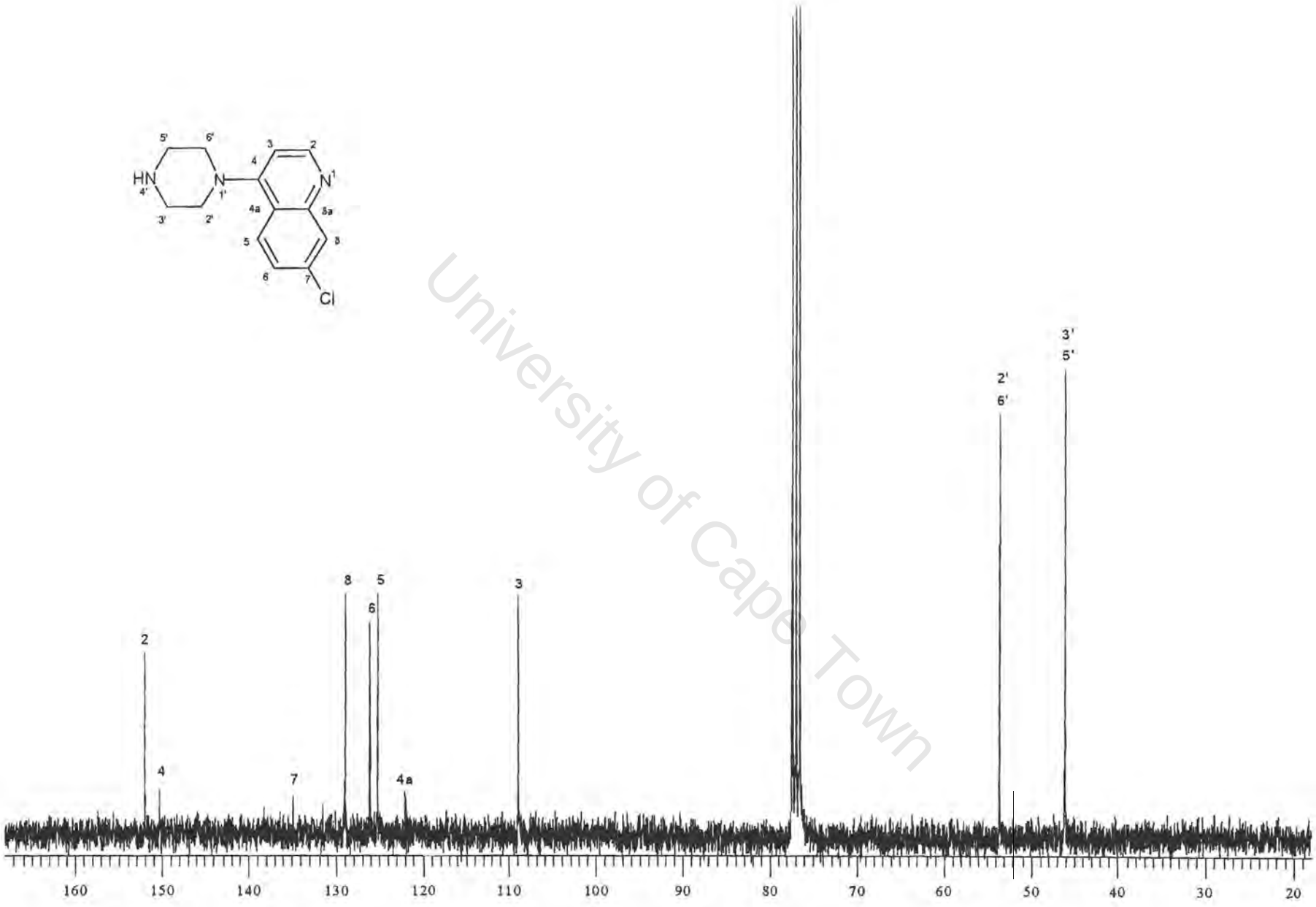

Figure A2.11.2 ^{13}C NMR spectrum of amine 3 in $CDCl_3$, 300MHz

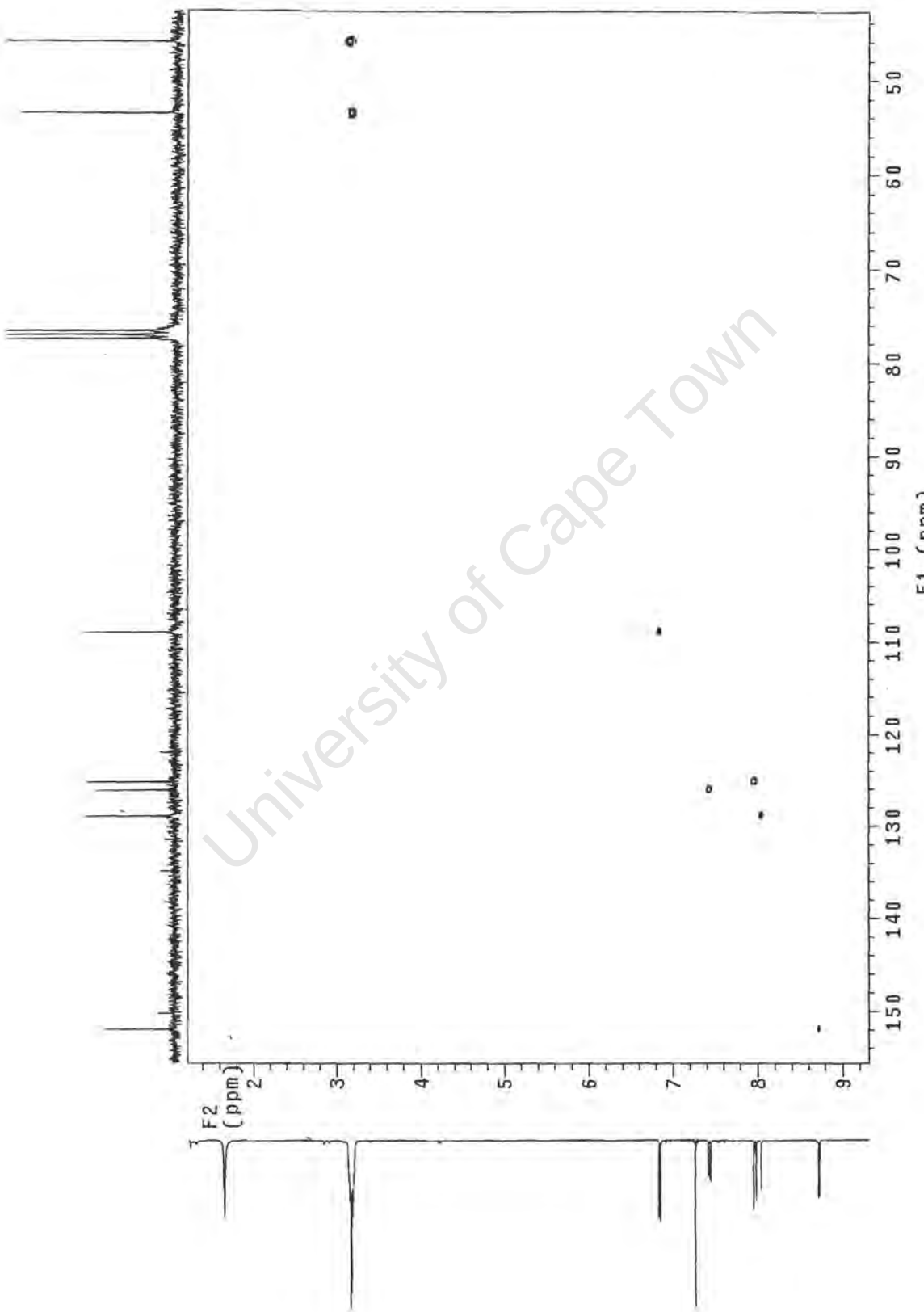

Figure A2.11.3 HSQC spectrum of amine **3** in $CDCl_3$, 300MHz